Pro-fibrotic effects of all-trans retinoic acid in transforming growth factor-1-induced fibrogenesis in renal fibroblasts

Rankin, Alexandra Catherine

Awarding institution:
King's College London

Pro-fibrotic effects of all-*trans* retinoic acid in transforming growth factor-β1-induced fibrogenesis in renal fibroblasts

A thesis submitted for the degree of Doctor of Philosophy

By Dr. Alexandra Catherine Rankin

King's College London School of Medicine

King's College London

University of London

1st April 2014

Abstract

Retinoids, including the prototypic vitamin A and its main bioactive form, all-*trans* retinoic acid (tRA), have both anti- and pro-fibrotic effects in renal disease models. To understand and prevent the pro-fibrotic effects of retinoids it is important to establish *in vitro* models. This work aimed to explore the mechanisms behind the fibrogenic effects of tRA in renal fibroblasts.

A picro-Sirius red-based *in vitro* assay was used to determine the effects of retinoids on total collagen accumulation with and without transforming growth factor (TGF)-β1 in NRK-49F normal rat kidney fibroblasts. Individual fibrotic markers and nuclear receptors were investigated using molecular biology approaches, activity assays and chemical agonists and inhibitors.

tRA dose-dependently increased total collagen deposition with and without TGF-β1 in NRK-49F cells. At the level of gene expression tRA showed dual potential, down-regulating mRNAs encoding a range of extracellular matrix proteins and matrix metalloproteinases (MMPs), while up-regulating others including plasminogen activator inhibitor (PAI)-1 and transglutaminase 2 (TG2). tRA alone and additively, with TGF-β1, reduced MMP activity and increased PAI-1 protein; the PAI-1 inhibitor tiplaxtinin reduced the increase in total collagen caused by tRA and TGF-β1 treatment. TG2 protein was not modulated by tRA and a TG2 inhibitor did not reduce tRA's pro-fibrotic effect.

NRK-49F cells expressed retinoid nuclear receptors and PPARβ/δ and nuclear receptor mRNAs were differentially regulated by tRA and TGF-β1. RAR and RXR antagonists reduced tRA's pro-fibrotic effect while a pan-RXR agonist more than a pan-RAR or PPARβ/δ agonist increased total collagen deposition. RAR isotype-selective agonists had less, if any, effect on fibrosis.

In summary, an *in vitro* model for the pro-fibrotic effects of retinoids has been established, which is associated with modulation of MMPs, PAI-1 and RAR/RXR. Further studies of RAR isotype-selective agonists might be of merit as they had reduced pro-fibrotic activities compared to less selective retinoids.

Acknowledgements

Firstly and foremostly I would like to thank Professor Bruce Hendry and Dr. Qihe Xu for giving me the opportunity to do this PhD and for their generosity of advice, support and encouragement. In so many different ways I would not be writing this without them. Thank you also to the renal research team (Andi, Joe, Qin, Fei, Lucy and Ayesha) and in particular Dr. Claire Sharpe for inciting scientific discussion which has been of enormous help to me and Mazzie Noor for throwing me many golden nuggets of scientific information. In addition I am extremely grateful for the support I have received from the King's Renal Research Fund and Kidney Research UK.

This PhD thesis would not have been possible without the unwavering support of my husband "Gorgeous Daniel" as he is known in the renal lab. who, had he known how absent a wife I would be at the start of this journey, might not have agreed to marry me! Daniel, thank you also for listening to my presentations countless times and giving me your constructive criticism on this thesis. In addition my very special son Oscar was born during the writing of this thesis. He has brought light and perspective to this work (and my life).

Finally to my other four favourite distractions, my nieces and nephew, Kristin, Iona, Phoebe and William who, along with Oscar, have the ability to make me forget all about my work worries!

Publications relating to this thesis

"An *in vitro* model for the pro-fibrotic effects of retinoids: Mechanisms of action."
Alexandra C. Rankin, Bruce M. Hendry, Jonathan P. Corcoran and Qihe Xu. Br J Pharmacol. 2013; 170(6): 1177-1189.

"Endogenous retinoic acid activity in principal cells and intercalated cells of mouse collecting duct system."
Yuen Fei Wong, Jeffrey B. Kopp, Catherine Roberts, Peter J. Scambler, Yoshifusa Abe, Alexandra C. Rankin, Neelanjana Dutt, Bruce M. Hendry and Qihe Xu. PLoS One. 2011 Feb 4; 6(2): e16770.

"NRK-49F cells as a model for studying the pro-fibrotic effects of all-*trans* retinoic acid: Roles for retinoid nuclear receptors and carrier proteins."
Alexandra C. Rankin, Bruce M. Hendry and Qihe Xu. J Am Soc Nephol. 2010; 21: 614A (abstract).

"Kidneys of Alb/TGF-beta1 transgenic mice are deficient in retinoic acid and exogenous retinoic acid shows dose-dependent toxicity."
Qihe Xu, Bruce M. Hendry, Malcolm Maden, Huiyan Lu, Yuen Fei Wong, Alexandra C. Rankin, Mazhar Noor and Jeffrey B. Kopp. Nephron Exp Nephrol. 2010; 114(4): e127-32.

"All-*trans* retinoic acid is pro-fibrotic in a normal rat kidney fibroblast cell line: A role for retinoid nuclear receptors and lipid binding proteins?"
Alexandra C. Rankin, Qihe Xu and Bruce M. Hendry. J Am Soc Nephol. 2009; 20: 492A (abstract).

Contents

List of figures and tables

Tables

Supplementary tables

Abbreviations used

ACE-I	Angiotensin converting enzyme inhibitors
ACN	Acetonitrile
ADH	Alcohol dehydrogenase
AF	Activation function
ANOVA	Analysis of variance
ANG II	Angiotensin II
AP-1	Activating protein-1
APL	Acute promyelocytic leukaemia
ARB	Angiotensin receptor blocker
αSMA	Alpha smooth muscle actin
BSA	Bovine serum albumin
Ca^{2+}	Calcium
CBP	CREB-binding protein
CDK	Cyclin-dependent kinase
CKD	Chronic kidney disease
COL	Collagen
COUP-TFII	Chicken ovalbumin upstream promoter-transcription 2
CRABP	Cellular retinoic acid binding protein
CRBP	Cellular retinol binding protein
CREB	Cyclic AMP-regulated enhancer-binding protein
CTGF	Connective tissue growth factor
CVD	Cardiovascular disease
CYP26	Cytochrome P450 family 26
DBD	DNA-binding domain
ddH_2O	Double distilled water
DMEM	Dulbecco's Modified Eagle Medium
DNA	Deoxyribonucleic acid
DR	Direct repeat
DTT	Dithiothreitol

ECM	Extracellular matrix
EC_{50}	Half maximal effective concentration
EDTA	Ethylenediaminetetraacetic acid
EMT	Epithelial-to-mesenchymal transition
ERK	Extracellular signal-regulated kinases
ESRD	End-stage renal disease
FABP5	Fatty acid binding protein 5
FCS	Foetal calf serum
FN	Fibronectin
GAPDH	Glyceraldehyde-3-phosphate dehydrogenase
GFR	Glomerular filtration rate
GOI	Gene of interest
GTP	Guanosine triphosphate
HGF	Hepatocyte growth factor
HKG	Housekeeping gene
HMC	Human mesangial cell
HPLC	high performance liquid chromatography
HRP	Horseradish peroxidase
HSC	Hepatic stellate cell
HSP	Heat shock protein
IC_{50}	Half maximal inhibitory concentration
IM	Intramuscular
IP	Intraperitoneal
IV	Intravenous
JNK	c-Jun N-terminal kinase
Kd	Binding efficiency
Ki	Inhibitor constant
LBD	Ligand-binding domain
LC/MS/MS	Liquid chromatography-tandem mass spectrometry
LDH	Lactate dehydrogenase
LRAT	Lecithin:retinol acyltransferase

LRP-1	Low-density lipoprotein receptor-related protein 1
MAP kinase	Mitogen-activated protein kinase
MEF	Mouse embryonal fibroblast
MMP	Matrix metalloproteinase
N-CoR	Nuclear receptor co-repressor
NFκB	Nuclear factor kappa-light-chain-enhancer of activated B
NRK	Normal rat kidney
NTD	N-terminal domain
PA	Plasminogen activator
PAI-1	Plasminogen activator inhibitor-1
PAR6	Partitioning defective 6
PBS	Phosphate buffered saline
PCR	Polymerase chain reaction
PDGF	Platelet-derived growth factor
PI3K	Phosphoinositide 3-kinase
PKC	Protein kinase C
PML	Promyelocytic leukaemia
PMSF	Phenylmethanesulphonylfluoride
PO	Per os
PPAR	Peroxisome proliferator-activated receptor
PPRE	Peroxisome proliferator response element
PSR	Picro-Sirius red
Q-ToF	Quadrupole time-of-flight
RA	Retinoic acid
RAAS	Renin-angiotensin-aldosterone system
RALDH	Retinaldehyde dehydrogenase
RAR	Retinoic acid receptor
RARE	Retinoic acid response element
RBP	Retinol binding protein
REH	Retinyl ester hydrolase
RhoA	Ras homolog gene family, member A

RMC	Rat mesangial cell
RNA	Ribonucleic acid
ROCK1	Rho-associated protein kinase 1
ROR-β	Retinoic acid receptor-related orphan receptor β
RPL13a	60S ribosomal protein L 13a
RRT	Renal replacement therapy
R-Smads	Receptor-activated Smads
RT-qPCR	Reverse transcription quantitative PCR
RXR	Retinoid X receptor
SARA	SMAD anchor for receptor activation
SC	Subcutaneous
SDR	Short-chain dehydrogenases/reductase
SDS	Sodium dodecyl sulphate
SDS-PAGE	SDS-polyacrylamide gel electrophoresis
siRNA	Short-interfering ribonucleic acid
SMRT	Silencing mediator of RA and TR
Smurf	Smad-ubiquitination-regulatory factor
SNx	Subtotal nephrectomy
SPARC	Secreted protein, acidic and rich in cysteine
STRA6	Stimulated by retinoic acid gene 6
TAK1	TGF-β activated kinase 1
TBS	Tris-buffered saline
TG2	Transglutaminase 2
TGIF	TGF β-induced factor homeobox 1
TGF-β	Transforming growth factor-β
TβRI	TGF-β receptor type I
TβRII	TGF-β receptor type II
TIMP	Tissue inhibitor of matrix metalloproteinase
TIF	Renal tubulointerstitial fibrosis
TNF	Tumour necrosis factor
tPA	Tissue-type plasminogen activator
tRA	All-*trans* retinoic acid

TSP-1	Thrombospondin-1
TTNPB	(E)-4-[2-(5,6,7,8-tetrahydro-5,5,8,8-tetramethyl-2-naphthalenyl)-1-propenyl] benzoic acid
TTR	Transthyretin
uPA	Urokinase-type plasminogen activator
UTI	Urinary tract infection
UUO	Unilateral ureteric obstruction
VAD	Vitamin A deficiency
VCAM	Vascular cell adhesion molecule
VSMC	Vascular smooth muscle cell
WSB	Western sample buffer
9cRA	9-*cis* retinoic acid
13cRA	13-*cis* retinoic acid

Chapter 1. Introduction

1.1 Chronic kidney disease (CKD)

Chronic kidney disease (CKD) is a major public health concern worldwide. In the UK, the prevalence of CKD stages 3-5 is as high as 8.5% (Stevens, O'Donoghue et al. 2007). It is caused by a variety of conditions including hypertension, diabetes mellitus and glomerulonephritis and is chronic and progressive, characterised by excessive and abnormal extracellular matrix (ECM) deposition leading to renal fibrosis and end-stage renal disease (ESRD). Patients with CKD are at significantly increased risk of cardiovascular disease (CVD) and death and this risk increases as their glomerular filtration rate (GFR) falls (Go, Chertow et al. 2004). Once ESRD has developed patients need to be established on renal replacement therapy (RRT) and this patient group have a poor prognosis with incident over 65 year olds having only a 74.9% and 25.1% 1- and 5- year survival, respectively (Ansell, Roderick et al. 2009).

In the general nephrology clinic management of CKD initially involves diagnosis and treatment of the underlying cause of kidney injury. More general measures are also undertaken to maintain stable kidney function and prevent CVD. These include lifestyle advice (achieving a healthy weight, taking regular exercise and smoking abstention) and pharmacological interventions, such as anti-hypertensive drugs to maintain adequate blood pressure control, treatment of hyperlipidaemia and medication to reduce proteinuria (National Collaborating Centre for Chronic Conditions 2008).

Novel strategies for the treatment of CKD include more comprehensive blockade of the renin-angiotensin-aldosterone system (RAAS) with direct renin inhibitors (Mende 2010), endothelin receptor antagonists (Turgut and Bolton 2010), drugs that target the transforming growth factor (TGF)-β system (Akhurst and Hata 2012) and connective tissue growth factor (CTGF) inhibitors (Reeves, Rawal et al. 2012). However, thus far, a therapy that directly targets renal fibrosis safely and effectively remains elusive.

Retinoids (vitamin A derivatives) have been proposed as potential therapies for the treatment of renal fibrosis (Xu, Lucio-Cazana et al. 2004). Retinoids and their signalling system have been shown to interfere with pathways involved in fibrogenesis including ECM production (Perez, Shull et al. 1992; Wang, Tankersley et al. 2002), TGF-β1 signalling (Morath, Dechow et al. 2001; Schaier, Jocks et al. 2003; Kishimoto, Kinoshita et al. 2011) and modulation of matrix turnover (Liu, Lu et al. 2008; Liu, Lu et al. 2011). However, despite evidence supporting a role for retinoids in the treatment of renal fibrosis, there remains a lack of consensus that they are, indeed, beneficial. This laboratory-based work uses a novel *in vitro* model to provide new insights into the effects of retinoids on progression of fibrosis in renal fibroblasts. The background of the current understanding of renal fibrosis, with particular focus on areas where retinoids may play a role, is reviewed here.

1.2 Renal tubulointerstitial fibrosis

Renal tubulointerstitial fibrosis (TIF) is characterised by excessive accumulation of ECM in the interstitium of the kidney. Integral to this process is the loss of tubules and peritubular capillaries and infiltration of mononuclear cells. TIF is an important predictor of progression to ESRD (Risdon, Sloper et al. 1968; Schainuck, Striker et al. 1970; Mackensen-Haen, Bader et al. 1981; Nath 1992) and is mediated by many different growth factors and cytokines, which exert pro-fibrotic effects on effector cells, particularly fibroblasts (Liu 2011). In this section the key roles of renal myofibroblasts, TGF-β and ECM remodelling in TIF will be reviewed.

1.2.1 Role of myofibroblasts

Myofibroblasts have long been identified as key cellular mediators of TIF. They are elongated, spindle-shaped cells with large, elliptical and speckled nuclei, dense rough endoplasmic reticulum, extensive Golgi apparatus and an absence of lysosomes (Hutchison, Fligny et al. 2012). Biochemically, they are characterised by expression of the intermediate filaments desmin, vimentin and the contractile protein alpha smooth muscle actin (αSMA), which is widely regarded as a myofibroblast marker, and morphologically, by the formation of

stress fibres (Hutchison, Fligny et al. 2012). They synthesise and secrete a complex array of pathological structural and non-structural ECM molecules, and of particular importance in fibrosis are collagen types I and III (Rodemann and Muller 1991; Hutchison, Fligny et al. 2012). In addition, they remodel the ECM through the production of proteinases, use autocrine and paracrine signalling systems to communicate with other cells (Jeon 2009) and contract matrix increasing its density (Kelynack, Hewitson et al. 2000).

Myofibroblasts are rarely identified in normal kidneys however following injury they are found in increasing numbers. The origin of renal myofibroblasts is a hotly debated subject however there is now strong evidence from genetic fate-mapping studies that they develop from mesenchymal precursors resident in the kidney as interstitial fibroblasts, perivascular fibroblasts and pericytes (Lin, Kisseleva et al. 2008; Humphreys, Lin et al. 2010; Asada, Takase et al. 2011). There are few distinguishing characteristics between these cells but include differences in their tissue location and anatomical connections with endothelial cells; however following kidney injury they become indistinguishable as myofibroblasts (Lin, Kisseleva et al. 2008; Picard, Baum et al. 2008; Humphreys, Lin et al. 2010; Hutchison, Fligny et al. 2012). Although, epithelial-to-mesenchymal transition (EMT) is reportedly a potential source of renal myofibroblasts and *in vitro* studies demonstrate that renal tubular cells can undergo EMT (Okada, Danoff et al. 1997), evidence for the biological significance of this effect *in vivo* is lacking (Iwano, Plieth et al. 2002; Humphreys, Lin et al. 2010; Koesters, Kaissling et al. 2010). Likewise, evidence for endothelial-to-mesenchymal transition remains unsubstantiated (Zeisberg, Potenta et al. 2008). In view of the emerging importance of resident mesenchymal precursors as a key source of myofibroblasts a focus on these fibroblastic cells when examining the direct effects of therapies on TIF would seem a reasonable approach.

Trans-differentiation of resident mesenchymal precursors into renal myofibroblasts occurs via various different mechanisms following renal injury. Tubular cells, leukocytes and fibroblasts themselves all produce cytokines and

growth factors that contribute to (myo)fibroblast differentiation, proliferation and collagen synthesis (Hewitson 2009). Implicated pro-fibrotic molecules include angiotensin (ANG) II and platelet-derived growth factor (PDGF) as well as disease-specific states such as hyperglycaemia in diabetes mellitus and mechanical stress (Darby and Hewitson 2007; Hewitson 2009). In addition, TGF-β has been identified as a group of premier cytokines involved in TIF.

1.2.2 Role of transforming growth factor (TGF)-β

TGF-β belongs to the TGF-β superfamily of cytokines, of which there are over 30 members in humans (Massague 2012). It plays important roles in embryogenesis and adult tissue homeostasis by regulating cell proliferation, differentiation and migration. TGF-β is made up of three isoforms, TGF-βs 1-3; TGF-β1 was initially identified by its ability to induce anchorage-independent growth of fibroblasts (Moses, Branum et al. 1981; Roberts, Anzano et al. 1981) and subsequently TGF-β2 was identified, cloned and sequenced (Hanks, Armour et al. 1988; Madisen, Webb et al. 1988) followed by TGF-β3 (Derynck, Lindquist et al. 1988; Jakowlew, Dillard et al. 1988; ten Dijke, Hansen et al. 1988).

TGF-β1 is the most broadly studied of the TGF-β isoforms and its role as a key mediator of renal fibrosis is well established as it increases ECM production and interferes with matrix turnover (Lan and Chung 2012). Evidence to support its importance in renal fibrogenesis includes its increased expression in virtually every animal model of CKD (Okuda, Languino et al. 1990; Coimbra, Wiggins et al. 1991; Yamamoto, Noble et al. 1994; Cheng, Orikasa et al. 1995; Hamaguchi, Kim et al. 1995; Moll, Menoud et al. 1995) as well as in human CKD (Yoshioka, Takemura et al. 1993; Yamamoto, Noble et al. 1996; Sharma, Ziyadeh et al. 1997), its ability to activate fibroblasts and mesangial cells and cause trans-differentiation of epithelial and endothelial cells into myofibroblasts *in vitro* (Border, Okuda et al. 1990; Fan, Ng et al. 1999; Han, Isono et al. 1999; Oldfield, Bach et al. 2001) and exogenous TGF-

β1 causes renal fibrosis while transgenic mice over-expressing TGF-β1 develop renal fibrosis (Sanderson, Factor et al. 1995; Mozes, Bottinger et al. 1999; Liu 2006). In addition TGF-β1 increases the expression of a variety of ECM molecules including collagens I, III and IV, fibronectin (FN) and also plasminogen activator inhibitor (PAI)-1, all of which are increased in TIF (MacKay, Striker et al. 1989; Tomooka, Border et al. 1992; McKay, Khong et al. 1993; Suzuki, Ebihara et al. 1993; Hansch, Wagner et al. 1995; Bertelli, Valenti et al. 1998; Poncelet and Schnaper 1998; Douthwaite, Johnson et al. 1999; Zhang, Ou et al. 2000). TGF-β1 also modulates the expression and activity of matrix metalloproteinases (MMPs) and their inhibitors resulting in reduced matrix degradation and a pro-fibrotic phenotype (Schnaper, Hayashida et al. 2003).

TGF-β1 is secreted as a homodimer consisting of two 12-kDa polypeptides linked by disulphide bonds and associated non-covalently with a latency-associated protein; this inactive complex may be covalently bound to a latent TGF-β-binding protein by disulphide bonds (Schnaper, Hayashida et al. 2003). Latent TGF-β1 deposits in the ECM and binds to matrix proteins such as FN (Dallas, Sivakumar et al. 2005). *In vitro,* release of active TGF-β1 occurs through a number of environmental triggers including heat, shear force, pH extremes and proteolysis (Munger, Harpel et al. 1997). *In vivo,* TGF-β1 activation is a complex and tightly regulated process: A non-proteolytic activation by integrins and thrombospondin-1 (TSP-1) has been identified (Jenkins 2008; Hayashi and Sakai 2012) and proteolytic activation also occurs, with proteases exerting their actions both indirectly, via integrins and other activating molecules, and directly, functioning in a coordinated manner with other activating molecules (Jenkins 2008).

TGF-β signalling is highly complex, context dependent and involves canonical and non-canonical pathways. An illustration of current knowledge of TGF-β signalling pathways is shown in Figure 1.1.

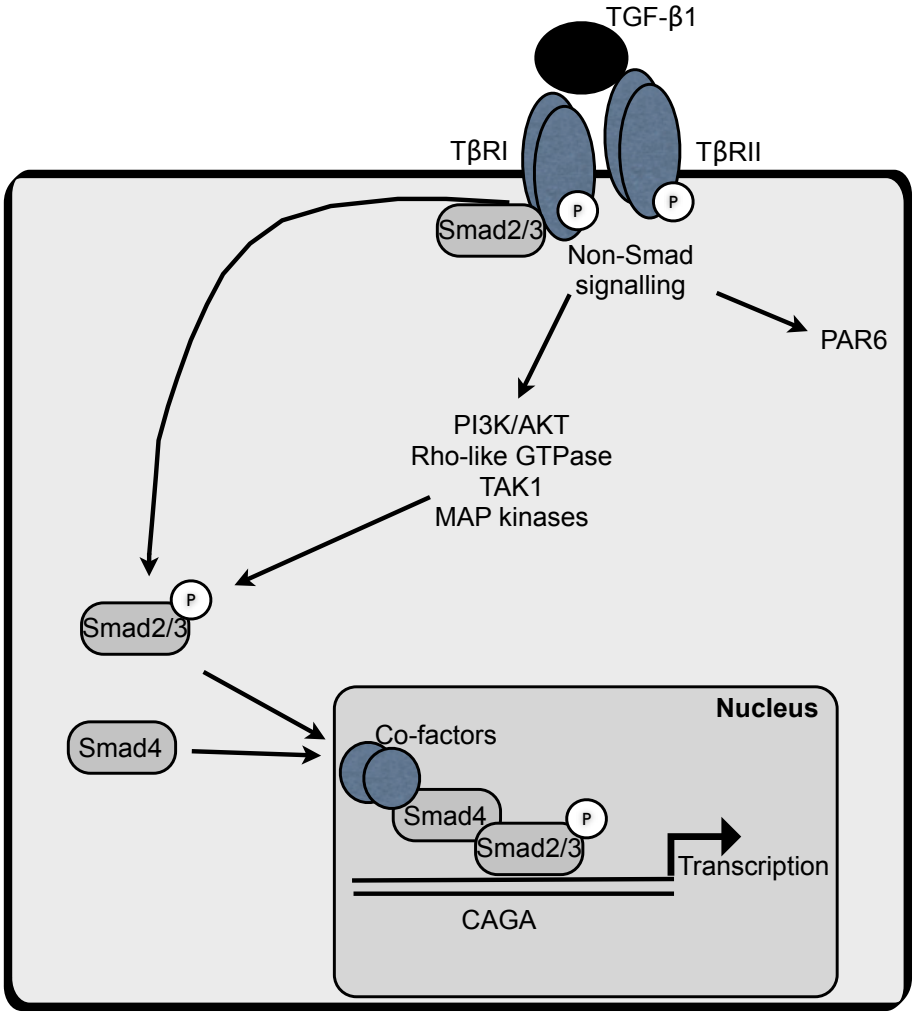

Figure 1.1. Signal-transduction pathways of TGF-β1 (adapted from Massague 2000, Doyle, Gerber et al. 2012 and Choi, Ding et al. 2012). Active TGF-β1 binds to TβRII causing phosphorylation and activation of TβRI. TβRI phosphorylates R-Smad, which binds to Smad4. The Smad complex is then imported into the nucleus where it binds to specific locations within TGF-β1-responsive genes, co-factors are recruited and transcription of specific genes can be initiated. TGF-β1 can also exert its effects via non-Smad signalling pathways. *MAP kinases:* mitogen-activated protein kinases; *PAR6:* partitioning defective 6; *PI3K:* phosphoinositide-3-kinase; *TAK1:* TGF-β-activated kinase 1; TGF-β activated kinase; *TβRI*: TGF-β receptor type I; *TβRII*: TGF-β receptor type II.

In canonical TGF-β signalling active TGF-β binds to a complex of two TGF-β receptor type I and two type II transmembrane receptors that possess cytoplasmic serine/threonine kinase domains (Massague 2000). On ligand binding, the type II receptors trans-phosphorylate the Gly-Ser (GS) domain of the type I receptors, which, in turn, phosphorylate carboxy-terminal serine residues of receptor-activated Smads (R-Smads), Smad2 and Smad3 (Bruce

and Sapkota 2012). R-Smads can also be phosphorylated by mediators other than TGF-β1, for example ANGII via MAP kinases, leading to TGF-β1-independent R-Smad signalling (Derynck and Zhang 2003). Once phosphorylated, R-Smads form a complex with Smad4 and enter the nucleus where regulation of transcription of target genes occurs (Shi and Massague 2003; Feng and Derynck 2005; Schmierer and Hill 2007).

In renal fibrosis phosphorylated Smad3 is considered to be pathogenic while Smad2 may be protective (Lan and Chung 2012). Evidence for the pathogenic effects of Smad3 include: 1) TGF-β1/Smad3 signalling targets fibrogenic genes such as COL1A1, COL1A2, COL3A1, COL5A2, COL6A1, COL6A3 and tissue inhibitor of matrix metalloproteinase (TIMP)-1 (Verrecchia, Chu et al. 2001); 2) Smad3 knockout mice show reduced fibrosis in murine models of renal disease (Fujimoto, Maezawa et al. 2003; Sato, Muragaki et al. 2003); and 3) A specific inhibitor of Smad3 reduces renal fibrosis in a mouse model of streptozotocin-induced diabetes (Li, Qu et al. 2010). The role of Smad2 in renal fibrosis requires clarification although there is some evidence to support a renoprotective role as conditional Smad2 knockout mice show increased renal fibrosis following unilateral ureteric obstruction (UUO) (Meng, Huang et al. 2010).

The transcriptional response of cells to TGF-β varies depending on three contextual determinants: 1) The extra- and intra-cellular composition of the TGF-β signal transduction system including concentration and activity of ligands, receptors and regulators; 2) Transcriptional factors, histone readers and modifiers and chromatin remodellers that bind to activated Smad proteins to regulate transcription and determine which genes are targeted; and 3) Epigenetic status of the cell (Massague 2012).

Control of TGF-β/Smad signalling is tightly regulated, occurs at multiple levels and has been found to be disrupted in renal diseases. For example, one of the inhibitory Smads, Smad7, helps maintain TGF-β homeostasis by increasing the degradation of the TGF-β receptor type I and R-Smads

(Kavsak, Rasmussen et al. 2000; Ebisawa, Fukuchi et al. 2001; Lan and Chung 2012) and Smad7 expression is induced by TGF-β1 resulting in a negative feedback mechanism (Afrakhte, Moren et al. 1998). However, in the pathological state of renal fibrosis, there is reduced renal Smad7 protein and increased degradation, which is associated with increased renal fibrosis (Lan 2008; Lan and Chung 2012).

It is now well established that TGF-β1 also signals via non-canonical pathways, which helps to explain the diverse actions of TGF-β1 that cannot be attributed to Smad-dependent signalling (Derynck and Zhang 2003; Zhang 2009; Massague 2012). For example, ligand activation of the TGF-β type II receptor can lead to direct phosphorylation of partitioning defective 6 (PAR6) in cells undergoing EMT (Massague 2012); TGF-β can also modulate TGF-β-activated kinase 1 (TAK1) activity, mitogen-activated protein (MAP) kinases, Rho-like guanosine triphosphatases and the phosphoinositide-3-kinase (PI3K) pathway independently of Smad activation (Funaba, Zimmerman et al. 2002; Derynck and Zhang 2003; Zhang 2009; Choi, Ding et al. 2012; Massague 2012).

In vitro evidence for the importance of non-canonical TGF-β1 signalling in renal fibrosis includes the association of TGF-β1-induced p38 MAP kinase activation and increased Col1a1 in mesangial cells (Chin, Mohsenin et al. 2001) and FN expression in proximal tubular epithelial cells (Niculescu-Duvaz, Phanish et al. 2007) and the association of TGF-β1-induced extracellular signal-regulated kinases (ERK) activation with FN accumulation and collagen mRNA production in mesangial cells (Hayashida, Poncelet et al. 1999; Inoki, Haneda et al. 2000). More recently, TAK1 has been identified as a major upstream molecule in TGF-β1-induced type I collagen and FN expression through activation of the MAP kinases in mesangial cells (Choi, Ding et al. 2012). Furthermore, *In vivo* studies have corroborated the importance of non-canonical TGF-β signalling in renal fibrosis (Choi, Ding et al. 2012). For example, conditional tak1 gene deletion in a mouse UUO model resulted in

suppression of interstitial myofibroblast accumulation, collagen deposition and expression of pro-fibrotic markers (Ma, Tesch et al. 2011).

1.2.3 Role of extracellular matrix (ECM) remodelling

In the normal kidney a balance between matrix production and degradation exists resulting in homeostasis of ECM turnover. The accumulation of ECM proteins, primarily collagens, leads to TIF resulting in loss of kidney function as normal tissue is replaced by scar tissue. Major pathological features of TIF include an increase in the amount of ECM protein usually present in the interstitium such as collagen types I, III, V and VII and FN, as well as those usually absent in normal interstitium such as collagen type IV and laminin (usually found in the tubular basement membrane) (Table 1.1) (Eddy 1996; Norman and Fine 1999).

It is generally accepted that over-production of ECM proteins leads to their accumulation in renal fibrosis however a reduction in matrix degradation can exacerbate the situation. Remodelling of the ECM occurs via two major degradation pathways, the serine protease plasminogen-plasmin system and the matrix metalloproteinases (MMPs). Together these two systems can degrade all components of the ECM.

Table 1.1. ECM proteins that accumulate in TIF (Eddy 1996; Norman and Fine 1999).

Interstitial matrix proteins	Collagens I, III, V, VI, VII, XV Fibronectin Tenascin
Basement membrane proteins	Collagen IV Laminin
Extracellular proteoglycans	Large chondroitin sulfate proteoglycans (aggrecan, versican) Small proteoglycans (decorin, fibromodulin, biglycan, fibromodulin) Basement membrane proteoglycans (heparin sulfate proteoglycan, perlecan)
Polysaccharides and glycoproteins	Hyaluronan Thrombospondin Secreted protein, acidic and rich in cysteine (SPARC) Osteopontin

In the serine protease plasminogen-plasmin system activation of plasminogen to plasmin by tissue-type plasminogen activator (tPA) or urokinase-type plasminogen activator (uPA) leads to proteolysis of matrix proteins including FN, laminin, entactin, tenascin, thrombospondin and perlecan, and also the activation of several MMPs (Eddy 2009). Plasminogen activator inhibitors, of which PAI-1 is the primary physiological inhibitor, regulate this system. PAI-1 has been implicated in the pathogenesis of CKD. It is a 50-kDa glycoprotein that is produced by adipocytes, and by the liver as an acute phase protein. It cannot be detected in normal kidney but is present in almost all human CKD specimens examined (Eddy and Fogo 2006; Eddy 2009) and its expression can be induced in fibroblasts, glomerular cells, tubular epithelial cells and macrophages in response to injury (Eddy 2009). Evidence of a causal role for PAI-1 in renal fibrosis includes: 1) Its non-inhibitory mutant inhibits collagen deposition in anti-Thy1 nephritis (Huang, Haraguchi et al. 2003) and renal fibrosis in experimental diabetic nephropathy (Huang, Border et al. 2008), and its deficiency reduces TIF in UUO (Oda, Jung et al. 2001) and TGF-β1 transgenic mice (Krag, Danielsen et al. 2005); and 2) PAI-1 transgenic mice

develop more fibrosis compared to wild-type in response to UUO injury (Matsuo, Lopez-Guisa et al. 2005).

The mechanisms through which PAI-1 exerts its fibrogenic effects are still not known. While it has been tempting to attribute its pathogenic activity to inhibition of plasminogen activation, studies suggest that this is unlikely to be its sole mechanism of action. In fact plasmin(ogen) and its activators have not been proven to attenuate renal fibrosis and even have pro-fibrotic effects. For example, in mouse models of UUO plasmin(ogen) deficiency reduced fibrosis (Edgtton, Gow et al. 2004; Zhang, Kernan et al. 2007); there was no change in renal fibrosis in uPA-deficient compared to wild-type mice (Yamaguchi, Lopez-Guisa et al. 2007); and tPA-deficient mice developed less severe fibrosis (Yang, Shultz et al. 2002). Potential mechanisms for the pro-fibrotic effects of PAI-1 include cell chemoattraction as higher levels of PAI-1 expression are associated with an increase in renal myofibroblasts and macrophages (Matsuo, Lopez-Guisa et al. 2005). In addition, PAI-1 can also influence integrin-dependent cell adhesion and migration via an interaction with the urokinase receptor and its bound ligand uPA (Zhang and Eddy 2008).

The MMPs make up the other major ECM degradation pathway. They are a family of zinc-dependent endopeptidases classified into six groups based on substrate and sequence homology consisting of the collagenases, gelatinases, stromelysins, matrilysins, membrane-type MMPs and “other MMPs” (Catania, Chen et al. 2007). They have multiple domains including a pro-domain, catalytic domain, hinge region and hemopexin-like domain (Catania, Chen et al. 2007). They are mostly secreted as zymogens (inactive enzyme precursors) and require activation by cleavage of the pro-domain by plasmin or other MMPs (Visse and Nagase 2003). Tissue inhibitors of matrix metalloproteinases (TIMPs), of which there are four members TIMPs-1-4, all have similar structures, which fit into the active site of the MMP catalytic domain to regulate MMP activity (Catania, Chen et al. 2007). Other MMP inhibitors also exist, for example tissue factor pathway inhibitor-2 (Herman, Sukhova et al. 2001).

Renal expression of the MMPs and TIMPs is complex, likely to be species dependent and their localisation in the kidney has not been fully characterised. MMPs -2, -3, -9, -13, -14, -24, -25, -27 and -28 and TIMPs -1, -2 and -3 have all been identified in renal tissue and in addition MMP-7 has been found in pathophysiological states (Catania, Chen et al. 2007). MMPs -2 and -9 (the gelatinases) cleave denatured collagens, laminin and some chemokines; MMP-3 (stromelysin) can degrade a variety of substrates including collagens, FN, laminin, gelatin and casein; MMP-13 (collagenase) cleaves collagen types I, II and III; MMPs -14, -24 and -25 are membrane-type MMPs; and the other MMPs are difficult to classify as they do not easily fit into the above categories. As well as targeting and degrading ECM proteins, MMPs can cleave non-ECM substrates including cell adhesion molecules, growth factors and growth factor receptors and can also activate each other, increasing the complexity of their actions in fibrosis (Somerville, Oblander et al. 2003).

MMP expression and activity are altered in a variety of renal disease states however changes can be variable depending on the renal disease model studied (Figure 1.2) (Catania, Chen et al. 2007). For example, in the UUO model in rabbits and rats an early increase in MMP-2 expression and activity (Sharma, Mauer et al. 1995; Iimura, Takahashi et al. 2004) and decreased MMP-1 and -9 expression (Iimura, Takahashi et al. 2004) have been documented as well as an increase in TIMP expression (Sharma, Mauer et al. 1995; Iimura, Takahashi et al. 2004). Other experimental models including a rat model of UUO and transgenic rats with renin-dependent hypertension mirror these findings of increased MMP-2 expression, reduced MMP-9 expression and increased TIMP-1 (Duymelinck, Dauwe et al. 2000; Bolbrinker, Markovic et al. 2006). However, levels of cortical MMP-2 and -9 are increased and activity of medullary MMP-7 and -9 increased in spontaneously hypertensive rats (Camp, Smiley et al. 2003) and in a rat model of diabetic nephropathy MMP-2 and -9 were down-regulated (McLennan, Kelly et al. 2002). Studies of human tissue have also shown increased TIMP-1 and -2 expression in glomerulosclerosis, increased TIMP-1

in the urine of CKD patients and increased MMP-2 but decreased MMP-9 levels in the plasma of CKD patients (Carome, Striker et al. 1993; Horstrup, Gehrmann et al. 2002; Chang, Yang et al. 2006).

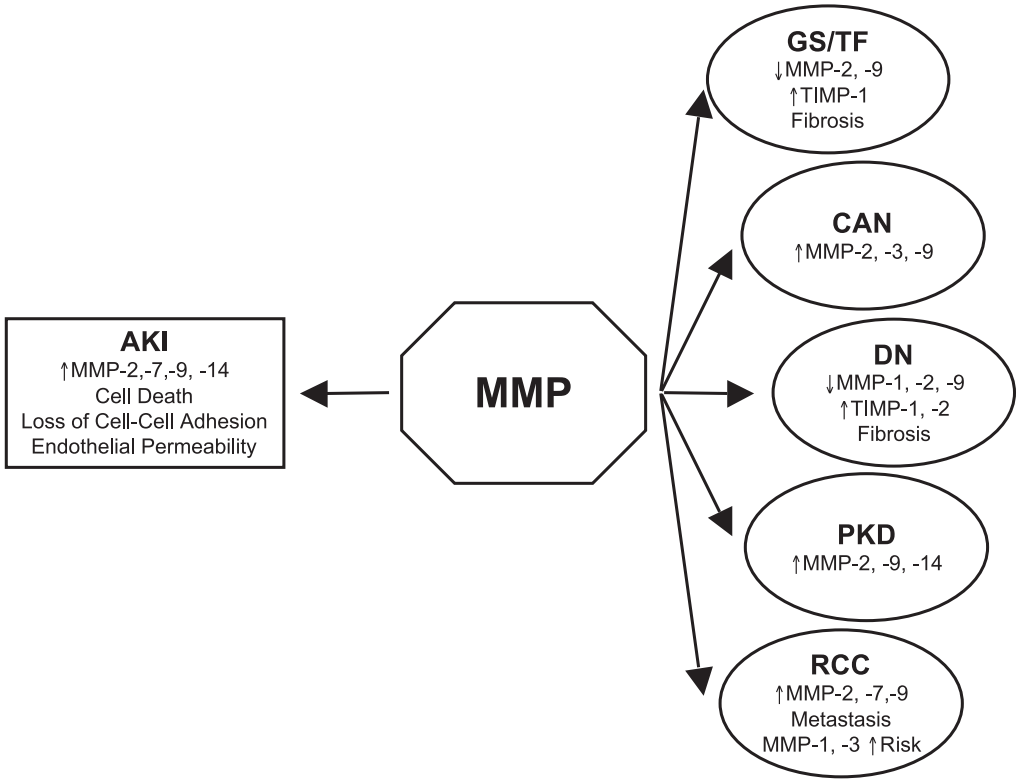

Figure 1.2. Changes in expression and activity of MMPs and TIMPs in acute and chronic renal diseases (Catania, Chen et al. 2007). *AKI:* acute kidney injury; *CAN:* chronic allograft nephropathy; *DN:* diabetic nephropathy; *GS/TF:* glomerulosclerosis/tubulointerstitial fibrosis; *PKD:* polycystic kidney disease; *RCC:* renal cell carcinoma.

TGF-β1 has been found to modulate MMPs in a variety of renal cell types although there are few reports of renal fibroblasts to date. For example, in TGF-β1-stimulated murine podocytes there was an increase in MMP-2 and -9 (Martin, Steadman et al. 1998; Asanuma, Shirato et al. 2002) and in TGF-β1-stimulated tubular epithelial cells MMP-2 expression was increased (Phanish, Wahab et al. 2006). However in mesangial cells TGF-β1 reduced MMP-2 activation (Baricos, Cortez et al. 1999; Singh, Song et al. 2001).

Due to their ability to degrade ECM proteins MMPs have been implicated as potential anti-fibrotic targets. However MMP knockout mice including those of MMP-2 and MMP-9 do not have a spontaneously fibrotic phenotype (Lelongt and Ronco 2002; Ronco and Chatziantoniou 2008; Rojiani, Alidina et al. 2010) and transgenic mice that over-express MMP-2 in renal proximal tubular cells develop tubular atrophy, glomerulosclerosis and TIF (Cheng, Pollock et al. 2006). Conversely, increasing MMP-2 activity was protective against fibrosis in rat models of diabetic nephropathy (Sun, Wang et al. 2006; Mankhey, Wells et al. 2007). The diverse effects of MMPs on fibrosis might be partly explained by their additional activities other than on matrix proteins. For example, MMP-2 accelerates macrophage infiltration following UUO possibly by degrading ECM components (Nishida, Okumura et al. 2007), is capable of inducing EMT in renal tubular cells *in vitro* and mediates EMT in a paracrine manner by activating TGF-β1 (Cheng and Lovett 2003). MMP-9 has been found to activate TGF-β (Ronco, Lelongt et al. 2007).

In addition to reduced matrix degradation, accelerated collagen deposition and matrix stabilisation may contribute to ECM accumulation (Fisher, Jones et al. 2009). Transglutaminase 2 (TG2) is an 80-kDa, calcium-dependent enzyme that catalyses an acyl-transfer reaction between the γ-carboxamide group of peptide-bound glutamine and the ε-amino group of peptide-bound lysine leading to a stable and proteolytic-resistant covalent dipeptide bond within a single peptide or between peptides. Cytosolic TG2 is unique amongst its family members in that a small proportion is secreted by cells. On release, TG2 is activated by the high calcium and low guanosine triphosphate (GTP) concentration in the interstitial space causing ε-(γ-glutamyl) lysine cross-linking of ECM proteins making them harder to degrade and increasing the rate of soluble collagen deposition (Fisher, Jones et al. 2009). Substrates for TG2 include FN, collagens, fibrinogen, oseopontin, laminin and nidogen (Mosher 1984; Martinez, Rich et al. 1989; Aeschlimann and Paulsson 1991; Kleman, Aeschlimann et al. 1995; Kaartinen, Pirhonen et al. 1999). TG2 can also activate TGF-β1 (Nunes, Gleizes et al. 1997; Annes, Munger et al. 2003; Shweke, Boulos et al. 2008) and TGF-β1 increases TG2 mRNA (Douthwaite,

Johnson et al. 1999). In addition, TG2 also plays diverse roles in cell signalling, cell adhesion, cell migration, cell-matrix interactions, cell death, apoptosis and autophagy (Nakaoka, Perez et al. 1994; Jones, Nicholas et al. 1997; Verderio, Nicholas et al. 1998; Oliverio, Amendola et al. 1999; Akimov and Belkin 2001; D'Eletto, Farrace et al. 2009; Rossin, D'Eletto et al. 2011).

Because of its ability to accelerate collagen deposition and stabilise matrix, TG2 has been identified as a possible target for renal fibrosis. Evidence that TG2 is involved in renal fibrogenesis includes that ε-(γ-glutamyl) lysine cross-links and TG2 expression are increased in numerous experimental models of renal disease including the streptozotocin-induced model of type 1 diabetes with (Huang, Haylor et al. 2009) and without uninephrectomy (Skill, Griffin et al. 2001) and the subtotal nephrectomy model (SNx) (Johnson, Skill et al. 1999) as well as in human diabetic nephropathy (El Nahas, Abo-Zenah et al. 2004) and a variety of other human CKD specimens (Johnson, El-Koraie et al. 2003). Furthermore, evidence supporting that TG2 is pathogenic and targeting TG2 improves renal outcome include the reduction of glucose-induced ECM accumulation in proximal tubular epithelial cells by TG inhibition (Skill, Johnson et al. 2004), the reduction in total and fibrillar collagen in TG2 knockout mice subjected to UUO (Shweke, Boulos et al. 2008) and the preservation of kidney function and amelioration of histological changes by an irreversible TG2 inhibitor in an animal model of diabetic nephropathy (Huang, Haylor et al. 2009) and the SNx model (Johnson, Fisher et al. 2007).

TG2 is also up-regulated in liver disease and fibrosis. However, following carbon tetrachloride-induced liver injury in wild-type and TG2 knockout mice, mice lacking TG2 failed to clear hepatic necrotic tissue, demonstrated increased ECM accumulation and inflammatory cells and had a 60% mortality compared to no deaths in the wild-type group (Nardacci, Lo Iacono et al. 2003). The same group found elevated levels of TG2 in the livers of HCV-infected patients during the initial stages of liver fibrosis but levels had decreased in the more advance stages leading them to hypothesise a protective role for TG2 (Nardacci, Lo Iacono et al. 2003). More recent studies

have shown that TG2 expression and activity, although increased in liver fibrosis, does not appear to contribute to stabilisation of collagen matrix or fibrogenesis (Popov, Sverdlov et al. 2011).

1.3 Retinoids

1.3.1 Vitamin A metabolism

Retinoids are a group of compounds related to vitamin A (retinol). They exert a wide range of biological effects on embryogenesis, tissue homeostasis, cell differentiation, proliferation and apoptosis. Retinoids can be classified into three groups: retinoic acid (RA) precursors (including retinol), naturally-occurring RAs (including tRA) and synthetic retinoids (Xu, Lucio-Cazana et al. 2004). Humans cannot synthesise retinoids and must gain their required daily intake from the diet as RA precursors that are subsequently converted to RA so that they may exert the majority of their biological effects. Figure 1.3 illustrates the molecular structures of some well-studied, naturally-occurring retinoids and demonstrates that they are small, lipophilic molecules with a basic structure consisting of a cyclic end group, polyene side chain and polar end group.

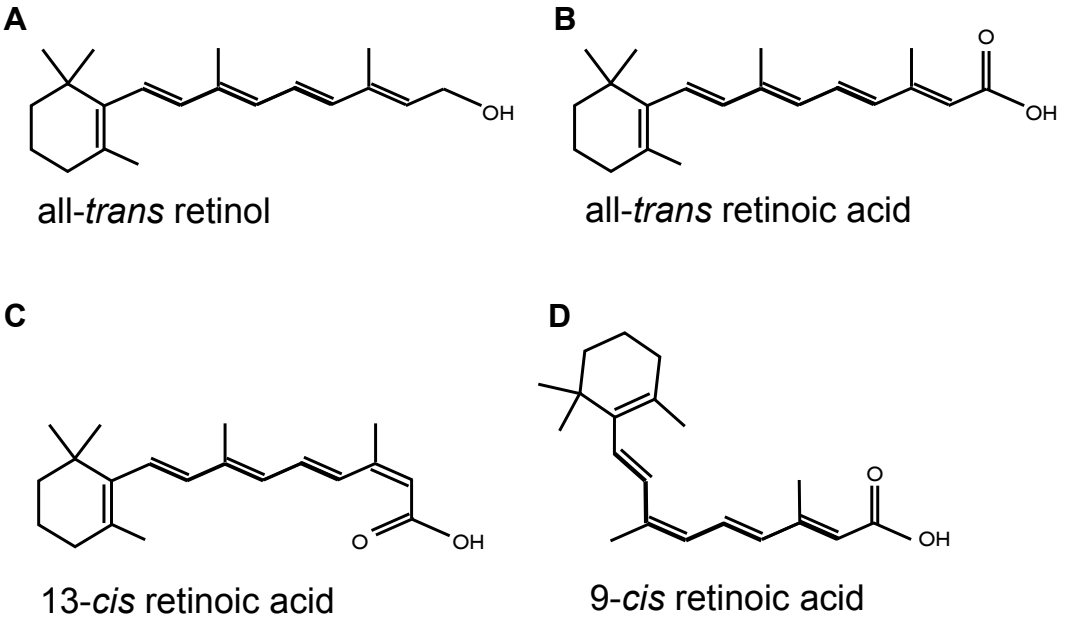

Figure 1.3. Molecular structure of retinoids. A- all-*trans* retinol; **B**- all-*trans* retinoic acid; **C**- 13-*cis* retinoic acid; and **D**- 9-*cis* retinoic acid.

Figure 1.4 demonstrates the pathway through which retinol is converted to RA and its subsequent metabolism in cells. Following absorption in the intestine and modification in hepatocytes, retinol (predominantly all-*trans* retinol) enters the circulation, transported in plasma in a one-to-one complex with retinol binding protein (RBP), thereby reducing its rate of metabolism (Theodosiou, Laudet et al. 2010; D'Ambrosio, Clugston et al. 2011) and to transthyretin (TTR), reducing the renal elimination of RBP (Blomhoff and Blomhoff 2006). Plasma levels of retinol:RBP are maintained at a steady state of approximately 2 µM while other retinoids including tRA and 13-*cis* RA (13cRA) are detectable only at around 5-10 nM bound to albumin (Blomhoff and Blomhoff 2006; Theodosiou, Laudet et al. 2010). Retinyl esters (most commonly retinyl palmitate) are also present in plasma, transported directly from the intestine to target tissues as chylomicron remnants (Theodosiou, Laudet et al. 2010). Retinyl esters and retinol:RBP, via the RBP receptor “stimulated by retinoic acid gene 6” (STRA6) (Kawaguchi, Yu et al. 2007), enter RA target cells where retinol can be stored as retinyl esters following esterification by microsomal lecithin:retinol acyltransferase (LRAT), or be converted to RA. The fatty acid binding proteins cellular retinol binding protein (CRBP) I, CRBPII and CRBPIII bind intracellular retinol and retinal and are thought to play roles in the uptake of retinol into cells, determination of intracellular retinol levels, facilitation of retinol esterification and protection of retinol from metabolism (Napoli 1999; Napoli 2000; Theodosiou, Laudet et al. 2010; Napoli 2012).

Retinol is converted to its active form in two steps. Firstly, it is reversibly oxidised to retinal by microsomal short-chain dehydrogenases/reductases (SDRs) with retinol dehydrogenase activity or by cytosolic alcohol dehydrogenases (ADHs) (Pares, Farres et al. 2008). Retinal then undergoes irreversible oxidation to the active RA, a reaction catalysed by retinaldehyde dehydrogenases (RALDHs) (Napoli 1999).

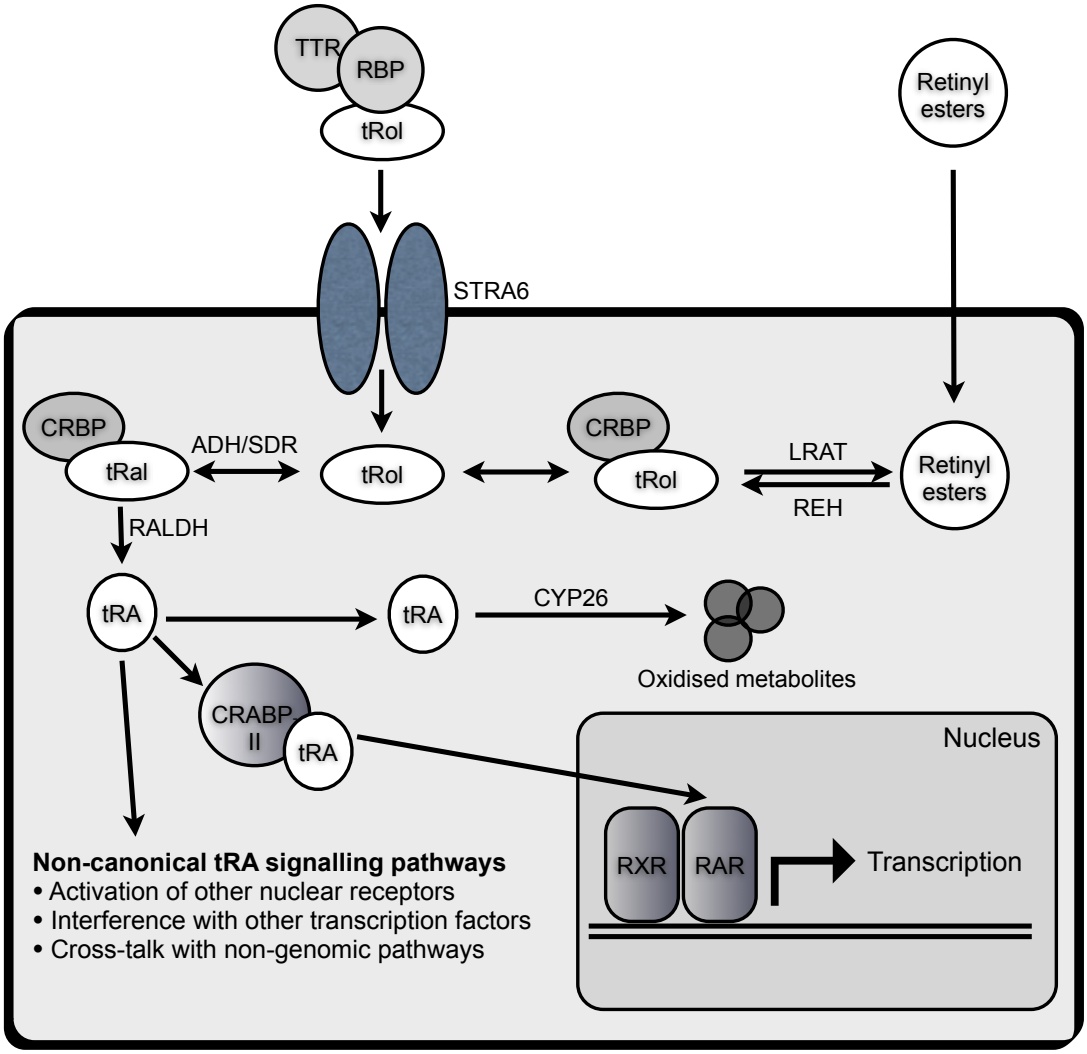

Figure 1.4. Metabolism of all-*trans* retinol to tRA in cells (adapted from Theodosiou, Laudet et al. 2010; D'Ambrosio, Clugston et al. 2011). *ADH:* alcohol dehydrogenase; *CRABP-II:* cellular retinoic acid binding protein-II; *CRBP:* cellular retinol binding protein; *CYP26:* cytochrome P450 family 26; *FABP5:* fatty acid binding protein 5; *LRAT:* lecithin:retinol acetyltransferase; *PPAR:* peroxisome proliferator activated receptor β/δ; *RALDH:* retinaldehyde dehydrogenases; *RAR:* retinoic acid receptor; *RBP:* retinol binding protein; *REH:* retinyl ester hydrolase; *RXR:* rexinoid receptor; *SDR:* short-chain dehydrogenase/ reductase; *STRA6:* stimulated by retinoic acid gene 6; *tRA:* all-*trans* retinoic acid; *tRal:* all-*trans* retinal; *tRol:* all-*trans* retinol; *TTR:* transthyretin.

Of the naturally-occurring biologically active RAs, tRA is the most abundant in mammalian embryos (Satre, Ugen et al. 1992; Scott, Walter et al. 1994; Horton and Maden 1995). Other endogenous retinoids reported to have biological activity include 9cRA, 13cRA, 11-*cis* retinaldehyde, 3,4-didehydro RA, 4-oxo RA and 4-oxo-retinol (Buck, Derguini et al. 1991; Achkar, Derguini

et al. 1996; Napoli 1996; Blaner 2001). While tRA can undergo isomerisation to 9cRA (Levin, Sturzenbecker et al. 1992; Blaner 2001) and 13cRA (Cullum and Zile 1985), isomerisation products of tRA have not been consistently detected in mammalian cells and their biological significance remains unclear (Germain, Chambon et al. 2006; Theodosiou, Laudet et al. 2010). Furthermore, while 13cRA is detectable in nature it does not have potent gene regulatory activity but undergoes isomerisation to the biologically active tRA and 9cRA, which may account for at least some of its physiological activity (Blaner 2001). Since tRA is the predominant endogenous, biologically active retinoid it is currently considered the most important (Germain, Chambon et al. 2006).

Once synthesised, active RA binds with high affinity to cytosolic cellular RA binding protein (CRABP)-I or CRABP-II. Although the distinct roles of the two CRABP isoforms have not been fully elucidated, it is proposed that they protect RA and aid its transport within the cell (Dong, Ruuska et al. 1999). In addition, CRABP-I may influence the metabolic fate of RA by increasing its degradation or sequestering RA (Boylan and Gudas 1991; Boylan and Gudas 1992). In adults, the widespread expression of CRABP-I and the more limited expression of CRABP-II implies a more specialised function for CRABP-II (Dong, Ruuska et al. 1999). Specifically, CRABP-II also appears to play a role in delivering RA to RA receptors (RARs) (Dong, Ruuska et al. 1999). Binding of RA to CRABP-II results in its translocation from cytosol to nucleus where RA is directly delivered by CRABP-II to RARs (Dong, Ruuska et al. 1999).

The cytosolic fatty acid binding protein 5 (FABP5) has also been postulated to bind RA then translocate to the nucleus to deliver RA directly to another nuclear receptor, peroxisome proliferator-activated receptor (PPAR) β/δ (Tan, Shaw et al. 2002; Schug, Berry et al. 2007). However this proposed RA signalling pathway is controversial as other groups have not been able to confirm tRA-induced PPARβ/δ activation in cells (Borland, Foreman et al. 2008; Rieck, Meissner et al. 2008) even with high intracellular FABP5 and PPARβ/δ expression (Borland, Khozoie et al. 2011).

Catabolism of RA into polar metabolites for excretion is controlled by the cytochrome P450 family 26 (CYP26) family of enzymes and is thought to be initiated by hydroxylation of the C4 or C18 position of the β-ionone ring of RA (Theodosiou, Laudet et al. 2010).

1.3.2 Canonical retinoic acid (RA) signalling pathway

Classical RA signalling occurs through retinoid nuclear receptors which function as transcriptional regulators. There are two classes of retinoid nuclear receptor, the retinoic acid receptors (RARs) and the retinoid X receptors (RXRs). RARs bind tRA and 9cRA whereas RXRs bind 9cRA but not tRA. Both RARs and RXRs consist of three isotypes, α, β and γ (Chambon 1996). RARα and RARγ have two isoforms (α1-2 and γ1-2) and RARβ has five isoforms (β1-5) (Leroy, Krust et al. 1991; Zelent, Mendelsohn et al. 1991; Peng, Maruo et al. 2004; Germain, Chambon et al. 2006). The RXR isotypes also have several isoforms, RXRα1-4, RXRβ1-4 and RXRγ1-2 (Lefebvre, Benomar et al. 2010). RAR and RXR isotypes are encoded by separate genes with the isoforms generated by differential promoter usage and alternative splicing (Chambon 1996; Pfahl and Chytil 1996).

RARs have a modular structure consisting of six well-defined regions designated A to F (Figure 1.5), with RXRs lacking the F region (Rochette-Egly and Germain 2009). The C and E regions contain a DNA-binding domain (DBD) and a ligand-binding domain (LBD), respectively, and are the most conserved and considered the most important regions with respect to canonical retinoid receptor signalling (Rochette-Egly and Germain 2009). The DBD confers sequence-specific DNA recognition and has a dimerisation interface; the LBD is complex and contains a ligand-binding pocket, a dimerisation interface and the ligand-dependent activation function (AF)-2 (Mader, Chen et al. 1993; Perlmann, Umesono et al. 1996; Laudet and Gronemeyer 2002). Regions A and B contain the N-terminal domain (NTD) which includes the AF-1 and region B is proline-rich with multiple phosphorylation sites; region D is poorly conserved and is thought to act as a hinge between the DBD and LBD; and the function of region F is still unknown

although it too has multiple phosphorylation sites that might alter RAR function (Rochette-Egly and Germain 2009).

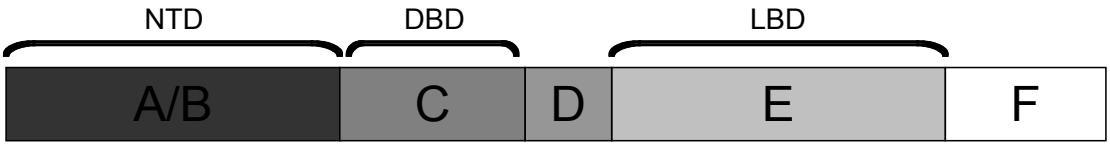

Figure 1.5. Schematic diagram of the functional domains of RARs (adapted from Rochette-Egly and Germain 2009). RARs consist of six regions, A to F, with regions C and E the most conserved. Regions A and B correspond to the N-terminal domain (NTD) that contains a proline-rich motif with phosphorylation sites for kinases; region C corresponds to the DNA-binding domain (DBD); and region E corresponds to the ligand-binding domain (LBD) which also contains the AF-2 domain, a dimerisation domain and phosphorylation sites for several kinases.

Retinoid nuclear receptors function as dimers with RXRs binding to RARs and RXRs (Yu, Delsert et al. 1991; Leid, Kastner et al. 1992; Germain, Chambon et al. 2006). RXRs also dimerise with numerous other nuclear receptors including PPARβ/δ, thyroid hormone and vitamin D nuclear receptors (Lefebvre, Benomar et al. 2010).

RXR-RAR heterodimers act as ligand-dependent transcriptional regulators by binding to specific retinoic acid response elements (RAREs) found in the promoter region of retinoid target genes (Germain, Chambon et al. 2006). RAREs are direct repeats (DRs) of polymorphic arrangements of the canonical motif 5'-PuG(G/T)TCA separated by five, two or one nucleotides (DR5, DR2, DR1) (Leid, Kastner et al. 1992; Mangelsdorf and Evans 1995). Heterodimers are organised as 5'-RXR-RAR-3' for DR5 and DR2 conferring activational gene activity but the polarity is reversed in DR1 elements (5'-RAR-RXR-3') leading to repressive activity (Perlmann, Rangarajan et al. 1993; Kurokawa, DiRenzo et al. 1994; Predki, Zamble et al. 1994; Zechel, Shen et al. 1994; Germain, Chambon et al. 2006). The unliganded RXR-RAR heterodimer prevents transcription due to the presence of co-repressors (Glass and Rosenfeld 2000) such as nuclear receptor co-repressor (N-CoR) (Horlein, Naar et al. 1995) and silencing mediator of RA and TR (SMRT)

(Chen and Evans 1995). On ligand binding to RAR the LBD undergoes a conformational change causing the dissociation of co-repressors and association of various co-activator complexes to initiate transcription (Rochette-Egly and Germain 2009). RXR LBD activation alone cannot induce the dissociation of co-repressors and activate transcription, a phenomenon referred to as RXR subordination or silencing (Chambon 2005; Germain, Chambon et al. 2006).

There is evidence to suggest that the RAR and RXR isotypes may have distinct physiological functions in development. For example, RAR isotypes display differential spacio-temporal distribution in mouse embryonal development (Dolle, Ruberte et al. 1990) and isotype-specific RAR knockout mice show differential signs of the vitamin A deficiency (VAD) syndrome as well as other congenital abnormalities (although many of these defects can be rescued with RA treatment suggesting functional redundancy among the RARs) (Germain, Chambon et al. 2006). In addition, different roles for individual RXR-RAR heterodimers have been demonstrated from experiments performed on F9 murine embryonal carcinoma cells. In these cells RXRα-RARγ heterodimers are necessary for growth arrest, visceral endodermal differentiation and primitive endodermal differentiation whereas RXRα-RARα heterodimers are required for parietal endodermal differentiation (Taneja, Rochette-Egly et al. 1997; Germain, Chambon et al. 2006).

In contrast, knowledge of the pathophysiological roles of the individual receptor isotypes post-natally and in adulthood is lacking due, in part, to functional redundancies observed between the RARs and the early mortality of various combinations of retinoid receptor null mutants from germline mutations (Germain, Chambon et al. 2006).

1.3.3 Non-canonical retinoid signalling pathways

The classical ligand-activated RXR-RAR/RARE pathway is well established as essential for RA signal transduction however it is becoming more apparent that retinoids also exert their effects via other, non-canonical pathways. For example, RA can bind to and activate other nuclear receptors than retinoid receptors such as retinoic acid receptor-related orphan receptor β (ROR-β) and the chicken ovalbumin upstream promoter-transcription 2 (COUP-TFII), although the relevance of these receptors in RA signalling *in vivo* is not yet clear (Stehlin-Gaon, Willmann et al. 2003; Kruse, Suino-Powell et al. 2008).

RA has also been found to bind and activate PPARβ/δ with nanomolar affinity and in so doing can activate the RXR-PPARβ/δ/peroxisome proliferator response element (PPRE) pathway (Shaw, Elholm et al. 2003; Berry and Noy 2007). This alternative signalling pathway of RA was shown to be important in studies of the RA-resistant mouse model of breast cancer, *MMTV-neu* (Schug, Berry et al. 2008). In this model RA preferentially activates PPARβ/δ rather than RAR due to a high FABP5:CRABP-II ratio diverting RA to PPARβ/δ (Schug, Berry et al. 2008). However if this ratio of FABP5 to CRABP-II is reduced, thus diverting RA back to RAR, suppression of tumour growth in this previously RA-resistant cancer model occurred (Schug, Berry et al. 2008).

Retinoids and/or their receptors may also interfere indirectly with transcriptional events. A well-established effect of RARs is the repression of activating protein-1 (AP-1) activation via ligand-dependent and ligand-independent mechanisms. Potential models for this repression include suppression of c-Fos and c-Jun expression, a direct interaction with Jun/Fos, disruption of Jun/Fos dimerisation and inhibition of c-Jun N-terminal kinase (JNK) (Fanjul, Dawson et al. 1994; Moreno-Manzano, Ishikawa et al. 1999; Konta, Xu et al. 2001; Rochette-Egly and Germain 2009). RA, via its retinoid nuclear receptors, can also interfere with nuclear factor kappa-light-chain-enhancer of activated B-cells (NFκB) signalling partly via a direct interaction and also competitive recruitment of transcription integrators between NFκB

and RXR (Na, Kang et al. 1999; Austenaa, Carlsen et al. 2004; Austenaa, Carlsen et al. 2009).

In addition retinoids can exert effects via non-genomic pathways. For example, RA rapidly activates MAP kinases subsequent to the activation of upstream kinases including phosphoinositide 3-kinase (PI3K) and protein kinase C δ (PKCδ) via retinoid receptor-dependent and independent pathways (Kambhampati, Li et al. 2003; Ochoa, Torrecillas et al. 2003; del Rincon, Guo et al. 2004; Pan, Kao et al. 2005; Bastien, Plassat et al. 2006; Masia, Alvarez et al. 2007). In line with this concept RARs have been identified not only in the nucleus but also in the cytosol and membranes of cells (Dey, De et al. 2007; Masia, Alvarez et al. 2007; Rochette-Egly and Germain 2009). RARα has also been purported to have a non-genomic role as an RNA-binding protein: Unliganded RARα interacts directly with mRNA in neurones resulting in repression of translation but on RA-binding the association of RARα with mRNA is reduced relieving translational repression (Chen, Onisko et al. 2008).

1.3.4 Role of retinoids in proliferation, differentiation and inflammation

The importance of a fully functioning retinoid signalling system has long been acknowledged in embryonic growth and patterning and much is now understood about the role of retinoids in embryogenesis (Niederreither and Dolle 2008). Likewise, the importance of retinoids, and, in particular, retinal, in the visual cycle is well recognised (Palczewski 2010). The role of retinoids post-natally however is less well understood. Vitamin A deficiency increases the risk of infection, nephrolithiasis, and growth retardation whereas an excess can lead to toxicity of multiple organs including liver and central nervous system (Theodosiou, Laudet et al. 2010). However, since this thesis explores the effects of pharmacological doses of exogenous retinoids on renal fibrosis, the following section will focus on the effects of exogenous retinoids on cell proliferation, differentiation and inflammation, as these processes are relevant to post-natal pathological disease states including kidney diseases and renal fibrosis.

Retinoids are known to be anti-proliferative, exerting their effects via different mechanisms including interference with cell cycle progression and apoptosis. RA inhibits cell cycle progression by blocking the G1 phase of the cell cycle with an increase in the proportion of cells in the G0/G1 phase and a decrease of those in the S phase (Mongan and Gudas 2007). They are known to modulate cyclins and cyclin-dependent kinases (CDKs) through a variety of mechanisms including changes in mRNA and protein expression (Ma, Feng et al. 2005) and they increase the expression and post-translational stability of CDK inhibitors (Tang and Gudas 2011). RARβ2 has been implicated as the predominant retinoid receptor mediating the inhibitory effects of RA on the cell cycle by targeting genes that mediate tRA-induced cell growth inhibition, for example the cell-cycle inhibitors $p21^{CIP1}$ (Suzui, Shimizu et al. 2004) and $p27^{KIP1}$ (Li, Faria et al. 2004).

Retinoids also induce apoptosis in different cancer cells however the processes through which they exert this effect are not fully elucidated and are likely to depend on cell type and environment (Tang and Gudas 2011). For example, RARα, RARβ and RARγ signalling pathways have all been identified as important in different situations (Hatoum, El-Sabban et al. 2001; Chikamori, Hill et al. 2006; Altucci, Leibowitz et al. 2007; Chen, Zhang et al. 2007; Luo, Lin et al. 2009). Conversely, retinoids are also anti-apoptotic in a variety of cell types and conditions via negative regulation of the AP-1 pathway (Moreno-Manzano, Ishikawa et al. 1999). Both nuclear receptor-dependent and independent mechanisms are important for this anti-apoptotic effect of retinoids (Konta, Xu et al. 2001).

In addition, retinoids can induce cell differentiation in various normal and cancer cells including breast, melanoma, neuroblastoma, squamous, osteosarcoma and F9 cells (Beere and Hickman 1993; Taneja, Rochette-Egly et al. 1997; Luo, Yang et al. 2010) with retinoid-suppressed phosphorylation of RARα being postulated as a potential mechanism of action (Luo, Yang et al. 2010).

Retinoids also play a major role in immune modulation and inflammation. Vitamin A deficiency (VAD) is known to have profound effects on the host defence against infection. RA has been implicated in regulation of thymic proliferation and selection processes, T-cell differentiation and behaviour and RA can determine the balance of Th1/Th2-type T cells and Th-17 cells (Mora, Iwata et al. 2008; Pino-Lagos, Benson et al. 2008). RA is known to modulate antigen presentation by altering dendritic cell function (Mora, Iwata et al. 2008; Pino-Lagos, Benson et al. 2008) and it exerts direct and indirect effects on B cell isotype switching and antibody production (Gudas, Sporn et al. 1994; Pino-Lagos, Benson et al. 2008). The anti-inflammatory effects of retinoids occur via a variety of different mechanisms including modulation of inflammatory cytokines and receptor expression as well as leukocyte behaviour. For example, tRA prevents tumour necrosis factor α (TNFα)-induced vascular cell adhesion molecule (VCAM)-1 expression and VCAM-1-dependent T-cell binding to TNFα-treated human dermal microvascular endothelial cells via effects of tRA on the activation of NFκB-dependent complex formation (Gille, Paxton et al. 1997); retinoids modulate trans-epidermal migration of polymorphonuclear leukocytes following epicutaneous challenge with leukotriene-B4 (Wozel, Chang et al. 1991); 9cRA reduces monocyte adhesion to foetal calf serum (FCS)-stimulated human mesangial cells (HMCs) (Manzano, Munoz et al. 2000); tRA inhibits constitutive expression of monocyte chemoattractant protein-1 in rat mesangial cells (RMCs) in a retinoid receptor-dependent manner (Lucio-Cazana, Nakayama et al. 2001); and tRA increases the expression of cyclooxygenases 1 and 2 and prostaglandin E_2 production in HMCs (Alique, Moreno et al. 2006) and RMCs (Alique, Lucio-Cazana et al. 2007).

The diverse effects of retinoids on cell cycle progression, programmed cell death, cytodifferentiation, immunity and inflammation have led to retinoid-based therapeutic strategies for the treatment of a variety of disease states. Furthermore, clinical trials of the effects of retinoids in a variety of disease states are currently being conducted including in a variety of cancers and autoimmune diseases.

In oncology, retinoid-induced cytodifferentiation forms the basis of treatment in acute promyelocytic leukaemia (APL). In most APL sufferers the RARα gene is rearranged and fused to the promyelocytic leukaemia (PML) gene creating a PML/RARα fusion protein. This causes a stoichiometric increase in the levels of histone deacetylases and associated DNA methyltransferase complexes resulting in silencing of retinoid-regulated genes including important regulators of myeloid differentiation (Villa, Morey et al. 2006). Pharmacological doses of tRA reduce the promoter occupancy of this fusion protein allowing transcription of previously silenced genes (Morey, Brenner et al. 2008). Tazarotene, a retinoid with RARβ and RARγ specificity, has been identified as a potential treatment for basal cell carcinomas and bexarotene, an RXR agonist, is used in the treatment of cutaneous T cell lymphomas. In dermatology, tazarotene is successfully used for plaque psoriasis and 13cRA is used for cystic acne vulgaris (Theodosiou, Laudet et al. 2010). Finally, tRA has been successfully used to improve clinical symptoms and laboratory parameters in a case series of patients with steroid-refractory lupus nephritis (Kinoshita and Funauchi 2012).

1.3.5 Effects of retinoids in non-renal fibrosis

The effects of retinoids in fibrosis have been explored in numerous fibrotic diseases including skin, liver and lung fibrosis. In the 1970s-1980s retinoids were trialled in two cutaneous disorders characterised by excessive deposition of collagen, namely keloid scars and hypertrophic scars. Topical RA treatment successfully reduced scar size in patients suffering these conditions (Janssen de Limpens 1980; Panabiere-Castaings 1988). Other reports however opposed this view of retinoids as anti-scarring agents as they were shown to enhance keloid formation in patients receiving dermabrasion (Rubenstein, Roenigk et al. 1986).

Reports in the literature of the effects of retinoids in liver fibrosis are also conflicting. Some evidence suggests that VAD can damage the liver as adult Wistar rats fed a diet deficient in vitamin A for 3 months expressed increased hepatic α-SMA in sinusoidal cells and there was an increase in FN, laminin

and collagen type IV in hepatic extracts (Aguilar, Genta et al. 2009). Furthermore, RA supplementation in liver disease can protect against liver fibrosis. For example, tRA-treated mice with CCl_4-induced liver fibrosis showed reduced fibrosis, attenuation of the increase in α2(I) collagen mRNA (Wang, Potter et al. 2007) and survival was also improved (Hisamori, Tabata et al. 2008); in a rat model of liver fibrosis induced by common bile duct ligation tRA reduced fibrosis and decreased the increase in collagen type I (Wang, Dan et al. 2008). Other reports, however, suggest that retinoids could aggravate fibrosis in an already damaged liver. For example, in the CCl_4 rat model high dietary uptake of retinoids acted as an accelerator of fibrotic liver disease (Vollmar, Heckmann et al. 2002) and, in liver fibrosis induced by peritoneal injections of porcine serum, polyprenoic acid facilitated liver fibrosis (Numaguchi, Okuno et al. 1994). In humans there is also evidence that retinoid treatment may be detrimental to the liver. In a group of 18 patients receiving long-term etretinate for psoriasis two suffered mild periportal fibrosis, one suffered chronic active hepatitis and one was diagnosed with cirrhosis (Camuto, Shupack et al. 1987).

In models of pulmonary fibrosis studies have suggested that retinoids have an anti-fibrotic effect. For example, tRA decreased fibrosis and α-SMA expression in a model of oxygen-induced lung injury in the newborn rat (Ozer, Kumral et al. 2005) and in a mouse model of bleomycin-induced pulmonary fibrosis tRA ameliorated fibrosis (Tabata, Kadokawa et al. 2006).

1.3.6 Effects of retinoids in renal fibrosis

The role of exogenous retinoids in renal fibrosis also remains unknown as, although the majority of published reports suggest that they have anti-fibrotic potential, a few studies also show a pro-fibrotic effect of retinoids on kidney scarring. Table 1.2 summarises the effects of different retinoids on renal fibrosis in various experimental renal disease models. Examples of the pro-fibrotic effect of retinoids include: 1) In the SNx model, a model considered to represent CKD in humans, while low-dose 13cRA was renoprotective, high-dose 13cRA caused an increase in glomerular sclerosis index in both sham

Table 1.2. Effects of retinoids on fibrosis in *in vivo* models of renal disease. *IM:* intramuscular; *IP:* intraperitoneal; *IV:* intravenous; *PO:* per os; *SC:* subcutaneous.

Model	Anti-fibrotic	Pro-fibrotic	Type and dose of retinoid	References
Pyelonephritis Wistar rats	✔		Vitamin A 60 kIU IM/IV/PO	(Kavukcu, Soylu et al. 1999)
Lupus nephritis NZB/W F1 mice	✔		tRA 0.5 mg IP thrice per week	(Kinoshita, Yoo et al. 2003)
Acute renal allograft rejection Fisher rat kidney grafted to Lewis rats	✔		13cRA 2 mg/kg/day PO 20 mg/kg/day PO	(Kiss, Adams et al. 2003)
Chronic allograft nephropathy Fisher rat kidney grafted to Lewis rats	✔		13cRA 2 mg/kg/day PO 20 mg/kg/day PO	(Adams, Kiss et al. 2005)
Anti-glomerular basement membrane glomerulonephritis Wistar and Lewis rats	✔	✔	tRA 5 mg/kg/day PO 30 mg/kg/day PO	(Datta, Reddy et al. 2001; Oseto, Moriyama et al. 2003)
Puromycin-induced nephrosis; Wistar rats	✔		tRA 10 mg/kg/day PO	(Moreno-Manzano, Mampaso et al. 2003)
acute anti-Thy1.1 mesangioproliferative nephritis in Wistar rats	✔		tRA 10 mg/kg/day SC 13cRA 40 mg/kg/day SC	(Wagner, Dechow et al. 2000; Morath, Dechow et al. 2001)
chronic anti-Thy1.1 mesangioproliferative nephritis in Wistar rats	✔		13cRA 2 mg/kg/day PO 10 mg/kg/day PO	(Schaier, Lehrke et al. 2001)
Subtotal nephrectomy in Sprague-Dawley rats	✔	✔	13cRA 10 mg/kg/day PO 40 mg/kg/day PO	(Morath, Ratzlaff et al. 2009)
UUO Wistar rats and C57BL/B6 mice	✔		13cRA 5 mg/kg/day SC 25 mg/kg/day SC tRA 20 mg/kg/day IP 15 mg/day PO	(Schaier, Jocks et al. 2003; Kishimoto, Kinoshita et al. 2011; Zhou, Qin et al. 2012)
Alb/TGF-β1 transgenic mice		✔	tRA SC 6-10.7 mg/kg/day 12.7-18.8 mg/kg/day 20.1-27.4 mg/kg/day	(Xu, Hendry et al. 2010)
Age-related renal disease in Fisher 344 rats	✔		tRA 1 mg/kg/day PO	(Moreno-Manzano, Rodriguez-Puyol et al. 1997)

and SNx groups as well as an increase in collagen IV staining and an increase in the interstitial area (Morath, Ratzlaff et al. 2009); and 2) In the kidneys of Alb/TGF-β1 transgenic mice, a model that over-expresses active TGF-β1 leading to progressive renal fibrosis, medium- and high-dose tRA exacerbated fibrosis and increased mortality although low-dose tRA did not alter the severity of renal fibrosis (Xu, Hendry et al. 2010). These two studies, in particular, highlight three important questions that remain unanswered: 1) Do different retinoids play different roles in renal fibrosis; 2) What is the optimal therapeutic dose of RA to avoid toxic effects; and 3) How are the activities of retinoids affected by experimental model used?

1.3.7 *In vivo* evidence of possible mechanisms for the effects of retinoids in renal fibrosis

The endogenous retinoid signalling system is disrupted in kidney diseases. Reduced levels of endogenous kidney RA occur in renal disease models, such as in Alb/TGF-β1 transgenic mice (Xu, Hendry et al. 2010), diabetic nephropathy (Starkey, Zhao et al. 2010) and anti-Thy1.1 nephritis (Liebler, Uberschar et al. 2004). In addition, changes in the expression of endogenous retinoid signalling molecules also occur. For example, in the acute anti-Thy1.1 nephritis model, there was time-dependent activation of the retinoid system with reduced mRNA expression of RXRα, RARβ and RARγ, retinol dehydrogenase 1 and 2 and RALDHs 1 and 2 on day 3 but an increase of RXRα, RARα, RARβ and RARγ as well as RARα protein on day 7 (Liebler, Uberschar et al. 2004); In the chronic anti-Thy1.1 glomerulonephritis model there was significantly greater RARα and RXRα mRNA expression compared to control animals and RARγ expression was decreased (Schaier, Liebler et al. 2004).

Interventional studies using retinoid receptor agonists suggest that, not only does retinoid nuclear receptor expression alter in renal disease, but retinoid receptor activation modulates fibrosis. The RAR and RXR agonists, Ro-137410 and Ro-257386, respectively, were found to reduce glomerular damage, procollagen I and FN I mRNAs and FN I protein in the acute anti-

Thy1.1 nephritis model (Lehrke, Schaier et al. 2002) and the RARα- and RXR-specific agonists, AGN195183 and AGN194204, respectively, reduced renal injury with a reduction in mesangial matrix expansion, glomerular sclerosis index and tubulointerstitial area in the chronic anti-Thy1.1 glomerulonephritis model (Schaier, Liebler et al. 2004).

These results demonstrate that the endogenous renal retinoid signalling system is altered in renal disease and suggest that it is at least partly via retinoid nuclear receptor signalling that modulation of renal fibrosis by retinoids occurs.

There are multiple potential targets for retinoids in renal fibrosis and one such target had been identified as TGF-β1. In the acute anti-Thy1.1 nephritis model, tRA was found to reduce urinary TGF-β1 excretion and lower glomerular TGF-β1 and TGF receptor type II protein; furthermore, tRA and 13cRA were found to attenuate the increase in cortical TGF-β1 and TGF-β receptor type II gene expression (Morath, Dechow et al. 2001). In the rat UUO model, 13cRA reduced the increases in TGF-β1 and TGF-β receptor type II mRNAs (Schaier, Jocks et al. 2003) and in the mouse UUO model the increase of TGF-β1 mRNA and protein was attenuated by prophylactic and therapeutic administration of tRA (Kishimoto, Kinoshita et al. 2011). The reduction in TGF-β1 expression by retinoids could in part be nuclear receptor-dependent as both RARα and RXR agonists (AGN195183 and AGN194204) exerted similar effects in the chronic anti-Thy1.1 glomerulonephritis model (Schaier, Liebler et al. 2004). Although infiltrating macrophages produce significant amounts of TGF-β1 therefore the reduction in TGF-β1 could be attributed to an anti-inflammatory effect of RA, Morath et al. showed that glomerular cells were a significant source of TGF-β1 and could be a target for RA treatment (Morath, Dechow et al. 2001).

There are also reports of retinoid-induced increases in TGF-β1 expression although this pro-fibrotic effect of retinoids is less well documented.

Glomerular TGF-β1 protein levels were increased by tRA treatment in experimental anti-GBM antibody-mediated glomerulonephritis (Datta, Reddy et al. 2001) and, in the SNx model, TGF-β1 gene and protein levels were increased by high-dose 13cRA associated with an increased glomerular sclerosis index, interstitial area and collagen IV staining (Morath, Ratzlaff et al. 2009).

Matrix degradation systems also appear to be targets for retinoids in *in vivo* renal disease models although again the mechanisms through which they exert their effects remain unclear. In a rat model of glomerulosclerosis induced by uninephrectomy and an injection of adriamycin, tRA reduced TIMP-1 mRNA and protein expression and enhanced MMP-2 and MMP-9 expression and activity associated with a reduction in collagen IV and fibronectin (Qin, Lei et al. 2009; Zhou, Qin et al. 2011). In the 5/6 nephrectomy rat model, tRA reduced the increase in PAI-1 observed associated with a reduction in αSMA, and this effect was independent of plasmin (Liu, Lu et al. 2011).

1.3.8 *In vitro* evidence of possible mechanisms for the effects of retinoids in renal fibrosis

Further insights into possible mechanisms underlying the effects of retinoids on fibrosis are available from cell models although, unfortunately, there are few *in vitro* renal cell models to refer to. Other *in vitro* models, however, suggest possible pathways through which RA might exert its effects in TIF, which are summarised in Table 1.3.

Firstly, the canonical retinoid signalling system has been shown to directly interfere with ECM production. For example, the mouse α2(I) collagen promoter has at least two RAREs (Perez, Shull et al. 1992) and tRA-induced suppression of α2(I) collagen in rat HSCs has been shown to be mediated by RARβ and RXRα via one or more RAREs (Wang, Tankersley et al. 2002; Wang, Tankersley et al. 2004). Another example is laminin B1: Its promoter

Table 1.3. Possible effects of retinoids on molecular markers of fibrosis in cellular models.

In vitro model	Effect of retinoid	Proposed mechanism of action	Possible effect on fibrosis	References
Rat hepatic stellate cells (HSCs)	Suppression of α2(I) collagen (tRA)	RARβ/ RXRα/ RARE-driven	Anti-fibrotic	Wang, Tankersley et al. 2002; Wang, Tankersley et al. 2004
Mouse F9 teratocarcinoma stem cells	Increased laminin B1 (tRA)	RARE-driven	Pro-fibrotic	Vasios, Gold et al. 1989
Mouse embryonal fibroblasts (MEFs)	Increased CTGF	RARE-driven	Pro-fibrotic	Brigstock 2003; Leask and Abraham 2003
HepG2 human hepatocellular cell line	Suppression of TGF-β transcription	Retinoid receptor-dependent antagonism of AP-1 activity	Anti-fibrotic	Salbert, Fanjul et al. 1993; Blomhoff 1997
HL-60 human promyelocytic leukaemia (APL) cells, rat vascular smooth muscle cells (VSMCs)	Increased TGF-β1 expression (tRA and 13cRA)	Increased TGF-β1 transcription	Pro-fibrotic	Falk, De Benedetti et al. 1991; Morath, Ratzlaff et al. 2009
Bovine endothelial cells, rat HSCs	Increased TGF-β1 activation (retinol and 9cRA)	Increase in plasminogen activator and plasmin	Pro-fibrotic	Kojima and Rifkin 1993; Okuno, Moriwaki et al. 1997
HL-60 cells	Reduced TGF-β-induced differentiation to monocytes (tRA)	RARα-dependent phosphatases that limit R-Smad phosporylation	Anti-fibrotic	Cao, Flanders et al. 2003
Human lung fibroblasts (WI-26)	Reduced Smad3/4-driven transcription	Direct interaction between RARs and Smad3	Anti-fibrotic	Pendaries, Verrecchia et al. 2003
NIH3T3 mouse embryo fibroblast cells	Increase in phosphorylated Smad2/3 compared to TGF-β treatment alone (bexarotene)	Direct interaction between RXRα and Smad2	Pro-fibrotic	Hoover, Burton et al. 2008
Human glomerular mesangial cells	Suppression of TGF-β1-induced αSMA, FN and PAI-1 (9cRA)	Induction of HGF mRNA and protein	Anti-fibrotic	Wen, Li et al. 2005
NB4 (APL) cell line	Increased Smad4 protein (tRA)	Decreased microRNA-146a	Pro-fibrotic	Zhong, Wang et al. 2010
Human VSMCs	increased PAI-1 mRNA (tRA and 9cRA)	Increased PAI-1 transcription via tyrosine kinases	Pro-fibrotic	Watanabe, Kanai et al. 2002
Keloid derived fibroblasts	suppression of MMP-13 (tRA)	Modulation of transcription	Pro-fibrotic	Uchida, Yoshimura et al.2003
CV-1 monkey kidney fibroblast cell line	Increased TG2 transcription	RARE-driven	Pro-fibrotic	Nagy, Saydak et al. 1996

also contains an RARE and RA-induced transcription results in a pro-fibrotic effect (Vasios, Gold et al. 1989).

Secondly, retinoids can interfere indirectly with ECM production via cross-talk with the TGF-β signalling system although they have variable and often opposing actions depending on cell type and environment. Evidence for antagonistic effects of retinoids on the TGF-β1 signalling system *in vitro* includes: 1) tRA suppresses production of TGF-β in rat HSCs (Davis, Kramer et al. 1990); 2) RA decreases TGF-β expression in chicken myocytes (Jakowlew, Cubert et al. 1992); 3) tRA reduces TGF-β1 production in irradiated human lung fibroblasts (Tabata, Kadokawa et al. 2006); and 4) Low-dose 13cRA decreases TGF-β1 gene expression in rat vascular smooth muscle cells (VSMCs) (Morath, Ratzlaff et al. 2009). Conversely, evidence for potentiation of the TGF-β signalling system by RA includes: 1) tRA induces TGF-β1 mRNA and protein expression in HL-60 cells (Falk, De Benedetti et al. 1991); 2) RA increases active TGF-β1 in bovine endothelial cells (Kojima and Rifkin 1993); 3) 9cRA increases the secretion and activation of TGF-β in rat HSCs (Okuno, Moriwaki et al. 1997); and 4) High-dose 13cRA increases TGF-β1 mRNAs in rat VSMCs (Morath, Ratzlaff et al. 2009).

The RA and TGF-β1 systems communicate through a variety of different mechanisms both at the transcriptional and post-transcriptional levels. For example, retinoids can inhibit TGF-β1 gene expression through their anti-AP-1 activity as TGF-β1 mRNA expression is largely governed by three AP-1 binding sites located in two promoters of the gene (Salbert, Fanjul et al. 1993; Blomhoff 1997). Retinoids may also interfere indirectly with TGF-β1 expression via cross-talk with the RAAS. tRA can block the ANG II-induced increase in TGF-β1 mRNA in rat VSMCs, the mechanism of which involves retinoid receptor-dependent mechanisms and anti-AP-1 activity. Specifically, there was abrogation of the increase in ANG II-induced c-fos mRNA by tRA and also down-regulation of AT_1 receptor mRNA expression, the promoter of which contains an AP-1 consensus site (Haxsen, Adam-Stitah et al. 2001).

Retinoids can also increase CTGF expression, which in turn promotes TGF-β1 signalling, as there is a conserved DR2 RARE in the CTGF gene of mouse embryonal fibroblasts (MEFs) (Brigstock 2003; Leask and Abraham 2003). Furthermore, RA can modulate TGF-β1 signalling through the serine protease plasminogen-plasmin system. RA has been shown to increase PA leading to an increase in plasmin activity, which in turn can activate latent TGF-β1 (Kojima and Rifkin 1993; Okuno, Moriwaki et al. 1997).

Other postulated mechanisms through which the retinoid signalling system interferes with TGF-β1 signalling include: 1) RAR-dependent phosphatases that limit R-Smad phosphorylation therefore reducing levels of nuclear Smad complexes (Cao, Flanders et al. 2003); 2) Direct interactions of RARs with Smad proteins which, in the absence of agonists, potentiate Smad signalling (Pendaries, Verrecchia et al. 2003); 3) Direct regulation of Smad2 activity by RXRα (Hoover, Burton et al. 2008); 4) Induction of the anti-fibrotic hepatocyte growth factor (HGF) (Wen, Li et al. 2005); and 5) Down-regulation of the Smad4-targeting microRNA-146a by tRA (Zhong, Wang et al. 2010).

Thirdly, retinoids can interfere with fibrosis via modulation of matrix degradation pathways without affecting TGF-β1 activity. For example, tRA can reduce the increase in PAI-1 protein following TGF-β1 treatment in RMCs, which is associated with reduced FN accumulation (Liu, Lu et al. 2008; Liu, Lu et al. 2011). Conversely, tRA and 9cRA induced PAI-1 gene expression in human VSMCs (Watanabe, Kanai et al. 2002). MMP expression and activity is also modulated by retinoids. In human skin fibroblasts, tRA reduced trypsin-activatable collagenase (Oikarinen, Oikarinen et al. 1985), in keloid-derived fibroblasts, tRA suppressed the increase in MMP-13 (Uchida, Yoshimura et al. 2003) and in 3T3 L1 preadipocytes as a model of HSCs, retinoids reduced collagenase activity (Numaguchi, Okuno et al. 1994).

Finally, RA also up-regulates TG2 expression as the TG2 gene promoter possesses an RARE providing a further mechanism for how retinoids interfere with renal fibrosis (Nagy, Saydak et al. 1996; Yan, Noonan et al. 1996).

1.4 Aims and objectives of this project

Despite numerous reports suggesting that retinoids might constitute promising new treatments for kidney diseases, there is growing evidence that they also have a pro-fibrotic potential in certain situations. The mechanisms of the pro-fibrotic effects of retinoids in renal diseases are poorly understood. In this project, the central hypothesis that renal fibroblasts are the target of the net fibrogenic effects of tRA is tested. Further this project aims to elucidate potential mechanisms behind the pro-fibrotic effects of tRA.

More specifically, the objectives of this project are to:

1) Establish the effect of tRA on net fibrogenesis in NRK-49F normal rat kidney fibroblasts in the absence and presence of TGF-β1;
2) Explore the roles of selected fibrotic markers in the effects of tRA on TGF-β1-induced fibrosis in NRK-49F cells;
3) Investigate the roles for retinoid nuclear receptors, tRA carrier proteins and retinoid nuclear receptor-independent pathways in the effects of tRA on TGF-β1-induced fibrosis in NRK-49F cells.

1.5 Experimental design

The normal rat kidney fibroblast cell line “NRK-49F” was used as a cell model for renal interstitial fibrosis. An *in vitro* assay was set up to determine the effects of tRA on total collagen deposition in the absence and presence of TGF-β1 using picro-Sirius red stain. Molecular biology techniques including reverse transcription quantitative polymerase chain reaction (RT-qPCR), Western blot analysis, immunocytochemistry, mass spectrometry, enzyme activity assays and gene silencing techniques were used to explore the contributions of fibrotic markers and retinoid signalling molecules to the effects of tRA on fibrosis in NRK-49F cells. Chemical agonists and antagonists further determined the actions of specific proteins. The effects of tRA on total collagen deposition in human foreskin fibroblasts was also determined.

Chapter 2. Materials and Methods

2.1 Materials

2.1.1 Cell culture

Plasticware: Cell lines and primary cultures were maintained in 75 cm^2 flasks purchased from Greiner Bio-One Ltd (Stonehouse, UK). For use in experiments, cell culture multi-well plates in 6, 12, and 24 well formats and 60 and 100 mm cell culture dishes were purchased from Corning B.V. Life Sciences (Amsterdam, The Netherlands), 35 mm dishes were purchased from Greiner Bio-One Ltd and 96 well collagen type-I coated tissue culture plates were purchased from BD Biosciences (Oxford, UK).

Cell culture medium and supplements: Dulbecco's Modified Eagle Medium (DMEM) high glucose (4.5g/L) with 584 mg/L L-glutamine and 110 mg/L sodium pyruvate, DMEM/Ham's F-12 (DMEM/F12) and RPMI-1640 were purchased from PAA Laboratories GmbH (Pasching, Austria) and supplemented with penicillin/streptomycin x100 (PAA Laboratories GmbH) and Fungizone amphotericin B (Invitrogen, Paisley, UK) to give final concentrations of 100 IU/ml penicillin, 100 µg/ml streptomycin and 0.25 µg/ml Fungizone, unless otherwise stated. Foetal calf serum (FCS; Sigma-Aldrich Company Ltd., Gillingham, UK), BD Nu-Serum culture supplement (BD Biosciences) and insulin-transferrin-sodium selenite Liquid Media Supplement x100 sterile-filtered (ITS; Sigma) were used to supplement culture media as described in methods.

2.1.2 Retinoid preparations and TGF-β1

tRA: tRA with a purity of 98% determined by high performance liquid chromatography (Sigma) was dissolved in 100% ethanol to a stock concentration of 10 mM and stored at -80^{O}C protected from light using aluminium foil. Stock solution was mixed by vortexing, incubated at 37^{O}C for 15 min, then vortexed again before use in experiments.

Other retinoids: AGN194204, AGN193109 (kind gifts from R.A.S. Chandraratna, Irvine, California, USA), HX531 (a kind gift from H. Kagechika, Tokyo, Japan) and CD437, CD2019 and AGN195183 (kind gifts from Dr J. Corcoran, London, UK) were dissolved in DMSO and stored at -80^{O}C; please refer to Table 2.1 and 2.2 for references for these chemicals. (E)-4-[2-(5,6,7,8-tetrahydro-5,5,8,8-tetramethyl-2-naphthalenyl)-1-propenyl] benzoic acid (TTNPB; Enzo Life Sciences, Exeter, UK), >98% purity, was dissolved in 100% ethanol and stored at -80^{O}C. Retinoid preparations were protected from light at all times using aluminium foil. Molecular structures and biological activities of retinoids are shown in Figure 2.1 and Tables 2.1 and 2.2. Binding efficiencies (Kd) were determined by *in vitro* assays and half maximal effective concentrations (EC_{50}) and half maximal inhibitory concentrations (IC_{50}) were determined using functional assays in a cellular context (see references in Tables 2.1 and 2.2 for details).

TGF-β1: Human platelet TGF-β1 (R&D Systems, Abingdon, UK) was reconstituted in a solution of 4 mM hydrochloric acid (HCl; VWR International Ltd, Lutterworth, UK) and 0.1% bovine serum albumin (BSA; PAA Laboratories GmbH) that had been filter-sterilised using a polyethersulfone membrane with 0.2 µm pore size. A stock solution of 10 ng/µl TGF-β1 was stored at -80^{O}C until use.

2.1.3 Other chemical agonists, antagonists and inhibitors

PPARβ/δ agonist GW0742 and PPARβ/δ antagonist GSK0660 (Sigma), both >98% purity by HPLC, TG2 inhibitor 1,3-dimethyl-2[(2-oxo-propyl)thio] imidazolium chloride (NTU283; Zedira, Darmstadt, Germany), >95% purity by HPLC, and PAI-1 inhibitor tiplaxtinin (Axon Medchem, Groningen, The Netherlands), purity 99%, were dissolved in DMSO and stored at -80^{O}C. Molecular structures and biological activities are shown in Figures 2.1 and 2.2 and Tables 2.1, 2.2 and 2.3. Binding efficiencies (Kd) were determined by *in vitro* assays and half maximal effective concentrations (EC_{50}) and half maximal inhibitory concentrations (IC_{50}) were determined using functional assays in a cellular context (see references in Tables 2.1- 2.3 for details).

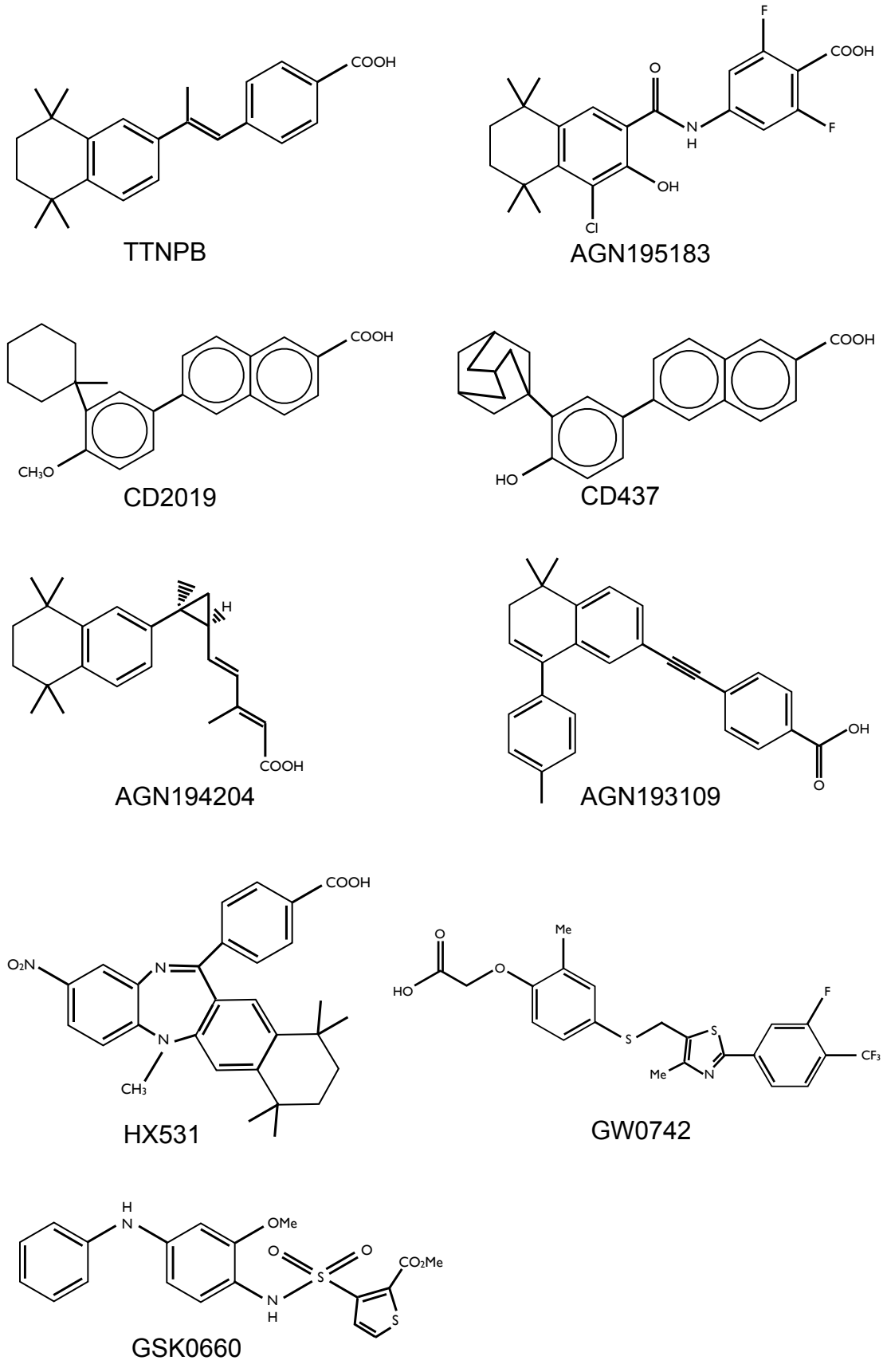

Figure 2.1. Molecular structures of nuclear receptor agonists and antagonists.

Table 2.1. Biological activity of nuclear receptor agonists used in experiments. *EC_{50}* half maximal effective concentration; *Kd* binding efficiency; *NA* not active.

Nuclear receptor agonist	Nuclear receptor target	Kd (nM)	EC_{50} (nM)	References
TTNPB	Pan-RAR agonist	RARα 2.5 RARβ 2.7 RARγ 1.8 RXRs>10000	RARα 10 RARβ 3.5 RARγ 2.5	(Pignatello, Kauffman et al. 1997; Pignatello, Kauffman et al. 1999)
AGN195183	RARα agonist	RARα 3 RARβ $>10^5$ RARγ $>10^5$	RARα 200 RARβ NA RARγ NA	(Allegretto, McClurg et al. 1993; Beard, Duong et al. 2002)
CD2019	RARβ agonist	RARα 920 RARβ 26 RARγ 160	RARα 19.8 RARβ 3.8 RARγ 46.9	(Bernard, Bernardon et al. 1992)
CD437	RARγ agonist	RARα 6500 RARβ 2480 RARγ 77	RARα 140 RARβ 28.4 RARγ 7.3	(Bernard, Bernardon et al. 1992)
AGN194204	Pan-RXR agonist	RARs >30000 RXRα 0.4 RXRβ 3.6 RXRγ 3.8	RARs NA RXRα 0.2 RXRβ 0.8 RXRγ 0.08	(Vuligonda, Thacher et al. 2001)
GW0742	PPARβ/δ agonist	-	PPARα 1100 PPARβ/δ 1 PPARγ 2000	(Sznaidman, Haffner et al. 2003)

Table 2.2. Biological activity of nuclear receptor antagonists used in experiments. *IC_{50}* half maximal inhibitory concentration; *Ki* inhibitor constant.

Nuclear receptor antagonist	Nuclear receptor target	Ki (nM)	IC_{50} (nM)	References
AGN193109	Pan-RAR antagonist	RARα 2 RARβ 2 RARγ 3 RXRs no binding	10	(Agarwal, Chandraratna et al. 1996)
HX531	Pan-RXR antagonist	-	18	(Ebisawa, Umemiya et al. 1999)
GSK0660	PPARβ/δ antagonist	PPARα >10000 PPARβ/δ 155 PPARγ >10000	300	(Shearer, Steger et al. 2008; Naruhn, Toth et al. 2011)

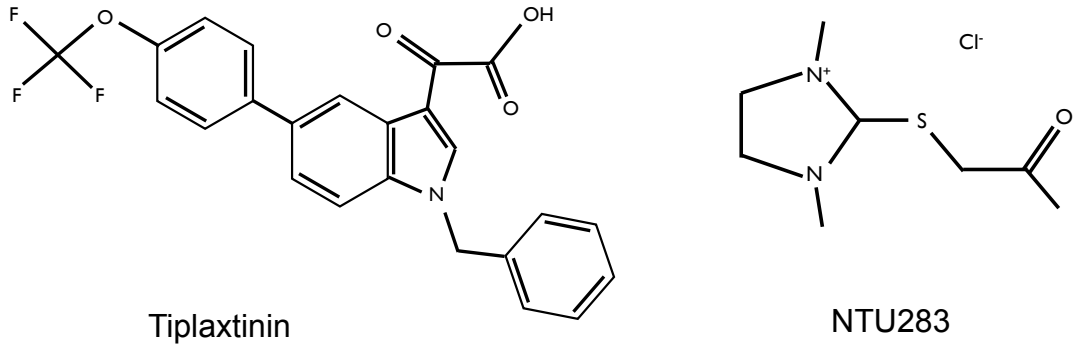

Tiplaxtinin NTU283

Figure 2.2. Molecular structures of tiplaxtinin and NTU283.

Table 2.3. Biological activity of chemical inhibitors used in experiments.

Chemical inhibitor	Target	Ki (nM)	IC_{50} (nM)	References
Tiplaxtinin	PAI-1	480	2700	(Elokdah, Abou-Gharbia et al. 2004)
NTU283	TG2	-	50000	(Skill, Johnson et al. 2004)

2.1.4 Immunocytochemistry and Western blotting

Antibodies: Table 2.4 lists the antibodies used in experiments and their sources. All antibodies were stored according to the recommendations of the supplier.

Positive controls: A-431 nuclear extract (sc-2122), human RXRγ transfected 293T total cell lysate (sc-177886), Sol8 nuclear extract (sc-2157), HeLa nuclear extract (sc-2120) and NIH/3T3 total cell lysate (sc-2210) were purchased from Santa Cruz biotechnology, inc. (Heidelberg, Germany). Rat recombinant TG2 was a kind gift from Dr T. Johnson (Sheffield, UK).

Table 2.4. List of antibodies used in experiments. *BP* blocking peptide; *GAPDH* glyceraldehyde-3-phosphate dehydrogenase; *HRP* horseradish peroxidase; *HSP* heat shock protein.

Antibody	Manufacturer
Anti-E-FABP rabbit polyclonal IgG (H-45, sc-50379) Anti-CRABP-II goat polyclonal IgG and BP (K-13, sc-10065) Anti-RARα rabbit polyclonal IgG and BP (C-20, sc-551) Anti-RARβ rabbit polyclonal IgG and BP (C-19, sc-552) Anti-RARγ mouse monoclonal IgG_{2A} (G-1, sc-7387) Anti-RXRα rabbit polyclonal IgG and BP (D-20, sc-553) Anti-RXRγ rabbit polyclonal IgG and BP (Y-20, sc-555) Anti-PPARβ rabbit polyclonal IgG (H-74, sc-7197) Anti-FN rabbit polyclonal IgG (H-300, sc-9068) Anti-Col4A1/3 goat polyclonal IgG (G-20, sc-9301) Anti-HSP-70 goat polyclonal IgG (K-20, sc-1060) Normal rabbit IgG control IgG (sc-2027) Normal goat IgG control IgG (sc-2028) Normal mouse IgG control IgG (sc-2025) Goat anti-rabbit IgG-HRP conjugated secondary antibody (sc-2004) Bovine anti-goat IgG-HRP conjugated secondary antibody (sc-2378)	Santa Cruz biotechnology, inc. (Heidelberg, Germany)
Anti-vimentin mouse monoclonal IgM (ab20346) Anti-cytokeratin mouse monoclonal IgG_1 (ab49779) Anti-collagen I rabbit polyclonal IgG (ab292) Anti-collagen III rabbit polyclonal IgG (ab7778) Anti-PAI-1 rabbit polyclonal IgG (ab7205) Anti-TG2 mouse monoclonal IgG_1 (ab2386) Anti-RXRβ rabbit polyclonal IgG (ab15032)	Abcam (Cambridge, UK)
Anti-αSMA mouse monoclonal IgG_{2A} (A2547)	Sigma (Gillingham, UK)
Anti-GAPDH mouse monoclonal antibody (MAB374)	Millipore (Durham, UK)
ECL sheep anti-mouse IgG-HRP conjugated secondary antibody (NA931V)	GE Healthcare UK Ltd (Chalfont St Giles, UK)
Alexa Fluor 488 goat anti-rabbit IgG secondary antibody (A11008) Alexa Fluor 555 donkey anti-goat IgG secondary antibody (A21432)	Invitrogen (Paisley, UK)
Anti-TG2 mouse monoclonal antibody IA12	A kind gift from Dr T. Johnson (Sheffield, UK)

2.1.5 Real-time quantitative polymerase chain reaction (qPCR)

Plasticware: RNase-, DNase-, DNA- and pyrogen-free bevelled filter pipette tips were purchased from Starlab (Milton Keynes, UK) and RNase-, DNase-, DNA- and PCR inhibitor-free 1.5 ml microcentrifuge tubes were purchased from Alpha Laboratories (Eastleigh, UK).

Gene expression assays: TaqMan gene expression assays were purchased from Applied Biosystems (Foster City, California, USA). SABiosciences RT^2 qPCR primer assays were purchased from SABiosciences (Frederick, Maryland, USA). Please refer to Table 2.5 for details of assays.

Table 2.5. Gene expression assays used in experiments.

TaqMan gene expression assays	SABiosciences RT^2 qPCR primer assays
Collagen type I alpha1 (col1A1; collagen_A1-I) Collagen type I alpha 2 (col1A2; Rn01638584_m1) Collagen type III alpha 1 (col3A1; Rn01437681_m1) Collagen type IV alpha 1 (col4A1; collagen_A1-IV) Fibronectin (FN; FN1_66s) Serine peptidase inhibitor, clade E, member 1 (PAI-1; Rn01481341_m1) TGF-β1 (Rn00572010_m1) TGF-β2 (Rn00579674_m1) TGF-β3 (Rn00565937_m1) TG2 (Rn01423105_m1) FABP5, epidermal (Rn00821817_g1) CRABP-II (Rn00568361_m1) GAPDH (Rn99999916_s1) 60S ribosomal protein L 13a (Rpl13a; Rn00821946_g1)	RARα (PPR52856A) RARβ (PPR51911A) RARγ (PPR51930A) RXRα (PPR56668B) RXRβ (PPR50385A) RXRγ (PPR49326A) PPARβ/δ (PPR53429A) MMP-2 (PPR43605C) MMP-3 (PPR48487B) MMP-13 (PPR45162A) GAPDH (PPR06557A) β-actin (PPR06570B) Rpl13a (PPR53027A)

Rat ECM and adhesion molecules PCR array: Rat ECM and adhesion molecules PCR arrays were purchased from SABiosciences.

2.2 Buffers and solutions

2.2.1 General solutions

Phosphate buffered saline (PBS): To make 1 L of 10x PBS, 80 g NaCl, 2 g KCl, 14.4 g Na_2PO_4 and 2.4 g KH_2PO_4 (all Sigma) were dissolved in double distilled water (ddH_2O) to a volume of 1 L and pH adjusted to 7.4 using 1 M sodium hydroxide (NaOH; Sigma). For use in experiments 1x PBS was made by adding 100 ml 10x PBS to 900 ml ddH_2O.

Tris-buffered saline (TBS): To make 1 L of 10x TBS, 80 g NaCl, 2 g KCl and 30 g Tris base (Merck, Darmstadt, Germany) were added to ddH_2O to a volume of 1 L and the pH adjusted to 7.4 using 5 M HCl. For use in experiments 1x TBS was made by adding 100 ml 10x TBS to 900 ml ddH_2O.

TBST (0.1%): 1 ml Tween 20 (Sigma) was added to 1 L 1xTBS.

2.2.2 Solutions for the 2 dimensional (2D) *in vitro* model of fibrosis

Picro-Sirius red (PSR) stain (0.1%): Approximately 1.5 g of picric acid (Sigma) was added to 100 ml ddH_2O to make saturated picric acid then 0.1 g of Direct Red 80 (Sigma) was added to make 0.1% PSR.

Acetic acid solution (0.1%): To make 1% stock solution, 5 ml of acetic acid (VWR International Ltd) was added to 500 ml of ddH_2O. Stock solution was further diluted 10x to make 0.1% acetic acid solution.

NaOH solution (0.1M): To make 1 M stock solution, 20 g of NaOH was added to 500 ml ddH_2O. Stock solution was then diluted 10x to make 0.1 M NaOH.

2.2.3 Immunocytochemistry

Paraformaldehyde solution (3.7%): 2 ml of 37% formaldehyde solution (Sigma) was added to 18 ml PBS.

Triton X solution (0.1%): 10 µl Triton X-100 (Sigma) was added to 10 ml PBS.

BSA blocking agent (1%): 0.1 g BSA was added to 10ml PBS.

2.2.4 Protein extraction and Western blotting

PBS-TDS cell lysis buffer: To make 4x stock, 40 ml 10x PBS, 4 ml Triton X-100, 2 g sodium deoxycholate (Sigma) and 0.4 g sodium dodecyl sulphate (SDS; VWR International Ltd) were added to 56 ml ddH_2O. For a working solution of 1x PBS-TDS with protease inhibitors, 5 ml of 4x stock solution was added to 15 ml ddH_2O and 2 µl 5 mg/ml leupeptin, 4 µl 5 mg/ml pepstatin, 40 µl 100 mM phenylmethanesulphonylfluoride (PMSF) and 40 µl 100 mM ethylenediaminetetraacetic acid (EDTA) (all Sigma) were added.

SDS (10%): 10 g SDS was added to 100 ml ddH_2O.

Tris 1.0 M (pH 6.8): 121.14 g Tris base was added to 1 L ddH_2O and the pH adjusted to 6.8.

Tris 1.5 M (pH 8.8): 181.71 g Tris base was added to 1 L ddH_2O and the pH adjusted to 8.8.

Ammonium persulphate (10%): 0.1 g ammonium persulphate (AppliChem UK Ltd, Lancaster, UK) was added to 1 ml of ddH_2O.

Stacking and resolving gels for Tris-glycine SDS-polyacrylamide gel electrophoresis (SDS-PAGE): ddH_2O, 30% acrylamide mix (Sigma), 1.5 M Tris (pH 8.8), 10% SDS, 10% ammonium persulphate and TEMED (Bio-Rad Laboratories, Hemel Hempstead, UK) were mixed in varying proportions to

produce 6-15% resolving gels. Stacking gels (5%) were made as above but using 1.0 M Tris instead of 1.5 M Tris.

Western sample buffer (WSB): To make 10x stock solution, 100 mg SDS and 2 mg bromophenol blue (Sigma) were added to 1 ml 1 M Tris HCl (pH 6.8) and 1 ml glycerol (Invitrogen). Stock solution was filtered using a polyethersulfone membrane with 0.2 µm pore size and stored at -20^{O}C until use.

Electrophoresis buffer: To make 5 L of 4x electrophoresis buffer, 60.4 g Tris base, 288 g glycine (Merck) and 20 g SDS were added to ddH_2O to a volume of 5 L. For use in experiments, 250 ml 4x electrophoresis buffer was added to 750 ml ddH_2O water and stored at 4^{O}C until use.

Towbin transfer buffer: To make 2.5 L of 4 x stock, 30.28 g Tris base and 144 g glycine were added to ddH_2O to a volume of 2.5 L. For use in experiments, 550 ml 4x Towbin transfer buffer and 440 ml methanol were added to 1210 ml ddH_2O and stored at 4^{O}C before use.

Milk blocking solution (5%): 2.5 g non-fat milk was added to 50 ml 0.1% TBST.

Mild stripping buffer: Mild stripping buffer was prepared according to Abcam's protocol:
http://www.abcam.com/ps/pdf/protocols/stripping%20for%20reprobing.pdf.
To make 1 L, 15 g glycine, 1 g SDS and 10 ml Tween 20 were added to ddH_2O to a volume of 1L and the pH adjusted to 2.2.

2.3 Cell culture

Cell cultures were maintained in 75 cm^2 flasks in Jencons Millenium incubators (Leighton Buzzard, UK) under humidified conditions at 37^{O}C and 5% CO_2. For passaging or use in experiments, cells were washed with sterile Dulbecco's PBS (PAA Laboratories GmbH) then trypsinised with 0.05%/ 0.02% trypsin-EDTA (PAA Laboratories GmbH) under humidified conditions at 37^{O}C and 5% CO_2 for 3-5 min. Cells were then resuspended in culture medium supplemented with FCS and counted using a haemocytometer.

2.3.1 NRK-49F cell line

Normal rat kidney fibroblast-like cells (NRK-49F; LGC Standards, Teddington, UK) were chosen as a suitable *in vitro* model for the study of the effects of tRA on renal interstitial fibroblasts. Long-term cell cultures were originally established from kidneys of adult non-inbred Osborne-Mendel rats (Huu, Rosenblum et al. 1966) and consisted of both fibroblastic and epithelioid cells. Subsequently, several independently isolated fibroblastic clones were developed one of which was designated "49F" (de Larco and Todaro 1978). The NRK-49F cell line consists of cells that are morphologically (Figure 2.3) and behaviourally similar to fibroblasts and stain positive for the fibroblast cell marker vimentin and negative for the epithelial cell marker cytokeratin (Figure 2.4). They express αSMA at low levels when quiescent, however αSMA is induced following treatment with TGF-β1 consistent with trans-differentiation of fibroblasts to myofibroblasts (Figure 2.5). NRK-49F cells have been used for operational definition of TGF-β activity (Roberts, Anzano et al. 1985) and as they characteristically respond to TGF-β1 they were selected as an appropriate cell line to study the effects of tRA in an *in vitro* model of fibrosis. Cells were propagated in DMEM supplemented with 5% FCS and subcultured before becoming confluent because of the risk of transformation. Cells between passages 5 to 20 (as they were designated passage 0 on arrival from supplier) were used for experiments.

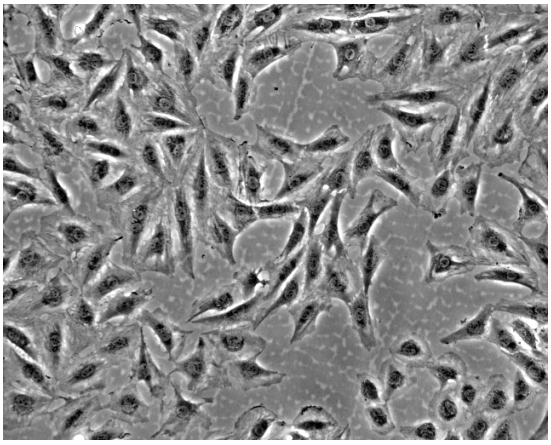

Figure 2.3. NRK-49F cells in culture. (Phase contrast microscopy, x200 magnification).

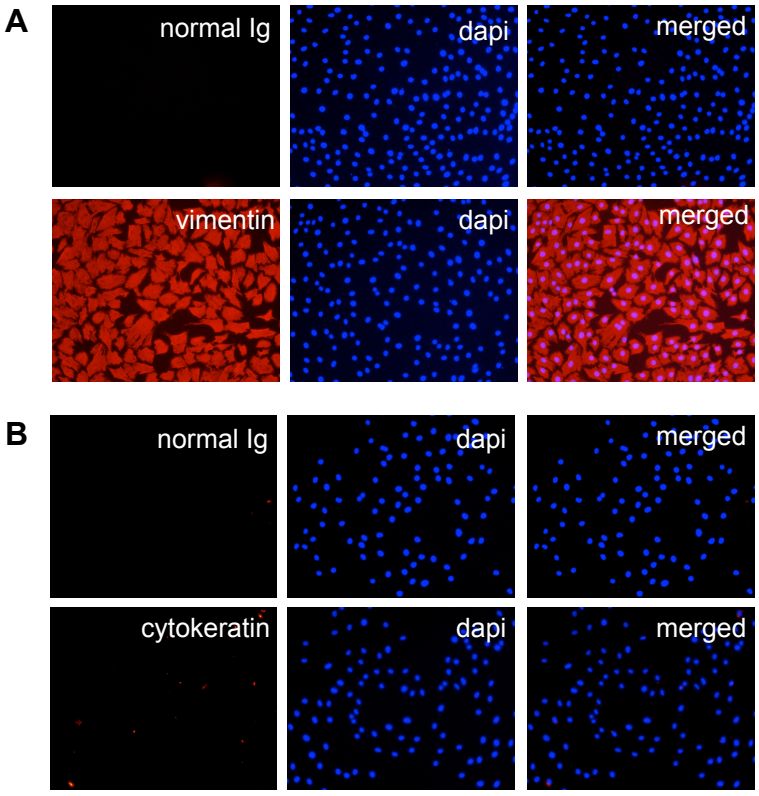

Figure 2.4. Characterisation of NRK-49F cells by immunocytochemistry. NRK-49F cells were seeded in 12 well plates in DMEM supplemented with 5% FCS and incubated overnight. Cells were fixed and permeabilised in 100% methanol at -20^{O}C for 10 min, then washed with PBS and blocked with 1% BSA for 1 h. Cells were then incubated in primary antibody for 1 h at room temperature, washed with PBS then incubated with Alexa Fluor secondary antibody overnight at 4^{O}C followed by further washing then finally counterstained with 4',6-diamidino-2-phenylindole (DAPI). Cells stained positive for vimentin (**A**) and negative for cytokeratin (**B**). (Fluorescence microscopy, x200 magnification).

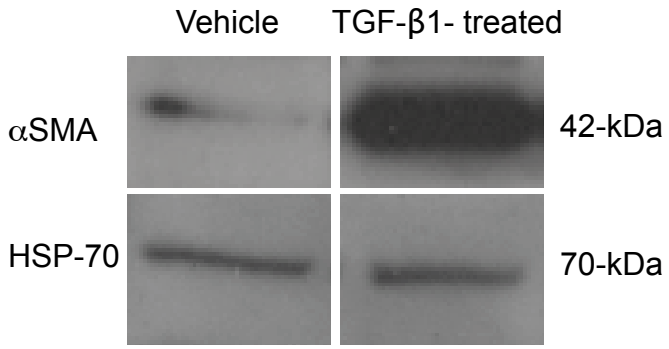

Figure 2.5. αSMA protein expression in NRK-49F cells by Western blot analysis. NRK-49F cells were cultured for 3 d in DMEM supplemented with 2.5% FCS and 2.5% Nu then for 4 d in DMEM supplemented with ITS then treated with 5 ng/ml TGF-β1 or vehicle for 48 h. NRK-49F total cell lysate was extracted and run on a 10% polyacrylamide gel under reducing and denaturing conditions then transferred onto a nitrocellulose membrane. The membrane was blocked with 5% milk and subjected to αSMA immunoblotting. HSP-70 was used as a loading control. The experiment was repeated twice. αSMA protein expression was induced by TGF-β1 treatment. For full protocol of protein extraction and Western blotting please see below.

2.3.2 Other primary cell cultures and cell lines

Human foreskin fibroblasts (a kind gift from Dr C. Yee, Bethesda, Maryland, USA) were maintained in DMEM supplemented with 10% FCS. This primary cell culture showed typical morphological appearances of fibroblasts (Figure 2.6) and stained positive for the (myo)fibroblast markers vimentin and αSMA but negative for the epithelial marker cytokeratin (Figure 2.7). Cells between passages 8-12 were used for experiments.

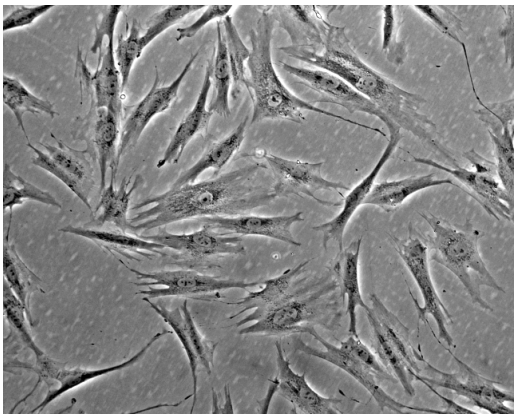

Figure 2.6. Human foreskin fibroblasts in culture. (Phase contrast microscopy, x200 magnification).

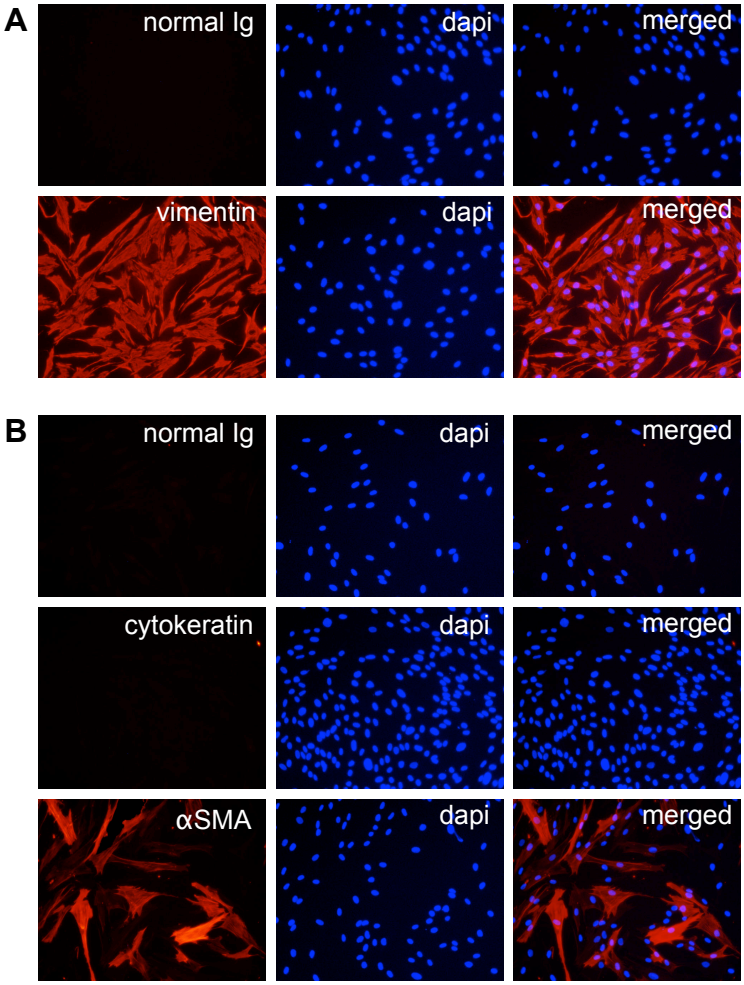

Figure 2.7. Characterisation of human foreskin fibroblasts by immunocytochemistry. Human foreskin fibroblasts were seeded in 12 well plates in DMEM supplemented with 10% FCS and incubated overnight. Cells were then subjected to immunocytochemical analysis as before. Cells stained positive for vimentin and αSMA (**A** and **B**) and negative for cytokeratin (**B**). (Fluorescence microscopy, x200 magnification).

The COS-7 kidney fibroblast cell line (a kind gift from Dr N. Bury, London, UK) was originally derived from the African green monkey and was established by transformation of CV-1 cells by an origin-defective mutant of SV40 which codes for wild type T antigen (Gluzman 1981). This cell line was maintained in DMEM supplemented with 10% FCS. On arrival, COS-7 cells were designated a passage of 1 and cells between passages 2-20 were used for experiments.

Primary rat mesangial cells isolated from the glomeruli of Wistar rats (a kind gift from Prof M. Rodriguez-Puyol, Madrid, Spain) were maintained in RPMI-1640 supplemented with 10% FCS; a primary rat mesangial cell culture isolated from the glomeruli of male Sprague-Dawley rats (Dominion Pharmakine, Bizkaia, Spain) was maintained in DMEM/F12 supplemented with 20% FCS; the SM43 rat mesangial cell line (established by Dr M. Kitamura, London, UK) was maintained in DMEM/F12 supplemented with 10% FCS; and the human mesangial cell line "HMCL" (a kind gift from Dr Xiong Zhong Ruan, London, UK) was maintained in RPMI-1640 supplemented with 5% FCS and ITS.

2.3.3 2D *in vitro* model of fibrosis

The 2D *in vitro* model of TGF-β1-induced fibrosis (Xu, Norman et al. 2007) was used to qualitatively and quantitatively determine the effects of tRA and other retinoids on collagen deposition in cells. This model uses the strong anionic dye PSR to stain and quantify total collagen, a technique that is well documented in other commercially available collagen quantification assays such as the QuickZyme collagen assays (QuickZyme Biosciences, Leiden, The Netherlands) and Sircol soluble collagen assay (Biocolor Ltd, Carrickfergus, UK). PSR consists of the small, anionic picric acid and the large, hydrophobic Sirius Red (Figure 2.8) and binds to collagens via the interaction of its acid sulphonic groups with the basic groups of collagen molecules. As collagen types I, II and III are rich in basic amino acids PSR reacts strongly with these collagens (Junqueira, Bignolas et al. 1979).

NRK-49F cells were seeded at a density of $1x10^4$/well in 96-well collagen type I-coated tissue culture plates in DMEM supplemented with 2.5% FCS and 2.5% Nu for 3 d then DMEM supplemented with ITS for 4 d, as previously defined (Grotendorst, Rahmanie et al. 2004). Cells, with or without 2 h pre-treatment with chemical antagonists/inhibitors, were then treated with retinoids and/or 5 ng/ml TGF-β1 in DMEM supplemented with ITS for a further 48 h protected from light with aluminium foil. Vehicle-treated cells (cells exposed to the same concentration of DMSO or ethanol as treated cells) were

included as controls. Changes in cell morphology were observed and captured by photomicroscopy using a Nikon Eclipse TE2000-S epifluorescence microscope (Nikon Instruments Europe BV, Amstelveen, The Netherlands) and a DXM1200F Nikon digital camera (Nikon UK Limited, Kingston upon Thames, UK). Cell detachment index was also recorded. The cell detachment index was a qualitative method of determining toxicity of treatment with a score of 0 representing no cell detachment and 0.5, 1, 1.5, 2, 2.5, 3 and 3.5 equating to cell detachment of 5%, 10%, 20%, 30%, 40%, 60% and 80%, respectively. A score of 4 corresponded to complete disruption of the cell monolayer. Some caution should be exercised when using this method to determine cytotoxicity as not all detached cells represent non-viable cells. The cells were then fixed with 100% ice-cold methanol overnight at -20^{O}C, rinsed then washed twice for 5 min with PBS before staining with 200 µl 0.1% PSR for ≥ 4 h on a rocking platform at room temperature. Excess PSR was removed by a rinse and two 5 min washes with 0.1% acetic acid after which the acetic acid was discarded and the plate air-dried overnight at room temperature. Cell staining for PSR was observed and captured by photomicroscopy then the PSR eluted with 200 µl 0.1 M sodium hydroxide for ≥ 2 h on a rocking platform at room temperature. Following elution, PSR staining was quantified by spectrophotometric analysis at 540 nm using a spectrophotometer (Dynex Technologies, Worthing, UK). Experiments were repeated at least three times.

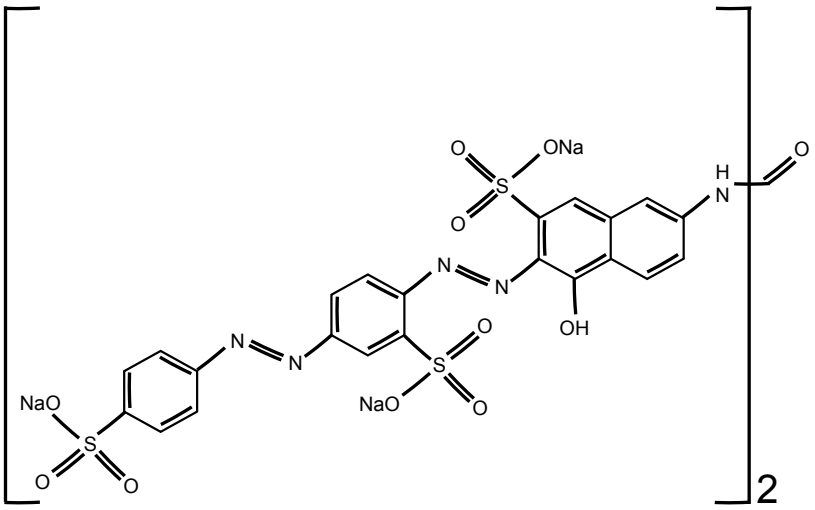

Figure 2.8. Molecular structure of Sirius Red.

2.4 Lactate dehydrogenase cytotoxicity assay

The effects of tRA, TGF-β1 and tiplaxtinin on NRK-49F cell toxicity were further assessed by measuring lactate dehydrogenase (LDH) release from cells using Promega's CytoTox 96® Non-Radioactive Cytotoxicity Assay (Promega, Southampton, UK). LDH is a cytosolic enzyme that converts pyruvate to lactate with the concomitant conversion of NADH to NAD^+ when oxygen is absent or in short supply. LDH is also released from necrotic cells and the amount of LDH present in conditioned medium can therefore be used as a measure of cytotoxicity. Promega's CytoTox 96® Non-Radioactive Cytotoxicity Assay measures LDH in conditioned medium by using a 30 minute coupled enzymatic reaction that results in the conversion of a tetrazolium salt into a red formazan product. This red formazan product can be measured by spectrophotometry with the amount of product being directly proportional to the number of necrotic cells.

NRK-49F cells were seeded in quadruplicate into 96 well collagen type I-coated plates and treated as per the protocol for the 2D *in vitro* model. A control for culture medium background absorbance, a volume correction control, a cell spontaneous LDH release control and a control to determine maximum LDH release from cells were included in the plate set up. Lysis solution at a volume of 20 µl (10 µl per 100 µl) was added to the volume correction control and to control cells for complete lysis and plates incubated under humidified conditions at 37^OC and 5% CO_2 for 45 min. Conditioned media at a volume of 50 µl from control wells and experimental wells were then transferred to 96 well flat bottom enzymatic assay plates (Nunc, Roskilde, Denmark) and an equal volume of substrate mix was added. Plates were incubated at room temperature for 30 min protected from light then 50 µl of stop solution was added to halt the reaction and the absorbance recorded at 490 nm using a spectrophotometer.

Percentage cytotoxicity for the test conditions was calculated as follows:

Maximum LDH release= (cells + lysis solution) - (medium + lysis solution)
Baseline LDH release= (cells alone) - (medium alone)
Test LDH release= (cells in test conditions) - (medium alone)

$$\% \text{ cytotoxicity} = \frac{(\text{test LDH release}) - (\text{baseline LDH release})}{\text{Maximum LDH release}} \times 100$$

% cytotoxicity was presented as an average of quadruplicates and experiments were repeated three times.

2.5 Immunocytochemistry

NRK-49F cells at a density of $3x10^4$ cells/well were seeded in 35 mm cell culture dishes in either DMEM supplemented with 5% FCS for 24 h or, if cells were to be treated with retinoids with and without TGF-β1, they were cultured as per the protocol for the 2D *in vitro* model (see above). Culture medium was then removed and the cells washed with PBS at room temperature before fixing with 3.7% paraformaldehyde on ice for 10 min. Cells were washed thrice with ice-cold PBS, then permeabilised with 0.1% Triton in PBS for 5 min at room temperature then again washed with PBS. Cells were blocked with 1% BSA at room temperature for 1 h followed by incubation in primary antibody or normal Ig (used as a negative control) in PBS for 1 h at room temperature. After further washes with PBS, cells were incubated in a 1 in 1000 dilution of secondary antibody labelled with fluorescent Alexa Fluor 488 or Alexa Fluor 555 fluorescent dyes overnight at $4^{O}C$. Finally cells were again washed thrice with PBS, counterstained with 1 mg/ml 4',6-diamidino-2-phenylindole (DAPI) in PBS at a 1 in 1000 dilution for 5 min followed by further washes then examined using fluorescence photomicroscopy.

2.6 Reverse transcription qPCR

Two-step reverse transcription (RT)-qPCR was used to determine the mRNA expression of retinoid nuclear receptors, PPARβ/δ and two tRA carrier proteins in NRK-49F cells and to investigate the effects of tRA on fibrosis-related genes. Experiments were carried out in an area of the laboratory designated for nucleic acid work and RNase ZAP (Sigma) was used to clean benches and gloves. All pipette tips and plasticware were commercially-purchased free of RNase, DNase, PCR inhibitors and pyrogens. Water used in experiments was either commercially-purchased and free of RNases or had been treated with 0.1% diethylpyrocarbonate (DEPC; Sigma).

2.6.1 RNA extraction

RNA extraction from cells- standard protocol: NRK-49F cells were seeded in 35 mm cell culture dishes at a density of $3x10^4$ cells/dish in DMEM supplemented with 2.5% FCS and 2.5% Nu for 3 d then DMEM supplemented with ITS for 4 d. Cells were then treated with vehicle, 2 μM tRA, 5 ng/ml TGF-β1 or tRA and TGF-β1 at variable time points (Figure 2.9). Total RNA was extracted using Qiagen's RNeasy Mini Kit according to the manufacturer's guidelines (Qiagen, Crawley, UK). Briefly, cell culture medium was removed then the cells lysed directly with Buffer RLT and 1% β-mercaptoethanol. Cell lysate was collected, mixed by pipetting then transferred to a QIA shredder spin column placed in a 2 ml collection tube and centrifuged for 2 min at full speed. An equal volume of 70% ethanol was then added to the homogenised lysate and mixed by pipetting before transferring to an RNeasy spin column placed in a 2 ml collection tube and centrifuged at 21.1 x *g*. The flow-through was discarded and the spin column membrane washed once with 700 μl Buffer RW1 and twice with 500 μl Buffer RPE, discarding the flow-through following centrifugation between each wash. The RNeasy spin column was then transferred to a new 2 ml collection tube and centrifuged at full speed for 1 min to eliminate any carry over of Buffer RPE. Finally, the RNeasy spin column was placed in a 1.5 ml collection tube, 30 μl of RNase-free water directly added to the spin column membrane and the spin column centrifuged

for 1 min at full speed. Purity of the eluted total RNA was confirmed using a Nanodrop ND1000 spectrophotometer (Labtech, Ringmer, UK). Total RNA was stored at -80^{O}C until use. Experiments were repeated three times.

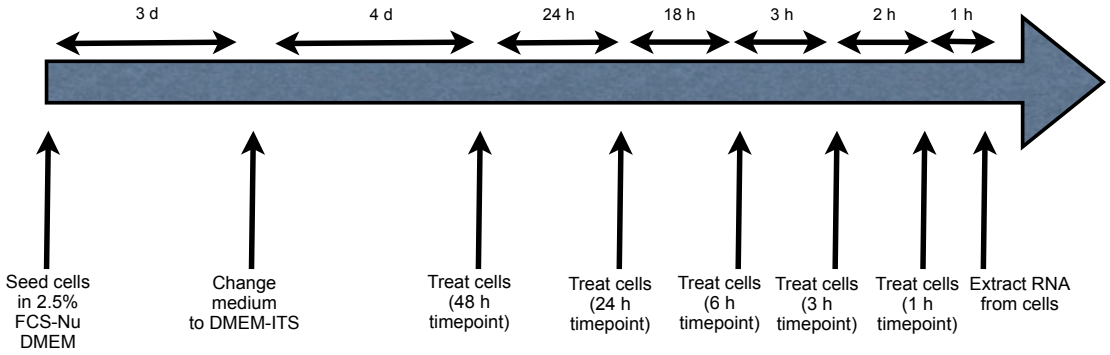

Figure 2.9. Protocol for RNA extraction of NRK-49F cells at different time points. NRK-49F cells were seeded in 35 mm dishes in DMEM supplemented with 2.5% FCS and 2.5% Nu for 3 d then DMEM supplemented with ITS for 4 d. Cells were then treated with 2 μM tRA and/or 5 ng/ml TGF-β1 at different time points. Total RNA was extracted at the end of the experiment.

RNA extraction from small samples of cells (<5x10^{5}): For extraction of total RNA from cells seeded in 96-well plates, the Qiagen RNeasy Micro Kit was used according to manufacturer's guidelines (Qiagen). Briefly, following removal of culture medium and direct cell lysis with Buffer RLT and 1% β-mercaptoethanol, cell lysate was collected in 1.5 ml eppendorf tubes and samples homogenised by vortexing for 1 min. An equal volume of 70% ethanol was then added to the lysates and samples were transferred to an RNeasy MinElute spin column, centrifuged at full speed then washed once with Buffer RW1. On-column DNase digestion was performed by adding DNase I incubation mix directly to the spin column membrane and incubating for 15 min at room temperature. Further washes were performed using Buffer RW1, Buffer RPE and 80% ethanol. The MinElute spin columns were then centrifuged in new 2 ml collection tubes with their lids open at full speed for 5 min to dry the spin columns and remove residual ethanol. Finally, RNA was eluted into 1.5 ml collection tubes by adding 14 μl of RNase-free water directly to the centre of the spin column membrane followed by centrifugation for 1 min at full speed. The purity of the eluted total RNA was confirmed using a Nanodrop ND1000 spectrophotometer and stored at -80^{O}C until use.

2.6.2 Reverse transcription

Total RNA was reverse transcribed into cDNA using the Omniscript Reverse Transcription Kit (Qiagen). Equal amounts of RNA for comparative samples (50 ng-2µg) were diluted in RNase-free water to a total volume of 13 µl then 2 µl each of Buffer RT, deoxyribonucleotide triphosphate (dNTP) mix and oligo-dT primers and 1 µl of Omniscript reverse transcriptase were added to start the reaction. Samples were incubated at 37^{O}C for 60 min then the resulting cDNA diluted with 80 µl water and stored until use at -20^{O}C.

2.6.3 qPCR

Two methodologies were used for the fluorescent identification of PCR product using qPCR based on the availability of pre-designed primers from either Applied Biosystems or SABiosciences:

1) TaqMan chemistry: TaqMan gene expression assays (Applied Biosystems) consist of 2 unlabelled primers for amplification and one 6-FAM-dye-labelled TaqMan probe for detection of the sequence of interest. When intact, the probe has a reporter (6-FAM) dye at its 5' end and a non-fluorescent quencher dye at the 3' end. The proximity of the reporter and quencher dyes results in suppression of the fluorescent signal from the reporter dye by fluorescence resonance energy transfer (FRET) through space. If the target of interest is present in the reaction mix then the forward and reverse primers anneal at the 3' end of the cDNA with the probe annealing between the forward and reverse primer sites. During the reaction DNA polymerase extends the primer sequences and, as it reaches the probe, its 5' nuclease activity cleaves the probe. The reporter is released and separates from the quencher dye resulting in increased fluorescent signal. The increase in fluorescence is used to monitor the accumulation of PCR product. The fluorogenic probes allow the detection of only the target of interest thus increasing the specificity of the reaction. TaqMan Universal 2x PCR Master mix (Applied Biosystems) was used with the 20x TaqMan gene expression assays which were supplied at a concentration of 18 µM for each primer and 5 µM for the probe.

2) SYBR Green chemistry: SABiosciences RT^2 qPCR primer assays consisting of forward and reverse primers use SYBR Green technology to identify PCR product. SYBR Green is a fluorogenic dye that emits little signal in solution but when bound to double-stranded DNA emits a strong signal. Thus, as qPCR product accumulates there is increased binding of SYBR Green dye and increased fluorescent signal allowing quantification of the amplified target sequence. As the SYBR Green dye will detect all double-stranded DNA this methodology is less specific than the TaqMan chemistry and may require optimisation. In addition, if comparison of expression between genes is desirable, then amplicon length between target genes should be considered as a longer amplicon will produce more fluorescent signal if the primer efficiencies are the same. RT^2 SYBR Green/ROX 2x qPCR Master Mix (SABiosciences) was used with the RT^2 qPCR primer assays which were supplied at a concentration of 10 µM.

To prepare the reactions, gene expression assay, qPCR Master Mix and RNase-free water, in the proportions shown in Table 2.6, were mixed in a 1.5 ml micro-centrifuge tube then transferred to a 384-well optical plate before adding cDNA. Each reaction was repeated in triplicate and no template controls (NTCs) were included in plate set up. Plates were sealed with optical adhesive film, centrifuged and run on an ABI7900HT PCR system using Sequence Detection Systems (SDS) 2.2 software (Applied Biosystems), which was programmed to run for 40 cycles. Each cycle consisted of denaturation of cDNA for 15 sec at $95^{O}C$ then annealing and extension for 1 min at $60^{O}C$. A melting curve program was also included in the cycling when SYBR Green technology was used to identify any primer-dimer or non-specific products in the reaction.

The cycle number at which the amount of amplified target reached a fixed threshold (Ct) was used to calculate relative changes in gene expression using the $2^{e-\Delta\Delta Ct}$ method (relative quantification) (Livak and Schmittgen 2001). This method involves normalisation of the gene of interest (GOI) to an endogenous control or housekeeping gene (HKG) (ΔCt= GOI Ct - HKG Ct)

then comparing the normalised vehicle-treated sample to the normalised treated sample (ΔΔCt= ΔCt of treated sample - ΔCt of vehicle-treated sample). Finally, the relative expression was determined by the formula $2^{-\Delta\Delta Ct}$, which represents the fold change in gene expression normalised to an endogenous reference gene and relative to the untreated control sample.

Table 2.6. Reactions prepared for TaqMan and SYBR Green qPCR 384 plate formats.

	TaqMan technology	**SYBR Green technology**
Gene expression assay (µl)	0.875	0.5
qPCR Master Mix (µl)	6.25	5
Water (µl)	2.875	3.5
cDNA (µl)	2.5	1
Total volume	**12.5**	**10**

2.6.4 Optimisation of qPCR

Identification of suitable HKGs: HKGs are genes that are constitutively expressed at relatively constant levels in cells and are often used as endogenous controls because their expression does not alter across experimental conditions. The HKGs GAPDH, β-actin and RPL13a were chosen for further investigation as suitable endogenous controls in NRK-49F cells. Therefore, their mRNA expression was determined at 0, 1, 3, 6, 24 and 48 h following treatment of cells with 2 µM tRA and/or 5 ng/ml TGF-β1, as per protocol. Fold change mRNA expression compared to the 0 h time point was determined by taking the difference between the 0 h sample and other time points (ΔCt) then calculating $2^{-\Delta Ct}$ (Figure 2.10-2.12).

There was a significant up-regulation of β-actin mRNA at 24 h following tRA, TGF-β1 and dual treatment with tRA and TGF-β1 ($p<0.001$), which was also present at 48 h following tRA treatment ($p<0.05$) and at 6 h and 48 h following TGF-β1 treatment ($p<0.01$) (Figure 2.11). β-actin was therefore eliminated as a suitable endogenous control. mRNA expression of Gapdh and Rpl13a was also modulated by treatment, albeit less so than for β-actin, with significant

increases in Gapdh mRNA expression at 24 h following tRA ($p<0.05$) and TGF-β1 treatment ($p<0.01$) (Figure 2.10) and significant decreases in Rpl13a mRNA expression at 1 and 3 h following dual treatment ($p<0.05$ and $p<0.01$, respectively) (Figure 2.12). Gapdh and Rpl13a were thus identified as more suitable HKGs for use as endogenous controls and Gapdh was ultimately chosen for use in experiments although data generated at the 24 h time point, which showed statistically significant changes, were interpreted with caution.

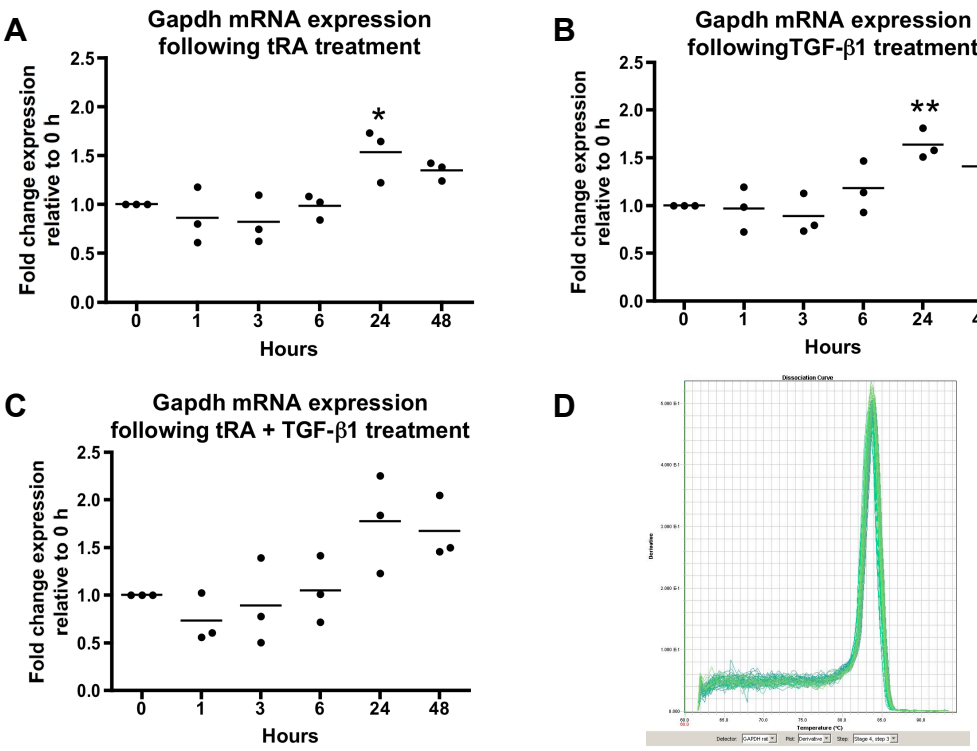

Figure 2.10. Effect of tRA in the absence and presence of TGF-β1 on Gapdh mRNA expression in NRK-49F cells. NRK-49F cells cultured as per protocol were treated with 2 μM tRA and/or 5 ng/ml TGF-β1 for 0, 1, 3, 6, 24 or 48 h. Total RNA was collected at 48 h. Two-step RT-qPCR using SYBR Green technology was used to determine changes in mRNA expression of Gapdh following treatment with tRA (**A**), TGF-β1 (**B**) and tRA and TGF-β1 (**C**). The dissociation curve is shown in **D**. Data represent mean ± SEM of 3 independent cell culture studies. Statistical analysis was performed on transformed data using repeated measures ANOVA. * $p<0.05$,** $p<0.01$ vs 0 h.

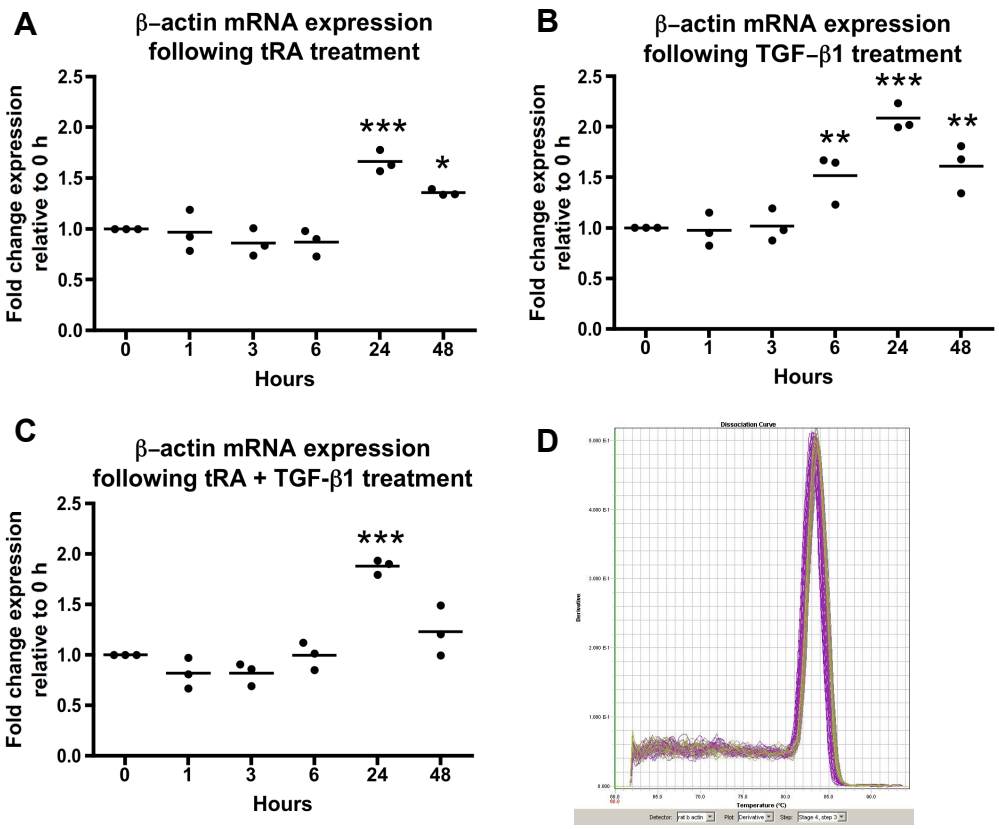

Figure 2.11. Effect of tRA in the absence and presence of TGF-β1 on β-actin mRNA expression in NRK-49F cells. NRK-49F cells cultured as per protocol were treated with 2 μM tRA and/or 5 ng/ml TGF-β1 for 0, 1, 3, 6, 24 or 48 h. Total RNA was collected at 48 h. Two-step RT-qPCR using SYBR Green technology was used to determine changes in mRNA expression of β-actin following treatment with tRA (**A**), TGF-β1 (**B**) and tRA and TGF-β1 (**C**). The dissociation curve is shown in **D**. Data represent mean ± SEM of 3 independent cell culture studies. Statistical analysis was performed on transformed data using repeated measures ANOVA. *p<0.05, **p<0.01, ***p<0.001 vs 0 h.

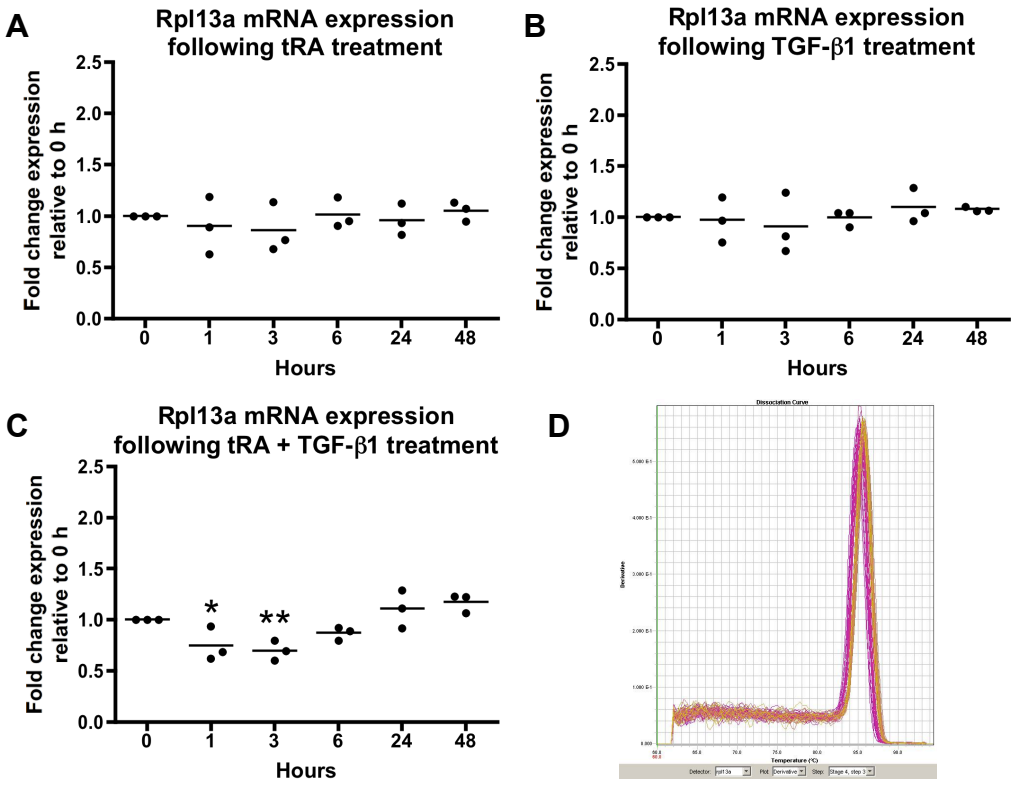

Figure 2.12. Effect of tRA in the absence and presence of TGF-β1 on Rpl13a mRNA expression in NRK-49F cells. NRK-49F cells cultured as per protocol were treated with 2 μM tRA and/or 5 ng/ml TGF-β1 for 0, 1, 3, 6, 24 or 48 h. Total RNA was collected at 48 h. Two-step RT-qPCR using SYBR Green technology was used to determine changes in mRNA expression of Rpl13a following treatment with tRA (**A**), TGF-β1 (**B**) and tRA and TGF-β1 (**C**). The dissociation curve is shown in **D**. Data represent mean ± SEM of 3 independent cell culture studies. Statistical analysis was performed on transformed data using repeated measures ANOVA. *p<0.05, **p<0.01 vs 0 h.

Optimisation of SABiosciences RT^2 qPCR primer assays: TaqMan and SABiosciences gene expression assays are purchased with a guarantee of adequate specificities and efficiencies. However, as part of the quality control process, a melting curve program was included in instrument set up for the gene expression assays that used SYBR Green technology to identify the presence of any non-specific products formed during the PCR reaction that could affect data analysis. Although the dissociation curves for the majority of gene expression assays displayed only one peak, those for Mmp-2 and Mmp-13 had more than one peak suggesting the presence of either primer-

dimer formation or non-specific product (Figure 2.13A, B). These gene expression assays required optimisation before use in experiments.

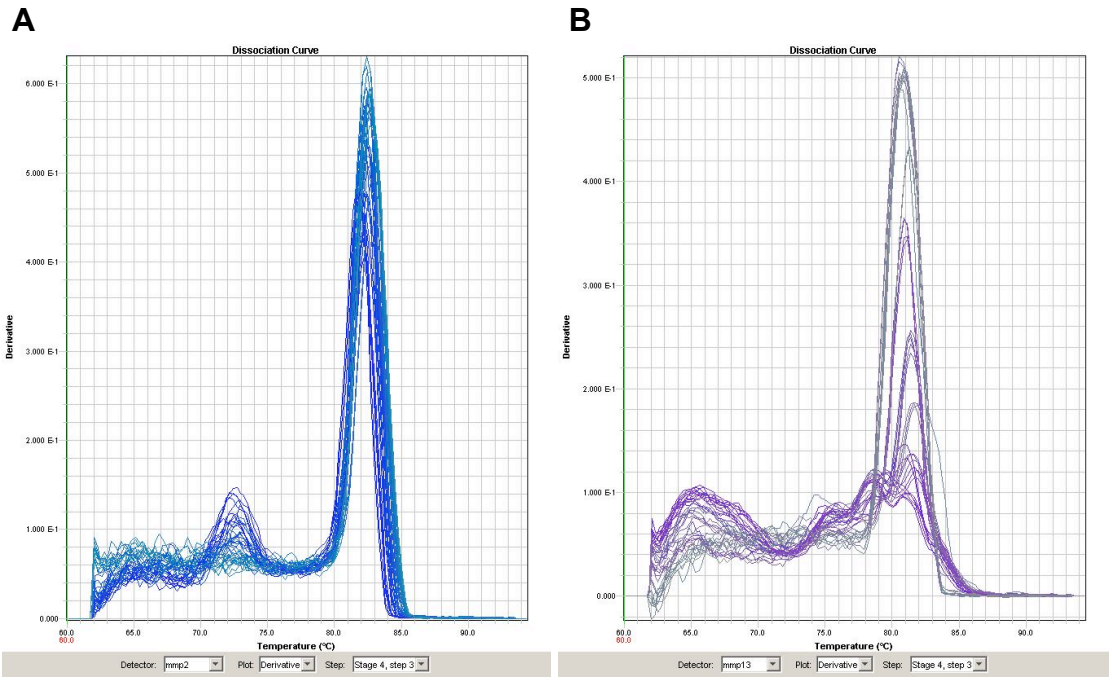

Figure 2.13. Dissociation curves for Mmp-2 and Mmp-13 PCR products. Dissociation curves for Mmp-2 (**A**) and Mmp-13 (**B**) RT-qPCR revealed more than one PCR product.

Primer concentration can affect the specificity of the reaction with high concentrations of primers increasing the yield of non-specific products. Therefore serial 1 in 2 dilutions of the 10 µM Mmp-2 and Mmp-13 stock primers were used to determine whether the non-specific peaks on the dissociation curves could be eliminated. A 1 in 4 dilution of Mmp-2 and Mmp-13 primers produced a single specific peak (Figures 2.14 and 2.15) and therefore this dilution was chosen for further optimisation experiments.

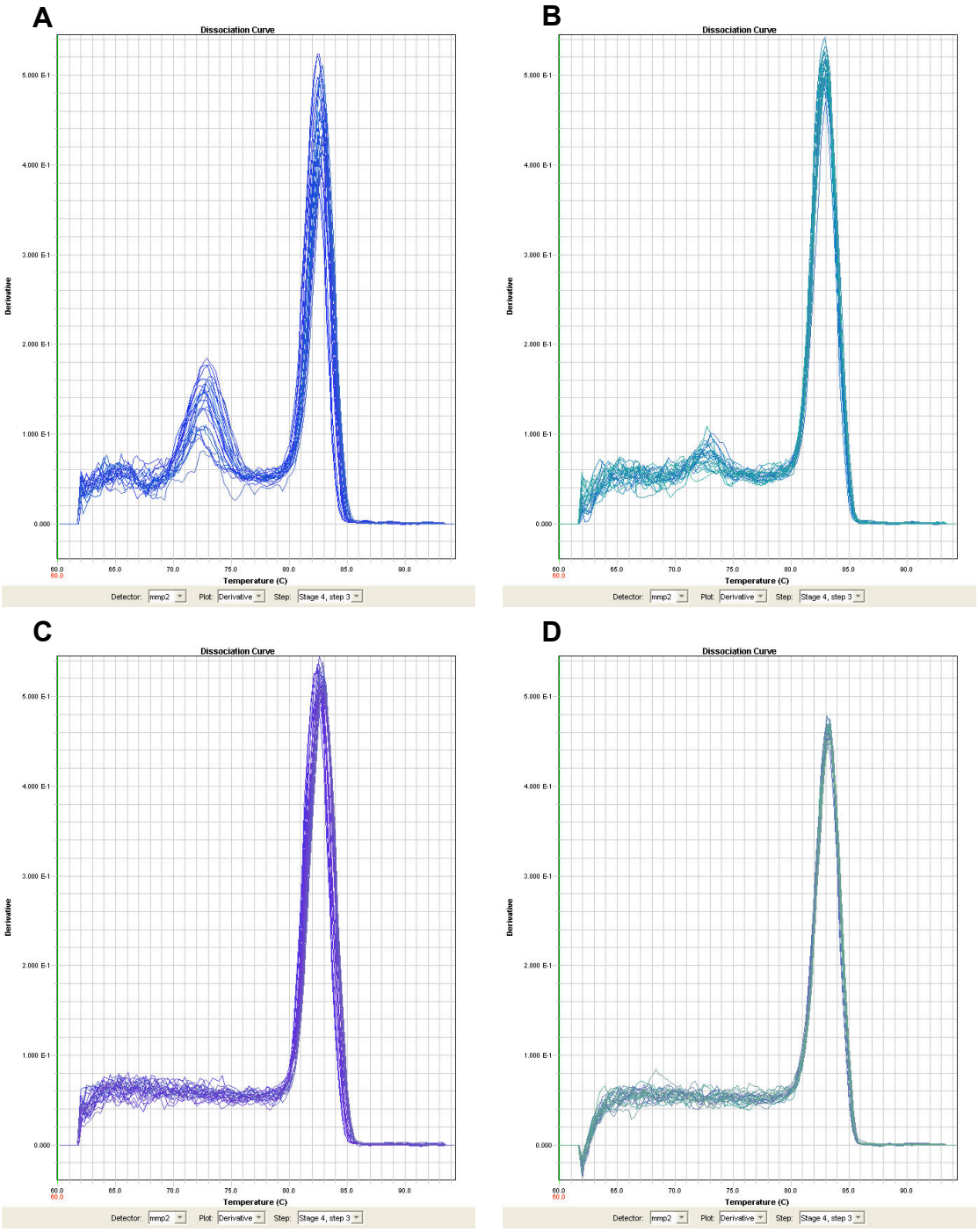

Figure 2.14. Dissociation curves for Mmp-2 PCR product following serial dilutions of primer. qPCR was performed on 1 in 2 serial dilutions of Mmp-2 primers using NRK-49F cDNA as template. **A**- no dilution of primer, **B**- 1 in 2 dilution, **C**- 1 in 4 dilution, **D**- 1 in 8 dilution.

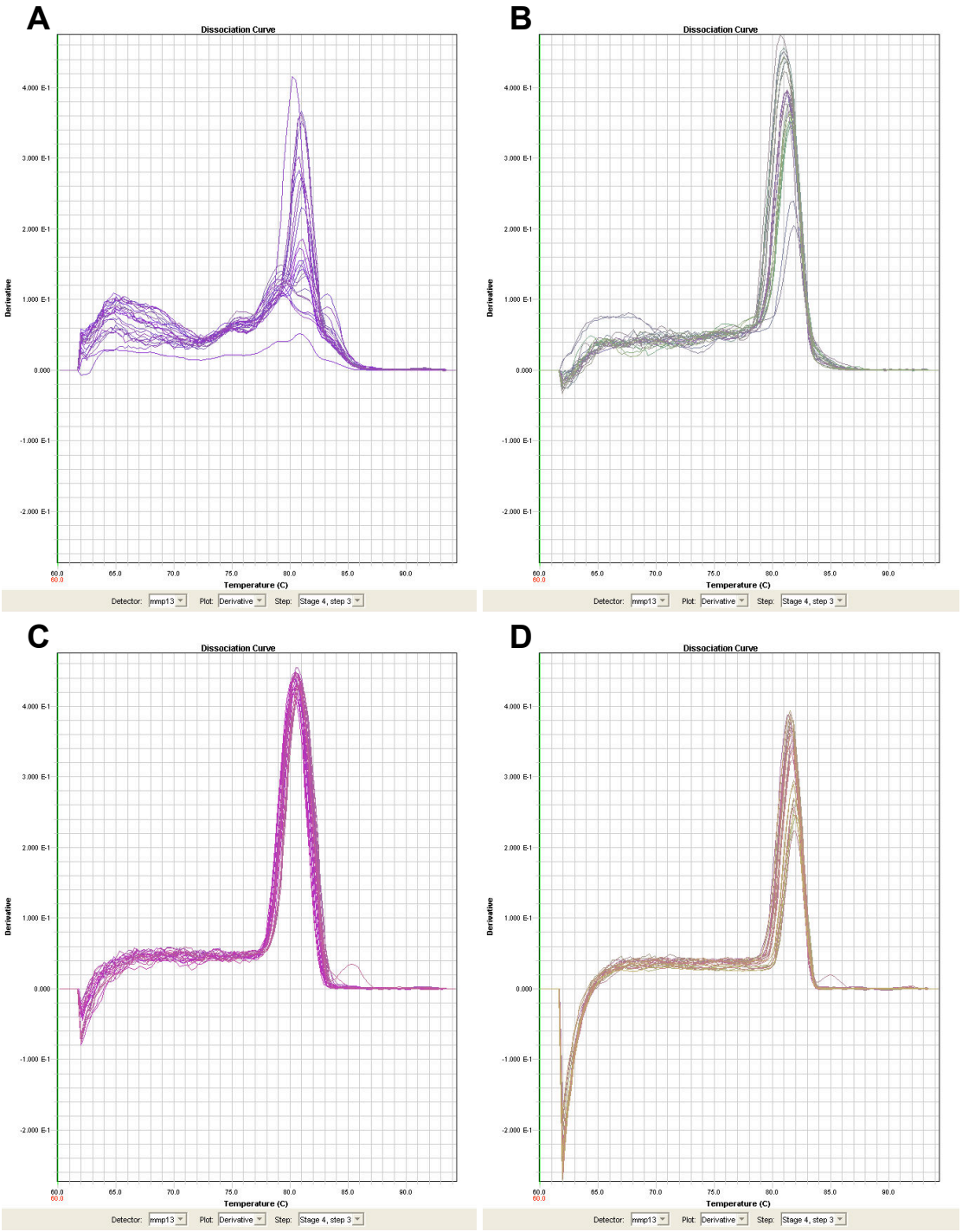

Figure 2.15. Dissociation curves for Mmp-13 PCR product following serial dilutions of primer. qPCR was performed on 1 in 2 serial dilutions of Mmp-13 primers using NRK-49F cDNA as template. **A**- no dilution of primer, **B**- 1 in 2 dilution, **C**- 1 in 4 dilution, **D**- 1 in 8 dilution.

Since the primers for Mmp-2 and Mmp-13 were to be diluted 1 in 4 in experiments it was necessary to show that they were present in excess in reactions, that diluting them did not limit the reaction and that their efficiencies were maintained and comparable to the efficiencies of the endogenous controls. Therefore, qPCR experiments were run on 1 in 3 serial dilutions of NRK-49F cDNA template using 1 in 4 dilutions of Mmp-2 and Mmp-13 primers and undiluted primers of HKGs Rpl13a and Gapdh.

The cDNA dilution series produced evenly spaced amplification curves for all four primers tested (Figure 2.16) and linear standard curves with coefficients of determination (R^2) >0.980 for all primers (Figure 2.17). The slopes of the standard curves were close to -3.32 suggestive of efficiencies of near 100% for all primers tested and the efficiencies calculated from the formula $10^{-1/slope}$ were 1.98, 2.02, 1.99 and 1.98 for Mmp-2, Mmp-13, Rpl13a and Gapdh, respectively. Finally, to further determine if two amplicons have the same efficiency, the ΔCt variation with template dilution can be compared (Livak and Schmittgen 2001). The Cts of the HKGs Rpl13a and Gapdh at different cDNA dilutions were subtracted from the corresponding Cts of Mmp-2 and Mmp-13. This showed that the ΔCts at different cDNA dilutions were comparable (Figure 2.18) and the absolute values of the slopes generated by linear regression were <0.1. Therefore, the Mmp-2 and Mmp-13 primers at dilutions of 1 in 4 were acceptable for use in experiments.

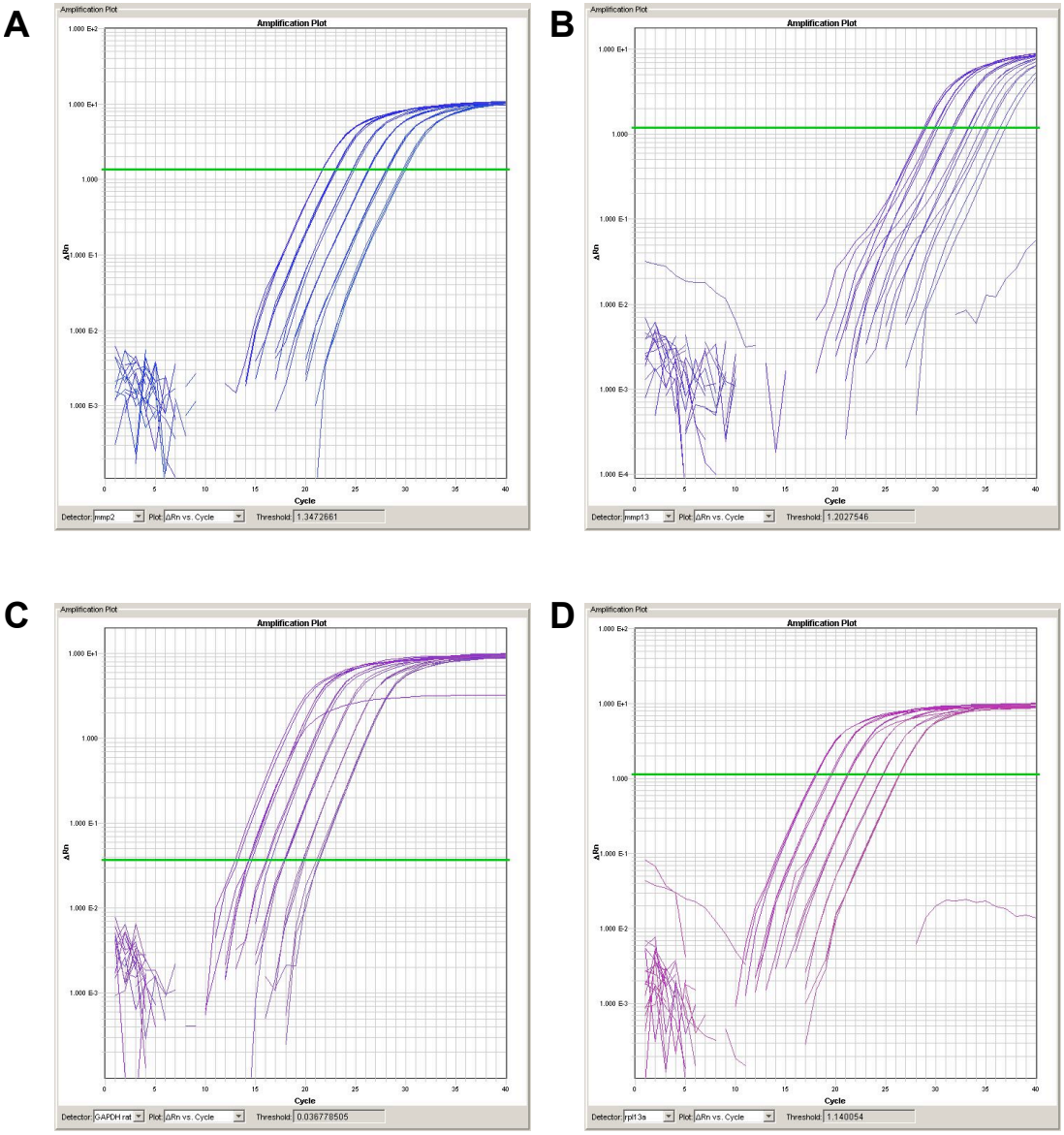

Figure 2.16. Amplification curves for Mmp-2, Mmp-13, Gapdh and Rpl13a using serial dilutions of NRK-49F cDNA. Serial 1 in 3 dilutions of NRK-49F cDNA were subjected to qPCR with Mmp-2 primers diluted 1 in 4 (**A**), Mmp-13 primers diluted 1 in 4 (**B**), undiluted Gapdh primers (**C**) and undiluted Rpl13a primers (**D**).

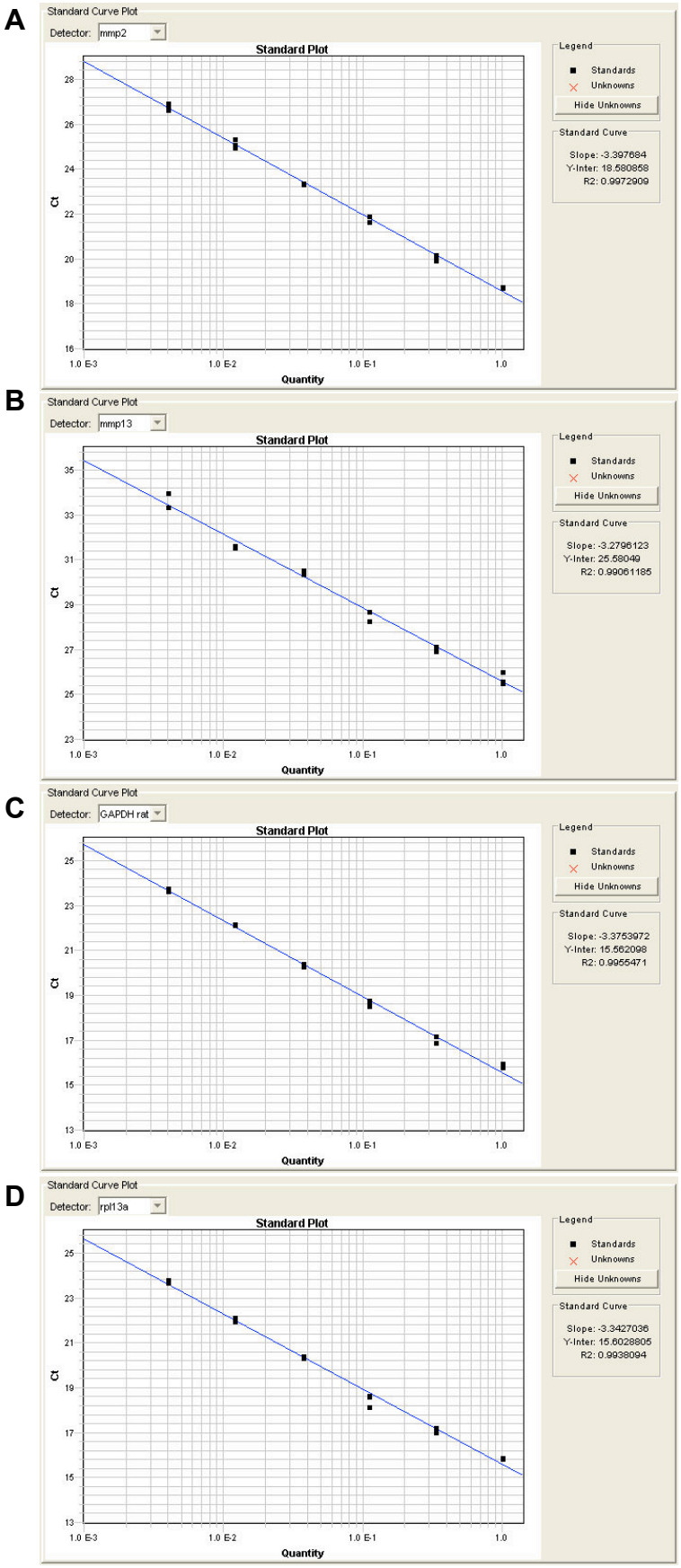

Figure 2.17. Standard curves for Mmp-2, Mmp-13, Gapdh and Rpl13a. Serial 1 in 3 dilutions of NRK-49F cDNA were subjected to qPCR. Standard curves for Mmp-2 (**A**), Mmp-13 (**B**), Gapdh (**C**) and Rpl13a (**D**) were generated using SDS 2.2 software.

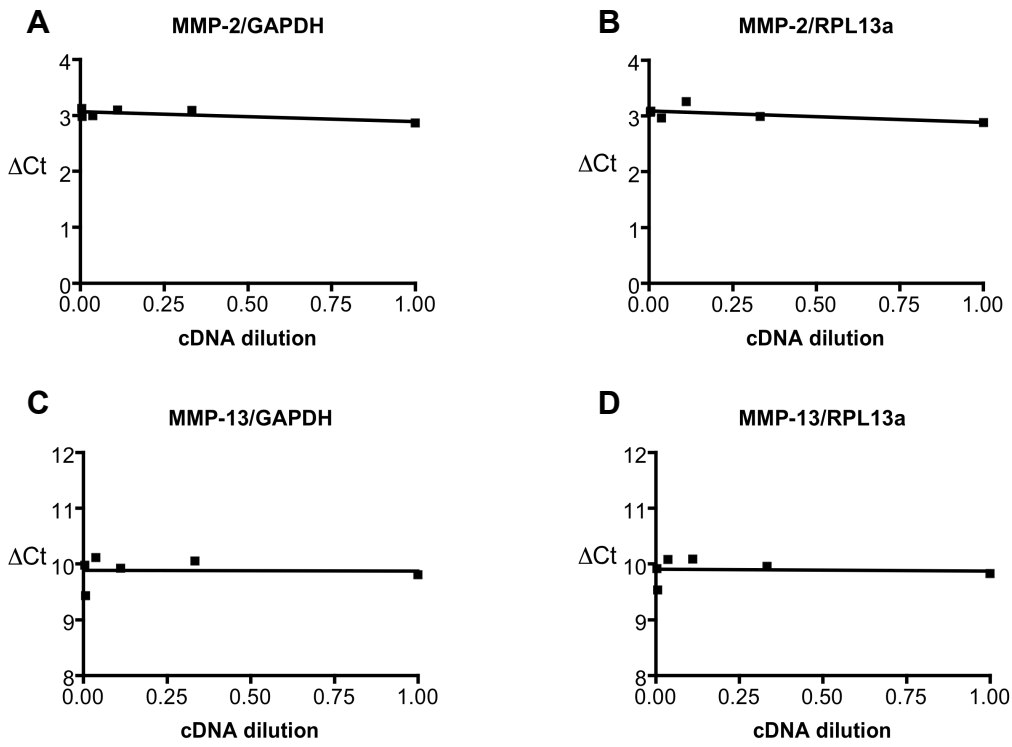

Figure 2.18. Validation of the $2^{-\Delta\Delta Ct}$ method. Serial 1 in 3 dilutions of NRK-49F cDNA were subjected to qPCR with the diluted Mmp-2 and Mmp-13 or undiluted Gapdh and Rpl13a gene expression assays. ΔCt was calculated by subtracting Gapdh or Rpl13a Ct from Mmp-2 or Mmp-13 Ct. Data were plotted as the average of triplicates and fit using linear regression analysis.

2.7 Rat ECM and adhesion molecules PCR array

A rat ECM and adhesion molecules PCR array (SABiosciences) was used to explore the changes in expression of 84 genes important in cell-cell and cell-matrix interactions in NRK-49F cells treated with tRA with and without TGF-β1. The RT^2 Profiler^{TM} PCR array uses SYBR Green technology and consists of a set of optimised real-time PCR primer assays on a 96-well plate format. It performs gene expression analysis with real-time PCR sensitivity and the multi-gene profiling capability of a microarray. The layout of the PCR array is shown in Figure 2.19.

RNA extracted from NRK-49F cells treated with vehicle, 2 μM tRA, 5 ng/ml TGF-β1 or both tRA and TGF-β1 was subjected to reverse transcription using SABiosciences RT^2 first strand kit according to the manufacturer's guidelines

	1	2	3	4	5	6	7	8	9	10	11	12
A	Adamts 1	Adamts 5	Adamt s8	Catna1	Ctnna2	Cd44	Cdh1	Cdh2	Cdh3	Cdh4	Cntn1	Col1a1
B	Col2a1	Col3a1	Col4a1	Col4a2	Col4a3	Col5a1	Col6a1	Col8a1	Cspg2	Ctgf	Ctnnb1	Ecm1
C	Emilin1	Entpd1	Fbln1	Fn1	Halpn1	Icam1	Itga2	Itga3	Itga4	Itga5	Itgad	Itgae
D	Itgal	Itgam	Itgav	Itgb1	Itgb2	Itgb3	Itgb4	Lama1	Lama2	Lama3	Lamb2	Lamb3
E	Lamc1	Mmp10	Mmp 11	Mmp 12	Mmp 13	Mmp 14	Mmp 15	Mmp 16	Mmp 1a	Mmp2	Mmp3	Mmp7
F	Mmp8	Mmp9	Ncam1	Ncam2	Pecam	Postn	RGD15 65950	Sele	Sell	Selp	Sgce	Sparc
G	Spock1	Spp1	Syt1	Tgfbi	Thbs1	Thbs2	Timp1	Timp2	Timp3	Tnc	Vcam1	Vtn
H	Rplp1	Hprt	Rpl13a	Ldha	Actb	RGDC	RTC	RTC	RTC	PPC	PPC	PPC

Figure 2.19. Rat ECM and adhesion molecules PCR array layout. A1-G12= target genes of interest; H1-H5= HKGs; H6= rat genomic DNA contamination control (RGDC); H7-H9= reverse transcription controls (RTC); H10-H12= positive PCR controls (PPC). *Adamts1, 5, 8* A disintegrin-like and metallopeptidase (reprolysin type) with thrombospondin type 1 motif, 1, 5, 8; *Catna1/Ctnna2* catenin (cadherin-associated protein) α 1, 2; *Cd44* CD44 antigen; *Cdh1-4* cadherin 1-4; *Cntn1* contactin 1; *Col1a1* procollagen type I α 1; *Col2a1* procollagen type II α 1; *Col3a1* procollagen type III α 1; *Col4a1-3* procollagen type IV α 1-3; *Col5a1* procollagen type V α 1; *Col6a1* procollagen type VI α 1; *Col8a1* procollagen type XIII α 1; *Cspg* chondroitin sulfate proteoglycan 2; *Ctgf* connective tissue growth factor; *Ctnnb1* catenin (cadherin associated protein beta 1); *Ecm1* extracellular matrix protein 1; *Emilin1* elastin microfibril interfacer 1; *Entpd1* ectonucleoside triphosphate diphosphohydrolase 1; *Fbln1* fibulin 1; *Fn1* fibronectin 1; *Hapln1* hyaluronan and proteogylcan link protein 1; *Icam1* intercellular adhesion molecule 1; *Itga2-5* integrin alpha2-5; *Itgad* integrin α D; *Itgae* integrin α E; *Itgal* integrin α L; *Itgam* integrin α M; *Itgav* integrin α V; *Itgb1-4* integrin β 1-4; *Lama1-3* laminin α 1-3; *Lamb2-3* laminin β 2-3; *Lamc1* laminin γ 1; *Mmp1a, 2-3, 7-9, 10-16* matrix metallopeptidase 1a, 2-3, 7-9, 10-16; *Ncam1-2* neural cell adhesion molecule 1-2; *Pecam* platelet/endothelial cell adhesion molecule; *Postn* periostin, osteoblast specific factor; *Rgd1565950* similar to A disintegrin-like and metalloprotease (reprolysin type) with thrombospondin type 1 motif 2; *Sele* selectin, endothelial cell; *Sell* selectin, lymphocyte; *Selp* selectin, platelet; *Sgce* sarcoglycan, epsilon; *Sparc* secreted acidic cysteine rich glycoprotein; *Spock1* sparc/osteonectin, cwcv and kazal-like domains proteogycan 1; *Spp1* secreted phosphoprotein 1; *Syt1* synaptotagmin 1; *Tgfbi* transforming growth factor beta induced; *Thbs1-2* thrombospondin 1-2; *Timp1-3* tissue inhibitor of metallopeptidase 1-3; *Tnc* tenascin C; *Vcam1* vascular cell adhesion molecule 1; *Vtn* vitronectin; *Rplp1* ribosomal protein, large, P1; *Hprt* hypoxanthine guanine phosphoribosyl transferase; *Rpl13a* ribosomal protein L13A; *Ldha* lactate dehydrogenase A; *Actb* actin, β.

(SABiosciences). This kit was used to transcribe cDNA from RNA for the PCR array as it has been designed and optimised for use with the RT^2 Profiler^{TM} PCR arrays. The kit includes a built-in external RNA control that helps monitor reverse transcription efficiency and also tests for enzyme inhibitors contaminating RNA samples. Briefly, a genomic DNA elimination mixture for each RNA sample was prepared by adding 2 µl 5x genomic DNA elimination buffer to 1 µg RNA and the volume made up to 10 µl with RNase-free water. The DNA elimination mixture was incubated at 42^{O}C for 5 min then placed on ice for 1 min. An equal volume of the reverse transcription cocktail consisting of a reverse transcriptase enzyme mix, reverse transcription buffer, random hexamers, oligo-dT primers, an external control mix and RNase-free water was then added to each reaction and samples incubated at 42^{O}C for 15 min. The mixture was then immediately incubated at 95^{O}C for 5 min to stop the reaction. First strand cDNA samples were diluted with RNase-free water and stored at -20^{O}C until use.

Reactions for the PCR array were prepared by adding cDNA samples to RT^2 SYBR Green/ROX 2x qPCR Master Mix and RNase-free water according to manufacturer's guidelines. Reactions were mixed thoroughly then 25 µl was added to each of the 96 wells of the PCR array. Included in the PCR array were 5 HKGs for normalisation of qPCR data, a genomic DNA control (GDC) that detects non-transcribed genomic DNA contamination, a reverse transcription control (RTC) that tests the efficiency of the RT^2 first strand kit reaction with a primer set that detects template synthesised from the kit's built in external RNA control, and a positive PCR control (PPC) that tests the efficiency of the PCR itself using a pre-dispensed artificial DNA sequence and the primer set that detects it. The sets of replicate control wells (RTC and PPC) also test for inter-well, intra-plate consistency. Once prepared the plate was sealed with optical thin-walled 8-cap strips, centrifuged at 1000 x *g* for 1 min at room temperature then run on an ABI7900HT PCR system using SDS 2.2 software. Data was analysed using SABiosciences PCR Array Data Analysis Web portal including calculation of $2^{e-\Delta\Delta Ct}$ (relative quantification). Each PCR array was repeated in triplicate.

For the GDC, a Ct of 35 or more is considered acceptable. Of the 12 plates run, 10 had GDC Cts of greater that 35 and 2 had GDC Cts of less than 35. Of the two samples that had Cts of less than 35, one sample was from the vehicle treated-group and had a Ct of 34.91 and one sample was from the tRA-treated group and had a Ct of 34.52. The efficiency of the RT^2 first strand kit reaction is considered acceptable if the ΔCt of RTC-PPC is 5 or less. The averages of the triplicate samples for all four groups passed this test. Finally, a PPC was used to test for the presence of different amounts of PCR amplification inhibitors in each sample. The average PPC Ct on each plate should be 20 +/- 2 and should not vary by more than two cycles between arrays being compared. All the plates passed this test. In general inter-plate, intraplate consistency was good with ΔCt of less than 0.5 between replicates.

2.8 Protein extraction

In order to determine protein expression of nuclear receptors and RA carrier proteins and changes in expression or activity of proteins involved in fibrosis following tRA treatment with and without TGF-β1, total protein was extracted and conditioned media stored from NRK-49F cell cultures.

NRK-49F cells were seeded in 10 cm cell culture dishes at a density of $1x10^5$ cells/dish in DMEM supplemented with 2.5% FCS and 2.5% Nu for 3 d then DMEM supplemented with ITS for 4 d; phenol red-free medium was used when collecting conditioned media (PAA Laboratories GmbH). Cells were then treated with vehicle, 2 μM tRA, 5 ng/ml TGF-β1 or dual treatment for 48 h and conditioned media stored at -80^OC until use. For extraction of total cell lysates, cell culture dishes were firstly placed on ice and the medium discarded. Cells were washed thrice with PBS then 500 μl of ice-cold PBS-TDS with protease inhibitors (except where the protease inhibitors would interfere with protein activity assays) was added to the cell monolayer to cover the cells. Dishes were incubated for 1 h on ice. Cell scrapers (Greiner Bio-One Ltd) were then used to collect total cell lysates and the lysates transferred to 1.5 ml microcentrifuge tubes (Greiner Bio-One Ltd) on ice. Intact cell membranes were broken up and DNA sheared using a 25 G needle

and syringe then the samples were centrifuged at full speed for 2 min. Supernatants were transferred to fresh microcentrifuge tubes and the protein concentration of samples determined by comparison with a set of protein standards using the bicinchoninic acid method (BCA) and BCA protein assay reagent (Pierce Protein Research products, Thermo Scientific, Rockford, USA). The BCA protein assay combines the reduction of Cu^{2+} to Cu^{1+} by protein in an alkaline medium with the highly sensitive and selective colorimetric detection of the cuprous cation (Cu^{1+}) by BCA. The resulting intense purple-coloured product can be measured by spectrophotometric analysis at 540 nm. NRK-49F total cell lysate was stored at -80^{O}C until use.

2.9 Western blot analysis

Immunoblotting was used for the detection and relative quantification of proteins of interest in samples. This technique uses gel electrophoresis to separate native or denatured proteins by the length of polypeptide (denatured protein) or by the 3-D structure of the protein (native/ non-denatured protein). Protein is then transferred from gel to a nitrocellulose membrane and the protein of interest detected using a specific antibody.

2.9.1 SDS polyacrylamide gel electrophoresis (SDS-PAGE)

Samples consisting of total cell lysate were diluted using PBS-TDS so that they contained equal amounts of protein for loading. Samples consisting of conditioned medium contained very small amounts of protein so these samples were not diluted and normalisation between samples was done using the corresponding undiluted total cell lysate as a loading control. Samples were prepared by mixing them with 10x WSB and 10% beta-mercaptoethanol (Sigma) then they were heated to 100^{O}C for 10 min on a heat block to denature the protein. The biotinylated protein ladder (Cell Signalling Technology, Danvers, Massachusetts, USA) was heated at 100^{O}C for 2 min. Samples, biotinylated protein ladder and Amersham's full range rainbow molecular weight marker (GE Healthcare, Little Chalfont, UK) were then loaded onto a polyacrylamide gel and run in an electrophoresis tank filled with pre-cooled electrophoresis buffer at 50 V for 30 min (through the stacking gel)

then at 200 V for a further 45-60 min (through the resolving gel). Protein was then transferred from gel to Amersham's Hybond C-super nitrocellulose membrane (GE Healthcare) in a transfer tank containing ice-cold Towbin transfer buffer at 100 V for 45 min. Adequate transfer was confirmed by Ponceau S staining (Sigma). The membrane was destained by washing with ddH_2O then blocked in 5% skimmed milk blocking solution for 2 h at room temperature on a rocking platform.

2.9.2 Immunodetection

Once blocking was complete the nitrocellulose membrane was incubated in primary antibody in 5% milk blocking solution overnight at 4^{O}C on a rocking platform (the biotinylated ladder was incubated in milk blocking solution alone). The membrane was then briefly rinsed then washed thrice for 10 min with 0.1% TBST before incubating with secondary antibody conjugated to horseradish peroxidase in milk blocking solution for 1 h at room temperature on a rocking platform. The membrane was again washed with 0.1% TBST then the membrane developed using Amersham's ECL Plus Western Blotting detection Reagents (GE Healthcare) and exposed to Amersham's Hyperfilm ECL chemiluminescence film (GE Healthcare) in a dark room.

Band densitometry was performed using Adobe Photoshop CS version 8.0 software (Adobe Direct, Rotterdam, The Netherlands). Films were scanned, converting to greyscale, inverted then the contrast and brightness of the image optimised. The lasso tool was used to draw around the bands and the mean x pixels recorded. Results were normalised to a loading control and presented as mean +/- SEM relative to the vehicle control of three independent cell culture studies.

2.10 Mass spectrometry

Liquid chromatography-tandem mass spectrometry (LC/MS/MS) was used to further determine the protein content of bands identified by TG2 and CRABP-II immunoblotting of NRK-49F total cell lysates.

2.10.1 Preparation of samples

General measures to avoid keratin contamination were taken including conducting experiments in a dust-free environment and wearing powder-free latex gloves.

Identification of protein bands of interest in polyacrylamide gels: NRK-49F total cell lysate and NIH/3T3 total cell lysate (used as a positive control for CRABP-II protein) were prepared as per the protocol for Western blot analysis (see above). Samples were loaded onto 8% (TG2) or 15% (CRABP-II) polyacrylamide gels with Amersham's full range rainbow molecular weight marker and run at 50 V for 30 min then 200 V for 45-60 min. Protein in the gels was then fixed in a solution of 10 ml methanol, 280 µl acetic acid and 29 ml ddH_2O for 30 min followed by staining with Brilliant Blue G-colloidal Coomassie stain (Sigma) made up of 4 parts stain and 1 part methanol at room temperature overnight on a rocking platform. Destaining consisted of one 10 min wash with the fixing solution followed by two 45-60 min washes with a solution of 10 ml methanol, 80 µl acetic acid and 29 ml ddH_2O until the bands appeared in good contrast to the background. Bands of interest were identified and cut out of the gels by comparison of the stained gels with immunoblots of TG2 and CRABP-II then cut into ~2 mm^2 pieces and transferred to a microcentrifuge tube. The remainder of the gels were stored in ddH_2O at $4^{O}C$.

Tryptic digestion: Trypsin was used for protein digestion because the proteolytic fragments produced contain a basic arginine and lysine amino acid residue which are suitable for positive ionisation mass spectrophotometric analysis. Gel cubes were initially washed with 100 mM ammonium bicarbonate (Sigma) in excess then acetonitrile (ACN; Fisher Scientific UK

Ltd, Loughborough, UK) was added to dehydrate the samples before drying in a SpeedVac vacuum concentrator for 5 min at 35^{O}C with the lids open. Samples were then rehydrated and the cysteine residues reduced with 10 mM dithiothreitol (DTT; Sigma) at 56^{O}C for 30 min. DTT was then discarded and ACN was again added before drying the samples as before. The gel pieces were then incubated in 55 mM iodoacetamide (IAA; Sigma) at room temperature in the dark for 20 min. IAA binds covalently to the thiol group of cysteine residues forming stable carbamidomethyl derivatives and preventing disulfide bond formation. The supernatant was subsequently discarded and the gel pieces again washed twice with 100 mM ammonium bicarbonate. Destaining was completed by washing with a 1:1 solution of 100 mM ammonium bicarbonate and ACN incubating at 37^{O}C with shaking for 30 min and the process repeated until all visible stain was removed. The samples were dehydrated once more with ACN and dried in a SpeedVac vacuum concentrator for 10 min. Trypsin diluted to a final concentration of 13 ng/µl in 50 mM ammonium bicarbonate was added to the gel pieces and samples incubated at 4^{O}C for 20 min. Excess trypsin was removed and a minimal volume of 50 mM ammonium bicarbonate added to cover the gel pieces and keep them moist during enzyme cleavage. The samples were incubated at 37^{O}C for 3-4 h then at room temperature overnight.

Peptide extraction: Following tryptic digestion the peptide-rich supernatant was collected in a fresh microcentrifuge tube. The gel pieces were washed with 50 mM ammonium bicarbonate then dehydrated with ACN and the supernatant pooled with the peptide samples already collected. This process of rehydrating with 50 mM ammonium bicarbonate and dehydrating with ACN was repeated until all peptide from the gel pieces had been collected. The peptide samples were lyophilised and stored at -80^{O}C until use.

2.10.2 Mass spectrometry

LC/MS/MS was performed using an Ultimate LC system (Dionex Ltd, Camberley, UK) where chromatographic separations of samples occurs before analysis by a quadrupole time-of-flight (Q-ToF) tandem mass

spectrometer (Q-Tof micro; Waters Ltd, Elstree, UK) operating under MassLynx v4.0 software (Waters Ltd).

Lyophilised peptide samples were initially prepared by resuspending them in 23 µl 50 mM ammonium bicarbonate and incubating at 37^{O}C with shaking. Samples were then taken up by an autosampler and transferred to a C18 guard (trapping) column where peptides bind and are washed with loading "buffer A" consisting of 0.1% formic acid and H_2O to remove salts and provide peptides with a positive charge. Separation of peptides was commenced by reversed phase chromatography on a 75 µm C18 PepMap analytical column (Dionex). This column captures small peptides (<50-kDa), which are then resolved with an increasing mixture of "Buffer B" (80% ACN, 0.1% formic acid and H_2O) added to "buffer A" so that the gradient of ACN increases causing elution of peptides at a flow rate of 200 nL/min over 60 min. The eluate then enters the Q-ToF mass spectrometer which consists of an ion source and ion optics to accelerate and focus ions through an aperture into the quadrupole filter, a collision cell and a time-of-flight analyser. The mass spectrometer is kept in a vacuum so that the ions do not collide with air molecules.

When the eluate initially passes through the ion source, which is held at a high potential (35 kV) at 200^{O}C, it undergoes electrospray ionisation with a Z-spray source fitted to the QTof-micro. Highly charged, vapourised ions are then accelerated through four parallel metal rods (a quadrupole), two of which are positively charged and two negatively charged, down a potential gradient. The applied voltages cause the ions to fly in a specific trajectory between the rods and peptides that are too big, too small or highly charged are thrown out of their original path. The quadrupole is responsible for filtering ions based on their mass-to-charge ratio (m/z) and the stability of their trajectories. The instrument was run in automated data-dependent switching mode so that precursor or parent ions are detected and selected based on their intensity for sequencing by collision-induced fragmentation (CID). This process is called the MS survey scan. Selected peptides then move to the collision cell where a voltage is applied that excites argon gas, which then collides with peptide

fragmenting it into product or daughter ions. A small focusing lens guides the amino acids into the flight tube where pusher and puller plates cause the amino acids to hit channel plates and a time-to-digital converter (TDC) allows data acquisition (MS/MS). The mass spectrometer then continues to cycle through the “duty cycle” consisting of two MS survey scans and two MS/MS cycles.

2.10.3 Peptide sequencing and database searching

Data acquired from LC/MS/MS was displayed as a mass spectrum using ProteinLynx Global Server v2.2.5 software (Waters Ltd), which creates a peak list from the data collected. The peak lists were searched against the Swiss-Prot and an “in-house” neuroproteins database using Mascot software v2.2 (Matrix Science Ltd, London, UK) and sequence information was obtained for the peptides identified. Experiments were performed once.

2.11 Matrix metalloproteinase activity assay

Molecular Probes EnzChek® Gelatinase/Collagenase Assay kit (Invitrogen) was used to determine changes in MMP activity in NRK-49F cells treated with tRA in the absence or presence of TGF-β1. This kit uses fluorescent DQ™ gelatin, which is efficiently digested by most gelatinases and collagenases, as substrate for the MMPs. DQ™ gelatin is so heavily labelled with fluorescein that the fluorescent signal is quenched however when it is digested by MMPs fluorescent peptides are produced with the fluorescent signal being proportional to proteolytic activity.

The kit was used according to the manufacturer’s guidelines to assay for gelatinase/collagenase activity in NRK-49F total cell lysates. Stock solution of 1 mg/ml DQ™ gelatin was prepared by adding 1 ml ddH_2O to the lyophilised substrate and protected from light. To each assay well of a 96 well flat bottom enzymatic assay plate, 20 µl of DQ™ gelatin (for a final concentration of 100 µg/ml) was added to 80 µl of 1x reaction buffer and the solution pipetted up and down to mix. NRK-49F total cell lysates (extracted from cells using PBS-TDS with protease inhibitors except EDTA as EDTA inhibits MMPs) were then

added at a volume of 100 µl to the assay wells. Reaction buffer alone was used as a negative control and *Clostridium* collagenase as a positive control. Reactions were performed in triplicate. The plate was incubated at room temperature protected from light for 2 h then fluorescence intensity measured using a BioTek FLx800 fluorescence microplate reader (BioTek UK, Potton, UK) at an absorption of 485 +/- 20 nm and fluorescence emission detection of 530 nm +/- 20 nm. Results were corrected for background fluorescence by subtracting the value derived from the negative control. Results were presented as mean of percentage change in fluorescence compared to vehicle-treated NRK-49F cells of three independent cell culture studies.

2.12 Gene silencing techniques: Short-interfering RNA transfection in NRK-49F cells

Ambion's *Silencer*® Select pre-designed short-interfering RNAs (siRNA; Applied Biosystems) were used to knockdown expression of TG2 and PAI-1 in NRK-49F cells (Table 2.7). Non-targeting *Silencer*® Select negative control # 1 siRNA (Applied Biosystems) was used as a negative control. Chemical-based transfection gave variable and inconsistent knockdown therefore a combination of electroporation and chemical-based transfection was used to attempt adequate silencing of gene expression.

Bio-Rad electroporation: A Bio-Rad Gene Pulser II electroporation system with the Capacitance Extender Plus accessory (Bio-Rad, Hemel Hempstead, UK) was used for electroporation of NRK-49F cells. This system delivers exponential decay pulses characterised by two parameters, the field strength (kV/cm) and the time constant, which can be adjusted by varying the voltage and capacitance.

Table 2.7. Sequences for Ambion's *Silencer*® Select siRNAs used for knockdown in NRK-49F cells.

siRNA target	siRNA ID number	Sequence
TG2	s132700	Sense: CUACCAGAGUGGUGACCAAtt Anti-sense: UUGGUCACCACUCUGGUAGgg
	s132701	Sense: CGGAUGACGUGUACCUAGAtt Anti-sense: UCUAGGUACACGUCAUCCGct
PAI-1	s128155	Sense: GAUGCUAUGGGAUUCAAUAtt Anti-sense: UAUUGAAUCCCAUAGCAUCtt
	s128156	Sense: GGAGAUGGUUUUAGACCGAtt Anti-sense: UCGGUCUAAAACCAUCUCCgt

A pilot study was performed to determine the optimal voltage and capacitance for delivery of siRNA into NRK-49F cells. Cy5-labelled siRNA (Dharmacon, Thermo Scientific, Loughborough, UK), to give a final concentration of 100 nM, was added to 1.5 x 10^6 cells/ml NRK-49F cells suspended in sterile PBS (without Ca^{2+} and Mg^{2+}). A negative control of untreated cells was included in experimental set up. Cell suspensions at a volume of 0.6 ml were then electroporated at 0-400 V and 250 or 500 µF in sterile Gene Pulser cuvettes with a 0.4 cm electrode gap (Bio-Rad) at room temperature. They were subsequently transferred to 35 mm cell culture dishes and cultured in antibiotic-free DMEM supplemented with 2.5% FCS and 2.5% Nu. Cell morphology was examined by photomicroscopy and transfection efficiency was determined by flow cytometry.

Flow cytometry was performed by trypsinising cells then resuspending them in PBS supplemented with 2.5% FCS and washing them two further times with PBS supplemented with 1% FCS. Cells were then subjected to flow cytometry using a BD FACSCanto II flow cytometer (BD Biosciences) and data analysed using FloJo Flow Cytometry Analysis Software (Ashland, USA).

Chemical and electrical transfection: On the basis of the results of the pilot study, optimal electroporation settings were selected as 300 V and 250 µF as these conditions achieved greatest transfection of Cy5-labelled siRNA while keeping cell death to a minimum (see Chapter 6 for further details). For subsequent experiments, cells were electroporated using the methods described above with some adaptations. Cells were suspended in Opti-MEM and 7.5 µl lipofectamine RNAiMAX transfection reagent (both Invitrogen) prior to electroporation, and a concentration of 20 nM targeting siRNA was used as per manufacturer's guidelines. Untreated cells and those treated with negative control siRNA were used as controls. Following electroporation, NRK-49F cells were plated in collagen type-I-coated 96-well plates and cultured in antibiotic-free DMEM supplemented with 2.5% FCS and 2.5% Nu for 3 d then antibiotic-free DMEM supplemented with ITS and a further dose of 20 nM siRNA and lipofectamine RNAiMAX for 4 d prior to treatment with 2 µM tRA and/or 5 ng/ml TGF-β1. Knockdown was determined by two-step RT-qPCR of RNA extracted on d 7 of tissue culture and the effects of knockdown on total collagen deposition determined using the 2D *in vitro* model of fibrosis (see protocol above). Experiments were repeated twice.

2.13 Statistical analysis

Data was statistically analysed using GraphPad Prism software (GraphPad Software, San Diego, California, USA). Parametric data was analysed using a paired t-test when comparing results between two groups and a repeated measures analysis of variance (ANOVA) with Tukey post-test was used to test for statistical significance between multiple groups. Results presented as fold change were logarithmically transformed before performing statistical analysis. $P<0.05$ was taken as statistically significant. Data was only analysed when 3 or more independent cell culture studies were performed. Although cell detachment index was analysed using the methodology described above the data could also be described as interval variables and statistically analysed as such.

Chapter 3. Effects of all-*trans* retinoic acid (tRA) on fibrogenesis in NRK-49F cells

3.1 Effect of tRA on total collagen deposition in the 2D *in vitro* model of fibrosis

There are few, if any, reports of the effects of retinoids on fibrosis in renal interstitial fibroblasts. Therefore, NRK-49F cells were used as a renal fibroblast cell model to determine the net effects of tRA on total collagen deposition using the 2D *in vitro* model of fibrosis. tRA at doses of 0.02-5 μM were chosen for initial experiments on the basis of doses of tRA used in other published data (Liu, Lu et al. 2008).

tRA at concentrations of 0.02-5 μM, with and without 5 ng/ml TGF-β1, dose-dependently increased PSR staining for total collagen (Figure 3.1A, B). Up to 5 μM tRA alone did not increase LDH release from cells, but, in the presence of TGF-β1, there was a significant increase in LDH release with the highest dose tested of 5 μM tRA (Figure 3.1C). tRA, with or without TGF-β1, did not significantly increase cell detachment index (Figure 3.1D).

3.2 Effects of tRA on selected fibrotic markers using a PCR array

In order to study the effects of tRA on fibrosis in more detail, a rat ECM and adhesion molecules PCR array was employed, which allowed the study of 84 genes associated with fibrosis. In this pilot study, NRK-49F cells were treated as per protocol then RNA extracted and subjected to the RT-qPCR array. tRA at a concentration of 2 μM was used in this and subsequent experiments because it consistently caused an increase in PSR staining both with and without TGF-β1, without evidence of toxicity, in the 2D *in vitro* model of fibrosis. Triplicate measurements of each RNA sample from a single biological study were recorded.

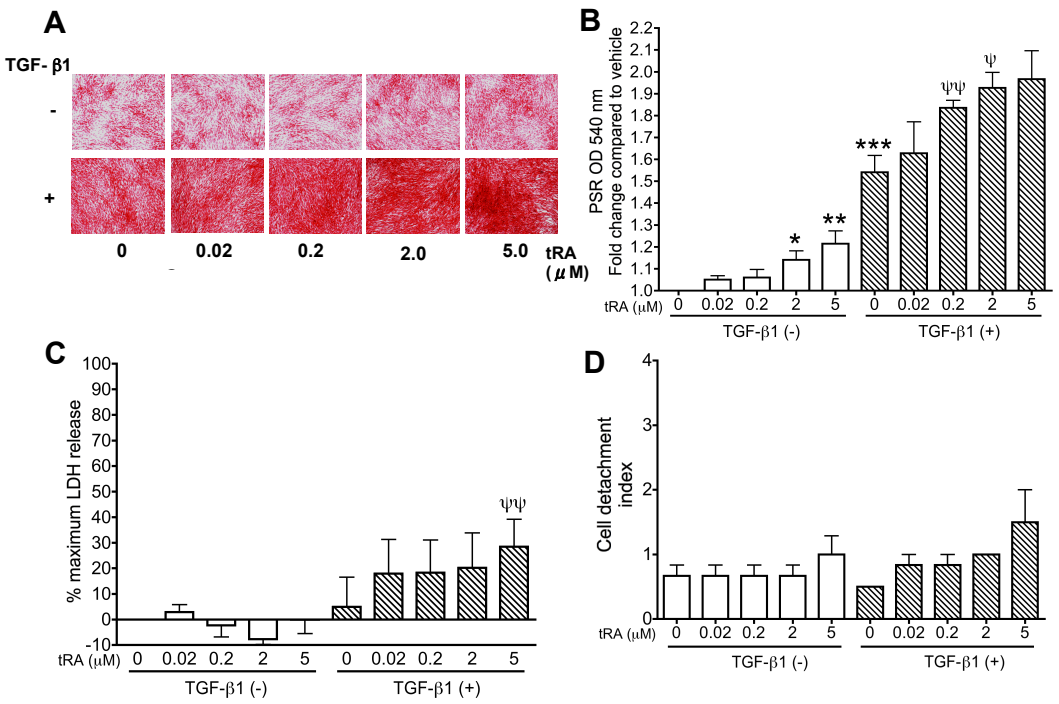

Figure 3.1. Effect of tRA in the absence and presence of TGF-β1 on total collagen deposition in NRK-49F cells. NRK-49F cells cultured as per protocol were treated with 0.02-5 μM tRA with and without 5 ng/ml TGF-β1 for 48 h. The effects on total collagen deposition were illustrated by representative photomicroscopy of PSR staining (x100 magnification) (**A**) and quantified by spectrophotometric analysis of eluted PSR, n=5 (**B**). Cytotoxicity was assessed by LDH release, n=3 (**C**) and cell detachment, n=3 (**D**). Data represent mean ± SEM of 3 or more independent cell culture studies. * $p<0.05$, ** $p<0.01$, *** $p<0.001$ vs vehicle; ψ $p<0.05$, ψ ψ $p<0.01$ vs TGF-β1-treated group.

From the 84 genes in the PCR array, those known to be important in ECM accumulation, including collagens, MMPs and TIMPs, were selected for further study in this chapter. However, a summary of all results from the PCR array dataset generated from SABiosciences PCR Array Data Analysis Web portal can be found in the Appendix section of this thesis (Supplementary tables 1-3) and there are changes in expression in some genes of unknown significance, that may also be worth more detailed study in the future.

Table 3.1 lists selected genes that demonstrated a two-fold or more up- or down-regulation by 2 μM tRA in the absence and presence of 5 ng/ml TGF-β1 and Figure 3.2 illustrates the effects of tRA with and without TGF-β1 on selected genes from the PCR array.

Table 3.1. Summary of relevant molecular markers up-regulated and down-regulated by tRA in the absence and presence of TGF-β1 in NRK-49F cells. Molecular markers that showed a two-fold or more up- or down-regulation following treatment with 2 μM tRA with or without 5 ng/ml TGF-β1 in the PCR array. Red= potential pro-fibrotic markers of tRA; green= potential anti-fibrotic markers of tRA.

	Markers up-regulated by tRA	Markers down-regulated by tRA
TGF-β1 (-)	Mmp-7	Ctgf, Mmp-3, Mmp-9, Mmp-10, Mmp-12, Mmp-13
TGF-β1 (+)	Col4a3, Mmp-7	Ctgf, Col6a1, Col8a1, Mmp-13, Mmp-14, Timp-1, Timp-2, Timp-3

TGF-β1 treatment of NRK-49F cells tended to up-regulate the majority of collagens and Fn1 as well as Timps -1 and -3; there was a tendency towards down-regulation of most MMPs although the mRNA of Mmps -9 and -10 tended to increase (Figures 3.2Ai, Aii). Overall these results are consistent with the concept that TGF-β1 is pro-fibrotic.

tRA treatment tended to down-regulate many collagen mRNAs as well as some other pro-fibrotic markers, including Col1a1, Col4a3, Col5a1, Col6a1, Col8a1, Ctgf and Fn1; conversely, there was evidence of up-regulation of other markers including Col3a1, Col4a1 and Col4a2 (Figure 3.2Bi). tRA tended to down-regulate the MMPs including Mmps -1a, -3, -9, -10, -12, -13, -15 and -16 although Mmps -2, -7 and -11 were up-regulated; there was a tendency towards down-regulation of Timps- 1-3 by tRA (Figure 3.2Bii).

In NRK-49F cells treated with both tRA and TGF-β1 compared to TGF-β1-treated cells alone there was a trend towards a down-regulation of Col3a1, Col4a1, Col4a2, Col5a1, Col6a1, Col8a1, Ctgf, Fn1, Timps- 1-3 and Mmps -2, -3, -10, -13, -14, -15 and -16 but a tendency towards up-regulation of Col4a3 and Mmps -7, -9, -11 and 12 (Figures 3.2Ci, Cii).

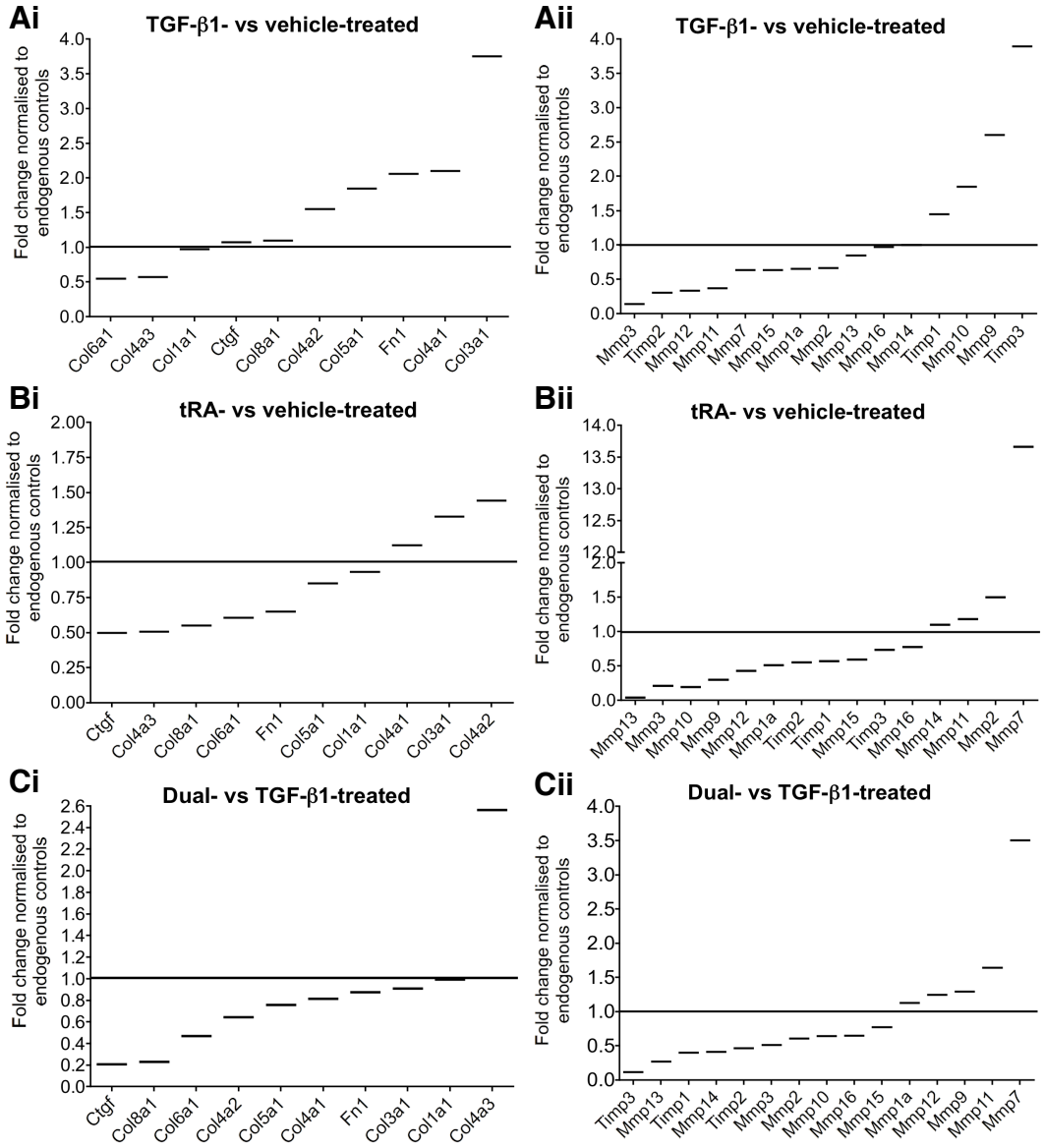

Figure 3.2. RT-qPCR array analysis of a pilot study of the effects of tRA in the absence and presence of TGF-β1 on mRNA expression of selected fibrotic markers in NRK-49F cells. NRK-49F cells cultured as per protocol were treated with 2 μM tRA with and without 5 ng/ml TGF-β1 for 48 h. Total RNA was extracted and subjected to an RT-qPCR array. Fold change in mRNA expression of collagens, Ctgf and Fn1 in TGF-β1- and tRA-treated cells vs vehicle-treated cells (**Ai, Bi**) and dual-treated cells vs TGF-β1-treated cells (**Ci**) are shown in the left panels. The right panels demonstrate fold changes in mRNA expression of the MMPs and TIMPs in TGF-β1- and tRA-treated cells vs vehicle-treated cells (**Aii, Bii**) and dual-treated cells vs TGF-β1-treated cells (**Cii**). Data represent average of triplicated measurements of samples from one cell culture study therefore statistical analysis was not performed.

3.3 Further evaluation of collagens and fibronectin

To confirm some of the results of the RT-qPCR array Col1a1, Col3a1 and Fn1 mRNA expression was studied using standard RT-qPCR. These molecular markers were chosen as they are known to be important in TIF. In addition, Col1a2 mRNA expression was explored as it is also important in fibrosis and was not included in the array. As well as the 48 h time point used in the RT-qPCR array, changes in mRNA expression at 6 h and 24 h were also studied.

Col1a1 mRNA expression was significantly suppressed by tRA and dual treatment at 24 h; by 48 h this effect of tRA alone had disappeared although there was a trend towards reduced Col1a1 mRNA expression by dual compared to TGF-β1 treatment (Figure 3.3A). Col1a2 mRNA was significantly suppressed at 48 h by tRA and there was a non-significant suppression by dual treatment compared to TGF-β1 treatment at this time point. There was a trend towards Col1a2 mRNA suppression by tRA at 24 h that reached significance in the dual treatment group and there was a significant suppression of Col1a2 mRNA by dual- versus TGF-β1 treatment at this time point (Figure 3.3B). Col3a1 mRNA expression was significantly suppressed at 24 h by tRA, however at 48 h there was an induction of Col3a1 mRNA in all three groups. There was a non-significant reduction in Col3a1 by dual treatment compared to TGF-β1 treatment at the 6 h, 24 h and 48 h time points (Figure 3.3C). Finally, Fn1 mRNA was significantly suppressed at 24 h by tRA although the effect did not reach significance at 48 h. There was a significant suppression of Fn1 expression by dual compared to TGF-β1 treatment at 24 h, an effect that appeared to be reversed at the 48 h time point (Figure 3.3D).

Standard RT-qPCR results at the 48 h time point for Col1a1 and Col3a1 were in agreement with results from the RT-qPCR array. However, results for Fn1 did differ between the two techniques: While tRA tended to down-regulate Fn1 mRNA in both standard RT-qPCR and the RT-qPCR array, there was evidence of Fn1 mRNA suppression following dual versus TGF-β1 treatment in the RT-qPCR array with no such trend seen for standard RT-qPCR.

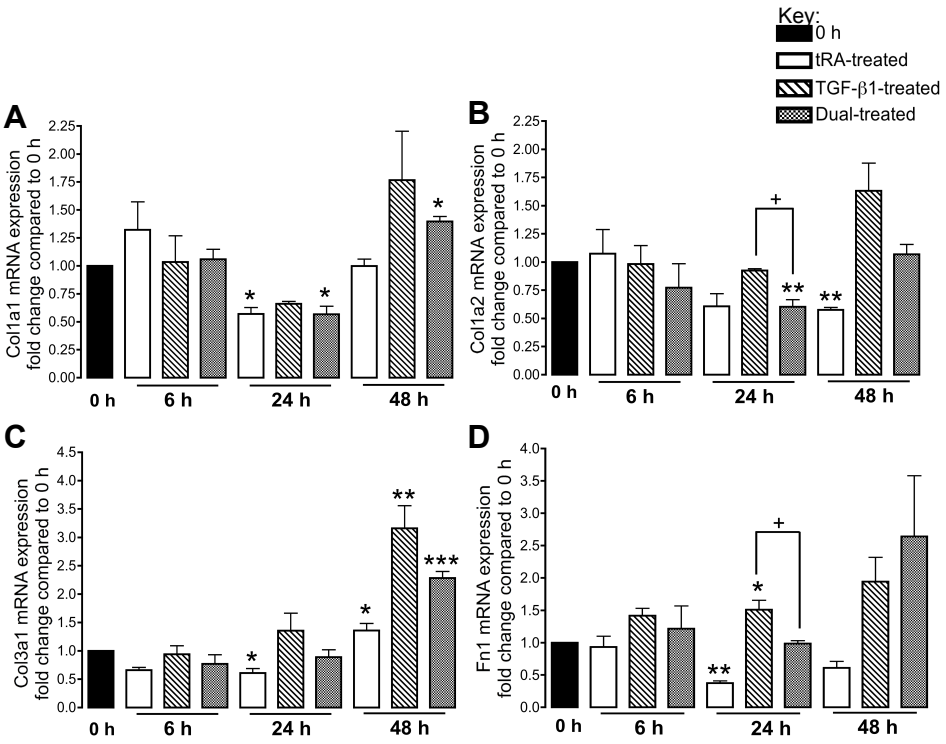

Figure 3.3. Effect of tRA in the absence and presence of TGF-β1 on Col1a1, Col1a2, Col3a1 and Fn1 mRNA expression. NRK-49F cells were cultured as per protocol and treated with 2 μM tRA with and without 5 ng/ml TGF-β1 for 0, 6, 24 or 48 h. Total RNA was extracted at 48 h and two-step RT-qPCR performed to determine changes in mRNA expression of Col1a1 (**A**), Col1a2 (**B**), Col3a1 (**C**) and Fn1 (**D**). Results were normalised to Gapdh and are presented as fold change compared to 0 h. Data represent mean ± SEM of 3 independent cell culture studies; clear bars= tRA-treated group, striped bars= TGF-β1-treated group, chequed bars= dual-treated group. Statistical analysis was performed on transformed data using repeated measures ANOVA. * $p<0.05$, ** $p<0.01$, *** $p<0.001$ vs 0 h group; + $p<0.05$, ++ $p<0.01$, +++ $p<0.001$ between groups indicated.

Because there was evidence of a dual effect of tRA on fibrosis at the level of gene expression, further analysis of collagens and FN at the protein level was done. Immunocytochemistry of collagen types I, III and IV suggested that the increase in PSR staining by tRA with and without TGF-β1 was due, at least in part, to increases in collagen types I and III (Figure 3.4), but not type IV (data not shown). Western blot analysis showed that FN protein expression was not altered by tRA treatment although dual treatment with tRA and TGF-β1 caused a trend towards an increase in FN compared to TGF-β1 treatment alone (Figure 3.5).

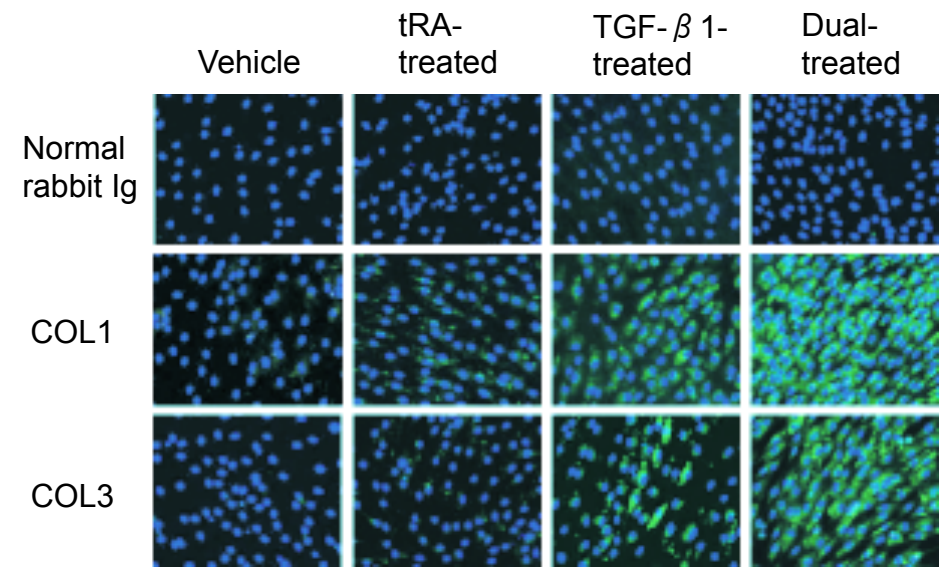

Figure 3.4. Effect of tRA in the absence and presence of TGF-β1 on collagen types I and III protein expression using immunocytochemistry. NRK-49F cells were cultured as per protocol and treated with 2 µM tRA with and without 5 ng/ml TGF-β1 for 48 h. Cells were fixed with 4% paraformaldehyde, permeabilised with 0.1% Triton X-100 and blocked with 1% BSA before the addition of primary then secondary antibodies. Staining of collagen types I and III was visualised using fluorescence microscopy x100 magnification.

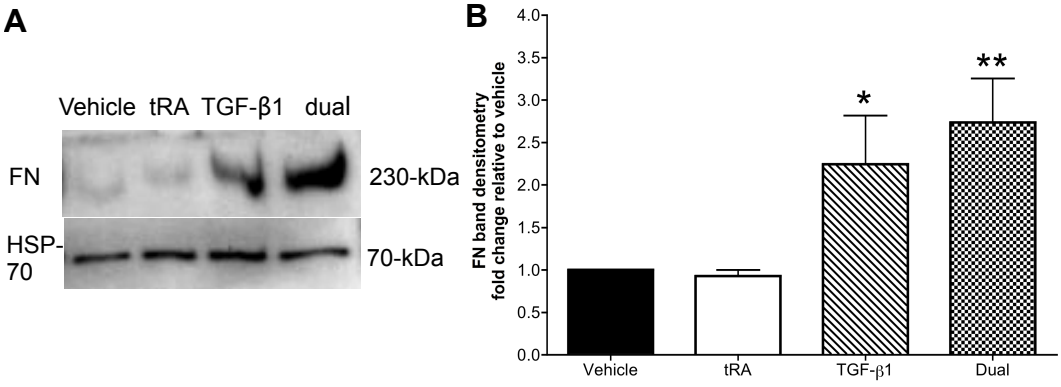

Figure 3.5. Effect of tRA in the absence and presence of TGF-β1 on FN protein expression using Western blot analysis. Total cell lysate was extracted from NRK-49F cells cultured as per the protocol and treated with 2 µM tRA with and without 5 ng/ml TGF-β1 for 48 h. Total cell lysate was loaded and run on 6% polyacrylamide gels under reducing and denaturing conditions then transferred onto a nitrocellulose membrane before blocking with 5% milk blocking solution and immunoprobing. **A**- Representive immunoblot of FN with HSP-70 used as a loading control; **B**- fold change of FN band densitometry relative to vehicle and normalised to HSP-70 loading control. Data represent mean ± SEM of 3 independent cell culture studies. Statistical analysis was done on transformed data using repeated measures ANOVA. * $p<0.05$, ** $p<0.01$ vs vehicle-treated group.

3.4 Further evaluation of MMPs

Results from the RT-qPCR array suggested that tRA in the absence and presence of TGF-β1 down-regulated several MMPs. To confirm these results standard RT-qPCR was performed on Mmps -2, -3 and -13. These MMPs were chosen for further evaluation because of their biological significance in fibrosis and because their Ct values were less than 30 suggesting that they might be expressed at protein level and play a role in matrix turnover in this cell model.

tRA caused a significant suppression of Mmp-2 mRNA at 24 h followed by an up-regulation at 48 h; dual treatment compared to TGF-β1 treatment alone caused a suppression of Mmp-2 at 24 h and 48 h (Figure 3.6A). Mmp-3 mRNA expression was significantly reduced in all three treatment groups at 24 h and 48 h and dual treatment compared to TGF-β1 treatment alone caused a significant suppression at 48 h (Figure 3.6B). Finally, tRA treatment caused a non-significant increase in Mmp-13 mRNA at 6 h followed by a significant suppression at 24 h in all three treatment groups (Figure 3.6C). These results were consistent with the RT-qPCR array data.

Although the majority of Mmps were down-regulated by tRA with and without TGF-β1 at the level of gene expression, the Timps were also down-regulated. Therefore, to determine whether tRA altered MMP activity as well as gene expression, NRK-49F total cell lysates were subjected to an MMP activity assay. The positive control of 0.025-0.2 U/ml *Clostridium* collagenase caused an increase in fluorescence confirming that the assay was working properly (data not shown). tRA and TGF-β1 both caused a significant reduction in fluorescence compared to the vehicle-treated group although no additive effect was observed in the dual-treated group (Figure 3.7).

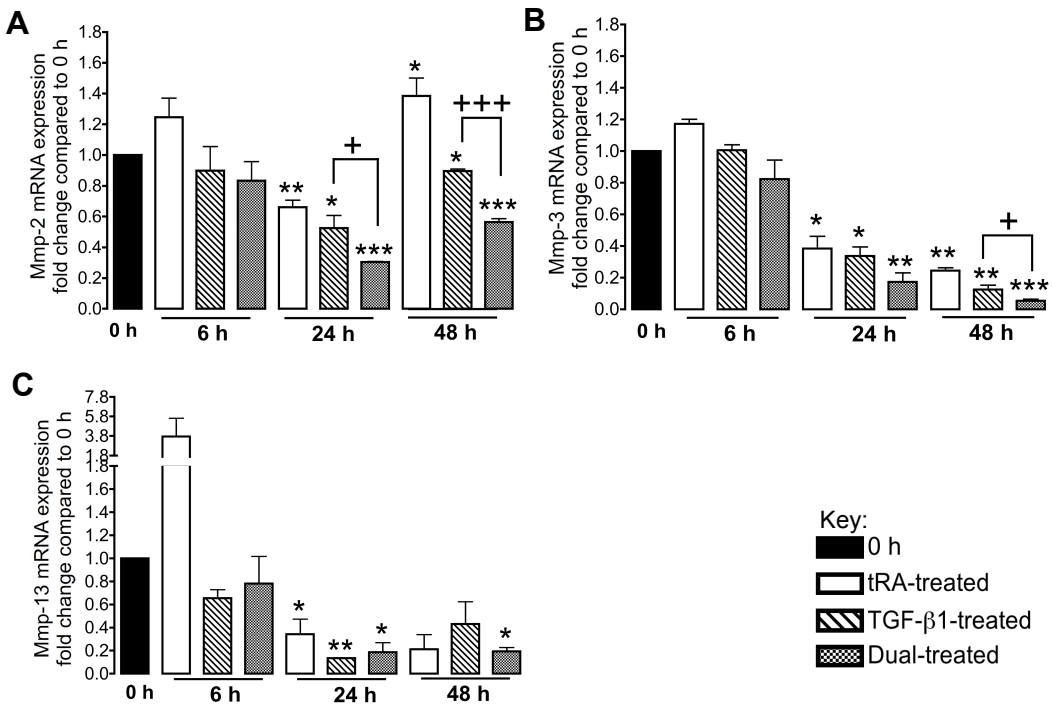

Figure 3.6. Effect of tRA in the absence and presence of TGF-β1 on Mmp-2, Mmp-3 and Mmp-13 mRNA expression. NRK-49F cells were cultured as per protocol and treated with 2 μM tRA with and without 5 ng/ml TGF-β1 for 0, 6, 24 or 48 h. Total RNA was extracted at 48 h and two-step RT-qPCR performed to determine changes in mRNA expression of Mmp-2 (**A**), Mmp-3 (**B**) and Mmp-13 (**C**). Results were normalised to Gapdh and are presented as fold change compared to 0 h. Data represent mean ± SEM of 3 independent cell culture studies; clear bars= tRA-treated group, striped bars= TGF-β1-treated group, chequed bars= dual-treated group. Statistical analysis was performed on transformed data using repeated measures ANOVA. *p<0.05, **p<0.01, ***p<0.001 vs 0 h; + p<0.05, ++ p<0.01, +++ p<0.001 between groups indicated.

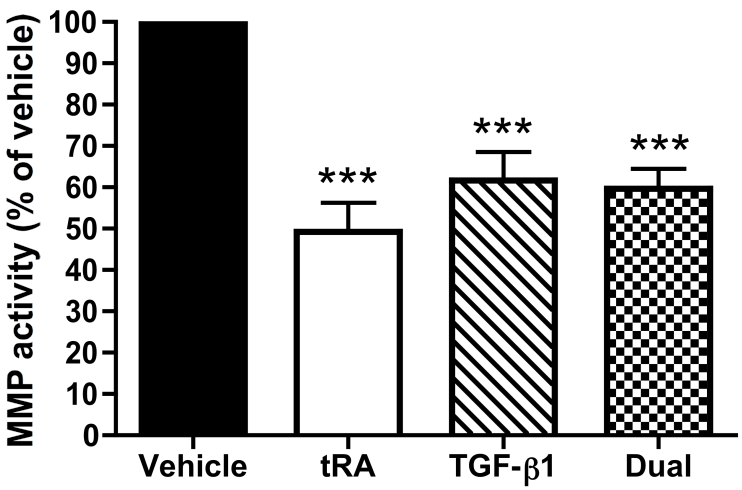

Figure 3.7. Effect of tRA in the absence and presence of TGF-β1 on MMP activity. NRK-49F cells were cultured as per protocol and treated with 2 μM tRA with and without 5 ng/ml TGF-β1. Total cell lysates were subjected to Molecular Probes' EnzChek Gelatinase/ Collagenase Assay as per manufacturer's guidelines. The reactions were incubated at room temperature for 2 h and fluorescence measured using a microplate reader with excitation at 485 +/- 20 nm and emission detection at 530 nm +/- 20 nm. Background fluorescence was subtracted from each value. Data represent mean +/- SEM of % change in fluorescence compared to vehicle-treated cells of 3 independent cell culture studies. Statistical analysis was done using repeated measures ANOVA. *** $p<0.001$ vs vehicle-treated cells.

3.5 Evaluation of other important molecular markers

The RT-qPCR array was a catalogued item and did not include all genes involved in fibrogenesis therefore the expression of some additional fibrogenic markers were examined using standard RT-qPCR.

The mRNA expression of Tgfbs 1-3 was examined as, although TGF-β1 is generally considered to be the major TGF-β isoform causing TIF, there is evidence that TGF-β2 and TGF-β3 also play a role (Figure 3.8A-C). TGF-β1 treatment caused a significant increase in Tgfb1 gene expression at 6 h consistent with TGF-β1 auto-induction; dual treatment caused a non-significant increase in Tgfb1 at the same time point although no additive effect of tRA compared to TGF-β1 alone was observed (Figure 3.8A). Conversely,

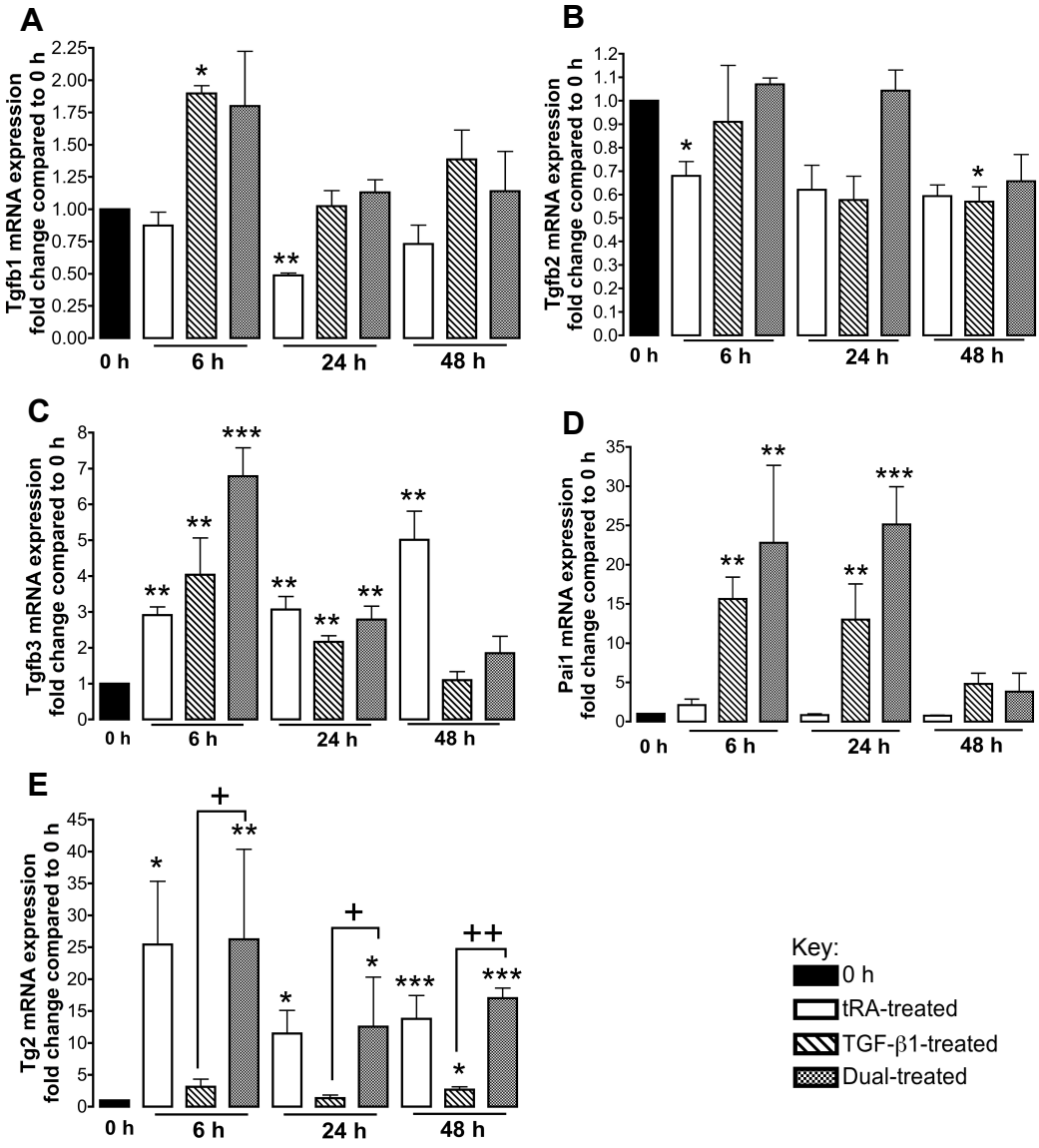

Figure 3.8. Effect of tRA in the absence and presence of TGF-β1 on Tgfb1, Tgfb2, Tgfb3, Pai1 and Tg2 mRNA expression. NRK-49F cells were cultured as per protocol and treated with 2 μM tRA with and without 5 ng/ml TGF-β1 for 0, 6, 24 or 48 h. Total RNA was extracted at 48 h and two-step RT-qPCR performed to determine changes in mRNA expression of Tgfb1 (**A**), Tgfb2 (**B**), Tgfb3 (**C**), Pai1 (**D**) and Tg2 (**E**). Results were normalised to Gapdh and are presented as fold change compared to 0 h. Data represent mean ± SEM of 3 independent cell culture studies; clear bars= tRA-treated group, striped bars= TGF-β1-treated group, chequed bars= dual-treated group. Statistical analysis was performed on transformed data using repeated measures ANOVA. *p<0.05, **p<0.01, ***p<0.001 vs 0 h; + p<0.05, ++ p<0.01 between groups indicated.

tRA significantly suppressed Tgfb1 at 24 h with evidence of on-going non-significant suppression at 48 h (Figure 3.8A). tRA suppressed Tgfb2 gene expression at 6 h with a tendency towards ongoing suppression at 24 and 48

h and at 48 h following dual treatment (Figure 3.8B). In contrast, Tgfb3 gene expression was induced by tRA, further increased by TGF-β1 and increased still more by dual treatment at 6 h; tRA treatment continued to cause a significant increase in Tgfb3 at 24 and 48 h but this induction was only maintained at 24 h in the dual treatment group (Figure 3.8C).

Pai1 and Tg2 gene expression were also studied. TGF-β1 caused a significant increase in Pai1 that was further increased by the addition of tRA at the 6 h and 24 h time points; tRA treatment alone caused a smaller, non-significant increase in Pai1 gene expression at 6 h (Figure 3.8D). tRA and dual treatment both caused a significant induction of Tg2 at 6, 24 and 48 h (Figure 3.8E).

3.6 Further investigation of the association between tRA-induced collagen accumulation and plasminogen activator inhibitor (PAI)-1

3.6.1 PAI-1 protein expression

As 2 μM tRA in the presence of 5 ng/ml TGF-β1 caused a significant increase in PAI-1 mRNA in NRK-49F cells with a smaller increase seen with tRA treatment alone, Western blot analysis was performed to determine whether PAI-1 protein was also modulated by tRA with and without TGF-β1. Both total cell lysates and conditioned media were studied as PAI-1 exerts its effects extracellularly. In total cell lysates and conditioned media, the anti-PAI-1 rabbit polyclonal antibody recognised a single band at ~50-kDa corresponding to the expected molecular weight of PAI-1 (Figure 3.9). In total cell lysates, both tRA and TGF-β1 induced a trend towards an increase in PAI-1 protein levels and dual treatment significantly increased PAI-1 protein expression; in conditioned media, PAI-1 protein was significantly increased by tRA treatment with further increases observed with TGF-β1 and dual treatment (Figure 3.9).

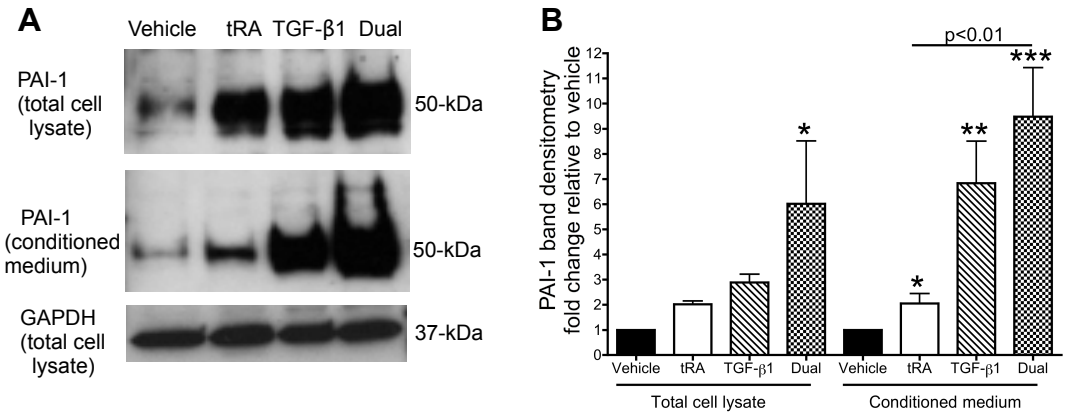

Figure 3.9. Western blot analysis of PAI-1 protein in NRK-49F total cell lysate and conditioned media. NRK-49F cells were cultured and treated as per protocol and total cell lysate and conditioned media were collected. Western blot analysis was performed using 10% polyacrylamide gels and membranes immunoprobed with rabbit polyclonal antibody to PAI-1. GAPDH was used as a loading control. **A**- Representative Western blot of PAI-1 protein; **B**- PAI-1 band densitometry presented as fold change compared to vehicle and normalised to GAPDH. Data represent mean ± SEM of 3 independent cell culture studies. Statistical analysis was performed on transformed data using repeated measures ANOVA. * $p<0.05$, ** $p<0.01$, *** $p<0.001$ vs vehicle-treated group.

3.6.2 Effect of the PAI-1 inhibitor tiplaxtinin on tRA-induced collagen accumulation

To determine if tRA-induced total collagen accumulation could be prevented by PAI-1 inhibition, cells were pre-treated for 2 h with the PAI-1 inhibitor tiplaxtinin then treated with 2 μM tRA and/or 5 ng/ml TGF-β1 for 48 h. Tiplaxtinin was chosen for use in experiments as it is the optimal PAI-1 inhibitor currently available commercially (Professor Daniel Lawrence, Ann Arbor, Michigan, USA, personal communication). However its use is limited by cytotoxicity. This is a particular problem as the Kd of tiplaxtinin is 480 nM and IC_{50} is 2.7 μM (Elokdah, Abou-Gharbia et al. 2004) therefore high concentrations are required to ensure PAI-1 inhibition.

Because of cytotoxicity at higher concentrations, doses of 1 and 2.5 μM tiplaxtinin were chosen for experiments (data not shown). As expected, a significant increase in PSR staining was observed following treatment of cells with tRA with and without TGF-β1 (Figure 3.10A). Tiplaxtinin at doses of 1 and

2.5 µM had no effect on PSR staining in vehicle and TGF-β1-treated cells, however 2.5 µM tiplaxtinin significantly reduced the increase in PSR staining caused by tRA and dual treatment (Figure 3.10A). There was a significant increase in LDH release by 2.5 µM tiplaxtinin although no significant increase in cell detachment index was demonstrated (Figure 3.10B, C).

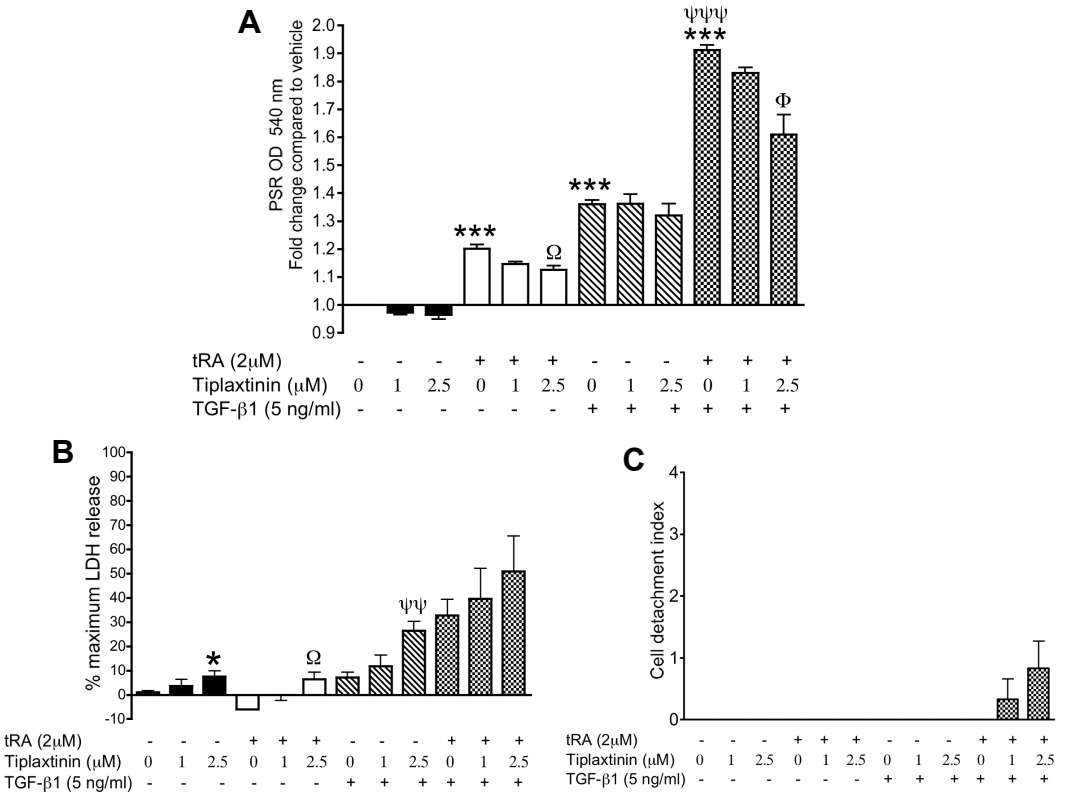

Figure 3.10. Effect of the PAI-1 inhibitor tiplaxtinin on tRA-induced total collagen accumulation. NRK-49F cells cultured as per protocol were treated with 0-2.5 µM tiplaxtinin, 2 µM tRA and/or 5 ng/ml TGF-β1 for 48 h. The effect on total collagen deposition was determined by spectrophotometric analysis of eluted PSR (**A**). Cytotoxicity was determined by LDH release (**B**) and cell detachment index (**C**). Data represent mean ± SEM of 3 independent cell culture studies. Statistical analysis was performed on transformed data using repeated measures ANOVA for A and using repeated measures ANOVA for B and C. * $p<0.05$, *** $p<0.001$ vs vehicle; ψψ $p<0.01$, ψψψ $p<0.001$ vs TGF-β1-treated group; Ω $p<0.05$ vs tRA-only treated group; Φ $p<0.05$ vs dual-treated group only.

3.7 Further investigation of the association between tRA-induced collagen accumulation and transglutaminase 2 (TG2)

3.7.1 TG2 protein expression

tRA at a dose of 2 μM in the absence and presence of 5 ng/ml TGF-β1 caused a significant increase in TG2 mRNA in NRK-49F cells. Therefore further experiments were performed to determine whether TG2 was also expressed at protein level and modulated by tRA.

Western blot analysis using anti-TG2 CUB7402 mouse monoclonal antibody was initially employed to determine whether NRK-49F cells expressed TG2 protein. Conditioned media was examined as well as NRK-49F total cell lysate as TG2 exerts its effects both intra- and extra-cellularly. Two bands were identified at ~70-kDa in NRK-49F total cell lysate and one band was seen at ~70-kDa in conditioned media (Figure 3.11). These bands were smaller than the expected molecular weight of TG2 of 75-85-kDa. There were also some smaller bands and larger bands observed at ~50-kDa and ~225-kDa, respectively, in NRK-49F total cell lysate (Figure 3.11).

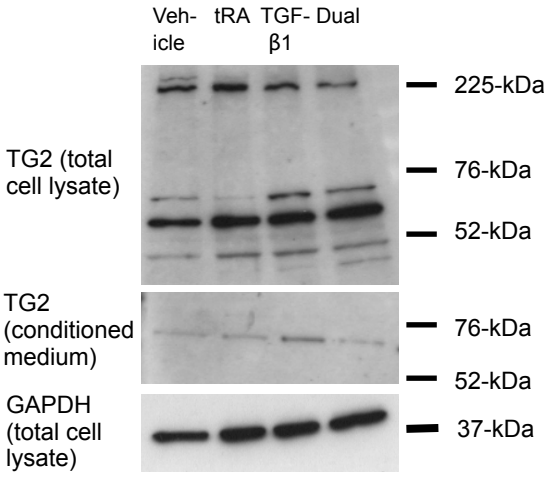

Figure 3.11. Western blot analysis of TG2 protein in NRK-49F total cell lysate and conditioned media using anti-TG2 CUB7402 mouse monoclonal antibody. NRK-49F cells were cultured and treated as per protocol and total cell lysate and conditioned media collected. Western blot analysis was performed using 8% polyacrylamide gels. Membranes were immunoprobed using CUB7402 mouse monoclonal antibody to TG2. GAPDH was used as a loading control.

Because it was unclear from TG2 Western blot analysis which bands, if any, represented TG2 protein, further determination of the effects of tRA was not done. Instead, LC/MS/MS analysis was performed on protein extracted from the ~70-kDa bands to confirm their identity (designated AR2_1 and AR2_2). These bands were chosen for further analysis because they were closest to the expected molecular weight of TG2.

Gel electrophoresis of NRK-49F total cell lysate using an 8% polyacrylamide gel was used to separate NRK-49F protein by weight then Coomassie blue staining was performed to identify the bands of interest, which were then cut out and analysed by mass spectrometry (Figure 3.12A, B). TG2 was not identified in samples using LC/MS/MS although other proteins between 50.9- and 83-kDa were present suggesting that the correct bands had been excised from the gel (please refer to Appendix, Supplementary table 4 for full list of proteins identified).

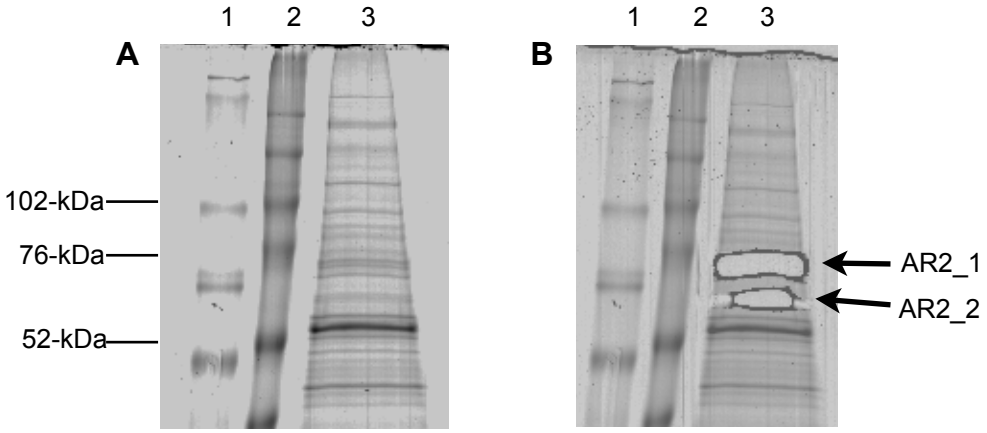

Figure 3.12. Colloidal Coomassie blue-stained electrophoresis gel of NRK-49F total cell lysate. NRK-49F total cell lysate was run on an 8% polyacrylamide gel under reducing and denaturing conditions then stained with brilliant blue G-colloidal Coomassie stain. **A**- Colloidal Coomassie blue-stained gel with colour markers; **B**- Colloidal Coomassie-stained gel following excision of the protein bands of interest (AR2_1 and AR2_2). Lanes 1 and 2- colour markers; Lane 3- NRK-49F total cell lysate.

Since TG2 protein was not identified in NRK-49F total cell lysates by mass spectrometry, Western blot analysis was revisited, this time using a positive control and a different anti-TG2 mouse monoclonal antibody, IA12. A band at ~76-kDa for both recombinant rat TG2 protein and NRK-49F total cell lysate

suggesting the presence of TG2 in NRK-49F total cell lysate and conditioned media (Figure 3.13Ai, Bi). However tRA with and without TGF-β1 did not alter TG2 protein expression significantly as determined by band densitometry although there was a trend towards an increase in dual-treated cells in NRK-49F total cell lysate (Figure 3.13Aii, Bii).

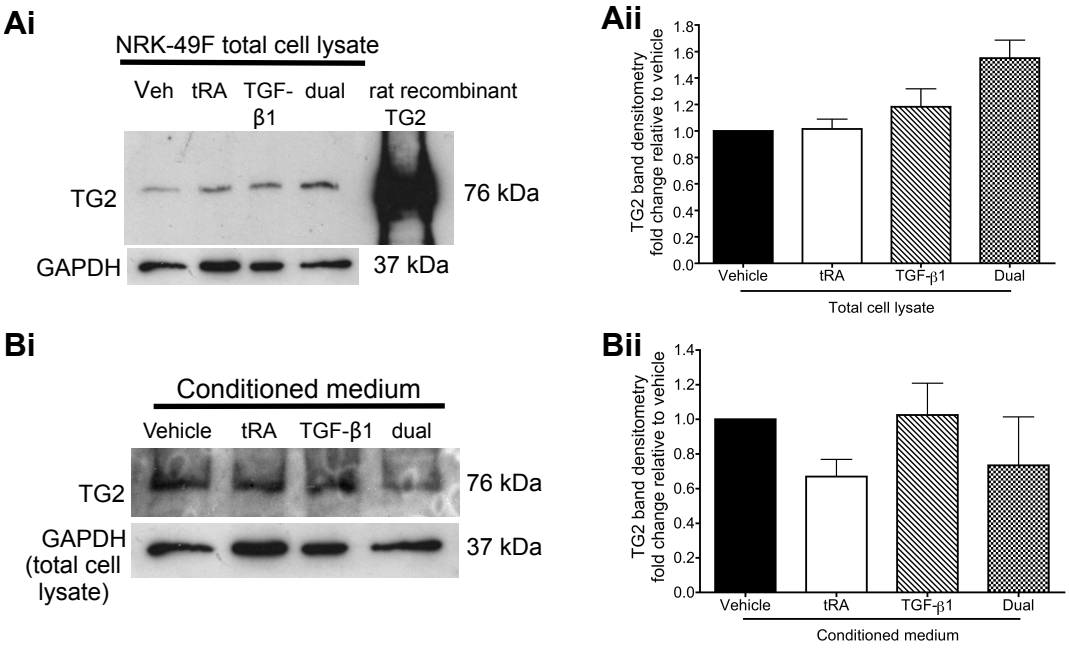

Figure 3.13. Western blot analysis of TG2 protein in NRK-49F total cell lysate and conditioned media using anti-TG2 IA12 mouse monoclonal antibody. NRK-49F cells were cultured and treated as per protocol and total cell lysate and conditioned media collected. Western blot analysis was performed using 8% polyacrylamide gels as before. Membranes were immunoprobed using IA12 mouse monoclonal antibody and GAPDH was used as a loading control. **Ai, Bi**- Western blot of NRK-49F total cell lysate (using rat recombinant TG2 as a positive control) and conditioned medium, respectively; **Aii, Bii**- TG2 band densitometry of NRK-49F total cell lysate and conditioned medium, respectively. Band densitometry data was presented as mean ± SEM fold change compared to vehicle and normalised to GAPDH of 3 independent cell culture studies. Statistical analysis was performed on transformed data using repeated measures ANOVA.

3.7.2 Effect of the TG2 inhibitor NTU283 on tRA-induced collagen accumulation

Although there was no significant change in TG2 protein expression in NRK-49F cells treated with tRA with or without TGF-β1, the effect of reducing TG2 activity on tRA-induced collagen accumulation was explored to further rule out that TG2 was contributing to the pro-fibrotic effects of tRA.

Figure 3.14 illustrates the effects of the TG2 inhibitor NTU283 at doses of 33-99 μM (Skill, Johnson et al. 2004) on PSR staining in NRK-49F cells treated with 0.2-2 μM tRA with and without 5 ng/ml TGF-β1. NTU283 alone had no effect on PSR staining however it caused a significant decrease in PSR staining in TGF-β1-treated cells (Figure 3.14Ai, Bi). There was a non-significant increase in PSR staining in cells treated with 0.2 μM tRA, which was further increased by the addition of 33-99 μM NTU283; a higher dose of 2 μM tRA did significantly increase PSR staining, which was further increased by NTU283 (Figure 3.14Ai). In the presence of TGF-β1, 0.2 and 2 μM tRA significantly increased PSR staining as expected, and PSR staining was increased further by NTU283 (Figure 3.14Bi). More cell detachment was observed in dual-treated cells with and without NTU283 (Figure 3.14Aii, Bii).

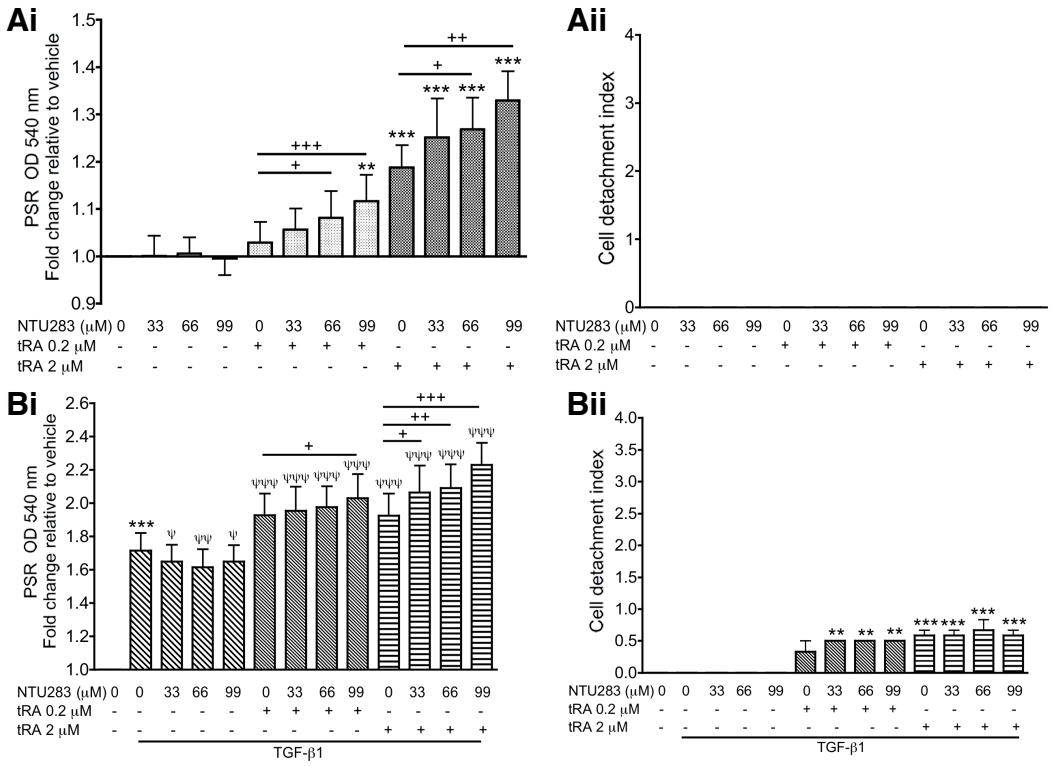

Figure 3.14. Effect of TG2 inhibitor NTU283 on tRA-induced total collagen accumulation. NRK-49F cells cultured as per protocol were pre-treated with NTU283 for 2 h then 0.2-2 μM tRA +/- 5 ng/ml TGF-β1 for 48 h. **Ai** and **Bi**- effect of NTU283 on PSR staining in tRA- and dual-treated cells, respectively; **Aii** and **Bii**- effect of NTU283 on cell detachment index in tRA- and dual-treated cells, respectively. Data for Ai and Bi represent mean ± SEM fold change relative to vehicle-treated cells and for Aii and Bii data represent mean ± SEM of 3 independent cell culture studies. Statistical analysis for Ai and Bi was performed on transformed data using repeated measures ANOVA and for Aii and Bii a repeated measures ANOVA was used. ** $p<0.01$, *** $p<0.001$ vs vehicle; ψ $p<0.05$, ψψ $p<0.01$, ψψψ $p<0.001$ vs TGF-β1-treated group; + $p<0.05$, ++ $p<0.01$, +++ $p<0.001$ between groups indicated.

3.8 Discussion

In this work, a novel *in vitro* model for the dose-dependent, pro-fibrotic effects of tRA has been established in a rat kidney fibroblast cell line supporting the hypothesis that tRA's fibrogenic effects are mediated through renal fibroblasts. Possible mechanisms through which tRA exerted its pro-fibrotic effects in this model included modulation of matrix degradation pathways, as there was evidence for reduced MMP expression and activity, and increased PAI-1 protein expression. Increased collagen production was less likely to play a role since the majority of collagen mRNAs were down-regulated by tRA with and without TGF-β1.

To establish the net effect of tRA on fibrosis *in vitro*, PSR was used to stain for total collagen protein. It is well accepted that excessive collagen accumulation causes TIF therefore this was a relevant method to use especially as it allowed quantification of collagen deposition. Since tRA can be toxic at high doses, which would affect the readout for the 2D *in vitro* model of fibrosis, two methods were used to determine cytotoxicity: Cell detachment index and LDH release from cells. There was agreement between the two assays that higher doses of tRA in the presence of TGF-β1 increased cytotoxicity and that treatment with tRA alone did not increase cell detachment or LDH release significantly (Figure 3.1D, E). These results suggest that the two methodologies for measuring cytotoxicity were comparable.

While at protein level tRA with and without TGF-β1 was pro-fibrotic, demonstrated by an increase in total collagen deposition and immunostaining for collagen types I and III (Figures 3.1 and 3.4), an RT-qPCR array showed a down-regulation as well as an up-regulation of various collagen mRNAs (Figure 3.2). Standard RT-qPCR of Col1a1, Col1a2, Col3a1 and Fn1 also showed differential regulation of fibrotic markers by tRA (Figure 3.3).

These results are important because they show that tRA can have directly opposing actions in the same cell model under the same conditions. Other published reports have also shown a dichotomous effect of RA in models of

renal fibrosis. For example, Xu et al. showed that tRA treatment suppressed selected fibrogenic molecular markers at the mRNA level in the kidneys of Alb/ TGF-β1 transgenic mice despite there being no evidence of improvement and even worsening of interstitial fibrosis with increasing doses of tRA (Xu, Hendry et al. 2010). In addition, this work shows that the time points chosen for measurements are also important when experimenting with tRA. tRA caused a biphasic response of Col3a1 and Mmp-2 mRNA demonstrating a time-dependent effect of tRA which has also been documented in other reports (Morath, Ratzlaff et al. 2009). Therefore, by selecting only a few molecular markers for experiments and variable time points to study, different biased conclusions could be drawn. These results also highlight the importance of confirming results obtained from screening tools such as RT-qPCR arrays as, although the results for Col1a1 and Col3a1 were consistent between the array and standard RT-qPCR, the results for Fn1 differed between the two techniques.

Since the RT-qPCR data did not definitively demonstrate evidence of an up-regulation of collagens to explain the pro-fibrotic effects of tRA, it was of interest that the majority of Mmps were down-regulated at mRNA level although there was also a down-regulation of Timps (Figure 3.2 and 3.6). In addition, PAI-1 expression was up-regulated by tRA alone and still more in the presence of TGF-β1 (Figure 3.9). Furthermore, an MMP activity assay demonstrated an overall reduction in MMP activity (Figure 3.7) and the PAI-1 inhibitor tiplaxtinin reduced the pro-fibrotic effects of tRA (Figure 3.10). tRA-induced reduced MMP activity may have been a result of reduced MMP expression but also decreased MMP activation as PAI-1 suppresses the conversion of plasminogen to plasmin, which is known to activate MMPs. Although caution should be applied when interpreting the effects of tiplaxtinin on tRA-induced collagen accumulation as tiplaxtinin caused significant cytotoxicity, overall, these results suggest decreased matrix degradation as a possible mechanism for the pro-fibrotic effect of tRA in NRK-49F cells.

MMP mRNA suppression by RA has been reported before as tRA suppresses ultraviolet irradiation-induced MMPs in human skin (Fisher and Voorhees 1998) and reduces plasma MMP activity and MMP9/TIMP-1 in cultured macrophages in patients with emphysema (Mao, Tashkin et al. 2003). A possible mechanism for this suppression is through inhibition of AP-1 as AP-1 binding sites have been identified in MMP genes (Benbow and Brinckerhoff 1997). tRA-induced PAI-1 expression has also been reported in VSMCs and may occur through tyrosine kinase-dependent pathways as tyrosine kinase inhibitors blocked retinoid-induced increase in PAI-1 mRNA in VSMCs (Watanabe, Kanai et al. 2002) or via retinoid receptor-dependent signalling through transcription factors such as Sp1 (Suzuki, Shimada et al. 1999).

tRA also caused a significant up-regulation of Tg2 mRNA in NRK-49F cells, which was further increased with the addition of TGF-β1 (Figure 3.8E). This result was not surprising because the TG2 gene has an RARE in its promoter (Nagy, Saydak et al. 1996; Yan, Noonan et al. 1996). However, TG2 protein was difficult to identify by both Western blot analysis and mass spectrometry in NRK-49F cells. Initially, TG2 immunoblotting using anti-TG2 CUB7402 mouse monoclonal antibody was performed and demonstrated multiple bands in NRK-49F total cell lysates that were not at the expected molecular weight for TG2 of 75-85-kDa (Figure 3.11). Two bands were identified at ~70-kDa, which could have represented TG2 protein, however, when protein extracted from the bands was analysed by LC/MS/MS, TG2 protein was not identified. Possible reasons that LC/MS/MS failed to identify TG2 protein in samples include: 1) Incorrect identification of the bands of interest from the polyacrylamide gel; 2) Absence of TG2 in NRK-49F total cell lysate; 3) The TG2 antibody was very sensitive and had a lower limit of detection than the mass spectrometer; and 4) Technical problems with TG2 identification by LC/MS/MS. The TG2 Western blot using anti-TG2 CUB7402 mouse monoclonal antibody also identified larger bands at 225-kDa, which might have consisted of TG2 bound to substrate and smaller bands at 50-kDa, which could have represented a shorter form of TG2, however it cannot be excluded that all the bands represented non-specific antibody binding (Figure 3.11).

Therefore Western blot analysis using another anti-TG2 mouse monoclonal antibody, IA12, was performed. This antibody recognised a band at ~76-kDa in NRK-49F total cell lysate and conditioned media similar to that identified in the positive control of recombinant rat TG2 protein and therefore was likely to represent TG2 protein (Figure 3.13). However, there was no evidence that tRA modulated TG2 protein expression either intra- or extra-cellularly using this method of TG2 protein detection (Figure 3.13). Furthermore, reducing TG2 activity using the TG2 inhibitor NTU283 did not prevent tRA-induced total collagen accumulation but rather potentiated the pro-fibrotic effect of tRA (Figure 3.14). This finding is consistent with some reports that TG2 might play a critical role in hepatic repair and a protective role in fibrosis (Nardacci, Lo Iacono et al. 2003). However, it may be that these fibrogenic effects of NTU283 were due to non-specific effects of the drug not related to TG2 inhibition especially as very little TG2 appeared to be present in conditioned media and published reports suggest that the major source of TG2 is tubular epithelial cells with only small contributions from mesangial and interstitial cells (Johnson, El-Koraie et al. 2003). Interestingly, NTU283 reduced the increase in PSR staining caused by TGF-β1 consistent with the role of TG2 as an activator of TGF-β1 (Figure 3.14) (Nunes, Gleizes et al. 1997).

In summary, the results presented in this chapter demonstrate a previously unreported dose-dependent, pro-fibrotic effect of tRA in an *in vitro* model of renal interstitial fibrosis and furthermore suggest possible mechanisms behind these detrimental effects of tRA. There are few reports of the effects of RA in renal fibroblast cell models to compare this work to perhaps partly because of the lack of availability of renal fibroblast primary cultures and cell lines. However, this work is somewhat similar to the effects of tRA in a transgenic mouse model of TIF caused by over-expression of TGF-β1, where high-dose tRA increased TIF (Xu, Hendry et al. 2010) akin to the pro-fibrotic effects of tRA in this *in vitro* model of TGF-β1-induced fibrosis presented here.

Chapter 4. Expression of retinoid nuclear receptors, PPARβ/δ and RA carrier proteins in NRK-49F cells

4.1 Expression of retinoid nuclear receptors and PPARβ/δ

4.1.1 mRNA expression of nuclear receptors

Results from the previous chapter showed that tRA treatment with and without TGF-β1 was able to modulate NRK-49F cell phenotype. Since RA is known to primarily signal via retinoid nuclear receptors, NRK-49F cells were characterised for retinoid nuclear receptor expression as a potential pathway through which tRA was exerting its effects. PPARβ/δ is also postulated to be a target receptor of tRA therefore the expression of this nuclear receptor was also studied (Shaw, Elholm et al. 2003).

mRNA expression of retinoid nuclear receptors and PPARβ/δ in NRK-49F cells was determined by extracting total RNA from quiescent cells then subjecting it to two-step RT-qPCR using pre-designed primers from SABiosciences and SYBR Green PCR technology. Relative quantification was used to compare expression of the different nuclear receptors on the assumption that the amplification efficiencies were similar between the targets (the standard curve method of absolute quantification could also have been used as an alternative to relative quantification). Of the tRA-binding nuclear receptors, Rara was the most highly expressed at mRNA level followed by Rarg then Pparbd; Rxrb was the most highly expressed RXR and Rxrg had the lowest mRNA expression relative to the other nuclear receptors (Figure 4.1).

4.1.2 Protein expression of nuclear receptors

Next the protein expression of the six retinoid nuclear receptors and PPARβ/δ was studied by Western blot analysis of NRK-49F total cell lysates. A single band was identified at ~50-52-kDa by the anti-RARα and anti-RARβ rabbit polyclonal antibodies corresponding to the expected molecular weight of RARα and RARβ proteins (Figure 4.2A, B). The anti-RARγ mouse

monoclonal antibody recognised two bands at ~50-52-kDa but only the 50-kDa band was present in the positive control of A431 nuclear extract, which is the expected molecular weight for RARγ (Figure 4.2C).

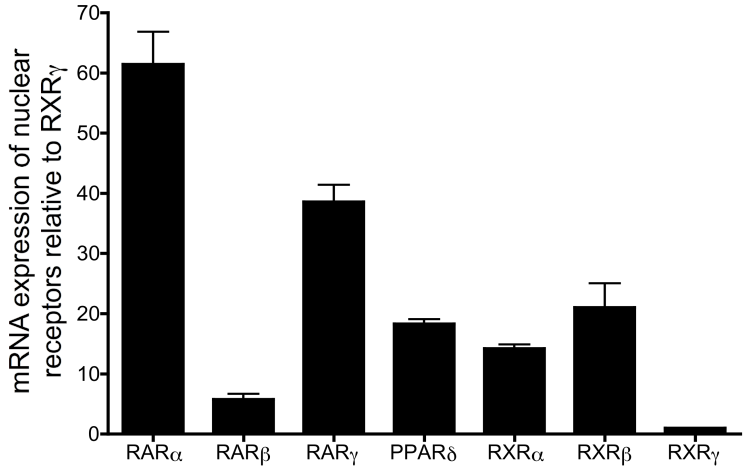

Figure 4.1. Relative mRNA expression of retinoid nuclear receptors and PPARβ/δ in NRK-49F cells. Total RNA was extracted from NRK-49F cells cultured for 3 d in DMEM supplemented with 2.5% FCS and 2.5% Nu then for 4 d in DMEM supplemented with ITS then two-step RT-qPCR was performed. mRNA expression of the retinoid nuclear receptors relative to the lowest expressed receptor, RXRγ, was determined. Data represent mean ± SEM of 9 independent cell culture studies.

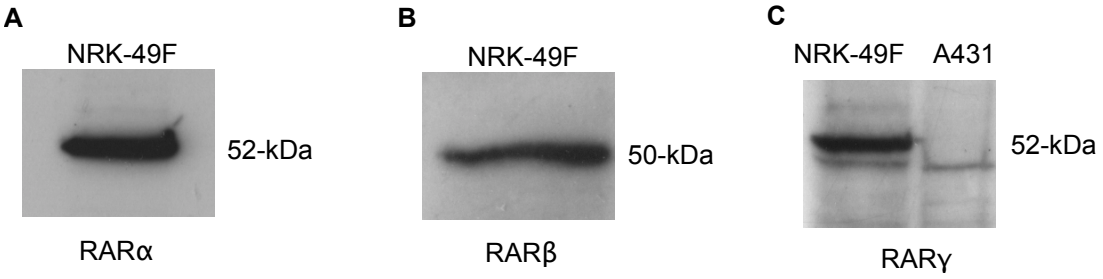

Figure 4.2. Western blot analysis of RARs. Total cell lysate was extracted from NRK-49F cells cultured as before and Western blot analysis performed using 10-12% polyacrylamide gels. Membranes were then subjected to immunoprobing. **A**- RARα immunoblot (1 in 20000 dilution of antibody); **B**- RARβ immunoblot (1 in 1000 dilution of antibody); **C**- RARγ immunoblot with A431 nuclear extract as a positive control (1 in 1000 dilution of antibody).

The rabbit polyclonal antibody to PPARβ/δ recognised multiple bands in NRK-49F total cell lysate, four of which were also present in the recommended positive control of Sol8 nuclear extract (Figure 4.3). The molecular weight of these bands were between 35- and 76-kDa. A blocking peptide was not available for this antibody.

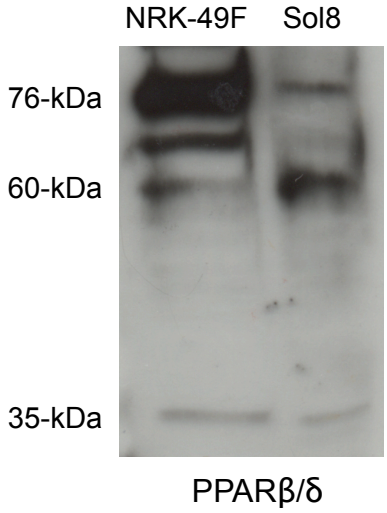

4.3. Western blot analysis of PPARβ/δ. Western blot analysis was performed on NRK-49F total cell lysate as before using 10% polyacrylamide gels. Membranes were immunblotted using a rabbit polyclonal antibody to PPARβ/δ (1 in 7500 antibody). Sol8 nuclear extract was used as a positive control.

Finally, RXR protein expression in NRK-49F total cell lysates was determined. Figure 4.4 shows relevant Ponceau S stains as well as representative RXR immunoblots to demonstrate equal protein loading where blocking peptides were used. The anti-RXRα rabbit polyclonal antibody recognised two bands at ~50-kDa and ~60-kDa (expected molecular weight 54-kDa) in both NRK-49F total cell lysate and the positive control of HeLa nuclear extract; these bands disappeared when the membrane was incubated with blocking peptide and antibody (Figure 4.4A). The rabbit polyclonal antibody to RXRβ recognised several bands in the positive control of HeLa nuclear extract, two of which were also present in NRK-49F total cell lysate at ~55-kDa and ~76-kDa (predicted molecular weight 48-kDa) (Figure 4.4B). A blocking peptide was not available for this antibody. Finally immunoprobing for RXRγ using a positive control of human RXRγ-transfected 293T total cell lysate revealed a cluster of bands with molecular weights ranging from ~52-kDa to 102-kDa for both NRK-49F total cell lysate and positive control. These blots were similar to the immunoblot on the Santa Cruz RXRγ antibody data sheet (see Appendix, Supplementary figure 1). These bands disappeared when the membrane was incubated with blocking peptide and antibody (Figure 4.4C).

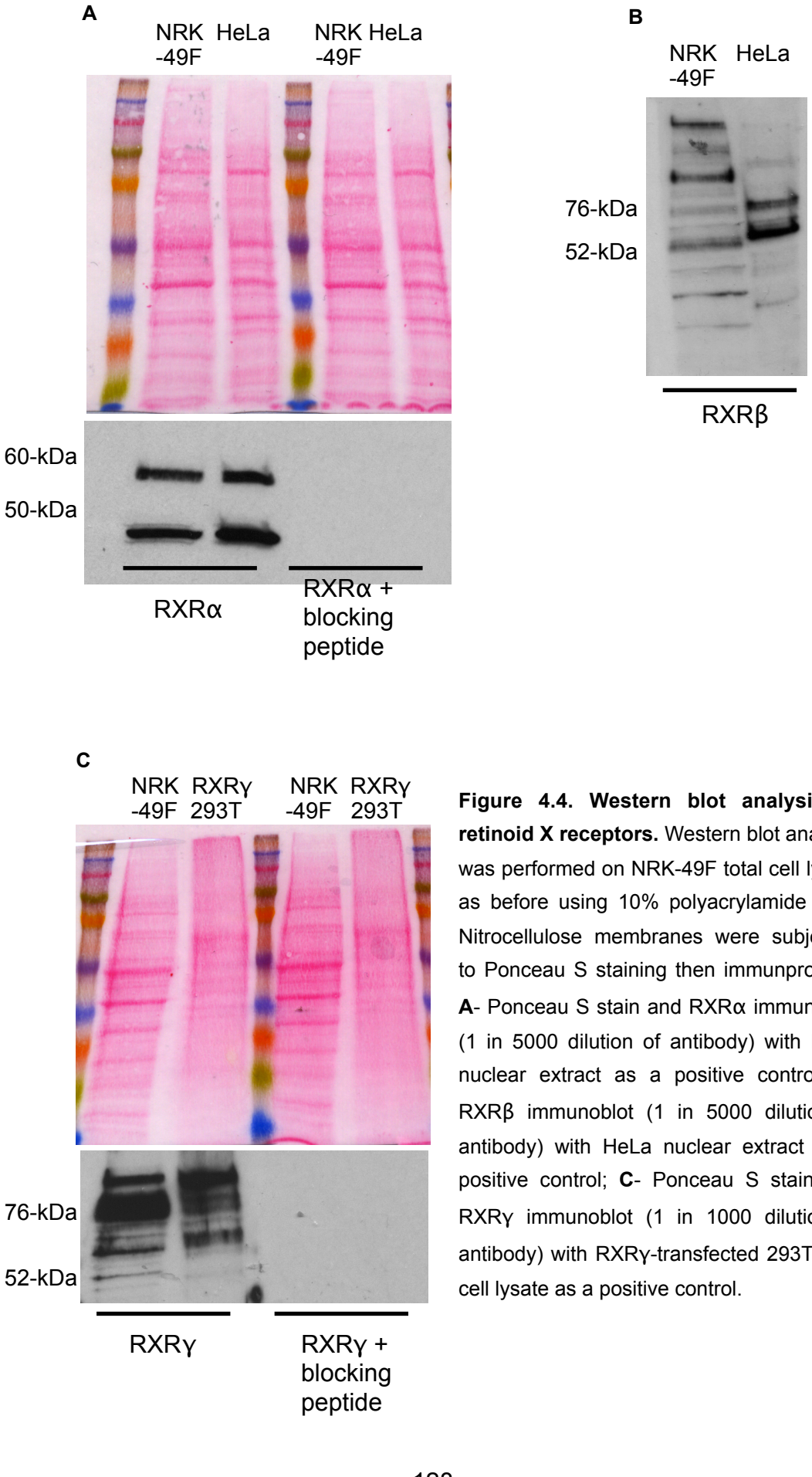

Figure 4.4. Western blot analysis of retinoid X receptors. Western blot analysis was performed on NRK-49F total cell lysate as before using 10% polyacrylamide gels. Nitrocellulose membranes were subjected to Ponceau S staining then immunprobing. **A**- Ponceau S stain and RXRα immunoblot (1 in 5000 dilution of antibody) with HeLa nuclear extract as a positive control; **B**- RXRβ immunoblot (1 in 5000 dilution of antibody) with HeLa nuclear extract as a positive control; **C**- Ponceau S stain and RXRγ immunoblot (1 in 1000 dilution of antibody) with RXRγ-transfected 293T total cell lysate as a positive control.

4.1.3 mRNA expression of nuclear receptors following treatment with tRA with and without TGF-β1

Since there was evidence that NRK-49F cells expressed retinoid nuclear receptors and possibly PPARβ/δ, change in nuclear receptor mRNA expression following treatment with 2 μM tRA with and without 5 ng/ml TGF-β1 was examined by standard two-step RT-qPCR.

tRA and dual treatment caused an early significant induction of Rara and Rarg mRNAs over 1-3 h and tRA also caused a later induction of Rarg mRNA at 48 h (Figure 4.5A, C). These inductions were followed by suppression of Rara mRNA by dual treatment at 6, 24 and 48 h and suppression of Rarb mRNA by tRA and dual treatment at 24 h and 48 h, respectively (Figure 4.5A, B). There was a significant suppression of Pparbd mRNA at 24 h in all three treatment groups (Figure 4.5D). Rxra, Rxrb and Rxrg mRNAs were all significantly suppressed by dual treatment at the 24 or 48 h time points (Figure 4.5E-G) and Rxra was also suppressed by treatment with tRA or TGF-β1 at 48 h (Figure 4.5E).

4.2 Expression of RA carrier proteins in NRK-49F cells

4.2.1 mRNA expression of RA carrier proteins

The expression of RA carrier proteins CRABP-II and FABP5 was also explored in NRK-49F cells because they have previously been reported to be important in the regulation of RA signalling (Dong, Ruuska et al. 1999; Tan, Shaw et al. 2002). Crabp2 and Fabp5 mRNA expression was determined by extracting total RNA from quiescent cells then subjecting it to two-step RT-qPCR using pre-designed primers and probes from Applied Biosystems and TaqMan technology.

Crabp2 mRNA was present at several hundred-fold higher levels than Fabp5 in NRK-49F cells (Figure 4.6). Fabp5 was expressed only at low levels, if at all, with Cts of 35 or above recorded by standard RT-qPCR.

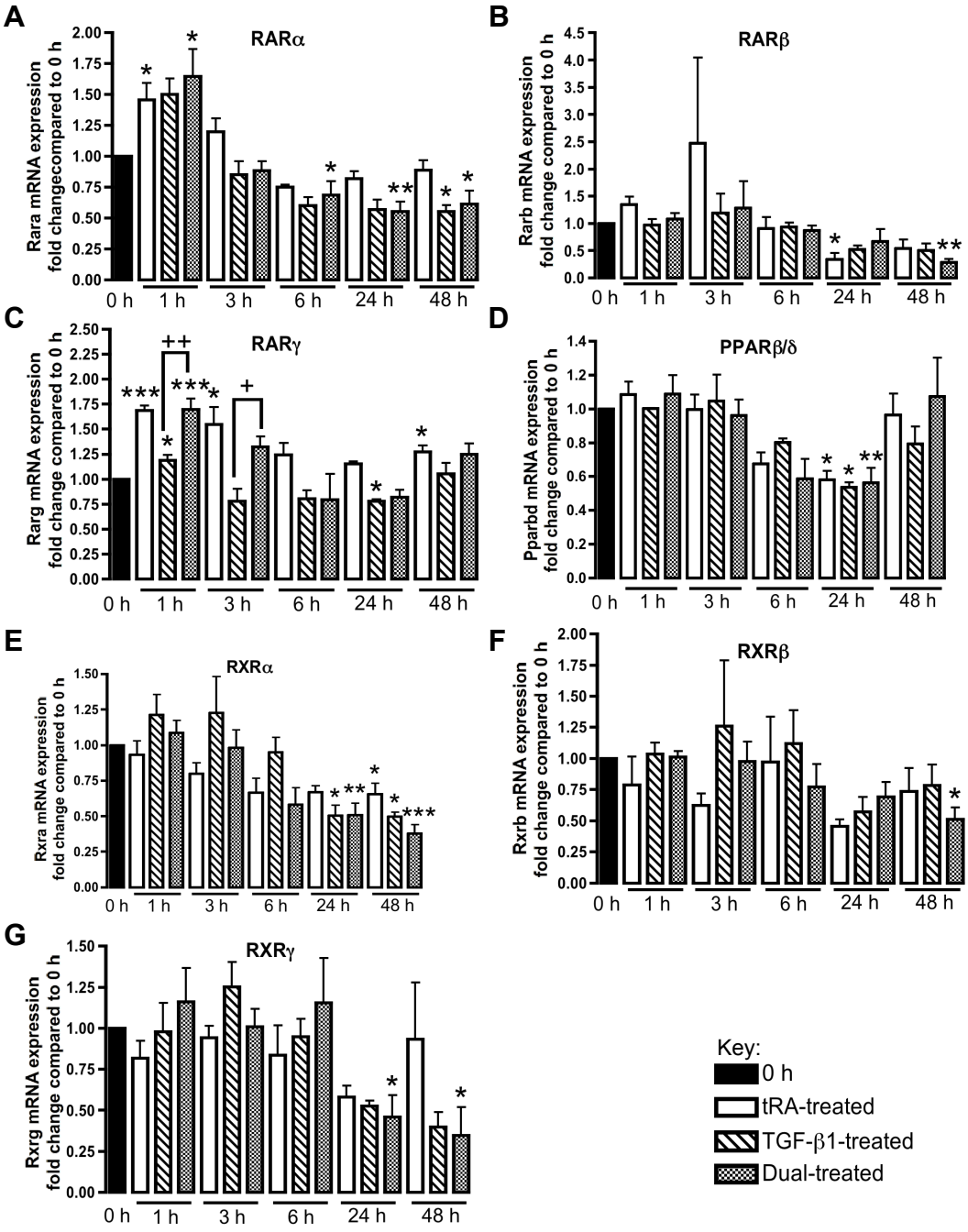

Figure 4.5. Change in mRNA expression of retinoid nuclear receptors and PPARβ/δ following tRA and TGF-β1 treatment. NRK-49F cells were cultured as per protocol and treated with 2 μM tRA with and without 5 ng/ml TGF-β1 for 0, 1, 3, 6, 24 or 48 h. Total RNA was extracted at 48 h and two-step RT-qPCR performed to determine changes in mRNA expression of Rara (**A**), Rarb (**B**), Rarg (**C**), Pparbd (**D**), Rxra (**E**), Rxrb (**F**) and Rxrg (**G**). Data represent mean ± SEM of 4 independent cell culture studies. Clear bars= tRA-treated group, striped bars= TGF-β1-treated group, chequed bars= dual-treated group. Statistical analysis was performed on transformed data using repeated measures ANOVA. * $p<0.05$, ** $p<0.01$, *** $p<0.001$ vs 0 h group; +$p<0.05$, ++$p<0.01$ between groups indicated.

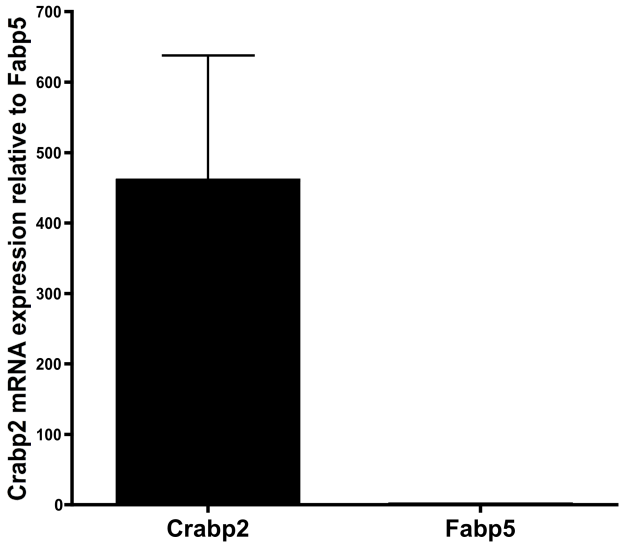

Figure 4.6. Relative mRNA expression of RA carrier proteins CRABP-II and FABP5 in NRK-49F cells. Total RNA was extracted from NRK-49F cells cultured as before then two-step RT-qPCR was performed. mRNA expression of the tRA carrier protein Crabp2 relative to Fabp5 was determined. Data represent mean ± SEM of 9 independent cell culture studies.

4.2.2 Protein expression of RA carrier proteins

Following the identification of CRABP-II and possibly FABP5 at mRNA level, their protein expression was explored by Western blot analysis of NRK-49F total cell lysate. A goat polyclonal antibody to CRABP-II recognised multiple bands in the positive control of NIH/3T3 total cell lysate and one band corresponded to the expected molecular weight of 15-kDa for CRABP-II protein (Figure 4.7). CRABP-II immunoprobing of NRK-49F total cell lysate also revealed multiple bands, four of which corresponded to bands seen in the positive control at ~20-, 31-, 35- and 80-kDa. The bands identified at 31-, 35- and 80-kDa disappeared with the addition of CRABP-II blocking peptide to the antibody (Figure 4.7).

A rabbit polyclonal antibody to FABP5 did not recognise any bands in NRK-49F total cell lysate although a positive control was not included to confirm that the technique had been successful (data not shown).

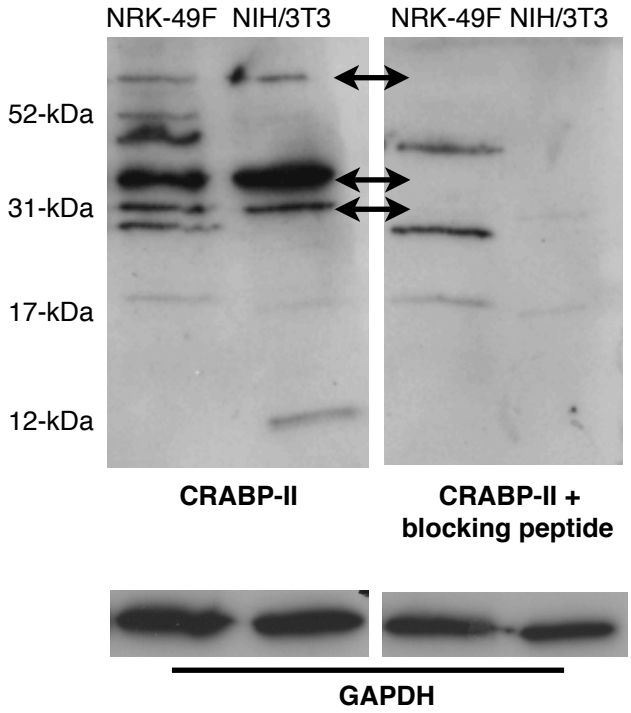

4.7. Western blot analysis of CRABP-II protein. Western blot analysis was performed on NRK-49F total cell lysate as before using 15% polyacrylamide gels. Membranes were subjected to immunoprobing with goat polyclonal antibody to CRABP-II (1 in 2000 dilution of antibody). NIH/3T3 total cell lysate was used as a positive control and GAPDH was used as a loading control. Arrows point to bands present in NRK-49F and NIH/3T3 total cell lysates that disappeared with the addition of blocking peptide.

Since immunoblotting did not definitively identify CRABP-II or FABP5 protein in NRK-49F cells, immunocytochemistry was also performed. However, there was no evidence of positive staining of cells with either an anti-CRABP-II goat polyclonal antibody or an anti-FABP5 rabbit polyclonal antibody although a positive control was not included to confirm that the technique had been successful (Figure 4.8).

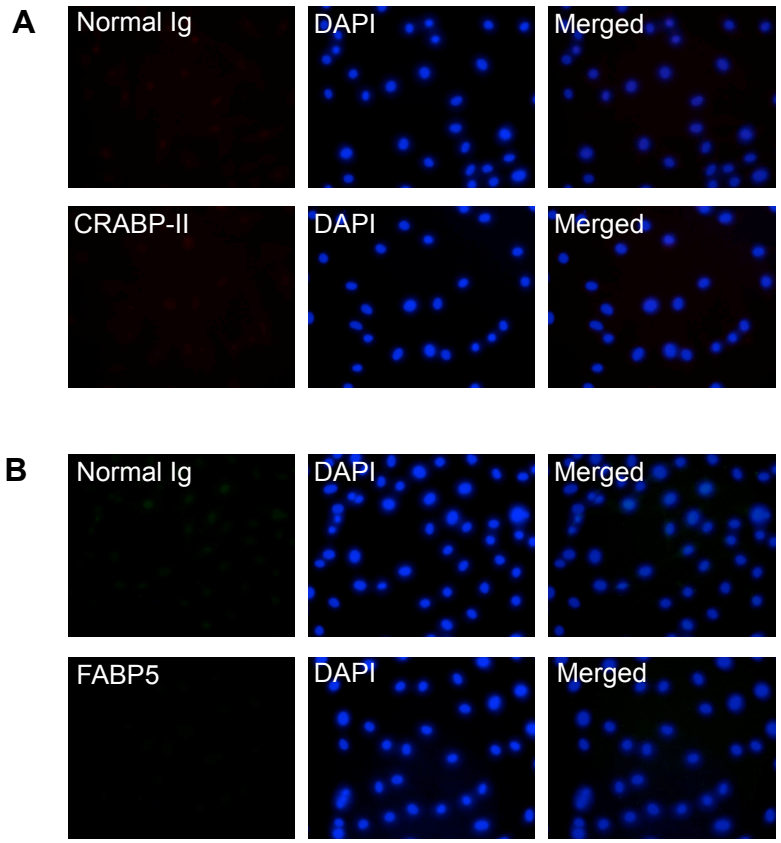

Figure 4.8. Immunocytochemistry of CRABP-II and FABP5 proteins. NRK-49F cells were fixed with paraformaldehyde and permeabilised with Triton X-100 then blocked with 1% BSA. Cells were then incubated with goat polyclonal antibody to CRABP-II (**A**) or rabbit polyclonal antibody to FABP5 (**B**) at a 1 in 100 dilution. Nuclei were counterstained with DAPI. Normal Ig was used as a negative control. (Fluorescence microscopy, x400 magnification).

Finally, since three bands at 31-, 35- and 80-kDa were identified by CRABP-II immunoblotting of both NRK-49F and NIH/3T3 total cell lysates, protein from these bands was extracted and further analysed by LC/MS/MS to determine whether CRABP-II protein was indeed present; in addition, protein from the 15-kDa band identified in NIH/3T3 total cell lysate was analysed to confirm the presence of CRABP-II in this band in the positive control (Figure 4.9). However, LC/MS/MS analysis did not identify CRABP-II protein in any of the selected samples (see Appendix, Supplementary table 4 for a list of proteins identified). Interestingly, CRABP-I and FABP5 proteins were present in protein from the 15-kDa band in NIH/3T3 total cell lysate and, as these proteins have the same expected molecular weight as CRABP-II, it suggests that the correct area of gel had been selected for analysis.

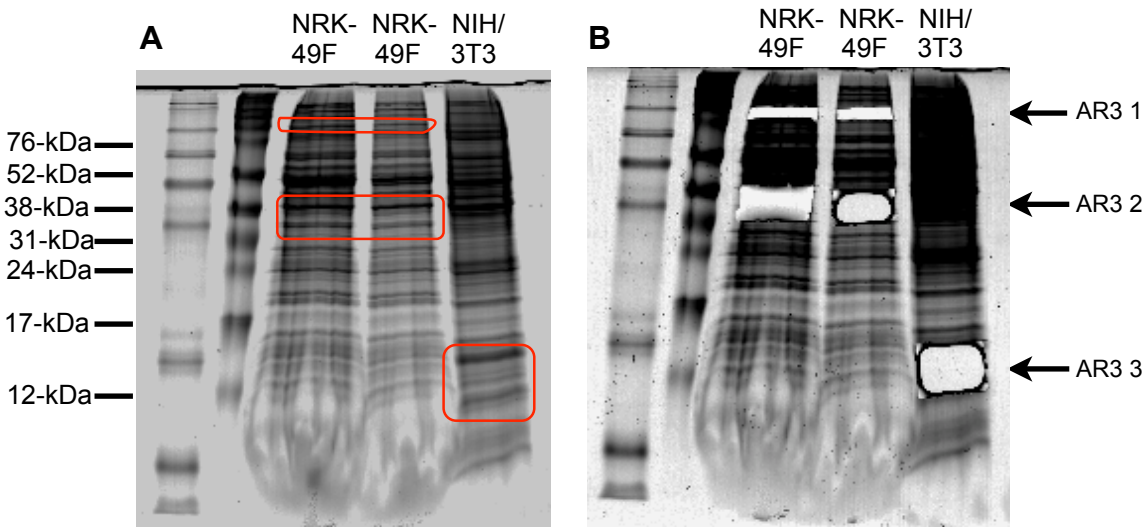

Figure 4.9. Colloidal Coomassie blue-stained electrophoresis gel of NRK-49F and NIH/3T3 total cell lysates. NRK-49F and NIH/3T3 total cell lysates were run on 15% polyacrylamide gels under reducing and denaturing conditions then the gel was stained with brilliant blue G-colloidal Coomassie stain. **A**- Colloidal Coomassie blue-stained gel with colour markers; **B**- Colloidal Coomassie blue-stained gel following excision of the protein bands of interest.

4.3 Discussion

The results presented in this chapter demonstrate the presence of key RA signalling machinery in NRK-49F cells. There was good evidence that NRK-49F cells expressed all three RAR isotypes and RXRα although the evidence for PPARβ/δ, RXRβ and RXRγ protein expression was weaker. Nuclear receptor mRNA expression was modulated by tRA treatment with and without TGF-β1 suggesting a role for these receptors in the response of NRK-49F cells to pro-fibrotic stimuli. However, there was little evidence that either CRABP-II or FABP5 were expressed at protein level and played a role in the pro-fibrotic effects of tRA.

In an effort to identify potential signalling pathways for the pro-fibrotic effects of tRA in NRK-49F cells retinoid receptor expression was determined as retinoids are known to exert their actions primarily via these receptors. All three RAR isotypes were identified at mRNA level in order of abundance

Rara>Rarg>Rarb (Figure 4.1). As Pparbd was present at lower levels than RAR, tRA signalling in NRK-49F cells likely predominantly occurs via the RARs and not PPARβ/δ. RXR mRNA was also detected in NRK-49F cells in order of abundance Rxrb>Rxra>Rxrg (Figure 4.1). Published data of retinoid receptor mRNA expression in mouse kidney by comparison shows that Rara is also the highest expressed RAR at mRNA level although Rxrα is the highest expressed RXR (Bookout, Jeong et al. 2005). However, mouse kidney samples consist of numerous cell types and only a minority of these will be fibroblasts. Although there are no published reports of retinoid receptor mRNA expression in renal fibroblast cell cultures to refer to, there is data on fibroblast cell cultures from other organs. For example, human dermal fibroblasts express RARα and RARγ but little RARβ (Redfern and Todd 1992; Tsou, Lee et al. 1994) and RXRα and RXRβ but not RXRγ (Tsou, Xie et al. 1997); rabbit corneal stromal and conjunctival fibroblasts expressed all the RARs and RXRs except RXRγ (Bossenbroek, Sulahian et al. 1998); and rat HSCs expressed all the RARs (Weiner, Blaner et al. 1992) while RXRα was the predominant RXR followed by RXRβ with RXRγ only weakly detected (Ohata, Lin et al. 1997). These reports are in agreement with the results presented here that Rara and Rarg are the most highly expressed RARs and Rxra and Rxrb are the most highly expressed RXRs at mRNA level in rat renal fibroblasts.

All three RARs were also identified at protein level by immunoblotting (Figure 4.2). The antibodies to RARα and RARβ recognised a single band at the expected molecular weight of RARα and RARβ. Although the antibody to RARγ recognised two bands at ~50-52-kDa, only the 50-kDa band was present in the positive control of A431 nuclear extract and was therefore likely to represent RARγ protein. The additional band could, however, have been an RARγ isoform. Although the relative expression of RAR proteins cannot be determined from this data as different antibodies have varying affinities for their epitopes, the anti-RARα rabbit polyclonal antibody was used at only a 1

in 20000 dilution suggesting that RARα might be the most abundant RAR in NRK-49F cells, in agreement with the mRNA data.

There was also evidence that NRK-49F cells expressed PPARβ/δ at protein level as the anti-PPARβ/δ rabbit polyclonal antibody recognised a band in both NRK-49F total cell lysate and the positive control at ~60-kDa likely to represent PPARβ/δ protein. However further bands were also seen at ~35-, 65- and 76-kDa (Figure 4.3). If specific, the 35-kDa band might represent a smaller molecular weight PPARβ/δ, which has previously been reported (Lundell, Thulin et al. 2007); the larger bands are unlikely to represent PPARβ/δ bound to other protein as the experiment was performed under reducing and denaturing conditions but are likely due to non-specific antibody binding.

In addition, the RXR immunoblots suggested that all three RXR isotypes were expressed at protein level in NRK-49F cells although the results were less definitive. The antibody to RXRα recognised two bands at ~50-kDa and ~60-kDa in both NRK-49F cells and the positive control and these bands disappeared with the addition of blocking peptide suggesting that they were specific for RXRα (Figure 4.4A). Although multiple bands were recognised by the anti-RXRβ antibody in NRK-49F total cell lysate, only two of these bands were also present in the positive control, at ~55-kDa and 76-kDa. The 55-kDa band is close to the predicted molecular weight of RXRβ and was therefore most likely to represent RXRβ protein (Figure 4.4B). Finally a cluster of bands were identified by the antibody for RXRγ in both NRK-49F and RXRγ-transfected 293T total cell lysate ranging from ~55-75-kDa, which compared to the immunoblot in the Santa Cruz RXRγ antibody data sheet (Appendix, Supplementary figure 1) and disappeared with the addition of blocking peptide suggesting these bands were specific for RXRγ antigen (Figure 4.4C).

There are several possible explanations for the multiple bands identified in the RXR immunoblots. Since RXRα and RXRβ have four isoforms and RXRγ has

two isoforms, the bands could represent different isoforms of RXRs (Lefebvre, Benomar et al. 2010). Post-translational modifications of protein could also provide an explanation for the additional bands. In addition, the bands with lower molecular weights might correspond to proteolytic products as reported previously (Rochette-Egly, Lutz et al. 1994). However, it cannot be excluded that the additional bands recognised in any of the immunoblots were caused by non-specific antibody binding and further analysis of NRK-49F total cell lysate and/or the bands would be required to confirm their identity.

Although nuclear receptor mRNA expression was modulated by tRA with and without TGF-β1 treatment in NRK-49F cells suggesting that these receptors might in some way be involved in the pro-fibrotic response, a candidate nuclear receptor responsible for these effects was not immediately identifiable (Figure 4.5). Despite this, there were some interesting and noteworthy findings. For example, Rara and Rarg were both up-regulated by tRA and dual treatment but also up-regulated more or less by the pro-fibrotic TGF-β1. It could therefore be extrapolated that RARα and/or RARγ are somehow involved in the pro-fibrotic response of tRA and TGF-β1 in NRK-49F cells. In addition, all the RXRs were down-regulated by tRA and dual treatment to a greater or lesser degree and in particular Rxra was suppressed by tRA, TGF-β1 and dual treatment. If this down-regulation of RXR mRNA is translated to reduced protein expression then the pathways through which tRA exerts it effects in NRK-49F cells could change with less canonical and more non-canonical signalling resulting in a different response of cells to tRA. Other published studies also report modulation of retinoid receptor expression in renal disease models. Liebler et al. demonstrated suppression followed by activation of the RARs and RXRα in experimental glomerulonephritis (Liebler, Uberschar et al. 2004) and the same group showed that in a chronic glomerulonephritis model RARα and RXRα mRNA were significantly increased (Schaier, Liebler et al. 2004).

It might have been predicted that Rarb mRNA would be induced by tRA treatment as there is an RARE in its promoter region, however other cell types

do not consistently demonstrate an induction of RARβ following treatment with tRA. For example, RARβ was not induced by RA in corneal epithelial cells (Bossenbroek, Sulahian et al. 1998). In addition, the reduction in Rarb mRNA by tRA with and without TGF-β1 was consistent with other reports of a reduction in RARβ expression in a rat model of hepatic fibrosis (Weiner, Blaner et al. 1992). Furthermore, since the *in vitro* model of fibrosis presented here involves minimal fibroblast proliferation and RARβ2 has been implicated as the predominant retinoid receptor interfering with cell cycle progression (Li, Faria et al. 2004; Suzui, Shimizu et al. 2004) it might be that RARβ has little role to play in this fibrogenic cell model.

In addition to the retinoid nuclear receptors, expression of the RA carrier proteins CRABP-II and FABP5 was explored in NRK-49F cells as they are also considered important in retinoid signal transduction. Despite the identification of Crabp2 mRNA in NRK-49F cells (Figure 4.6) CRABP-II immunoblotting did not identify a band at the expected molecular weight of 15-kDa (Figure 4.7). However multiple other bands were recognised by the anti-CRABP-II antibody and four bands corresponded to those seen in the positive control of NIH/3T3 total cell lysate at ~20-, 31-, 35- and 80-kDa of which three (the 31-, 35- and 80-kDa bands) disappeared with the addition of blocking peptide (Figure 4.7). If these three bands are indeed specific then they could represent post-translational modifications or different splicing products of CRABP-II. However they could also represent non-specific antibody binding. Therefore immunocytochemistry and mass spectrometry were performed to further determine if CRABP-II protein was present in NRK-49F total cell lysate but neither technique could positively identify CRABP-II protein (Figure 4.8). Somewhat surprisingly, LC/MS/MS did not even identify CRABP-II protein in the 15-kDa band in the positive control lysate that was consistent with CRABP-II protein. Possible explanations for this result include: 1) The wrong band was excised for analysis due to difficulty aligning the immunoblot with the gel; 2) The anti-CRABP-II antibody was very sensitive in its detection of the target protein and may have a lower limit of detection than the mass spectrometer; 3) CRABP-II was not present in the samples (despite NIH/3T3

total cell lysate being a positive control); and 4) There were technical problems with analysis of samples using the mass spectrometer. In addition, this methodology inevitable results in the excision of numerous proteins potentially reducing the sensitivity of the test.

Immunoblotting and immunocytochemistry also failed to identify FABP5 protein in NRK-49F cells, however this was not unexpected as the Ct of FABP5 was generally above 35 suggesting that FABP5 was expressed at low levels, if at all, in NRK-49F cells.

In summary, results presented in this chapter demonstrate the presence of retinoid nuclear receptors in NRK-49F cells and the modulation of retinoid receptor mRNA expression in response to tRA with and without TGF-β1. Overall, this data suggests that retinoid nuclear receptors may be involved in the pro-fibrotic effects of tRA in NRK-49F cells.

Chapter 5. Effects of nuclear receptor agonists and antagonists on total collagen accumulation in the 2D *in vitro* model of fibrosis in NRK-49F cells

In the previous chapters, tRA in the absence and presence of TGF-β1 caused a dose-dependent increase in total collagen accumulation in NRK-49F cells, which might be partly mediated by nuclear receptor signalling as there was evidence of retinoid nuclear receptor and PPARβ/δ expression in NRK-49F cells. In this chapter, the roles of the individual nuclear receptors in fibrogenesis in NRK-49F cells were studied. Two approaches were undertaken: Firstly, nuclear receptor agonists were used to explore the effects of retinoid receptor isotype and PPARβ/δ activation on fibrogenesis and, secondly, nuclear receptor antagonists were used to determine if tRA-induced total collagen accumulation could be prevented.

5.1 Effects of selective nuclear receptor agonists on total collagen accumulation

5.1.1 Effects of a pan-RAR and pan-RXR agonist

tRA is known to activate RAR. Therefore another pan-RAR agonist, TTNPB, was used to determine whether activation of RAR by TTNPB could mimic the effects of tRA on total collagen deposition.

TTNPB alone caused a small but significant increase in PSR staining at the highest dose tested (2 μM), in contrast to tRA, which was also pro-fibrotic at ten-fold lower concentrations (Figure 5.1Ai). In the presence of TGF-β1, 0.02-2 μM TTNPB caused a significant increase in PSR staining, similar to the effects of 0.02 μM tRA (Figure 5.1Ai), without causing significant cell detachment (Figure 5.1Aii).

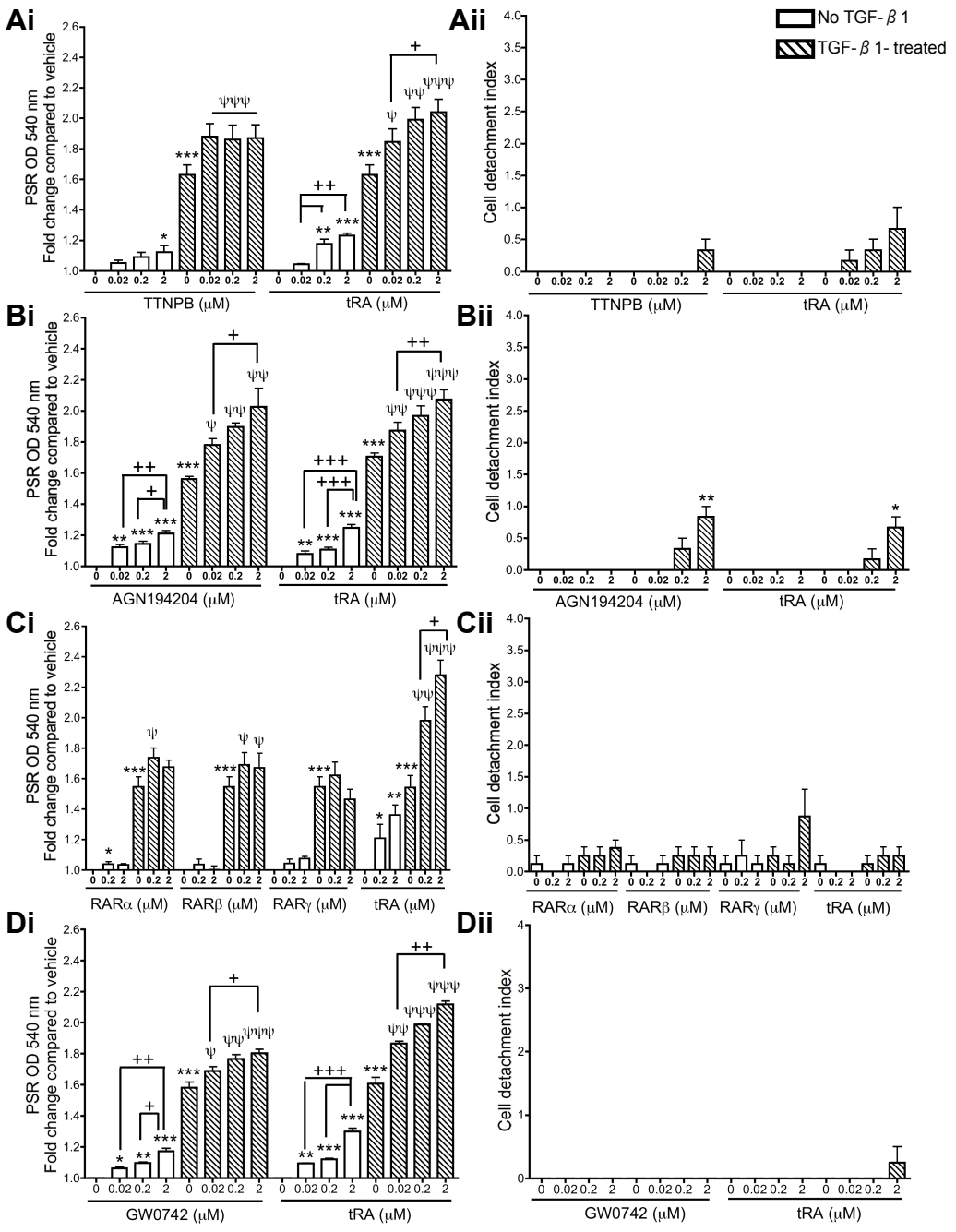

Figure 5.1. Effects of synthetic RAR, RXR and PPARβ/δ agonists on total collagen deposition in the absence and presence of TGF-β1 in NRK-49F cells. NRK-49F cells were cultured as per protocol then treated with nuclear receptor agonists +/- TGF-β1 for 48 h. Collagen deposition was quantified by spectrophotometric analysis of eluted PSR staining (**Ai-Di**) and cytotoxicity determined by cell detachment index (**Aii-Dii**). **A**- pan-RAR agonist TTNPB; **B-** pan-RXR agonist AGN194204; **C**-Isotype-selective agonists AGN195183 (RARα), CD2019 (RARβ) and CD437 (RARγ); **D**- PPARβ/δ agonist GW0742. Data represent mean ± SEM of three independent cell culture studies. Statistical analysis for Ai-Di was performed on transformed data using repeated measures ANOVA and for Aii-Dii using repeated measures ANOVA. * p<0.05, ** p<0.01, *** p<0.001 vs vehicle; ψ p<0.05, ψψ p<0.01, ψψψ p<0.001 vs TGF-β1-treated group; +p<0.05,++p<0.01 between groups indicated.

Next, the effects of the pan-RXR agonist AGN194204 were explored since, although tRA does not activate RXR, it could undergo isomerisation to RAs that do activate RXR *in vitro,* and thus play a role in tRA's pro-fibrotic effects.

NRK-49F cells treated with 0.02-2 μM AGN194204 showed a dose-dependent increase in PSR staining both with and without TGF-β1 similar to that seen with tRA (Figure 5.1Bi). There was significant cell detachment caused by 2 μM AGN194204 in the presence of TGF-β1 (Figure 5.1Bii).

5.1.2 Effects of RAR isotype-selective agonists

As pan-RAR agonist TTNPB showed a smaller pro-fibrotic effect in NRK-49F cells, the effects of RAR isotype-selective agonists on total collagen deposition were also explored.

The RARα-selective agonist AGN195183 at a dose of 0.2 μM with and without TGF-β1 caused a significant increase in PSR staining (Figure 5.1Ci). 0.2 and 2 μM RARβ-selective agonist CD2019 alone did not increase PSR staining however in the presence of TGF-β1 both doses mildly but significantly increased PSR staining (Figure 5.1Ci). Finally, the RARγ-selective agonist CD437 did not cause a change in PSR staining at the doses tested of 0.2 and 2 μM with or without TGF-β1 (Figure 5.1Ci). None of the RAR isotype-selective agonists caused significant cell detachment (Figure 5.1Cii).

5.1.3 Effect of a PPARβ/δ agonist

Finally, since tRA has been reported to bind and activate PPARβ/δ, the PPARβ/δ agonist GW0742 was used to investigate the role of this nuclear receptor in total collagen accumulation in NRK-49F cells.

GW0742 caused a dose-dependent, statistically significant increase in PSR staining both alone and in the presence of TGF-β1 although the effect was milder than that seen with tRA treatment (Figure 5.1Di). GW0742 did not cause a significant increase in cell detachment (Figure 5.1Dii).

5.2 Effects of nuclear receptor antagonists on tRA-induced total collagen accumulation

5.2.1 Effect of a pan-RAR and pan-RXR antagonist

Next, the pan-RAR antagonist AGN193109 and pan-RXR antagonist HX531 were used to determine if the pro-fibrotic effects of tRA on total collagen accumulation could be prevented by blocking RAR or RXR activation. Because of the doses of antagonists required to block RAR and RXR signalling (Johnson, Klein et al. 1995; Kanayasu-Toyoda, Fujino et al. 2005), 0.2 μM tRA was chosen for use in experiments to keep cytotoxicity to a minimum. This dose of tRA is the lowest dose that, in the presence of TGF-β1, caused a consistent increase in PSR staining however in the absence of TGF-β1 it did not cause a consistent increase in total collagen. Therefore the effects of AGN193109 and HX531 on tRA-induced total collagen accumulation in NRK-49F cells in the presence of TGF-β1 were studied.

AGN193109 and HX531 at doses of 1 μM had no effect on TGF-β1-induced total collagen deposition (Figure 5.2Ai, Bi). As expected, tRA at a dose of 0.2 μM in the presence of TGF-β1 caused a significant increase in PSR staining in comparison with TGF-β1-treated cells alone; however pre-treating cells with either AGN193109 or HX531 significantly suppressed this increase in PSR staining (Figure 5.2Ai, Bi). Neither AGN193109 nor HX531 caused significant cell detachment (Figure 5.2Aii, Bii).

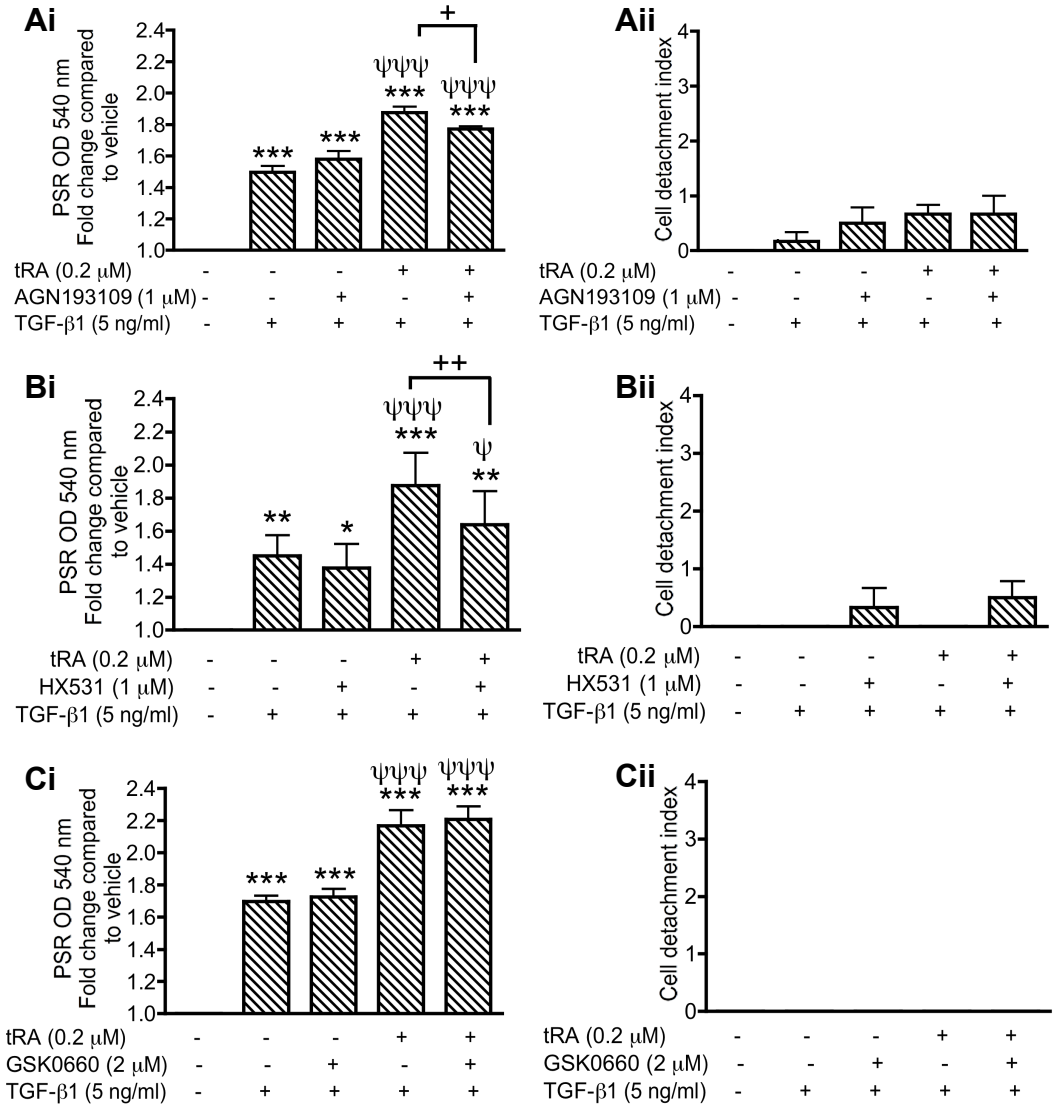

Figure 5.2. Effect of RAR, RXR and PPARβ/δ antagonists on tRA-induced total collagen accumulation in the presence of TGF-β1 in NRK-49F cells. NRK-49F cells cultured as per protocol were pre-treated with pan-RAR antagonist AGN193109 (**A**), pan-RXR antagonist HX531 (**B**) or PPARβ/δ antagonist GSK0660 (**C**) for 2 h then with 0.2 μM tRA and/or 5 ng/ml TGF-β1 for 48 h. Total collagen deposition was quantified by spectrophotometric analysis of eluted PSR staining (**Ai-Ci**) and cytotoxicity was assessed by cell detachment index (**Aii-Cii**). Data represent mean ± SEM of three independent cell culture studies. Statistical analysis for Ai-Ci was performed on transformed data using repeated measures ANOVA and for Aii-Cii was performed using repeated measures ANOVA.* p<0.05, ** p<0.01, *** p<0.001 vs vehicle-treated group; ψ p<0.05, ψψψ p<0.001 vs TGF-β1-treated group; + p<0.05, ++ p<0.01 between groups indicated.

5.2.2 Effect of a PPARβ/δ antagonist

Finally, the effect of the PPARβ/δ antagonist GSK0660 on tRA-induced total collagen accumulation was investigated. GSK0660 is a PPARβ/δ antagonist with a half maximal inhibitory concentration (IC_{50}) of 300 nM (Table 2.2) (Shearer, Steger et al. 2008) and was therefore used at a dose of 2 μM to ensure adequate blockade of PPARβ/δ ligand binding was achieved. This dose was well tolerated by NRK-49F cells causing no increase in cell detachment either alone or in combination with 0.2 μM tRA and 5 ng/ml TGF-β1 (Figure 5.2Cii). GSK0660 did not affect PSR staining in either TGF-β1-treated cells or cells treated with both tRA and TGF-β1 (Figure 5.2Ci).

5.3 Discussion

In the results presented here, treatment of NRK-49F cells with the pan-RXR agonist AGN194204 increased total collagen accumulation to a similar degree as tRA. Furthermore, the pan-RXR antagonist HX531 partially blocked the pro-fibrotic effects of tRA in the presence of TGF-β1. Although the pan-RAR agonist TTNPB and the PPARβ/δ agonist GW0742 also increased PSR staining, their effects were milder than that seen with either tRA or AGN194204, and the isotype-selective RAR agonists caused only minor changes. The pan-RAR antagonist AGN193109 partially blocked tRA-induced total collagen accumulation in the presence of TGF-β1 however the PPARβ/δ antagonist GSK0660 had no effect.

The most striking findings in this chapter were the effects of the pan-RXR agonist AGN194204 on total collagen deposition, and the effects of the pan-RXR antagonist HX531 on total collagen accumulation in dual-treated cells (Figure 5.1Bi). RXR activation mimicked the effect of tRA while blocking RXR signalling partially blocked the pro-fibrotic effects of tRA in the presence of TGF-β1 suggesting that RXRs, at least in part, play a role in the pro-fibrotic effects of tRA. However, since tRA cannot bind and activate RXRs, RXR activation by tRA must occur indirectly by conversion of tRA to metabolites, such as 9cRA, that can activate RXRs (Urbach and Rando 1994).

RXRs have been implicated as modulators of fibrosis in other organ systems. For example, in liver fibrosis a reduction in RXR expression was found to convert HSCs into their active form and increasing RXR expression inhibited HSC activation and proliferation (Ohata, Lin et al. 1997; Hellemans, Verbuyst et al. 2004); and in a rat model of hepatic fibrosis induced by CCl_4, increased expression of RXRα was associated with a decrease in α-SMA and type I collagen (Wang, Xu et al. 2011). Data supporting a role for RXRs in renal fibrosis is more scarce although there are some examples. In a rat model of experimental glomerulonephritis the RXR agonist Ro-257386 ameliorated renal damage (Lehrke, Schaier et al. 2002) and in a chronic model of glomerulosclerosis AGN194204 reduced glomerulosclerosis index as well as other parameters of renal damage (Schaier, Liebler et al. 2004). These studies suggest that fibrogenesis is associated with a reduction in RXR expression and increasing RXR expression/activation improves fibrosis. In contrast, the results presented here show the opposite: RXR agonism increased collagen deposition, and RXR antagonism reduced the pro-fibrotic effect of tRA. The discrepancy in these results are likely a demonstration of the variable nature of retinoids dependent on retinoid type, cell type and model used.

Although AGN194204 could be exerting its pro-fibrotic effects via canonical retinoid signalling there are other possible mechanisms through which it is functioning. For example, Hoover et al. have shown that RXR signalling can directly interfere with TGF-β signalling (Hoover, Burton et al. 2008); the RXR agonist bexarotene, in the presence of TGF-β, caused a rapid increase in Smad2 and Smad3 phosphorylation in MEFs and, furthermore, loss of RXRα resulted in increased Smad2 phosphorylation in response to TGF-β (Hoover, Burton et al. 2008). Alternatively, the effects of AGN194204 might be via RXR-independent pathways in a cell that has reduced RXR expression (although this is in conflict with the RXR antagonist data). The reduction in RXR mRNA demonstrated in the previous chapter could be an appropriate protective response in NRK-49F cells if the RXR signalling pathway is pro-fibrotic.

The pan-RAR agonist TTNPB also caused an increase in PSR staining in NRK-49F cells, however the effect was not dose-dependent and much weaker then that for tRA. The RAR antagonist AGN193109 reduced the pro-fibrotic effects of dual treatment. These results suggest that the pro-fibrotic effect of tRA might also occur partly via RAR signalling (Figure 5.1Ai, 5.2Ai). As RARα, RARβ and RARγ agonists each had only minor effects on total collagen deposition, there was no evidence that individual RAR isotypes were responsible for the pro-fibrotic effect of tRA although they could each have had additive functions (Figure 5.1Ci). Of note, different RAR agonists had different fibrogenic potencies in the order tRA>TTNBP>RARα/RARβ>RARγ (Figure 5.1Ci).

Published literature suggests that RAR agonism in a variety of cell and animal renal disease models confers protection against renal damage (Wagner, Dechow et al. 2000; Morath, Dechow et al. 2001; Schaier, Lehrke et al. 2001; Lehrke, Schaier et al. 2002; Schaier, Jocks et al. 2003; Schaier, Liebler et al. 2004; Liu, Lu et al. 2008; Morath, Ratzlaff et al. 2009; Liu, Lu et al. 2011). However there are also reports of RAR agonists exacerbating fibrosis in a dose-dependent (Morath, Ratzlaff et al. 2009; Xu, Hendry et al. 2010), time-dependent (Morath, Ratzlaff et al. 2009) and environment-dependent (Liu, Lu et al. 2008; Morath, Ratzlaff et al. 2009) manner. Although the work here has not identified an anti-fibrotic potential of the retinoids tested, given that isotype-selective retinoids have shown promising efficacy in CKD models, the use of RAR isotype-selective retinoids could be a plausible strategy to avoid unwanted pro-fibrotic effects of tRA.

Possible mechanisms for the pro-fibrotic effects of RAR agonists include canonical signalling (Perez, Shull et al. 1992) and/or interference of the TGF-β1 pathway (Cao, Flanders et al. 2003; Pendaries, Verrecchia et al. 2003), although further experiments to deduce specific mechanisms of action in this cell model are required.

However, if the pro-fibrotic effects of tRA are mediated through RAR activation then it is unclear why the pan-agonist TTNPB did not have as great a response as tRA on total collagen deposition. TTNPB binds RARs with 10-fold less efficiency than tRA, which might explain its reduced effects (Pignatello, Kauffman et al. 1997). In addition, tRA, as well as activating RARs directly, might be converted to retinoids that activate RXRs *in vitro* (Urbach and Rando 1994) therefore potentiating the effect of tRA on RXR-RAR activation, an effect that could be particularly relevant if endogenous RA activity was present in NRK-49F cell culture. In addition tRA could have nuclear receptor-independent effects as well as its RAR-dependent activities although the finding that an RAR antagonist reduced tRA-induced total collagen accumulation in the presence of TGF-β1 suggests that at least some of the pro-fibrotic effect of tRA is via RAR signalling (Figure 5.2Ai).

Finally, while the PPARβ/δ agonist GW0742 also caused a mild increase in PSR staining in NRK-49F cells, the PPARβ/δ antagonist GSK0660 could not prevent tRA-induced total collagen accumulation in the presence of TGF-β1 (Figure 5.1Di, and 5.2Ci). This suggests that activation of PPARβ/δ by tRA is not involved in the fibrogenic effects of tRA unless tRA binds to PPARβ/δ in such a way that GSK0660 does not prevent receptor activation. It cannot be excluded that a small proportion of tRA undergoes isomerisation *in vitro* to a ligand of RXRs causing RXR/PPARβ/δ activation and a pro-fibrotic response.

In summary, there is significant evidence for an RXR-mediated pro-fibrotic effect of tRA and some evidence for an RAR-mediated effect in NRK-49F cells. While all RAR and RXR agonists, with the exception of the RARγ-selective agonist CD437, caused an increase collagen deposition, the RAR isotype-selective agonists had a minimal effect on fibrosis and might therefore provide a viable option for the safe use of retinoids in CKD.

Chapter 6. Gene silencing using short-interfering RNA (siRNA) in NRK-49F cells

6.1 Pilot study to determine optimal settings for electroporation of siRNA into NRK-49F cells

Experiments thus far have used chemical agonists and antagonists to investigate mechanisms behind tRA-induced total collagen accumulation. However chemicals may exert effects not related to their target that cannot be predicted. Therefore it was important to corroborate these results use a different strategy and gene silencing using siRNA was chosen for this purpose.

In early experiments it was established that chemical-based transfection of siRNA was unsuitable for gene silencing in NRK-49F cells as the knockdown achieved was variable and inconsistent (data not shown). Therefore a combination of electroporation and chemical-based transfection was used to attempt adequate silencing of gene expression.

Firstly, a pilot study was performed to determine the optimal voltage and capacitance for electroporation of siRNA into NRK-49F cells. Cells were electroporated at 0-400 V and 250 or 500 µF in the presence of 100 nM Cy5-labelled siRNA and cell morphology examined by photomicroscopy and transfection efficiency determined by flow cytometry using a BD FACSCanto II flow cytometer. Data was analysed using FloJo Flow Cytometry Analysis Software.

Following electroporation, cell morphology of NRK-49F cells was altered with cells appearing larger and more spiculated. In addition the confluency of cells decreased as the voltage increased (Figure 6.1).

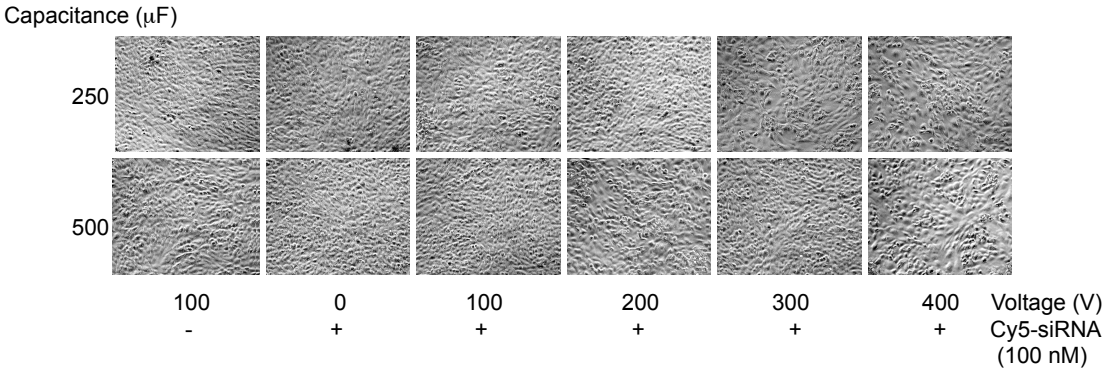

Figure 6.1. Photomicroscopy of NRK-49F cells 48 h after electroporation. NRK-49F cells at a density of 1.5 x 10^6 /ml were electroporated in the presence of 100 nM Cy5-labelled siRNA. Cells were then cultured for 48 h in DMEM supplemented with 2.5% FCS and 2.5% Nu prior to photomicroscopy (phase contrast, x200 magnification).

Figure 6.2 shows the relative fluorescence of NRK-49F cells following electroporation with Cy5-labelled siRNA at different voltages and capacitances. Negative control cells (cells not treated with siRNA) subjected to electroporation at 100 V and 250 or 500 μF had less fluorescent signal relative to cells electroporated with Cy5-labelled siRNA; as voltage and capacitance increased, relative fluorescence of Cy5-labelled siRNA-treated NRK-49F cells increased (Figure 6.2A, B).

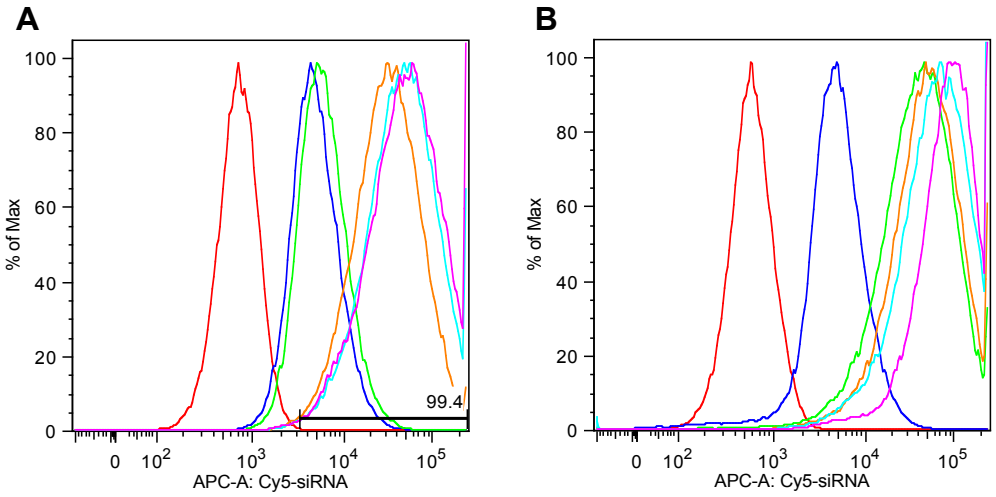

Figure 6.2. A single parameter histogram showing relative fluorescence of NRK-49F cells electroporated with Cy-5-labelled siRNA. NRK-49F cells were electroporated with Cy-5-labelled siRNA, cultured for 3 d in DMEM supplemented with 2.5% FCS and 2.5% Nu then subjected to flow cytometry. **A**- cells subjected to electroporation at a capacitance of 250 μF; **B**- cells subjected to electroporation at a capacitance of 500 μF. Red= 100 V, negative control (no siRNA), blue= 0 V, green= 100 V, yellow= 200 V, turquoise= 300 V, pink= 400 V.

70-80% of unelectroporated cells treated with Cy5-labelled siRNA gave a fluorescent signal and this increased to 100% when 200 V or more was delivered to cells (Figure 6.3A). The median intensity of signal increased as the voltage increased and cells exposed to a capacitance of 500 µF compared to 250 µF had a higher median intensity (Figure 6.3B). Although the percentage of cells within the live gate was >85% in all groups, cell density was reduced at voltages above 100 V and was most marked in the group receiving 500 µF and 400 V (Figure 6.3C, D). Therefore, for future experiments, electroporation settings were set at 300 V and 250 µF as these conditions achieved greatest transfection of Cy5-labelled siRNA while keeping cell death to a minimum.

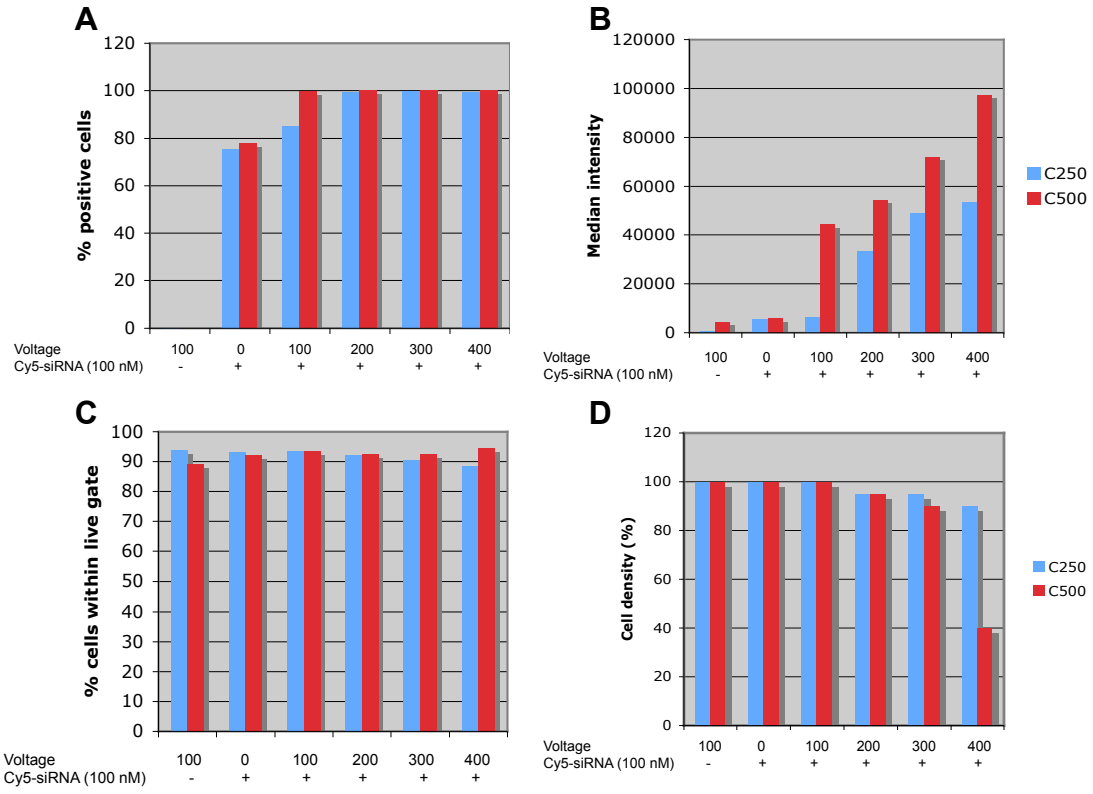

Figure 6.3. Flow cytometry of NRK-49F cells electroporated with Cy5-labelled siRNA under varying conditions. NRK-49F cells were electroporated with Cy-5-labelled siRNA then subjected to flow cytometry after 3 d culture as before. **A**- percentage of NRK-49F cells positive for Cy5-labelled siRNA; **B**- fluorescent intensity of NRK-49F cells following electroporation; **C**- percentage of cells within the live gate; **D**- percentage cell density at different electroporation settings.

6.2 Chemical and electrical transfection of NRK-49F cells using siRNA targeting PAI-1 and TG2

Results from Chapter 3 suggested that PAI-1 was one possible mediator of the pro-fibrotic effects of tRA. Therefore knockdown of PAI-1 gene expression was attempted using a combination of electroporation and chemical transfection, as described in methods. A concentration of 20 nM siRNA was used according to manufacturer's guidelines. Two controls were included in the experimental design: Cells electroporated without siRNA and those treated with negative control siRNA.

Unfortunately, two different siRNAs targeting PAI-1 (designated "siRNA1" and "siRNA2") achieved insufficient gene knockdown of only 29% and 44% for "siRNA1" and 15% and 28% for "siRNA2" in comparison with untreated cells in two independent cell culture studies (Figure 6.4).

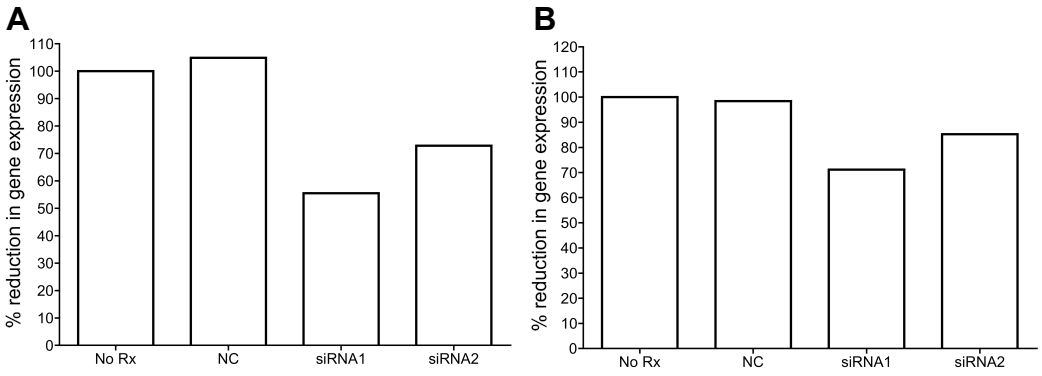

Figure 6.4. siRNA knockdown of PAI-1 in NRK-49F cells. NRK-49F cells were electroporated at 300 V and 250 µF with no siRNA ("no Rx"), 20 nM negative control siRNA ("NC") or 20 nM each of two siRNAs targeting PAI-1 ("siRNA1" and "siRNA2"). Cells were then seeded in collagen type-I-coated 96-well plates and cultured for 3 d in DMEM supplemented with 2.5% FCS and 2.5% Nu then for 4 d in DMEM supplemented with ITS and a further dose of 20 nM siRNA. Total RNA was extracted from cells and subjected to two-step RT-qPCR. **A** and **B** show the % reduction in PAI-1 mRNA expression in comparison with the "no Rx" group in two independent cell culture experiments.

Knockdown of TG2 gene expression was also attempted using two different siRNAs targeting TG2. “siRNA1” achieved adequate gene knockdown of >75% in comparison with untreated cells whereas “siRNA2” did not (Figure 6.5). Therefore “siRNA1” was used to examine the effects of TG2 gene knockdown on tRA-induced total collagen accumulation.

Two independent cell culture studies were performed to examine the effects of TG2 knockdown on tRA-induced increase in PSR staining (Figure 6.6). In the first experiment, negative control siRNA did not have any significant effect on PSR staining compared to untreated cells; in addition, knockdown of TG2 gene expression by “siRNA1” did not alter PSR staining in vehicle-, tRA- and TGF-β1-treated groups although there was a significant increase in PSR staining in the dual-treated group (Figure 6.6A). In the second independent cell culture study, negative control siRNA caused a reduction in PSR staining in comparison with the non-transfected group and “siRNA1” caused a further significant reduction in PSR staining in the vehicle-, tRA- and TGF-β1-treated groups compared cells treated with negative control siRNA (Figure 6.6B).

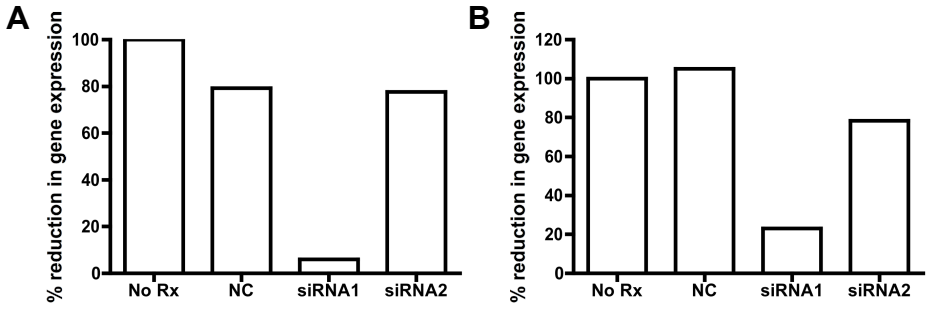

Figure 6.5. siRNA knockdown of TG2 in NRK-49F cells. NRK-49F cells were electroporated then cultured as before. Total RNA was extracted from cells and subjected to RT-qPCR. **A** and **B** show the % reduction in TG2 mRNA expression in comparison with the “No Rx” group in two independent cell culture experiments. *NC:* cells treated with negative control siRNA; *No Rx:* untreated cells; *siRNA1 and 2:* cells treated with siRNAs “1” and “2”.

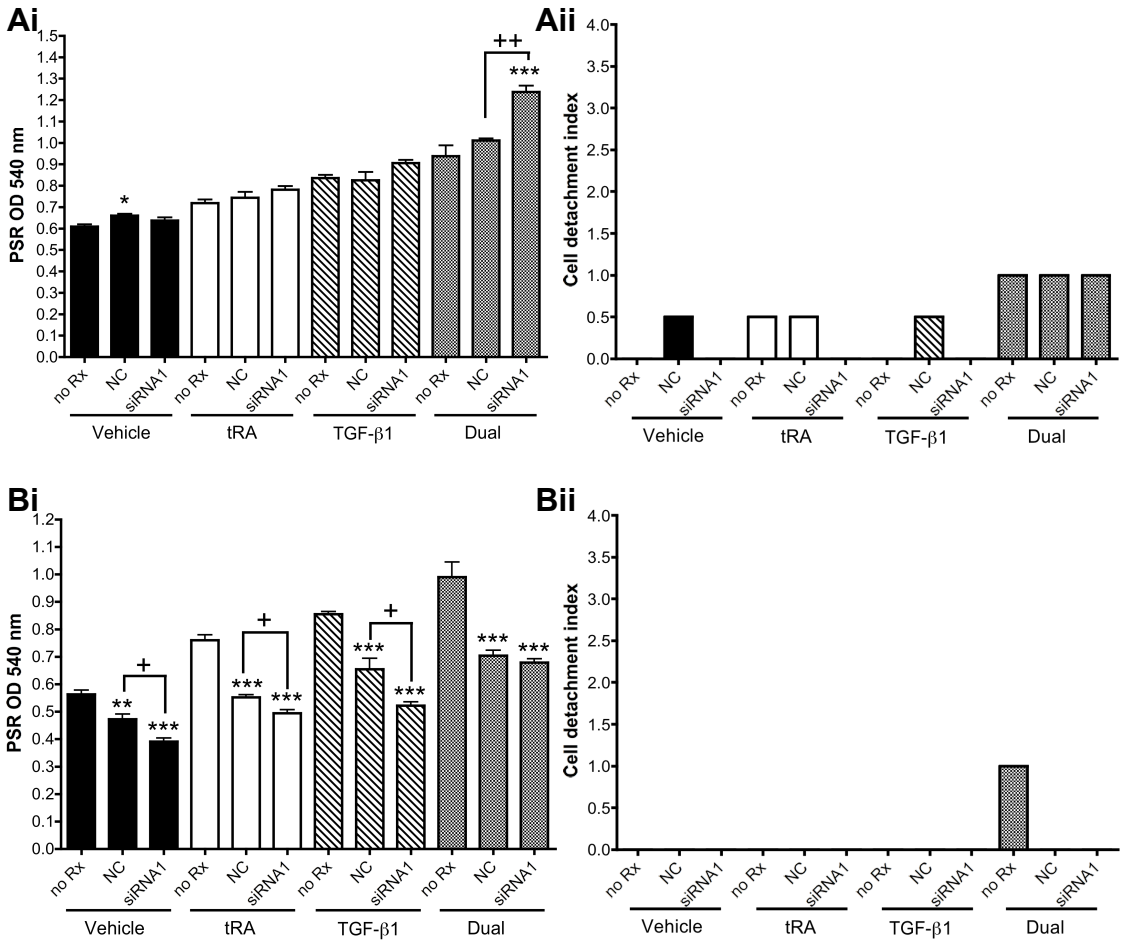

Figure 6.6. Effect of TG2 knockdown on tRA-induced total collagen accumulation in the absence and presence of TGF-β1. NRK-49F cells were transfected as before. Cells were then treated with 2 μM tRA with and without 5 ng/ml TGF-β1 for 48 h. Eluted PSR stain was used to quantify total collagen deposition (**Ai, Bi**) and cell detachment index was also recorded (**Aii, Bii**) in two independent experiments. Data for Ai and Bi represent mean ± SEM of quadruplicate wells; statistical analysis was performed using a one-way ANOVA. * $p<0.05$, ** $p<0.01$, *** $p<0.001$ vs "no Rx" group in each of the vehicle-, tRA-, TGF-β1- and dual-treated groups; + $p<0.05$, ++ $p<0.01$ between groups indicated.

6.3 Discussion

The results presented here show that, despite a successful pilot study, NRK-49F cells were difficult to successfully transfect with targeting siRNAs. Furthermore, although one of the four siRNAs ("siRNA1" targeting TG2) tested did achieve >75% gene knockdown of TG2, experimentation with this siRNA using the 2D *in vitro* model of fibrosis produced inconsistent and therefore unreliable results.

The pilot study was designed to determine optimal settings for electroporation of NRK-49F cells and was performed as previous experiments using chemical transfection had been unsuccessful. As expected, increasing the voltage and capacitance applied to NRK-49F cells increased delivery of Cy5-labelled siRNA into cells, but with the consequence of more cell loss (Figure 6.3). Optimal electroporation settings were therefore chosen as 300 V and 250 µF as these conditions achieved greatest transfection of Cy5-labelled siRNA while keeping cell death to a minimum.

However, despite optimising electroporation settings using fluorescent-labelled siRNA, electroporation of NRK-49F cells with Ambion's *Silencer*® select pre-designed targeting siRNAs was largely unsuccessful with only one siRNA out of four producing adequate knockdown of gene expression. There are several possible reasons for this failure of the technique: 1) There was a change in the protocol from the pilot experiment with alterations in electroporation solution used and culture time before determining knockdown. Opti-MEM and lipofectamine RNAiMAX transfection reagent were used to suspend cells in an attempt to further encourage siRNA uptake and gene knockdown was determined after 7 d culture because it was important to demonstrate gene knockdown at the point at which treatment of cells was to occur. Both these changes may have affected the success of gene knockdown; 2) Cell culture conditions were generally unfavourable for transfection because cells were confluent as required for the 2D *in vitro* model of fibrosis; 3) There was a reduction in siRNA dose from 100 nM for the Cy5-labelled siRNA to 20 nM for the targeting siRNAs; 4) The siRNAs may not have been functional or may have been of poor quality prior to use in experiments; 5) The RNAi pathway may not have been functioning in NRK-49F cells; 6) Delivery of Cy5-labelled siRNA into cells does not necessarily determine success of knockdown only that siRNA has entered cells.

Since “siRNA1” targeting TG2 achieved >75% knockdown, two independent experiments were performed to determine the effect of reducing TG2 gene expression on tRA-induced collagen accumulation. However these two studies produced very variable results and it was therefore difficult to draw any conclusions from the work. The technique of electroporation is well known to damage cells and the higher the voltage the worse the damage that occurs (Wells 2010). Electroporation of NRK-49F cells may not only have harmed cells but also altered their behaviour making experimentation with them and interpretation of results difficult.

There are many different factors to consider when performing electroporation including electrode design, pulse pattern, and pulse magnitude and duration (Wells 2010). Amaxa Nucleofector Technology, owned by Lonza Group Ltd, is based on electroporation and uses cell-type-specific reagents, with optimised protocols for difficult to transfect cell types including NRK-49F cells. Given the difficulties in transfection of NRK-49F cells arising from this work this technology might be a relevant next step to take as it reportedly offers high efficiency, high viability transfection with maintenance of cell functionality.

Chapter 7. Other cell models for the study of the pro-fibrotic effects of tRA

7.1 Effect of tRA on total collagen deposition in a human foreskin fibroblast primary culture

Since NRK-49F cells are a cell line and therefore might not represent the behaviour of other fibroblasts it was important to determine the effects of tRA on fibrosis in other fibroblast cell cultures and, in particular, primary cell cultures, as they are considered to more closely represent the *in vivo* setting. However primary renal fibroblast cell cultures are not available commercially therefore a human foreskin fibroblast primary culture was used to determine the effects of tRA with and without TGF-β1 on total collagen deposition using the 2D *in vitro* model of fibrosis.

2-5 μM tRA alone and 0.02-0.2 μM tRA in the presence of TGF-β1 caused a dose-dependent increase in PSR staining (Figure 7.1A, B). No change in cell detachment index was detected in any of the treatment groups (data not shown).

7.2 Other fibroblast and mesangial cell cultures

7.2.1 COS-7 kidney fibroblast cell line and the 2D *in vitro* model of fibrosis

As another example of a renal fibroblast cell line, COS-7 cells were also considered for use in investigations of the effects of tRA with and without TGF-β1 on total collagen deposition. However, this cell line had a rapid growth rate, produced large amounts of collagen even when quiescent, as demonstrated by PSR staining, and treatment with TGF-β1 did not induce an increase in collagen deposition (Figure 7.2). Therefore COS-7 cells were not suitable for further investigations of the effects of tRA on fibrosis with and without TGF-β1.

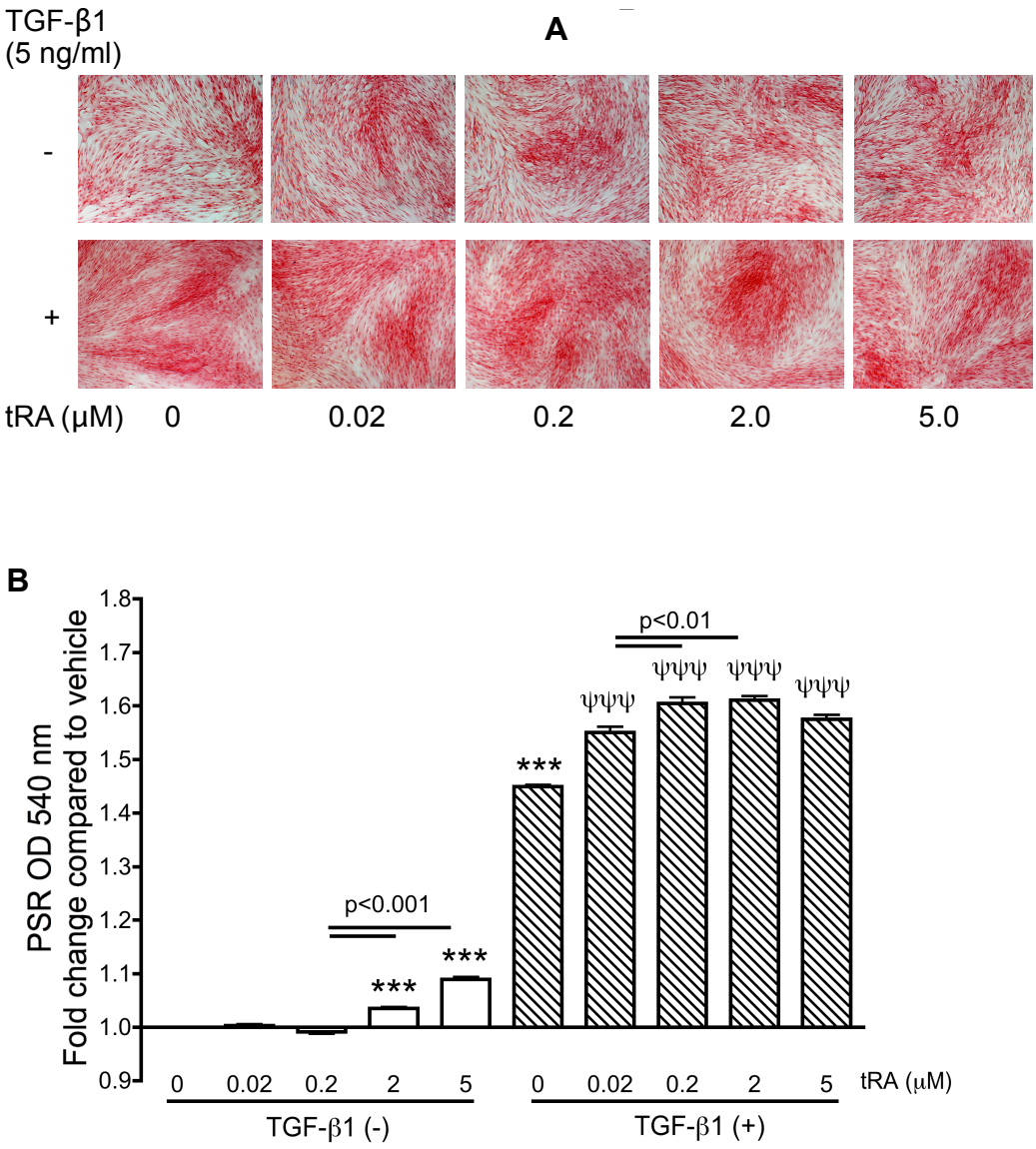

Figure 7.1. Effect of tRA treatment with and without TGF-β1 on total collagen deposition in human foreskin fibroblasts. Human foreskin fibroblasts cultured in collagen type-I-coated 96-well plates as per protocol were treated with increasing doses of tRA in the absence and presence of TGF-β1 for 48 h. Total collagen deposition was determined by photomicroscopy of PSR staining (x100 magnification) (**A**) and quantified by spectrophotometric analysis of eluted PSR (**B**). Data represent mean ± SEM of 3 independent cell culture studies. Statistical analysis on B was performed on transformed data using repeated measures ANOVA. *** p<0.001 vs vehicle; ψψψ p<0.001 vs TGF-β1-treated group.

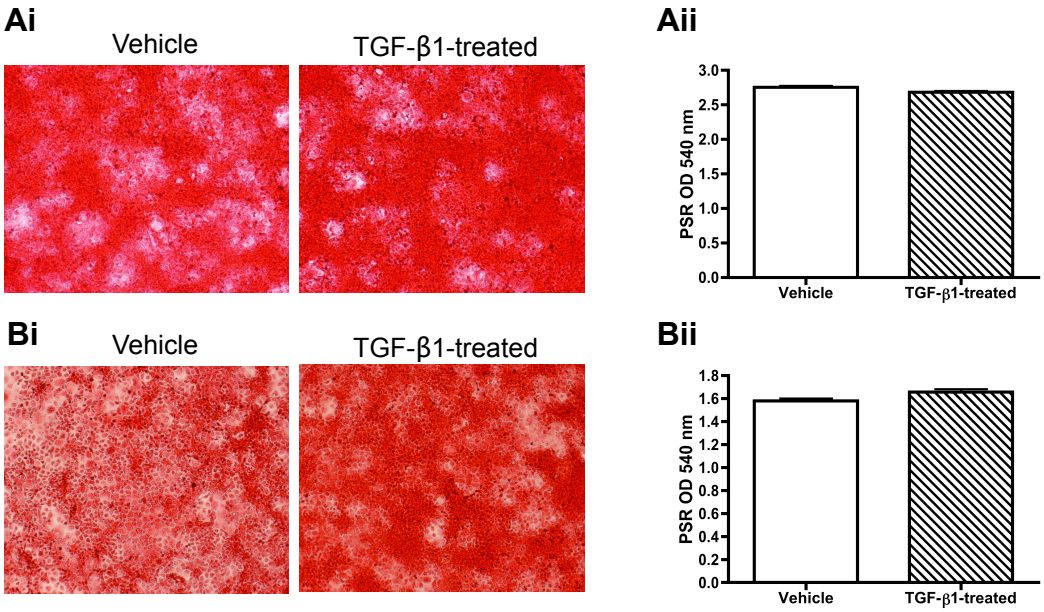

Figure 7.2. Effect of TGF-β1 treatment on total collagen deposition in COS-7 cells. COS-7 cells cultured at a density of $1x10^4$/well for 3 d in DMEM supplemented with 2.5% FCS and 2.5% Nu then for 4 d in DMEM supplemented with ITS (**A**) or at a density of $0.25x10^4$/well for 3 d in DMEM supplemented with 2.5% FCS and 2.5% Nu then for 1 d in DMEM supplemented with ITS (**B**) were treated with 5 ng/ml TGF-β1 for 48 h. The effect on total collagen deposition was determined by photomicroscopy of PSR staining (x100 magnification) (**Ai, Bi**) and quantified by spectrophotometric analysis of eluted PSR (**Aii, Bii**). Data represent eight replicates of one cell culture study.

7.2.2 Mesangial cells and the 2D *in vitro* model of fibrosis

Since mesangial cells are important in the development of glomerulosclerosis, mesangial cell lines and primary cultures were also tested for their suitability for use in the 2D *in vitro* model of fibrosis. Two primary rat mesangial cell cultures isolated from the glomeruli of Sprague-Dawley and Wistar rats, respectively, the SM43 rat mesangial cell line and the human mesangial cell line "HMCL" were each treated with 5 ng/ml TGF-β1 then stained for total collagen as per protocol for the 2D *in vitro* model of fibrosis. As there was no significant increase in PSR staining by TGF-β1 in any of the mesangial cell cultures tested they did not represent appropriate fibrotic models and therefore were not used for further experiments (Figure 7.3).

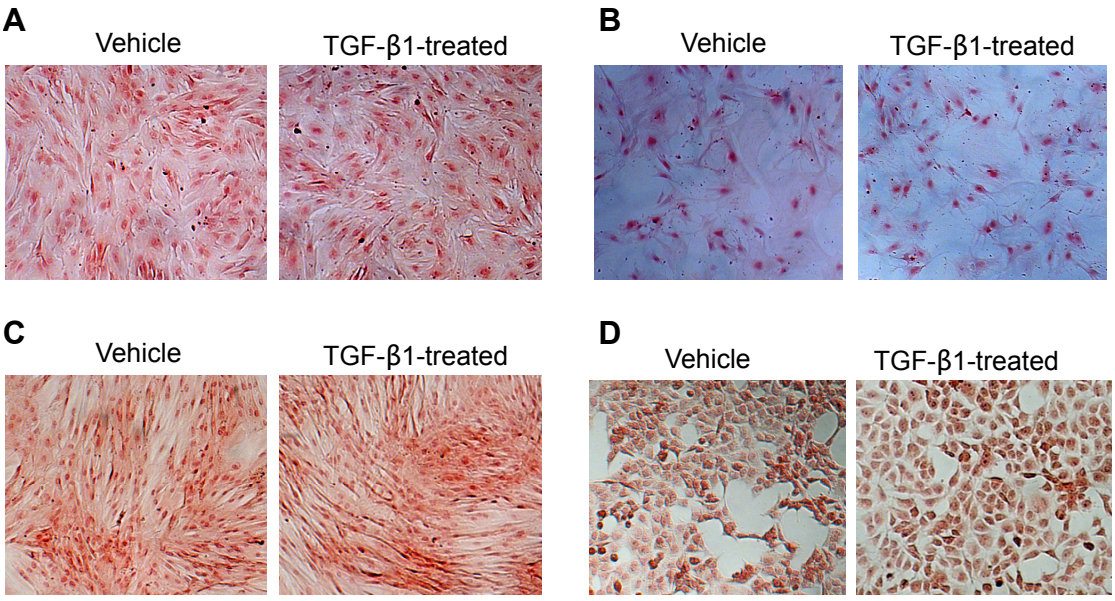

Figure 7.3. Effect of TGF-β1 treatment on total collagen deposition in mesangial cell cultures. Quiescent RMC primary cultures from Sprague-Dawley (**A**) and Wistar (**B**) rats and mesangial cell lines SM43 (**C**) and HMCL (**D**) were treated with 5 ng/ml TGF-β1 for 48 h. The effect on total collagen deposition was determined by photomicroscopy of PSR staining (x100 magnification).

7.3 Discussion

The results presented here demonstrate that a human foreskin fibroblast primary culture responded to tRA and dual treatment similarly to NRK-49F cells by increasing net collagen deposition. This result is important because it shows that the pro-fibrotic effect of tRA in NRK-49F cells is not idiosyncratic and supports the hypothesis that the pro-fibrotic effects of tRA occur through fibroblast activation.

Unfortunately, the net effect of tRA on fibrogenesis could not be tested in another renal fibroblast cell line, COS-7, and various mesangial cell cultures as they did not demonstrate increased PSR staining following TGF-β1 treatment and therefore could not be used as appropriate *in vitro* models of TGF-β1-induced fibrosis. There are several possible explanations why TGF-β1 treatment did not cause an increase in total collagen deposition in these cell cultures. Firstly, a cell's response to TGF-β1 can vary markedly

depending on a variety of factors such as confluency, serum content of media and whether the cells are actively proliferating or quiescent (Sutton, Canfield et al. 1991). In addition, cell behaviour may alter significantly depending on the plastic-ware used, for example if cells are seeded onto tissue culture-treated plates (Lewis and Norman 1998) and further, the dose of TGF-β1 can determine a cell's response (Alvarez, Sun et al. 1992). Secondly, the 2D *in vitro* model of fibrosis may not have been sensitive enough to detect small changes in collagen accumulation between groups. If cells already have a high basal collagen secretion (which may be a particular problem if cultures are maintained in FCS as it contains TGF-β1) or they do not produce enough collagen in response to TGF-β1 to be detected by PSR staining then this model cannot be used.

Chapter 8. Conclusions, perspectives and future work

8.1 Summary of findings

The work presented in this thesis shows that tRA, in the absence and presence of TGF-β1, is pro-fibrotic in NRK-49F cells by causing an increase in total collagen accumulation determined by PSR staining. This pro-fibrotic effect of tRA with and without TGF-β1 was also observed in a human foreskin fibroblast primary cell culture. Despite the tRA-induced increase in total collagen protein in NRK-49F cells, an RT-qPCR array showed there to be opposing actions of tRA at the level of gene expression with evidence of anti-fibrotic as well as pro-fibrotic potentials. Many of the MMPs were down-regulated at mRNA level and MMP activity was also reduced providing a potential mechanism through which tRA is pro-fibrotic. In addition, PAI-1 protein expression was up-regulated by tRA and further increased by dual treatment with tRA and TGF-β1 suggesting that it is through up-regulation of PAI-1 that dual treatment might cause more collagen accumulation than tRA alone. The PAI-1 inhibitor tiplaxtinin reduced tRA-induced collagen accumulation supporting the concept that PAI-1 contributes to the pro-fibrotic effect of tRA. There was no evidence to suggest that TG2 was involved in the pro-fibrotic effects of tRA as it was not up-regulated at protein level and a TG2 inhibitor did not prevent but rather exacerbated tRA-induced total collagen accumulation.

The pathways through which tRA might be exerting its fibrogenic effects include retinoid receptor signalling as retinoid receptors were expressed in NRK-49F cells and their mRNA expression was modulated by tRA and dual treatment. However tRA carrier proteins were less likely to be important as their protein expression was not detected in NRK-49F cells. A pan-RAR and RARα- and RARβ-selective agonists, a PPARβ/δ agonist but most of all a pan-RXR agonist all increased total collagen deposition; however, only a pan-RAR and pan-RXR antagonist, and not a PPARβ/δ antagonist, decreased the pro-fibrotic effects of tRA in the presence of TGF-β1, implicating RXRs and possibly also RARs as mediators of the pro-fibrotic effects of tRA.

8.2 Relevance of this work

CKD is a clinically important disease in the UK causing high morbidity and mortality and is a financial burden on the National Health Service. Whatever the cause of CKD it is renal fibrosis that is the final common pathway to ESRD. However there remains no direct treatment for renal fibrosis. Retinoids have been proposed as potential therapies for a variety of renal diseases because of their anti-inflammatory, anti-proliferative and possibly anti-fibrotic effects. Indeed, there are case reports of the successful use of retinoids in the treatment of PML in a CKD patient (Yamane, Tsukamoto et al. 2009) and in patients with lupus nephritis (Kinoshita and Funauchi 2012). However, retinoids are not benign drugs. Systemic administration has been associated with mucocutaneous side effects, headaches, musculoskeletal abnormalities, hairloss, hyperlipidaemia, liver toxicity, psychiatric disturbances and teratogenicity. In addition, as well as reports of the favourable effects of retinoids in renal disease models, there is also evidence that retinoids may exacerbate renal fibrosis.

The development of less toxic, pathway specific retinoids has occurred with the aim of reducing the unpleasant side effects of less selective retinoids and to aid research into the biological actions of individual retinoid signalling pathways. Disease-targeted retinoids would be particularly desirable in the CKD patient population because they are often asymptomatic and therefore will not readily accept treatments that make them feel unwell.

There is currently a lack of understanding of the specific pathways through which retinoids exert their pro-fibrotic effects. This work aimed to explore the mechanisms behind the fibrogenic effects of tRA in a cell model of renal interstitial fibrosis so that a strategy for the safe use of retinoids in renal diseases can be proposed.

8.2.1 NRK-49F cells as a suitable *in vitro* model for studying the effects of retinoids in renal interstitial fibrosis

There are few reports of the effects of retinoids on fibrosis in kidney fibroblasts despite their role as key mediators of TIF. This work hypothesised that the pro-fibrotic effects of retinoids occurred through renal fibroblasts and the NRK-49F cell line was chosen as a suitable renal fibroblast cell model to test this hypothesis. NRK-49F cells are derived from normal rat kidneys and are morphologically and behaviourally similar to fibroblasts (Huu, Rosenblum et al. 1966; de Larco and Todaro 1978). In the past, NRK-49F cells have been widely used in fibrogenesis studies, especially those induced by TGF-β1 (Roberts, Sporn et al. 1986; Grotendorst, Rahmanie et al. 2004). Furthermore, the NRK-49F cell culture conditions to minimise cell proliferation and maximise the fibrogenic response to TGF-β have already been established (Grotendorst, Rahmanie et al. 2004). For these reasons, NRK-49F cells were used to determine the effects of retinoids on renal fibroblasts in an *in vitro* model of TGF-β1-induced fibrosis.

However it is well recognised that cell lines are not recommended for extrapolating *in vitro* findings to the *in vivo* setting because they are immortalised, with the ability to proliferate indefinitely and may not retain all their original characteristics. However they remain useful research tools as, in theory, their phenotype does not change during passaging thus providing a consistent environment for the study of intracellular signalling pathways and they are also a continual source of cells. However, the effects of tRA on fibrosis were also studied in a human foreskin fibroblast primary cell culture to determine if the effects of tRA were reproducible in other fibroblast cell cultures.

8.2.2 The 2D *in vitro* model of fibrosis as a suitable fibrotic model for studying the effects of tRA

It is currently common practice in research to select a few molecular markers of fibrosis for study in cell culture experiments. However, as demonstrated by the RT-qPCR array data presented here, tRA with or without TGF-β1 can

differentially regulate different markers of fibrosis. Therefore, if only a few molecular markers are chosen to study, different biased conclusions could be drawn. To avoid this, the 2D *in vitro* model of fibrosis was used in this research. It represents one of the only validated, reproducible cell models of fibrosis currently available and uses the dye PSR to visualise total collagen protein deposition, which can be further quantified by spectrophotometric analysis of eluted stain (Xu, Norman et al. 2007). As collagens constitute a large component of the abnormal ECM in TIF, this model can be used to define changes in net fibrogenesis between treatments and was therefore suitable for determining the effects of different retinoids with and without TGF-β1 on fibrogenesis in NRK-49F cells. While there are numerous *in vivo* models of renal fibrosis available they are not appropriate or ethical to use to further define mechanisms behind harmful treatments. This work therefore underlines the clear need for the development of fibrotic cell models that can better represent the *in vivo* setting and can determine the effects of treatments on global fibrosis.

8.2.3 Effect of tRA on fibrosis in NRK-49F cells

The work presented in this thesis for the first time shows a net pro-fibrotic effect of tRA, in the absence and presence of TGF-β1, in a normal rat kidney fibroblast cell line (Figure 3.1). This fibrogenic effect of tRA was also observed in a human foreskin fibroblast primary culture (Figure 7.1) suggesting that the effects of tRA were not idiosyncratic to NRK-49F cells. These findings are of interest because there are few, if any, published reports of the effects of retinoids in renal fibroblasts and much of the evidence of their effects in other kidney cells, such as mesangial cells, demonstrates an anti-fibrotic effect (Wen, Li et al. 2005; Liu, Lu et al. 2008). Possible reasons for the deficit of reports of the effects of retinoids in renal fibroblasts include the lack of availability of renal fibroblast cultures commercially and publication bias where researchers and editors only seek to publish results that are favourable. In addition, as discussed above, if only one or two fibrogenic markers are selected for study then there is a risk of data being misinterpreted.

Despite its net pro-fibrotic effect, with and without TGF-β1, tRA had both anti- and pro-fibrotic activities at the level of gene expression with a down-regulation as well as an up-regulation of selected collagen mRNAs (Figure 3.2). The opposing actions of retinoids are not unique to this work. Suppression of collagen synthesis by retinoids has been reported in human keratinocytes (Chen, Goyal et al. 1997), skin fibroblasts (Shigematsu and Tajima 1995; Meisler, Parrelli et al. 1997), scleroderma fibroblasts (Ohta and Uitto 1987), lung fibroblasts (Krupsky, Fine et al. 1994; Redlich, Delisser et al. 1995) and HSCs (Hellemans, Verbuyst et al. 2004). However an induction of collagen synthesis has been reported in chicken chondrocytes (Wu, Ishikawa et al. 1997), quail chondrocytes (Sanchez, Gionti et al. 1993) and rat lung epithelial cells (Federspiel, DiMari et al. 1990). While the opposing actions of tRA at the level of gene expression are of interest because strategies to potentiate the anti-fibrotic and reduce the pro-fibrotic actions of retinoids might lead to the development of new treatments for fibrosis, mRNA changes are only relevant if they translate to a biologically significant effect at the functional level. This is exemplified by the collagen and TG2 data presented here where there was a down-regulation of many collagens at mRNA level despite collagen accumulation at protein level (Figures 3.1-3.4) and an up-regulation of TG2 mRNA but not protein following tRA and dual treatment (Figures 3.8E and 3.13).

However, in agreement with the RT-qPCR data, which showed a down-regulation of Mmp mRNAs (Figures 3.2 and 3.6), an MMP activity assay demonstrated that MMP activity was also reduced by tRA with and without TGF-β1 (Figure 3.7). This suggested that a reduction in matrix degradation by decreased MMP activity may contribute to the pro-fibrotic effect of tRA in NRK-49F cells. The published literature is scarce on the effects of tRA on MMP expression and activity in renal disease and there has tended to be focus on a few MMPs thought to be important in renal fibrosis despite evidence that at least ten isoforms are expressed in kidney tissue in health and disease (Catania, Chen et al. 2007). In light of the results presented here a review of the RT-qPCR data highlighted several individual MMPs that might

be of interest to explore in future studies. In particular, Mmp-13 (a collagenase), Mmps -3 and -10 (stromelysins) and Mmps -2 and -9 (gelatinases) showed a marked down-regulation at mRNA level following tRA and/or dual treatment. Roles for MMPs -2 and -9 are well established in renal fibrosis (Sharma, Mauer et al. 1995; Gonzalez-Avila, Iturria et al. 1998; Ronco and Chatziantoniou 2008) and MMPs -3, -10 and -13 together are known to breakdown FN, collagens and gelatins, which are all important in TIF. In addition, in murine models of experimental liver fibrosis, MMP-13 was found to facilitate resolution of hepatic fibrosis (Fallowfield, Mizuno et al. 2007) and MMP-13 over-expression reduced liver fibrosis associated with an increase in MMPs -2 and -9 activity (Endo, Niioka et al. 2011).

One other noteworthy result from the MMP RT-qPCR array was the up-regulation of Mmp-7 by tRA and dual treatment (Figure 3.2). While no conclusions can be drawn from this single result generated from a one cell culture study, it is intriguing that an increase in MMP-7 expression has been identified in diseased human kidney biopsy specimens and that it is a potential marker for renal Wnt/β-catenin signalling in progressive CKD (Surendran, Simon et al. 2004; He, Tan et al. 2011).

PAI-1 protein was also modulated by tRA with evidence of an increase in protein that was further increased by dual treatment in NRK-49F cells (Figure 3.9). Furthermore the PAI-1 inhibitor tiplaxtinin caused a reduction in tRA-induced collagen accumulation with and without TGF-β1 (Figure 3.10). These results could help to explain why dual treatment caused more collagen accumulation than tRA alone. In addition, they could partly explain the reduction in MMP activity by tRA and dual treatment as plasmin is known to activate MMPs.

While down-regulation of MMPs by tRA has been reported before (Benbow and Brinckerhoff 1997; Fisher and Voorhees 1998; Mao, Tashkin et al. 2003), the increase in PAI-1 expression was somewhat unexpected as a down-regulation of PAI-1 following tRA treatment in TGF-β1-stimulated mesangial

cells (Wen, Li et al. 2005; Liu, Lu et al. 2008) and in the SNx model have been reported (Liu, Lu et al. 2011). Furthermore, RAR agonists and antagonists have been found to suppress and potentiate TGF-β-induced PAI-1 promoter activity, respectively (Pendaries, Verrecchia et al. 2003). It is unclear whether these results represent true cell type specificity of tRA on PAI-1 expression between mesangial cells and fibroblasts, the two main effector cells in glomerulosclerosis and TIF, respectively. However, tRA induction of PAI-1 in NRK-49F cells is reminiscent of its effects in VSMCs, in which it induced PAI-1 mRNA expression (Watanabe, Kanai et al. 2002).

Although PAI-1 is widely reported to be pro-fibrotic the mechanisms through which it exerts its effects are complex, not fully understood and involve protease-independent as well as protease-dependent pathways. The primary role of PAI-1 is as an inhibitor of uPA and tPA, which convert plasminogen to plasmin. There are several mechanisms through which a decrease in renal plasmin might reduce fibrosis in this cell model. Firstly, plasmin is known to activate several latent MMPs as well as degrade fibrin (Nagase 1997), therefore a reduction in plasmin-induced MMP activation might exacerbate ECM accumulation. Secondly, if fibrinogen/fibrin is proved to be involved in renal scar formation then a reduction in plasmin would exacerbate fibrosis (Eddy and Fogo 2006). Finally, plasmin is also known to degrade some ECM components such as FN (Huang, Border et al. 2006). In addition, reduction in uPA and tPA activity by PAI-1 could contribute to the pro-fibrotic effects of PAI-1 independent of plasmin (Eddy and Fogo 2006). For example, uPA can degrade ECM components such as FN and activate anti-fibrotic molecules such as HGF. Therefore reduced uPA activity will favour development of fibrosis (Naldini, Vigna et al. 1995). Furthermore PAI-1 can exert its effects through receptor-mediated modulation of cell behaviour including cell detachment and migration (Eddy and Fogo 2006).

8.2.4 Contribution of the nuclear receptor signalling pathways to the pro-fibrotic effects of tRA

Results of experiments designed to determine the roles of the retinoid nuclear receptors and PPARβ/δ in the pro-fibrotic effects of tRA suggested that RXRs were likely mediators of these effects, and RARs possible mediators, because: 1) NRK-49F cells expressed retinoid nuclear receptors and their mRNA expression was modulated by tRA and dual treatment (Figures 4.1-4.2 and 4.4-4.5); 2) RXR pan-agonists more than RAR pan-agonists and RAR-isotype-selective agonists showed pro-fibrotic effects but RAR and RXR antagonists did not (Figure 5.1); and 3) RAR and RXR antagonists partially blocked tRA-induced total collagen deposition in the presence of TGF-β1 (Figure 5.2).

Retinoid receptor signalling has also been shown to be relevant in other experimental models of renal diseases. In particular, Juergen Wagner's group from the University of Heidelberg has demonstrated improvement in renal parameters in acute and chronic glomerulonephritis models by RAR- and RXR-specific agonists (Lehrke, Schaier et al. 2002; Schaier, Liebler et al. 2004). This work is important as it establishes that receptor-selective retinoids can be used successfully for the treatment of renal diseases.

Although in these published studies no differential effects were noted between RAR and RXR agonists, RAR and RXR agonists have been shown to play different roles in matrix synthesis in cell models of liver disease (Hellemans, Verbuyst et al. 2004). For example, in activated HSCs synthetic RXR agonists reduced collagen type I and FN synthesis however RAR agonists reduced collagen types I and III and FN (Hellemans, Verbuyst et al. 2004). In the work presented here there was also evidence that RARs and RXRs had differential roles in total collagen accumulation. The pan-RXR agonist HX531 caused an increase in PSR staining that was dose-dependent and similar in size to the effect seen with tRA, however the pan-RAR agonist TTNPB had only a small non-dose-dependent effect that was much less comparable with that seen

with tRA (Figure 5.1). These results are more consistent with tRA acting through RXR.

However, it is difficult to relate reports of the anti-fibrotic effects of RAR and RXR agonists in renal disease models to the work presented here where agonists of RARs and RXRs caused a pro-fibrotic effect. But renal disease models such as those of glomerulonephritis may not be directly applicable to TIF and more appropriate experimental models may better determine the effect of retinoid type in TIF, for example the Alb/TGF-β1 transgenic mouse model of renal fibrosis (Xu, Hendry et al. 2010).

The receptor-selective retinoids tested in this work had different pro-fibrotic potencies in the order: tRA and AGN194204 > TTNPB > AGN195183 and CD2019 > CD437 (Figure 5.1). Although the RARα and RARβ isotype-selective agonists tested were less fibrogenic and the RARγ agonist had no fibrogenic potential, none demonstrated a net anti-fibrotic potential and it remains largely unknown how retinoids exert their anti-fibrotic effects. Since receptor-selective agonists have already been used successfully in renal disease models (Schaier, Liebler et al. 2004; Zhong, Wu et al. 2011) the use of RAR isotype-selective retinoids could be a plausible strategy to avoid the unwanted pro-fibrotic effects of tRA and deserves a focus in future research.

Thus far, there are several reported possible mechanisms through which retinoid receptor signalling could result in fibrosis, summarised in Figure 8.1. Firstly, they could be exerting their effects via RAREs by increasing the transcription of RA-responsive genes (Vasios, Gold et al. 1989). Secondly, retinoid receptors could directly interfere with TGF-β intracellular signalling. Hoover et al. showed that dual treatment of dispersed hearts and NIH3T3 cells with retinoids (particularly an RXR agonist) and TGF-β resulted in an increase in phosphorylated R-Smads compared to TGF-β alone and loss of RXRα had a similar effect (Hoover, Burton et al. 2008). This suggests a direct interaction between retinoid receptors and Smads where agonists/loss of retinoid receptors would prevent this interaction making available R-Smads for

phosphorylation and activation (Hoover, Burton et al. 2008). In addition, Smad and RXR signalling may communicate at the level of TGIF. When the TGF-β signalling pathway is active TGIF binds to Smads preventing them from interacting with their co-activators thus blunting Smad-mediated transcription; however, TGIF can also bind to RXREs therefore preventing communication between TGIF and Smads (Bertolino, Reimund et al. 1995; Wotton, Lo et al. 1999). Thirdly, retinoids have been shown to increase TGF-β expression in some renal diseases models (Datta, Reddy et al. 2001; Morath, Ratzlaff et al. 2009). Finally, activation of RAR and RXR receptors can modulate other important intracellular signalling cascades such as the MAP kinases. These in turn could potentiate the effects of R-Smads leading to a heightened response to TGF-β1 (Rochette-Egly and Germain 2009).

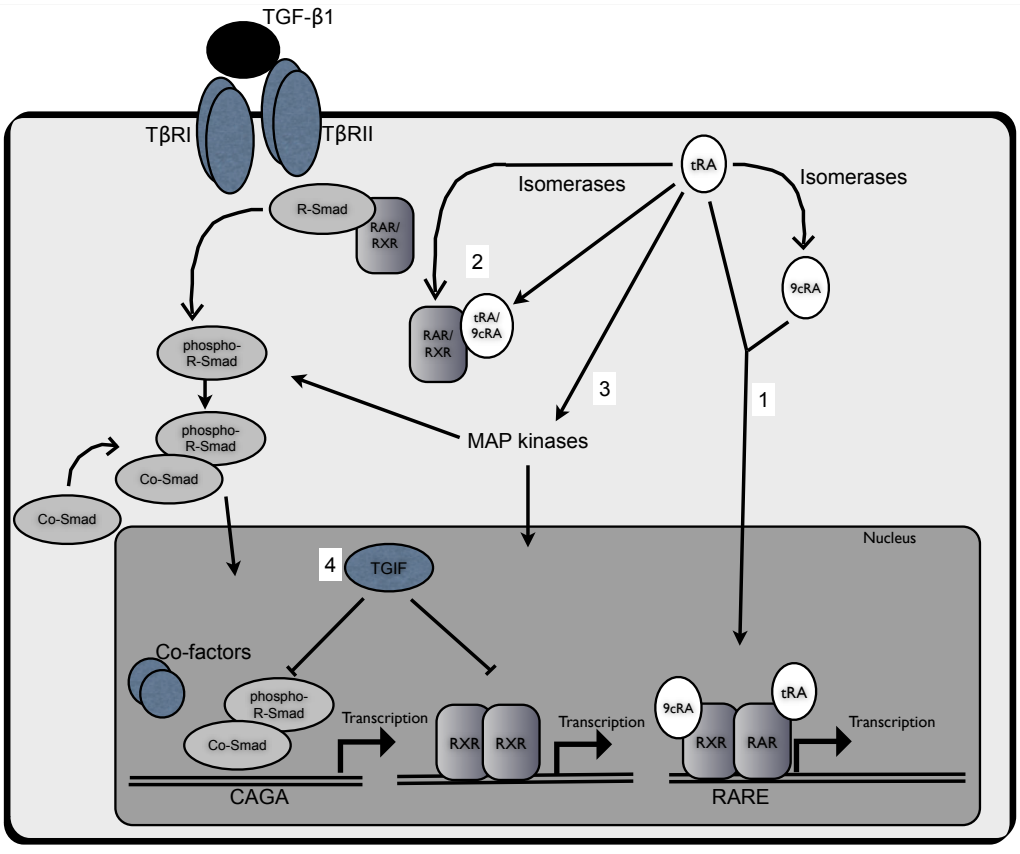

Figure 8.1. Potential mechanisms for the RAR/RXR-dependent pro-fibrotic effects of retinoids. 1) tRA or isomers of tRA directly affect transcriptional events by binding to RXR/ RAR dimers that bind to RAREs; 2) tRA or isomers of tRA bind to retinoid receptor/ R-Smad complexes and R-Smad is released and made available for phosphorylation; 3) tRA activates MAP kinases via retinoid receptor-dependent; 4) TGIF binds RXRE making available more Smad complex for Smad-mediated transcription.

8.2.5 Dual potential of retinoids

This work has confirmed the complex and opposing actions that retinoids can have even in the same cell system. The effects of tRA in NRK-49F cells varied depending on dosage, time points studied, cell culture conditions and retinoid type. Examples include the dose-dependent increase in total collagen accumulation by tRA (Figure 3.1); the opposing actions of tRA at the level of gene expression with both up-regulation and down-regulation of collagen mRNAs (Figure 3.2); the time-dependent regulation of Mmp-2 and Mmp-13 mRNAs with opposing actions of tRA at different time points (Figure 3.6); the environment-dependent regulation of FN protein following tRA treatment with no change seen in quiescent NRK-49F cells but a tendency towards an increase in TGF-β1-treated cells (Figure 3.5); and the differential effects of receptor-selective retinoids on total collagen accumulation (Figure 5.1).

With respect to retinoid dose, Morath et al. have shown that dose of 13cRA was crucial in determining outcome in a rat SNx model of renal fibrosis (Morath, Ratzlaff et al. 2009). Specifically, low-dose 13cRA (10 mg/kg body weight) had an anti-fibrotic effect, but high doses (40 mg/kg body weight) aggravated kidney scarring; the low-dose group also showed reduced TGF-β1 staining whereas high-dose treatment caused an increase in TGF-β1 mRNA expression (Morath, Ratzlaff et al. 2009). Another example is the effect of tRA on fibrosis in the Alb/TGF-β1 transgenic mouse model of renal fibrosis (Xu, Hendry et al. 2010). Xu et al. showed that low-dose tRA (6-10.7 mg/kg/day) caused a tendency towards suppression of some fibrogenic markers including FN, COL1A1 and COL1A2 mRNAs although no change in interstitial fibrosis or glomerulosclerosis score was seen, however high-dose tRA (20.1-27.4 mg/kg/day) exacerbated fibrosis (Xu, Hendry et al. 2010).

With respect to time point studied, similar to the results presented here for Mmp-2 and -13 mRNAs, Morath et al. showed a time-dependent effect of 13cRA on collagen IV and TGF-β1 mRNAs in VSMC cultures with a down-regulation of collagen IV mRNA at 4 h but an up-regulation at 24 h and a

down-regulation of TGF-β1 mRNA at 4 h but no change at 24 h (Morath, Ratzlaff et al. 2009).

Furthermore, environmental conditions also been found to affect the actions of retinoids in other studies. For example, Liu et al. showed that tRA increased FN protein in quiescent RMCs but reduced FN protein in TGF-β1-stimulated RMCs (Liu, Lu et al. 2008). A further example is the reduced procollagen production and type I and type III procollagen mRNA expression in scleroderma and normal human skin fibroblasts by tRA and 13cRA (Ohta and Uitto 1987) but the increase in FN, thrombospondin, laminin and collagen type I by tRA seen in growth-inhibited human skin fibroblasts (Varani, Mitra et al. 1990).

Moreover, retinoid type appears to be crucial in determining outcome. For example, in activated HSCs, tRA inhibited synthesis of procollagen types I, II, and IV, as well as FN and laminin, but 9cRA increased procollagen I mRNA without affecting the expression of other matrix proteins (Hellemans, Grinko et al. 1999). Naturally-occurring RAs and synthetic RAR/RXR-selective retinoids have also been shown to exert differential effects in activated HSCs (Hellemans, Verbuyst et al. 2004).

Thus, given the contrary nature of retinoids, this work corroborates that extra care should be taken when considering dosage, time points studied, environmental conditions and selectivity of retinoid.

8.3 Limitations of this work

8.3.1 Choice of cell model and the 2D *in vitro* model of fibrosis

NRK-49F cells were chosen as an appropriate fibroblast cell model as they are derived from normal rat kidneys, are phenotypically fibroblast-like and they are known to respond to TGF-β1 (Roberts, Sporn et al. 1986; Grotendorst, Rahmanie et al. 2004). However, they are a cell line and therefore may not retain their original characteristics. In addition they are of rat origin and, while this would be advantageous for further *in vivo* work using

rat experimental models, the results may not be applicable to human renal fibrosis which is ultimately the target for this research. Although the effects of tRA on total collagen deposition were reproducible in a human foreskin fibroblast primary culture, these cells may not behave similarly to human renal fibroblasts. Therefore to strengthen this data the effects of tRA in suitable rat and human renal fibroblast primary cultures could be determined. However, of course no cell culture is ideal as the phenotype of even primary cultures will change following contact with plastic-ware, different growth media and the loss of contact with other cell types, ECM and growth factors.

The 2D *in vitro* model of fibrosis was used as a validated, reproducible and rapid model for determining the net effects of different retinoids on total collagen deposition *in vitro* (Xu, Norman et al. 2007). However this model has its limitations. Firstly, it cannot be used if TGF-β1-treated cells do not produce enough collagen for the change to be detected by PSR staining. Indeed this model proved unsuitable for a variety of cell types that are known to be important in TIF and glomerulosclerosis. Secondly, as PSR stains for collagen, relevant changes in non-collagenous ECM components will be overlooked in this model. Finally, this model relies on an intact cell monolayer and disruption of this monolayer or contraction of cells could affect the readout. Furthermore, a confluent fibroblast monolayer does not represent the *in vivo* fibrotic setting. Thus, while the 2D *in vitro* model of fibrosis represents a useful cell model of fibrosis, there is a clear need for the development of improved *in vitro* fibrotic models that are applicable to a variety of cell types and mimic better the complex 3D environment that cells reside in *in vivo*.

8.3.2 Use of chemical agonists and inhibitors and gene silencing technology

This work has relied heavily on the use of chemical agonists and inhibitors of PAI-1, TG2 and the nuclear receptors. While agonists and inhibitors are useful in cell culture experiments because they can be transferred into *in vivo* work, they can often have unpredictable effects not related to their expected target and also can cause cytotoxicity. Therefore, ideally, results obtained using

chemicals should be confirmed with either a second agonist/inhibitor or, better still, via different technologies such as gene over-expression or knockdown, and blocking antibodies. In this work, transient transfection was used for this purpose, however, despite numerous attempts using different methodologies, gene knockdown using targeted siRNAs in NRK-49F cells was largely unsuccessful.

8.3.3 Roles of the matrix degradation pathways in the pro-fibrotic effects of tRA

The results presented in this thesis demonstrate an association between reduced MMP activity and a pro-fibrotic effect of tRA. However, interventional studies to further examine this relationship have not been performed. In addition, which particular MMP isoforms are involved has not been addressed. It is relevant to identify specific MMP isoforms as it would not only help develop a focus on disease-specific pathways but also facilitate transfer of this work into the *in vivo* setting as targeting multiple MMPs *in vivo* may have widespread biological implications.

tRA and dual treatment also caused an increase in PAI-1 expression and inhibiting PAI-1 activity reduced the pro-fibrotic effect of tRA. This provided another mechanism through which tRA might exert its actions. However, this work only looked at the effects of tRA on PAI-1 in isolated fibroblast cultures. Since PAI-1 acts through multiple serine protease-dependent and independent mechanisms, its effects on fibrosis are likely to be cell-type and species specific and may also depend on the region of the kidney affected, i.e. glomerular or tubulointerstitial, where expression of modulators of PAI-1 activity, such as cell surface receptors, may vary (Eddy and Fogo 2006). Therefore, *in vivo* experiments are necessary to further dissect the effects of tRA on PAI-1 in a complex setting where multiple cell types, growth factors and cytokines all play a role.

8.3.4 Roles for retinoid receptor-dependent and -independent pathways in the pro-fibrotic effects of tRA

This work has explored the effects of individual nuclear receptor activation on fibrosis in NRK-49F cells by using the end point of total collagen accumulation as a read out for fibrosis. However, the actions of each of the nuclear receptors on specific markers of fibrosis have not been explored. This is relevant as different nuclear receptors may play differential roles in fibrosis that remain unidentified by this work.

In addition, the intracellular signalling pathways through which the retinoid receptors exert their pro-fibrotic effects have not been elucidated and, furthermore, the contributions of retinoid receptor-independent pathways have not been explored in detail. Retinoid receptor-independent mechanisms might be involved in the pro-fibrotic effects of tRA as RAR and RXR antagonists did not fully inhibit tRA-induced total collagen accumulation suggesting that other pathways may also be active. Thus, future experiments could further dissect out the roles of individual retinoid receptors in fibrogenesis and the role of receptor-independent pathways in the pro-fibrotic effects of tRA.

8.4 Future work

8.4.1 *in vitro* work

To further investigate the roles of the MMPs in the pro-fibrotic effects of tRA protein expression of MMP isoforms could initially be performed. Zymography or MMP isoform-selective activity assays could subsequently be employed to identify which MMP isoforms are involved at the functional level. In addition, interventional studies using MMP inhibitors and gene silencing could be used to determine if the pro-fibrotic effects of tRA can be mimicked, and increasing MMP activity, for example by over-expression of MMPs, could be used to ascertain if the pro-fibrotic effects of tRA can be prevented. It would also be interesting to determine if the mechanism behind the effect of tRA on MMP expression is AP-1-dependent, as described in other publications (Benbow and Brinckerhoff 1997).

With respect to the finding that inhibiting PAI-1 activity using tiplaxtinin reduced the pro-fibrotic effect of tRA, this result needs to be confirmed using a second chemical inhibitor or a different technology, especially as tiplaxtinin was toxic in NRK-49F cells. In view of the lack of suitable chemical agonists/ inhibitors for PAI-1, blocking antibodies designed to inhibit the function of their target could be used. Stable transfection of NRK-49F cells could also be considered or easier-to-transfect cell cultures explored. Furthermore, it would be interesting to investigate the pathways through which PAI-1 is up-regulated by tRA; for example, is the mechanism of PAI-1 up-regulation tyrosine-kinase dependent (Watanabe, Kanai et al. 2002)?

The results obtained using chemical agonists and antagonists to retinoid receptors also need to be confirmed using different chemicals or technologies. In addition, it would be important to determine the retinoid receptor isotype with the least detrimental effect on MMP and PAI-1 regulation, which could be done using RT-qPCR, Western blotting and functional assays, in a similar way to the work presented here.

8.4.2 Translation of this work into an *in vivo* model

This work has focused on the effects of retinoids on fibrosis in renal fibroblasts. However in reality TIF is a highly complex process involving multiple cell types, growth factors and cytokines. The MMPs are well known to have roles much more diverse than simply matrix degradation and the effects of PAI-1 depend on the multiple cell types, growth factors and cytokines present in the *in vivo* setting. Therefore, to take this work further, it would be important to explore the effects of different retinoids on renal fibrosis in an equivalent *in vivo* model and there are numerous experimental models of TIF that could be considered.

The Alb/TGF-β1 transgenic mouse model is worth particular consideration from a mechanistic viewpoint as it is an *in vivo* model of TGF-β1-induced renal fibrosis and therefore is comparable to the *in vitro* model of TGF-β1-induced fibrosis presented here. This model over-expresses active TGF-β1 in

the liver leading to high serum TGF-β1 levels and renal fibrosis develops rapidly (Mozes, Bottinger et al. 1999). tRA has been shown to exacerbate renal fibrosis in this mouse model therefore it constitutes an *in vivo* pro-fibrotic model of the effects of tRA (Xu, Hendry et al. 2010). Ethically, it is inappropriate to consider a harmful treatment for an *in vivo* model, however it would be interesting to examine the mechanisms behind the pro-fibrotic effects of tRA in the renal tissue preserved from previous experiments, if available (Xu, Hendry et al. 2010). In addition, the effects of other, more selective retinoids could be explored in this model once their effects on fibrosis have been better defined *in vitro*.

8.5 Concluding remarks

This work has identified fibroblasts as a key cellular mediator of the pro-fibrotic effects of tRA and, furthermore, potential pathways involved (Figure 8.2). While an anti-fibrotic retinoid was not identified through this work, receptor-selective retinoids with no/less pro-fibrotic potential were identified, which may provide a safer option for use in CKD patients and reduce the side effect profile of less selective retinoids. The increased fibrogenic effect of tRA in the presence of TGF-β1 in renal fibroblasts highlights issues regarding the prescription of retinoids to CKD patients who over-express renal TGF-β1. In view of the emerging clinical use of retinoids in CKD there is justification to better define the fibrogenic effects of tRA so that the long-term safety profile of retinoids is improved and eventually a viable retinoid-based therapy for CKD devoid of the unwanted pro-fibrotic effects can be developed.

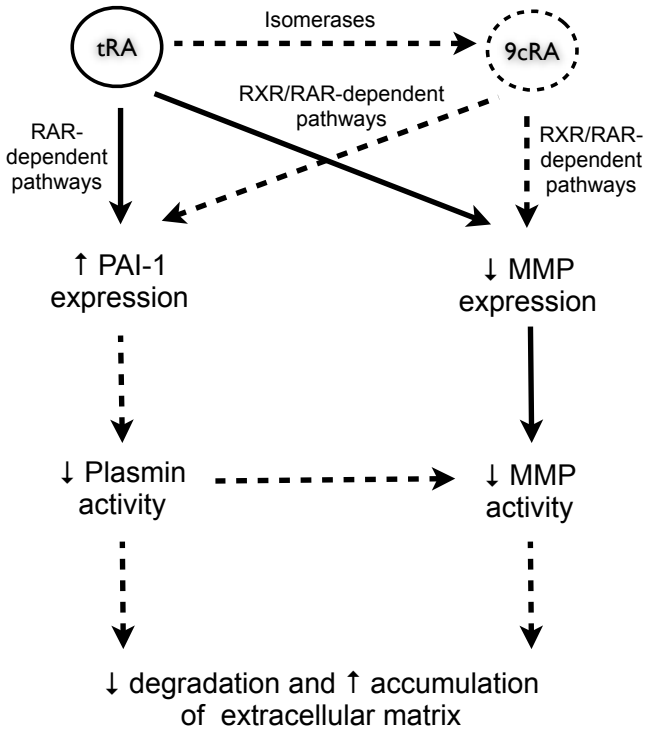

Figure 8.2. Diagram of the proposed pathways of the pro-fibrotic effects of tRA in NRK-49F cells. tRA-induced pro-fibrotic effects in NRK-49F cells are associated with increased PAI-1 and reduced MMP expression. tRA-induced PAI-1 could lead to reduced plasminogen activation into plasmin, which in turn could lead to reduced degradation of ECM proteins either directly or through reduced activation of MMPs by plasmin. Thus, both PAI-1 induction and MMP reduction could contribute to decreased degradation and increased accumulation of ECM. Both RXR and RAR pathways are likely involved in the pro-fibrotic effects of tRA, with tRA activation of RXR signalling hypothesised to occur by isomerisation of tRA into 9cRA. In terms of the pro-fibrotic effects, RAR agonists had only weak effects however the RXR agonist AGN194204 was as potent as tRA, suggesting that RXR-activating metabolites might play a larger role in the pro-fibrotic effects of tRA. Solid lines represent pathways directly supported by data and dashed lines represent hypothesised pathways.

Chapter 9. Bibliography

Achkar, C. C., F. Derguini, et al. (1996). "4-Oxoretinol, a new natural ligand and transactivator of the retinoic acid receptors." Proc Natl Acad Sci U S A **93**(10): 4879-4884.

Adams, J., E. Kiss, et al. (2005). "13-cis retinoic acid inhibits development and progression of chronic allograft nephropathy." Am J Pathol **167**(1): 285-298.

Aeschlimann, D. and M. Paulsson (1991). "Cross-linking of laminin-nidogen complexes by tissue transglutaminase. A novel mechanism for basement membrane stabilization." J Biol Chem **266**(23): 15308-15317.

Afrakhte, M., A. Moren, et al. (1998). "Induction of inhibitory Smad6 and Smad7 mRNA by TGF-beta family members." Biochem Biophys Res Commun **249**(2): 505-511.

Agarwal, C., R. A. Chandraratna, et al. (1996). "AGN193109 is a highly effective antagonist of retinoid action in human ectocervical epithelial cells." J Biol Chem **271**(21): 12209-12212.

Aguilar, R. P., S. Genta, et al. (2009). "Vitamin A deficiency injures liver parenchyma and alters the expression of hepatic extracellular matrix." J Appl Toxicol **29**(3): 214-222.

Akhurst, R. J. and A. Hata (2012). "Targeting the TGFbeta signalling pathway in disease." Nat Rev Drug Discov **11**(10): 790-811.

Akimov, S. S. and A. M. Belkin (2001). "Cell surface tissue transglutaminase is involved in adhesion and migration of monocytic cells on fibronectin." Blood **98**(5): 1567-1576.

Alique, M., F. J. Lucio-Cazana, et al. (2007). "Upregulation of cyclooxygenases by retinoic acid in rat mesangial cells." Pharmacology **79**(1): 57-64.

Alique, M., V. Moreno, et al. (2006). "Kinase-dependent, retinoic acid receptor-independent up-regulation of cyclooxygenase-2 by all-trans retinoic acid in human mesangial cells." Br J Pharmacol **149**(2): 215-225.

Allegretto, E. A., M. R. McClurg, et al. (1993). "Transactivation properties of retinoic acid and retinoid X receptors in mammalian cells and yeast. Correlation with hormone binding and effects of metabolism." J Biol Chem **268**(35): 26625-26633.

Altucci, L., M. D. Leibowitz, et al. (2007). "RAR and RXR modulation in cancer and metabolic disease." Nat Rev Drug Discov **6**(10): 793-810.

Alvarez, R. J., M. J. Sun, et al. (1992). "Biosynthetic and proliferative characteristics of tubulointerstitial fibroblasts probed with paracrine cytokines." Kidney Int **41**(1): 14-23.

Annes, J. P., J. S. Munger, et al. (2003). "Making sense of latent TGFbeta activation." J Cell Sci **116**(Pt 2): 217-224.

Ansell, D., P. Roderick, et al. (2009). "UK Renal Registry 12th Annual Report (December 2009): Chapter 7: Survival and causes of death of UK adult patients on renal replacement therapy in 2008: national and centre-specific analyses." Nephron Clin Pract **115 Suppl 1**: c117-144.

Asada, N., M. Takase, et al. (2011). "Dysfunction of fibroblasts of extrarenal origin underlies renal fibrosis and renal anemia in mice." J Clin Invest **121**(10): 3981-3990.
Asanuma, K., I. Shirato, et al. (2002). "Selective modulation of the secretion of proteinases and their inhibitors by growth factors in cultured differentiated podocytes." Kidney Int **62**(3): 822-831.
Austenaa, L. M., H. Carlsen, et al. (2004). "Vitamin A status significantly alters nuclear factor-kappaB activity assessed by in vivo imaging." Faseb J **18**(11): 1255-1257.
Austenaa, L. M., H. Carlsen, et al. (2009). "Retinoic acid dampens LPS-induced NF-kappaB activity: results from human monoblasts and in vivo imaging of NF-kappaB reporter mice." J Nutr Biochem **20**(9): 726-734.
Baricos, W. H., S. L. Cortez, et al. (1999). "Transforming growth factor-beta is a potent inhibitor of extracellular matrix degradation by cultured human mesangial cells." J Am Soc Nephrol **10**(4): 790-795.
Bastien, J., J. L. Plassat, et al. (2006). "The phosphoinositide 3-kinase/Akt pathway is essential for the retinoic acid-induced differentiation of F9 cells." Oncogene **25**(14): 2040-2047.
Beard, R. L., T. T. Duong, et al. (2002). "Synthesis and biological activity of retinoic acid receptor-alpha specific amides." Bioorg Med Chem Lett **12** (21): 3145-3148.
Beere, H. M. and J. A. Hickman (1993). "Differentiation: a suitable strategy for cancer chemotherapy?" Anticancer Drug Des **8**(4): 299-322.
Benbow, U. and C. E. Brinckerhoff (1997). "The AP-1 site and MMP gene regulation: what is all the fuss about?" Matrix Biol **15**(8-9): 519-526.
Bernard, B. A., J. M. Bernardon, et al. (1992). "Identification of synthetic retinoids with selectivity for human nuclear retinoic acid receptor gamma." Biochem Biophys Res Commun **186**(2): 977-983.
Berry, D. C. and N. Noy (2007). "Is PPARbeta/delta a Retinoid Receptor?" PPAR Res **2007**: 73256.
Bertelli, R., F. Valenti, et al. (1998). "Cell-specific regulation of alpha1(III) and alpha2(V) collagen by TGF-beta1 in tubulointerstitial cell models." Nephrol Dial Transplant **13**(3): 573-579.
Bertolino, E., B. Reimund, et al. (1995). "A novel homeobox protein which recognizes a TGT core and functionally interferes with a retinoid-responsive motif." J Biol Chem **270**(52): 31178-31188.
Blaner, W. S. (2001). "Cellular metabolism and actions of 13-cis-retinoic acid." J Am Acad Dermatol **45**(5): S129-135.
Blomhoff, R. (1997). "Retinoids may increase fibrotic potential of TGF-beta: crosstalk between two multi-functional effectors." Hepatology **26**(4): 1067-1068.
Blomhoff, R. and H. K. Blomhoff (2006). "Overview of retinoid metabolism and function." J Neurobiol **66**(7): 606-630.
Bolbrinker, J., S. Markovic, et al. (2006). "Expression and response to angiotensin-converting enzyme inhibition of matrix metalloproteinases 2 and 9 in renal glomerular damage in young transgenic rats with renin-dependent hypertension." J Pharmacol Exp Ther **316**(1): 8-16.

Bookout, A. L., Y. Jeong, et al. (2005). "www.nursa.org/10.1621/datasets.02001."
Border, W. A., S. Okuda, et al. (1990). "Transforming growth factor-beta regulates production of proteoglycans by mesangial cells." Kidney Int **37**(2): 689-695.
Borland, M. G., J. E. Foreman, et al. (2008). "Ligand activation of peroxisome proliferator-activated receptor-beta/delta inhibits cell proliferation in human HaCaT keratinocytes." Mol Pharmacol **74**(5): 1429-1442.
Borland, M. G., C. Khozoie, et al. (2011). "Stable over-expression of PPARbeta/delta and PPARgamma to examine receptor signaling in human HaCaT keratinocytes." Cell Signal **23**(12): 2039-2050.
Bossenbroek, N. M., T. H. Sulahian, et al. (1998). "Expression of nuclear retinoic acid receptor and retinoid X receptor mRNA in the cornea and conjunctiva." Curr Eye Res **17**(5): 462-469.
Boylan, J. F. and L. J. Gudas (1991). "Overexpression of the cellular retinoic acid binding protein-I (CRABP-I) results in a reduction in differentiation-specific gene expression in F9 teratocarcinoma cells." J Cell Biol **112**(5): 965-979.
Boylan, J. F. and L. J. Gudas (1992). "The level of CRABP-I expression influences the amounts and types of all-trans-retinoic acid metabolites in F9 teratocarcinoma stem cells." J Biol Chem **267**(30): 21486-21491.
Brigstock, D. R. (2003). "The CCN family: a new stimulus package." J Endocrinol **178**(2): 169-175.
Bruce, D. L. and G. P. Sapkota (2012). "Phosphatases in SMAD regulation." FEBS Lett.
Buck, J., F. Derguini, et al. (1991). "Intracellular signaling by 14-hydroxy-4,14-retro-retinol." Science **254**(5038): 1654-1656.
Camp, T. M., L. M. Smiley, et al. (2003). "Mechanism of matrix accumulation and glomerulosclerosis in spontaneously hypertensive rats." J Hypertens **21**(9): 1719-1727.
Camuto, P., J. Shupack, et al. (1987). "Long-term effects of etretinate on the liver in psoriasis." Am J Surg Pathol **11**(1): 30-37.
Cao, Z., K. C. Flanders, et al. (2003). "Levels of phospho-Smad2/3 are sensors of the interplay between effects of TGF-beta and retinoic acid on monocytic and granulocytic differentiation of HL-60 cells." Blood **101**(2): 498-507.
Carome, M. A., L. J. Striker, et al. (1993). "Human glomeruli express TIMP-1 mRNA and TIMP-2 protein and mRNA." Am J Physiol **264**(6 Pt 2): F923-929.
Catania, J. M., G. Chen, et al. (2007). "Role of matrix metalloproteinases in renal pathophysiologies." Am J Physiol Renal Physiol **292**(3): F905-911.
Chambon, P. (1996). "A decade of molecular biology of retinoic acid receptors." Faseb J **10**(9): 940-954.
Chambon, P. (2005). "The nuclear receptor superfamily: a personal retrospect on the first two decades." Mol Endocrinol **19**(6): 1418-1428.
Chang, H. R., S. F. Yang, et al. (2006). "Relationships between circulating matrix metalloproteinase-2 and -9 and renal function in patients with chronic kidney disease." Clin Chim Acta **366**(1-2): 243-248.

Chen, H., H. Zhang, et al. (2007). "HOXA5 acts directly downstream of retinoic acid receptor beta and contributes to retinoic acid-induced apoptosis and growth inhibition." Cancer Res **67**(17): 8007-8013.
Chen, J. D. and R. M. Evans (1995). "A transcriptional co-repressor that interacts with nuclear hormone receptors." Nature **377**(6548): 454-457.
Chen, M., S. Goyal, et al. (1997). "Modulation of type VII collagen (anchoring fibril) expression by retinoids in human skin cells." Biochim Biophys Acta **1351**(3): 333-340.
Chen, N., B. Onisko, et al. (2008). "The nuclear transcription factor RARalpha associates with neuronal RNA granules and suppresses translation." J Biol Chem **283**(30): 20841-20847.
Cheng, Q. L., M. Orikasa, et al. (1995). "Progressive renal lesions induced by administration of monoclonal antibody 1-22-3 to unilaterally nephrectomized rats." Clin Exp Immunol **102**(1): 181-185.
Cheng, S. and D. H. Lovett (2003). "Gelatinase A (MMP-2) is necessary and sufficient for renal tubular cell epithelial-mesenchymal transformation." Am J Pathol **162**(6): 1937-1949.
Cheng, S., A. S. Pollock, et al. (2006). "Matrix metalloproteinase 2 and basement membrane integrity: a unifying mechanism for progressive renal injury." Faseb J **20**(11): 1898-1900.
Chikamori, K., J. E. Hill, et al. (2006). "Downregulation of topoisomerase IIbeta in myeloid leukemia cell lines leads to activation of apoptosis following all-trans retinoic acid-induced differentiation/growth arrest." Leukemia **20**(10): 1809-1818.
Chin, B. Y., A. Mohsenin, et al. (2001). "Stimulation of pro-alpha(1)(I) collagen by TGF-beta(1) in mesangial cells: role of the p38 MAPK pathway." Am J Physiol Renal Physiol **280**(3): F495-504.
Choi, M. E., Y. Ding, et al. (2012). "TGF-beta signaling via TAK1 pathway: role in kidney fibrosis." Semin Nephrol **32**(3): 244-252.
Coimbra, T., R. Wiggins, et al. (1991). "Transforming growth factor-beta production in anti-glomerular basement membrane disease in the rabbit." Am J Pathol **138**(1): 223-234.
Cullum, M. E. and M. H. Zile (1985). "Metabolism of all-trans-retinoic acid and all-trans-retinyl acetate. Demonstration of common physiological metabolites in rat small intestinal mucosa and circulation." J Biol Chem **260**(19): 10590-10596.
D'Ambrosio, D. N., R. D. Clugston, et al. (2011). "Vitamin A metabolism: an update." Nutrients **3**(1): 63-103.
D'Eletto, M., M. G. Farrace, et al. (2009). "Transglutaminase 2 is involved in autophagosome maturation." Autophagy **5**(8): 1145-1154.
Dallas, S. L., P. Sivakumar, et al. (2005). "Fibronectin regulates latent transforming growth factor-beta (TGF beta) by controlling matrix assembly of latent TGF beta-binding protein-1." J Biol Chem **280**(19): 18871-18880.
Darby, I. A. and T. D. Hewitson (2007). "Fibroblast differentiation in wound healing and fibrosis." Int Rev Cytol **257**: 143-179.
Datta, P. K., R. S. Reddy, et al. (2001). "Effects of all-trans-retinoic acid (atRA) on inducible nitric oxide synthase (iNOS) activity and transforming

growth factor beta-1 production in experimental anti-GBM antibody-mediated glomerulonephritis." Inflammation **25**(6): 351-359.
Davis, B. H., R. T. Kramer, et al. (1990). "Retinoic acid modulates rat Ito cell proliferation, collagen, and transforming growth factor beta production." J Clin Invest **86**(6): 2062-2070.
de Larco, J. E. and G. J. Todaro (1978). "Epithelioid and fibroblastic rat kidney cell clones: epidermal growth factor (EGF) receptors and the effect of mouse sarcoma virus transformation." J Cell Physiol **94**(3): 335-342.
del Rincon, S. V., Q. Guo, et al. (2004). "Retinoic acid mediates degradation of IRS-1 by the ubiquitin-proteasome pathway, via a PKC-dependant mechanism." Oncogene **23**(57): 9269-9279.
Derynck, R., P. B. Lindquist, et al. (1988). "A new type of transforming growth factor-beta, TGF-beta 3." EMBO J **7**(12): 3737-3743.
Derynck, R. and Y. E. Zhang (2003). "Smad-dependent and Smad-independent pathways in TGF-beta family signalling." Nature **425** (6958): 577-584.
Dey, N., P. K. De, et al. (2007). "CSK controls retinoic acid receptor (RAR) signaling: a RAR-c-SRC signaling axis is required for neuritogenic differentiation." Mol Cell Biol **27**(11): 4179-4197.
Dolle, P., E. Ruberte, et al. (1990). "Retinoic acid receptors and cellular retinoid binding proteins. I. A systematic study of their differential pattern of transcription during mouse organogenesis." Development **110**(4): 1133-1151.
Dong, D., S. E. Ruuska, et al. (1999). "Distinct roles for cellular retinoic acid-binding proteins I and II in regulating signaling by retinoic acid." J Biol Chem **274**(34): 23695-23698.
Douthwaite, J. A., T. S. Johnson, et al. (1999). "Effects of transforming growth factor-beta1 on renal extracellular matrix components and their regulating proteins." J Am Soc Nephrol **10**(10): 2109-2119.
Duymelinck, C., S. E. Dauwe, et al. (2000). "TIMP-1 gene expression and PAI-1 antigen after unilateral ureteral obstruction in the adult male rat." Kidney Int **58**(3): 1186-1201.
Ebisawa, M., H. Umemiya, et al. (1999). "Retinoid X receptor-antagonistic diazepinylbenzoic acids." Chem Pharm Bull (Tokyo) **47**(12): 1778-1786.
Ebisawa, T., M. Fukuchi, et al. (2001). "Smurf1 interacts with transforming growth factor-beta type I receptor through Smad7 and induces receptor degradation." J Biol Chem **276**(16): 12477-12480.
Eddy, A. A. (1996). "Molecular insights into renal interstitial fibrosis." J Am Soc Nephrol **7**(12): 2495-2508.
Eddy, A. A. (2009). "Serine proteases, inhibitors and receptors in renal fibrosis." Thromb Haemost **101**(4): 656-664.
Eddy, A. A. and A. B. Fogo (2006). "Plasminogen activator inhibitor-1 in chronic kidney disease: evidence and mechanisms of action." J Am Soc Nephrol **17**(11): 2999-3012.
Edgtton, K. L., R. M. Gow, et al. (2004). "Plasmin is not protective in experimental renal interstitial fibrosis." Kidney Int **66**(1): 68-76.
El Nahas, A. M., H. Abo-Zenah, et al. (2004). "Elevated epsilon-(gamma-glutamyl)lysine in human diabetic nephropathy results from increased

expression and cellular release of tissue transglutaminase." Nephron Clin Pract **97**(3): c108-117.
Elokdah, H., M. Abou-Gharbia, et al. (2004). "Tiplaxtinin, a novel, orally efficacious inhibitor of plasminogen activator inhibitor-1: design, synthesis, and preclinical characterization." J Med Chem **47**(14): 3491-3494.
Endo, H., M. Niioka, et al. (2011). "Matrix metalloproteinase-13 promotes recovery from experimental liver cirrhosis in rats." Pathobiology **78**(5): 239-252.
Falk, L. A., F. De Benedetti, et al. (1991). "Induction of transforming growth factor-beta 1 (TGF-beta 1), receptor expression and TGF-beta 1 protein production in retinoic acid-treated HL-60 cells: possible TGF-beta 1-mediated autocrine inhibition." Blood **77**(6): 1248-1255.
Fallowfield, J. A., M. Mizuno, et al. (2007). "Scar-associated macrophages are a major source of hepatic matrix metalloproteinase-13 and facilitate the resolution of murine hepatic fibrosis." J Immunol **178**(8): 5288-5295.
Fan, J. M., Y. Y. Ng, et al. (1999). "Transforming growth factor-beta regulates tubular epithelial-myofibroblast transdifferentiation in vitro." Kidney Int **56**(4): 1455-1467.
Fanjul, A., M. I. Dawson, et al. (1994). "A new class of retinoids with selective inhibition of AP-1 inhibits proliferation." Nature **372**(6501): 107-111.
Federspiel, S. J., S. J. DiMari, et al. (1990). "Extracellular matrix biosynthesis by cultured fetal rat lung epithelial cells. II. Effects of acute exposure to epidermal growth factor and retinoic acid on collagen biosynthesis." Lab Invest **63**(4): 455-466.
Feng, X. H. and R. Derynck (2005). "Specificity and versatility in tgf-beta signaling through Smads." Annu Rev Cell Dev Biol **21**: 659-693.
Fisher, G. J. and J. J. Voorhees (1998). "Molecular mechanisms of photoaging and its prevention by retinoic acid: ultraviolet irradiation induces MAP kinase signal transduction cascades that induce Ap-1-regulated matrix metalloproteinases that degrade human skin in vivo." J Investig Dermatol Symp Proc **3**(1): 61-68.
Fisher, M., R. A. Jones, et al. (2009). "Modulation of tissue transglutaminase in tubular epithelial cells alters extracellular matrix levels: a potential mechanism of tissue scarring." Matrix Biol **28**(1): 20-31.
Fujimoto, M., Y. Maezawa, et al. (2003). "Mice lacking Smad3 are protected against streptozotocin-induced diabetic glomerulopathy." Biochem Biophys Res Commun **305**(4): 1002-1007.
Funaba, M., C. M. Zimmerman, et al. (2002). "Modulation of Smad2-mediated signaling by extracellular signal-regulated kinase." J Biol Chem **277** (44): 41361-41368.
Germain, P., P. Chambon, et al. (2006). "International Union of Pharmacology. LX. Retinoic acid receptors." Pharmacol Rev **58**(4): 712-725.
Gille, J., L. L. Paxton, et al. (1997). "Retinoic acid inhibits the regulated expression of vascular cell adhesion molecule-1 by cultured dermal microvascular endothelial cells." J Clin Invest **99**(3): 492-500.
Glass, C. K. and M. G. Rosenfeld (2000). "The coregulator exchange in transcriptional functions of nuclear receptors." Genes Dev **14**(2): 121-141.

Gluzman, Y. (1981). "SV40-transformed simian cells support the replication of early SV40 mutants." Cell **23**(1): 175-182.
Go, A. S., G. M. Chertow, et al. (2004). "Chronic kidney disease and the risks of death, cardiovascular events, and hospitalization." N Engl J Med **351** (13): 1296-1305.
Gonzalez-Avila, G., C. Iturria, et al. (1998). "Changes in matrix metalloproteinases during the evolution of interstitial renal fibrosis in a rat experimental model." Pathobiology **66**(5): 196-204.
Grotendorst, G. R., H. Rahmanie, et al. (2004). "Combinatorial signaling pathways determine fibroblast proliferation and myofibroblast differentiation." FASEB J **18**(3): 469-479.
Gudas, L. J., M. B. Sporn, et al. (1994). "Cellular biology and biochemistry of the retinods. In The Retinoids: Biology, Chemistry, and Medicine, 2nd Edition." Raven Press Ltd., New York, NY 443-520.
Hamaguchi, A., S. Kim, et al. (1995). "Transforming growth factor-beta 1 expression and phenotypic modulation in the kidney of hypertensive rats." Hypertension **26**(1): 199-207.
Han, D. C., M. Isono, et al. (1999). "High glucose stimulates proliferation and collagen type I synthesis in renal cortical fibroblasts: mediation by autocrine activation of TGF-beta." J Am Soc Nephrol **10**(9): 1891-1899.
Hanks, S. K., R. Armour, et al. (1988). "Amino acid sequence of the BSC-1 cell growth inhibitor (polyergin) deduced from the nucleotide sequence of the cDNA." Proc Natl Acad Sci U S A **85**(1): 79-82.
Hansch, G. M., C. Wagner, et al. (1995). "Matrix protein synthesis by glomerular mesangial cells in culture: effects of transforming growth factor beta (TGF beta) and platelet-derived growth factor (PDGF) on fibronectin and collagen type IV mRNA." J Cell Physiol **163**(3): 451-457.
Hatoum, A., M. E. El-Sabban, et al. (2001). "Overexpression of retinoic acid receptors alpha and gamma into neoplastic epidermal cells causes retinoic acid-induced growth arrest and apoptosis." Carcinogenesis **22** (12): 1955-1963.
Haxsen, V., S. Adam-Stitah, et al. (2001). "Retinoids inhibit the actions of angiotensin II on vascular smooth muscle cells." Circ Res **88**(6): 637-644.
Hayashi, H. and T. Sakai (2012). "Biological Significance of Local TGF-beta Activation in Liver Diseases." Front Physiol **3**: 12.
Hayashida, T., A. C. Poncelet, et al. (1999). "TGF-beta1 activates MAP kinase in human mesangial cells: a possible role in collagen expression." Kidney Int **56**(5): 1710-1720.
He, W., R. J. Tan, et al. (2011). "Matrix Metalloproteinase-7 as a Surrogate Marker Predicts Renal Wnt/beta-Catenin Activity in CKD." J Am Soc Nephrol.
Hellemans, K., I. Grinko, et al. (1999). "All-trans and 9-cis retinoic acid alter rat hepatic stellate cell phenotype differentially." Gut **45**(1): 134-142.
Hellemans, K., P. Verbuyst, et al. (2004). "Differential modulation of rat hepatic stellate phenotype by natural and synthetic retinoids." Hepatology **39** (1): 97-108.

Herman, M. P., G. K. Sukhova, et al. (2001). "Tissue factor pathway inhibitor-2 is a novel inhibitor of matrix metalloproteinases with implications for atherosclerosis." J Clin Invest **107**(9): 1117-1126.
Hewitson, T. D. (2009). "Renal tubulointerstitial fibrosis: common but never simple." Am J Physiol Renal Physiol **296**(6): F1239-1244.
Hisamori, S., C. Tabata, et al. (2008). "All-trans-retinoic acid ameliorates carbon tetrachloride-induced liver fibrosis in mice through modulating cytokine production." Liver Int **28**(9): 1217-1225.
Hoover, L. L., E. G. Burton, et al. (2008). "Retinoids regulate TGFbeta signaling at the level of Smad2 phosphorylation and nuclear accumulation." Biochim Biophys Acta **1783**(12): 2279-2286.
Horlein, A. J., A. M. Naar, et al. (1995). "Ligand-independent repression by the thyroid hormone receptor mediated by a nuclear receptor co-repressor." Nature **377**(6548): 397-404.
Horstrup, J. H., M. Gehrmann, et al. (2002). "Elevation of serum and urine levels of TIMP-1 and tenascin in patients with renal disease." Nephrol Dial Transplant **17**(6): 1005-1013.
Horton, C. and M. Maden (1995). "Endogenous distribution of retinoids during normal development and teratogenesis in the mouse embryo." Dev Dyn **202**(3): 312-323.
Huang, L., J. L. Haylor, et al. (2009). "Transglutaminase inhibition ameliorates experimental diabetic nephropathy." Kidney Int **76**(4): 383-394.
Huang, Y., W. A. Border, et al. (2006). "Noninhibitory PAI-1 enhances plasmin-mediated matrix degradation both in vitro and in experimental nephritis." Kidney Int **70**(3): 515-522.
Huang, Y., W. A. Border, et al. (2008). "A PAI-1 mutant, PAI-1R, slows progression of diabetic nephropathy." J Am Soc Nephrol **19**(2): 329-338.
Huang, Y., M. Haraguchi, et al. (2003). "A mutant, noninhibitory plasminogen activator inhibitor type 1 decreases matrix accumulation in experimental glomerulonephritis." J Clin Invest **112**(3): 379-388.
Humphreys, B. D., S. L. Lin, et al. (2010). "Fate tracing reveals the pericyte and not epithelial origin of myofibroblasts in kidney fibrosis." Am J Pathol **176**(1): 85-97.
Hutchison, N., C. Fligny, et al. (2012). "Resident mesenchymal cells and fibrosis." Biochim Biophys Acta.
Huu, D.-N., E. N. Rosenblum, et al. (1966). "Persistent infection of a rat kidney cell line with Rauscher murine leukemia virus." J Bacteriol **92**(4): 1133-1140.
Iimura, O., H. Takahashi, et al. (2004). "Effect of ureteral obstruction on matrix metalloproteinase-2 in rat renal cortex." Clin Exp Nephrol **8**(3): 223-229.
Inoki, K., M. Haneda, et al. (2000). "Role of mitogen-activated protein kinases as downstream effectors of transforming growth factor-beta in mesangial cells." Kidney Int Suppl **77**: S76-80.
Iwano, M., D. Plieth, et al. (2002). "Evidence that fibroblasts derive from epithelium during tissue fibrosis." J Clin Invest **110**(3): 341-350.
Jakowlew, S. B., J. Cubert, et al. (1992). "Differential regulation of the expression of transforming growth factor-beta mRNAs by growth

factors and retinoic acid in chicken embryo chondrocytes, myocytes, and fibroblasts." J Cell Physiol **150**(2): 377-385.
Jakowlew, S. B., P. J. Dillard, et al. (1988). "Complementary deoxyribonucleic acid cloning of a novel transforming growth factor-beta messenger ribonucleic acid from chick embryo chondrocytes." Mol Endocrinol **2**(8): 747-755.
Janssen de Limpens, A. M. (1980). "The local treatment of hypertrophic scars and keloids with topical retinoic acid." Br J Dermatol **103**(3): 319-323.
Jenkins, G. (2008). "The role of proteases in transforming growth factor-beta activation." Int J Biochem Cell Biol **40**(6-7): 1068-1078.
Jeon, K. W. (2009). "International Review of cytology (vol205)."
Johnson, A. T., E. S. Klein, et al. (1995). "Synthesis and characterization of a highly potent and effective antagonist of retinoic acid receptors." J Med Chem **38**(24): 4764-4767.
Johnson, T. S., A. F. El-Koraie, et al. (2003). "Tissue transglutaminase and the progression of human renal scarring." J Am Soc Nephrol **14**(8): 2052-2062.
Johnson, T. S., M. Fisher, et al. (2007). "Transglutaminase inhibition reduces fibrosis and preserves function in experimental chronic kidney disease." J Am Soc Nephrol **18**(12): 3078-3088.
Johnson, T. S., N. J. Skill, et al. (1999). "Transglutaminase transcription and antigen translocation in experimental renal scarring." J Am Soc Nephrol **10**(10): 2146-2157.
Jones, R. A., B. Nicholas, et al. (1997). "Reduced expression of tissue transglutaminase in a human endothelial cell line leads to changes in cell spreading, cell adhesion and reduced polymerisation of fibronectin." J Cell Sci **110 (Pt 19)**: 2461-2472.
Junqueira, L. C., G. Bignolas, et al. (1979). "Picrosirius staining plus polarization microscopy, a specific method for collagen detection in tissue sections." Histochem J **11**(4): 447-455.
Kaartinen, M. T., A. Pirhonen, et al. (1999). "Cross-linking of osteopontin by tissue transglutaminase increases its collagen binding properties." J Biol Chem **274**(3): 1729-1735.
Kambhampati, S., Y. Li, et al. (2003). "Activation of protein kinase C delta by all-trans-retinoic acid." J Biol Chem **278**(35): 32544-32551.
Kanayasu-Toyoda, T., T. Fujino, et al. (2005). "HX531, a retinoid X receptor antagonist, inhibited the 9-cis retinoic acid-induced binding with steroid receptor coactivator-1 as detected by surface plasmon resonance." J Steroid Biochem Mol Biol **94**(4): 303-309.
Kavsak, P., R. K. Rasmussen, et al. (2000). "Smad7 binds to Smurf2 to form an E3 ubiquitin ligase that targets the TGF beta receptor for degradation." Mol Cell **6**(6): 1365-1375.
Kavukcu, S., A. Soylu, et al. (1999). "The role of vitamin A in preventing renal scarring secondary to pyelonephritis." BJU Int **83**(9): 1055-1059.
Kawaguchi, R., J. Yu, et al. (2007). "A membrane receptor for retinol binding protein mediates cellular uptake of vitamin A." Science **315**(5813): 820-825.

Kelynack, K. J., T. D. Hewitson, et al. (2000). "Human renal fibroblast contraction of collagen I lattices is an integrin-mediated process." Nephrol Dial Transplant **15**(11): 1766-1772.
Kinoshita, K. and M. Funauchi (2012). "[Therapeutic effect of retinoic acid in lupus nephritis]." Nihon Rinsho Meneki Gakkai Kaishi **35**(1): 1-7.
Kinoshita, K., B. S. Yoo, et al. (2003). "Retinoic acid reduces autoimmune renal injury and increases survival in NZB/W F1 mice." J Immunol **170** (11): 5793-5798.
Kishimoto, K., K. Kinoshita, et al. (2011). "Therapeutic Effect of Retinoic Acid on Unilateral Ureteral Obstruction Model." Nephron Exp Nephrol **118** (3): e69-e78.
Kiss, E., J. Adams, et al. (2003). "Isotretinoin ameliorates renal damage in experimental acute renal allograft rejection." Transplantation **76**(3): 480-489.
Kleman, J. P., D. Aeschlimann, et al. (1995). "Transglutaminase-catalyzed cross-linking of fibrils of collagen V/XI in A204 rhabdomyosarcoma cells." Biochemistry **34**(42): 13768-13775.
Koesters, R., B. Kaissling, et al. (2010). "Tubular overexpression of transforming growth factor-beta1 induces autophagy and fibrosis but not mesenchymal transition of renal epithelial cells." Am J Pathol **177** (2): 632-643.
Kojima, S. and D. B. Rifkin (1993). "Mechanism of retinoid-induced activation of latent transforming growth factor-beta in bovine endothelial cells." J Cell Physiol **155**(2): 323-332.
Konta, T., Q. Xu, et al. (2001). "Selective roles of retinoic acid receptor and retinoid x receptor in the suppression of apoptosis by all-trans-retinoic acid." J Biol Chem **276**(16): 12697-12701.
Krag, S., C. C. Danielsen, et al. (2005). "Plasminogen activator inhibitor-1 gene deficiency attenuates TGF-beta1-induced kidney disease." Kidney Int **68**(6): 2651-2666.
Krupsky, M., A. Fine, et al. (1994). "Retinoic acid-induced inhibition of type I collagen gene expression by human lung fibroblasts." Biochim Biophys Acta **1219**(2): 335-341.
Kruse, S. W., K. Suino-Powell, et al. (2008). "Identification of COUP-TFII orphan nuclear receptor as a retinoic acid-activated receptor." PLoS Biol **6**(9): e227.
Kurokawa, R., J. DiRenzo, et al. (1994). "Regulation of retinoid signalling by receptor polarity and allosteric control of ligand binding." Nature **371** (6497): 528-531.
Lan, H. Y. (2008). "Smad7 as a therapeutic agent for chronic kidney diseases." Front Biosci **13**: 4984-4992.
Lan, H. Y. and A. C. Chung (2012). "TGF-beta/Smad signaling in kidney disease." Semin Nephrol **32**(3): 236-243.
Laudet, V. and H. Gronemeyer (2002). "The nuclear receptor facts book."
Leask, A. and D. J. Abraham (2003). "The role of connective tissue growth factor, a multifunctional matricellular protein, in fibroblast biology." Biochem Cell Biol **81**(6): 355-363.

Lefebvre, P., Y. Benomar, et al. (2010). "Retinoid X receptors: common heterodimerization partners with distinct functions." Trends Endocrinol Metab **21**(11): 676-683.
Lehrke, I., M. Schaier, et al. (2002). "Retinoid receptor-specific agonists alleviate experimental glomerulonephritis." Am J Physiol Renal Physiol **282**(4): F741-751.
Leid, M., P. Kastner, et al. (1992). "Multiplicity generates diversity in the retinoic acid signalling pathways." Trends Biochem Sci **17**(10): 427-433.
Leid, M., P. Kastner, et al. (1992). "Purification, cloning, and RXR identity of the HeLa cell factor with which RAR or TR heterodimerizes to bind target sequences efficiently." Cell **68**(2): 377-395.
Lelongt, B. and P. Ronco (2002). "Role of matrix metalloproteinases in kidney development and glomerulopathy: lessons from transgenic mice." Nephrol Dial Transplant **17 Suppl 9**: 28-31.
Leroy, P., A. Krust, et al. (1991). "Multiple isoforms of the mouse retinoic acid receptor alpha are generated by alternative splicing and differential induction by retinoic acid." EMBO J **10**(1): 59-69.
Levin, A. A., L. J. Sturzenbecker, et al. (1992). "9-cis retinoic acid stereoisomer binds and activates the nuclear receptor RXR alpha." Nature **355**(6358): 359-361.
Lewis, M. P. and J. T. Norman (1998). "Differential response of activated versus non-activated renal fibroblasts to tubular epithelial cells: a model of initiation and progression of fibrosis?" Exp Nephrol **6**(2): 132-143.
Li, J., X. Qu, et al. (2010). "Blockade of endothelial-mesenchymal transition by a Smad3 inhibitor delays the early development of streptozotocin-induced diabetic nephropathy." Diabetes **59**(10): 2612-2624.
Li, R., T. N. Faria, et al. (2004). "Retinoic acid causes cell growth arrest and an increase in p27 in F9 wild type but not in F9 retinoic acid receptor beta2 knockout cells." Exp Cell Res **294**(1): 290-300.
Liebler, S., B. Uberschar, et al. (2004). "The renal retinoid system: time-dependent activation in experimental glomerulonephritis." Am J Physiol Renal Physiol **286**(3): F458-465.
Lin, S. L., T. Kisseleva, et al. (2008). "Pericytes and perivascular fibroblasts are the primary source of collagen-producing cells in obstructive fibrosis of the kidney." Am J Pathol **173**(6): 1617-1627.
Liu, X., L. Lu, et al. (2011). "Amelioration of glomerulosclerosis with all-trans retinoic acid is linked to decreased plasminogen activator inhibitor-1 and alpha-smooth muscle actin." Acta Pharmacol Sin **32**(1): 70-78.
Liu, X., L. Lu, et al. (2008). "All-trans retinoic acid inhibits the increases in fibronectin and PAI-1 induced by TGF-beta1 and Ang II in rat mesangial cells." Acta Pharmacol Sin **29**(9): 1035-1041.
Liu, Y. (2006). "Renal fibrosis: new insights into the pathogenesis and therapeutics." Kidney Int **69**(2): 213-217.
Liu, Y. (2011). "Cellular and molecular mechanisms of renal fibrosis." Nat Rev Nephrol **7**(12): 684-696.

Livak, K. J. and T. D. Schmittgen (2001). "Analysis of relative gene expression data using real-time quantitative PCR and the 2(-Delta Delta C(T)) Method." Methods **25**(4): 402-408.
Lucio-Cazana, J., K. Nakayama, et al. (2001). "Suppression of constitutive but not Il-1beta-inducible expression of monocyte chemoattractant protein-1 in mesangial cells by retinoic acids: intervention in the activator protein-1 pathway." J Am Soc Nephrol **12**(4): 688-694.
Lundell, K., P. Thulin, et al. (2007). "Alternative splicing of human peroxisome proliferator-activated receptor delta (PPAR delta): effects on translation efficiency and trans-activation ability." BMC Mol Biol **8**: 70.
Luo, P., M. Lin, et al. (2009). "Function of retinoid acid receptor alpha and p21 in all-trans-retinoic acid-induced acute T-lymphoblastic leukemia apoptosis." Leuk Lymphoma **50**(7): 1183-1189.
Luo, P., X. Yang, et al. (2010). "Retinoid-suppressed phosphorylation of RARalpha mediates the differentiation pathway of osteosarcoma cells." Oncogene **29**(19): 2772-2783.
Ma, F. Y., G. H. Tesch, et al. (2011). "TGF-beta1-activated kinase-1 regulates inflammation and fibrosis in the obstructed kidney." Am J Physiol Renal Physiol **300**(6): F1410-1421.
Ma, Y., Q. Feng, et al. (2005). "Retinoid targeting of different D-type cyclins through distinct chemopreventive mechanisms." Cancer Res **65**(14): 6476-6483.
MacKay, K., L. J. Striker, et al. (1989). "Transforming growth factor-beta. Murine glomerular receptors and responses of isolated glomerular cells." J Clin Invest **83**(4): 1160-1167.
Mackensen-Haen, S., R. Bader, et al. (1981). "Correlations between renal cortical interstitial fibrosis, atrophy of the proximal tubules and impairment of the glomerular filtration rate." Clin Nephrol **15**(4): 167-171.
Mader, S., J. Y. Chen, et al. (1993). "The patterns of binding of RAR, RXR and TR homo- and heterodimers to direct repeats are dictated by the binding specificites of the DNA binding domains." EMBO J **12**(13): 5029-5041.
Madisen, L., N. R. Webb, et al. (1988). "Transforming growth factor-beta 2: cDNA cloning and sequence analysis." DNA **7**(1): 1-8.
Mangelsdorf, D. J. and R. M. Evans (1995). "The RXR heterodimers and orphan receptors." Cell **83**(6): 841-850.
Mankhey, R. W., C. C. Wells, et al. (2007). "17beta-Estradiol supplementation reduces tubulointerstitial fibrosis by increasing MMP activity in the diabetic kidney." Am J Physiol Regul Integr Comp Physiol **292**(2): R769-777.
Manzano, V. M., J. C. Munoz, et al. (2000). "Human renal mesangial cells are a target for the anti-inflammatory action of 9-cis retinoic acid." Br J Pharmacol **131**(8): 1673-1683.
Mao, J. T., D. P. Tashkin, et al. (2003). "All-trans retinoic acid modulates the balance of matrix metalloproteinase-9 and tissue inhibitor of metalloproteinase-1 in patients with emphysema." Chest **124**(5): 1724-1732.

Martin, J., R. Steadman, et al. (1998). "Differential regulation of matrix metalloproteinases and their inhibitors in human glomerular epithelial cells in vitro." J Am Soc Nephrol **9**(9): 1629-1637.
Martinez, J., E. Rich, et al. (1989). "Transglutaminase-mediated cross-linking of fibrinogen by human umbilical vein endothelial cells." J Biol Chem **264**(34): 20502-20508.
Masia, S., S. Alvarez, et al. (2007). "Rapid, nongenomic actions of retinoic acid on phosphatidylinositol-3-kinase signaling pathway mediated by the retinoic acid receptor." Mol Endocrinol **21**(10): 2391-2402.
Massague, J. (2000). "How cells read TGF-beta signals." Nat Rev Mol Cell Biol **1**(3): 169-178.
Massague, J. (2012). "TGFbeta signalling in context." Nat Rev Mol Cell Biol **13**(10): 616-630.
Matsuo, S., J. M. Lopez-Guisa, et al. (2005). "Multifunctionality of PAI-1 in fibrogenesis: evidence from obstructive nephropathy in PAI-1-overexpressing mice." Kidney Int **67**(6): 2221-2238.
McKay, N. G., T. F. Khong, et al. (1993). "The effect of transforming growth factor beta 1 on mesangial cell fibronectin synthesis: increased incorporation into the extracellular matrix and reduced pI but no effect on alternative splicing." Exp Mol Pathol **59**(3): 211-224.
McLennan, S. V., D. J. Kelly, et al. (2002). "Decreased matrix degradation in diabetic nephropathy: effects of ACE inhibition on the expression and activities of matrix metalloproteinases." Diabetologia **45**(2): 268-275.
Meisler, N. T., J. Parrelli, et al. (1997). "All-trans-retinoic acid inhibition of Pro alpha1(I) collagen gene expression in fetal rat skin fibroblasts: identification of a retinoic acid response element in the Pro alpha1(I) collagen gene." J Invest Dermatol **108**(4): 476-481.
Mende, C. W. (2010). "Application of direct renin inhibition to chronic kidney disease." Cardiovasc Drugs Ther **24**(2): 139-149.
Meng, X. M., X. R. Huang, et al. (2010). "Smad2 protects against TGF-beta/Smad3-mediated renal fibrosis." J Am Soc Nephrol **21**(9): 1477-1487.
Moll, S., P. A. Menoud, et al. (1995). "Induction of plasminogen activator inhibitor type 1 in murine lupus-like glomerulonephritis." Kidney Int **48**(5): 1459-1468.
Mongan, N. P. and L. J. Gudas (2007). "Diverse actions of retinoid receptors in cancer prevention and treatment." Differentiation **75**(9): 853-870.
Mora, J. R., M. Iwata, et al. (2008). "Vitamin effects on the immune system: vitamins A and D take centre stage." Nat Rev Immunol **8**(9): 685-698.
Morath, C., C. Dechow, et al. (2001). "Effects of retinoids on the TGF-beta system and extracellular matrix in experimental glomerulonephritis." J Am Soc Nephrol **12**(11): 2300-2309.
Morath, C., K. Ratzlaff, et al. (2009). "Chronic low-dose isotretinoin treatment limits renal damage in subtotally nephrectomized rats." J Mol Med **87**(1): 53-64.
Moreno-Manzano, V., Y. Ishikawa, et al. (1999). "Suppression of apoptosis by all-trans-retinoic acid. Dual intervention in the c-Jun n-terminal kinase-AP-1 pathway." J Biol Chem **274**(29): 20251-20258.

Moreno-Manzano, V., F. Mampaso, et al. (2003). "Retinoids as a potential treatment for experimental puromycin-induced nephrosis." Br J Pharmacol **139**(4): 823-831.
Moreno-Manzano, V., M. Rodriguez-Puyol, et al. (1997). "Prevention by tretinoin (all-trans-retinoic acid) of age-related renal changes." Int J Vitam Nutr Res **67**(6): 427-431.
Morey, L., C. Brenner, et al. (2008). "MBD3, a component of the NuRD complex, facilitates chromatin alteration and deposition of epigenetic marks." Mol Cell Biol **28**(19): 5912-5923.
Moses, H. L., E. L. Branum, et al. (1981). "Transforming growth factor production by chemically transformed cells." Cancer Res **41**(7): 2842-2848.
Mosher, D. F. (1984). "Cross-linking of fibronectin to collagenous proteins." Mol Cell Biochem **58**(1-2): 63-68.
Mozes, M. M., E. P. Bottinger, et al. (1999). "Renal expression of fibrotic matrix proteins and of transforming growth factor-beta (TGF-beta) isoforms in TGF-beta transgenic mice." J Am Soc Nephrol **10**(2): 271-280.
Munger, J. S., J. G. Harpel, et al. (1997). "Latent transforming growth factor-beta: structural features and mechanisms of activation." Kidney Int **51** (5): 1376-1382.
Na, S. Y., B. Y. Kang, et al. (1999). "Retinoids inhibit interleukin-12 production in macrophages through physical associations of retinoid X receptor and NFkappaB." J Biol Chem **274**(12): 7674-7680.
Nagase, H. (1997). "Activation mechanisms of matrix metalloproteinases." Biol Chem **378**(3-4): 151-160.
Nagy, L., M. Saydak, et al. (1996). "Identification and characterization of a versatile retinoid response element (retinoic acid receptor response element-retinoid X receptor response element) in the mouse tissue transglutaminase gene promoter." J Biol Chem **271**(8): 4355-4365.
Nakaoka, H., D. M. Perez, et al. (1994). "Gh: a GTP-binding protein with transglutaminase activity and receptor signaling function." Science **264** (5165): 1593-1596.
Naldini, L., E. Vigna, et al. (1995). "Biological activation of pro-HGF (hepatocyte growth factor) by urokinase is controlled by a stoichiometric reaction." J Biol Chem **270**(2): 603-611.
Napoli, J. L. (1996). "Biochemical pathways of retinoid transport, metabolism, and signal transduction." Clin Immunol Immunopathol **80**(3 Pt 2): S52-62.
Napoli, J. L. (1999). "Interactions of retinoid binding proteins and enzymes in retinoid metabolism." Biochim Biophys Acta **1440**(2-3): 139-162.
Napoli, J. L. (2000). "A gene knockout corroborates the integral function of cellular retinol-binding protein in retinoid metabolism." Nutr Rev **58**(8): 230-236.
Napoli, J. L. (2012). "Physiological insights into all-trans-retinoic acid biosynthesis." Biochim Biophys Acta **1821**(1): 152-167.
Nardacci, R., O. Lo Iacono, et al. (2003). "Transglutaminase type II plays a protective role in hepatic injury." Am J Pathol **162**(4): 1293-1303.

Naruhn, S., P. M. Toth, et al. (2011). "High-Affinity Peroxisome Proliferator-Activated Receptor {beta}/{delta}-Specific Ligands with Pure Antagonistic or Inverse Agonistic Properties." Mol Pharmacol **80**(5): 828-838.
Nath, K. A. (1992). "Tubulointerstitial changes as a major determinant in the progression of renal damage." Am J Kidney Dis **20**(1): 1-17.
National Collaborating Centre for Chronic Conditions (2008). "Chronic kidney disease: national clinical guideline for early identification and management in adults in primary and secondary care." London: Royal College of Physicians.
Niculescu-Duvaz, I., M. K. Phanish, et al. (2007). "The TGFbeta1-induced fibronectin in human renal proximal tubular epithelial cells is p38 MAP kinase dependent and Smad independent." Nephron Exp Nephrol **105**(4): e108-116.
Niederreither, K. and P. Dolle (2008). "Retinoic acid in development: towards an integrated view." Nat Rev Genet **9**(7): 541-553.
Nishida, M., Y. Okumura, et al. (2007). "MMP-2 inhibition reduces renal macrophage infiltration with increased fibrosis in UUO." Biochem Biophys Res Commun **354**(1): 133-139.
Norman, J. T. and L. G. Fine (1999). "Progressive renal disease: fibroblasts, extracellular matrix, and integrins." Exp Nephrol **7**(2): 167-177.
Numaguchi, S., M. Okuno, et al. (1994). "Modulation of collagen synthesis and degradation by retinoids and cytokines in 3T3 L1 preadipocytes." Intern Med **33**(6): 309-316.
Nunes, I., P. E. Gleizes, et al. (1997). "Latent transforming growth factor-beta binding protein domains involved in activation and transglutaminase-dependent cross-linking of latent transforming growth factor-beta." J Cell Biol **136**(5): 1151-1163.
Ochoa, W. F., A. Torrecillas, et al. (2003). "Retinoic acid binds to the C2-domain of protein kinase C(alpha)." Biochemistry **42**(29): 8774-8779.
Oda, T., Y. O. Jung, et al. (2001). "PAI-1 deficiency attenuates the fibrogenic response to ureteral obstruction." Kidney Int **60**(2): 587-596.
Ohata, M., M. Lin, et al. (1997). "Diminished retinoic acid signaling in hepatic stellate cells in cholestatic liver fibrosis." Am J Physiol **272**(3 Pt 1): G589-596.
Ohta, A. and J. Uitto (1987). "Procollagen gene expression by scleroderma fibroblasts in culture. Inhibition of collagen production and reduction of pro alpha 1(I) and pro alpha 1(III) collagen messenger RNA steady-state levels by retinoids." Arthritis Rheum **30**(4): 404-411.
Oikarinen, H., A. I. Oikarinen, et al. (1985). "Modulation of procollagen gene expression by retinoids. Inhibition of collagen production by retinoic acid accompanied by reduced type I procollagen messenger ribonucleic acid levels in human skin fibroblast cultures." J Clin Invest **75**(5): 1545-1553.
Okada, H., T. Danoff, et al. (1997). "Early role of Fsp1 in epithelial-mesenchymal transformation." Am J Physiol Renal Physiol **273**(4): F563-F574.
Okuda, S., L. R. Languino, et al. (1990). "Elevated expression of transforming growth factor-beta and proteoglycan production in experimental

glomerulonephritis. Possible role in expansion of the mesangial extracellular matrix." J Clin Invest **86**(2): 453-462.
Okuno, M., H. Moriwaki, et al. (1997). "Retinoids exacerbate rat liver fibrosis by inducing the activation of latent TGF-beta in liver stellate cells." Hepatology **26**(4): 913-921.
Oldfield, M. D., L. A. Bach, et al. (2001). "Advanced glycation end products cause epithelial-myofibroblast transdifferentiation via the receptor for advanced glycation end products (RAGE)." J Clin Invest **108**(12): 1853-1863.
Oliverio, S., A. Amendola, et al. (1999). "Inhibition of "tissue" transglutaminase increases cell survival by preventing apoptosis." J Biol Chem **274**(48): 34123-34128.
Oseto, S., T. Moriyama, et al. (2003). "Therapeutic effect of all-trans retinoic acid on rats with anti-GBM antibody glomerulonephritis." Kidney Int **64** (4): 1241-1252.
Ozer, E. A., A. Kumral, et al. (2005). "Effect of retinoic acid on oxygen-induced lung injury in the newborn rat." Pediatr Pulmonol **39**(1): 35-40.
Palczewski, K. (2010). "Retinoids for treatment of retinal diseases." Trends Pharmacol Sci **31**(6): 284-295.
Pan, J., Y. L. Kao, et al. (2005). "Activation of Rac1 by phosphatidylinositol 3-kinase in vivo: role in activation of mitogen-activated protein kinase (MAPK) pathways and retinoic acid-induced neuronal differentiation of SH-SY5Y cells." J Neurochem **93**(3): 571-583.
Panabiere-Castaings, M. H. (1988). "Retinoic acid in the treatment of keloids." J Dermatol Surg Oncol **14**(11): 1275-1276.
Pares, X., J. Farres, et al. (2008). "Medium- and short-chain dehydrogenase/ reductase gene and protein families : Medium-chain and short-chain dehydrogenases/reductases in retinoid metabolism." Cell Mol Life Sci **65**(24): 3936-3949.
Pendaries, V., F. Verrecchia, et al. (2003). "Retinoic acid receptors interfere with the TGF-beta/Smad signaling pathway in a ligand-specific manner." Oncogene **22**(50): 8212-8220.
Peng, X., T. Maruo, et al. (2004). "A novel RARbeta isoform directed by a distinct promoter P3 and mediated by retinoic acid in breast cancer cells." Cancer Res **64**(24): 8911-8918.
Perez, J. R., S. Shull, et al. (1992). "Glucocorticoid and retinoid regulation of alpha-2 type I procollagen promoter activity." J Cell Biochem **50**(1): 26-34.
Perlmann, T., P. N. Rangarajan, et al. (1993). "Determinants for selective RAR and TR recognition of direct repeat HREs." Genes Dev **7**(7B): 1411-1422.
Perlmann, T., K. Umesono, et al. (1996). "Two distinct dimerization interfaces differentially modulate target gene specificity of nuclear hormone receptors." Mol Endocrinol **10**(8): 958-966.
Pfahl, M. and F. Chytil (1996). "Regulation of metabolism by retinoic acid and its nuclear receptors." Annu Rev Nutr **16**: 257-283.
Phanish, M. K., N. A. Wahab, et al. (2006). "The differential role of Smad2 and Smad3 in the regulation of pro-fibrotic TGFbeta1 responses in human proximal-tubule epithelial cells." Biochem J **393**(Pt 2): 601-607.

Picard, N., O. Baum, et al. (2008). "Origin of renal myofibroblasts in the model of unilateral ureter obstruction in the rat." Histochem Cell Biol **130**(1): 141-155.
Pignatello, M. A., F. C. Kauffman, et al. (1997). "Multiple factors contribute to the toxicity of the aromatic retinoid, TTNPB (Ro 13-7410): binding affinities and disposition." Toxicol Appl Pharmacol **142**(2): 319-327.
Pignatello, M. A., F. C. Kauffman, et al. (1999). "Multiple factors contribute to the toxicity of the aromatic retinoid TTNPB (Ro 13-7410): interactions with the retinoic acid receptors." Toxicol Appl Pharmacol **159**(2): 109-116.
Pino-Lagos, K., M. J. Benson, et al. (2008). "Retinoic acid in the immune system." Ann N Y Acad Sci **1143**: 170-187.
Poncelet, A. C. and H. W. Schnaper (1998). "Regulation of human mesangial cell collagen expression by transforming growth factor-beta1." Am J Physiol **275**(3 Pt 2): F458-466.
Popov, Y., D. Y. Sverdlov, et al. (2011). "Tissue transglutaminase does not affect fibrotic matrix stability or regression of liver fibrosis in mice." Gastroenterology **140**(5): 1642-1652.
Predki, P. F., D. Zamble, et al. (1994). "Ordered binding of retinoic acid and retinoid-X receptors to asymmetric response elements involves determinants adjacent to the DNA-binding domain." Mol Endocrinol **8**(1): 31-39.
Qin, Y. H., F. Y. Lei, et al. (2009). "Effect of all-trans retinoic acid on renal expressions of matrix metalloproteinase-2, matrix metalloproteinase-9 and tissue inhibitor of metalloproteinase-1 in rats with glomerulosclerosis." Pediatr Nephrol **24**(8): 1477-1486.
Redfern, C. P. and C. Todd (1992). "Retinoic acid receptor expression in human skin keratinocytes and dermal fibroblasts in vitro." J Cell Sci **102 (Pt 1)**: 113-121.
Redlich, C. A., H. M. Delisser, et al. (1995). "Retinoic acid inhibition of transforming growth factor-beta-induced collagen production by human lung fibroblasts." Am J Respir Cell Mol Biol **12**(3): 287-295.
Reeves, W. B., B. B. Rawal, et al. (2012). "Therapeutic Modalities in Diabetic Nephropathy: Future Approaches." Open J Nephrol **2**(2): 5-18.
Rieck, M., W. Meissner, et al. (2008). "Ligand-mediated regulation of peroxisome proliferator-activated receptor (PPAR) beta/delta: a comparative analysis of PPAR-selective agonists and all-trans retinoic acid." Mol Pharmacol **74**(5): 1269-1277.
Risdon, R. A., J. C. Sloper, et al. (1968). "Relationship between renal function and histological changes found in renal-biopsy specimens from patients with persistent glomerular nephritis." Lancet **2**(7564): 363-366.
Roberts, A. B., M. A. Anzano, et al. (1981). "New class of transforming growth factors potentiated by epidermal growth factor: isolation from non-neoplastic tissues." Proc Natl Acad Sci U S A **78**(9): 5339-5343.
Roberts, A. B., M. A. Anzano, et al. (1985). "Type beta transforming growth factor: a bifunctional regulator of cellular growth." Proc Natl Acad Sci U S A **82**(1): 119-123.
Roberts, A. B., M. B. Sporn, et al. (1986). "Transforming growth factor type beta: rapid induction of fibrosis and angiogenesis in vivo and

stimulation of collagen formation in vitro." Proc Natl Acad Sci U S A **83** (12): 4167-4171.
Rochette-Egly, C. and P. Germain (2009). "Dynamic and combinatorial control of gene expression by nuclear retinoic acid receptors (RARs)." Nucl Recept Signal **7**: e005.
Rochette-Egly, C., Y. Lutz, et al. (1994). "Detection of retinoid X receptors using specific monoclonal and polyclonal antibodies." Biochem Biophys Res Commun **204**(2): 525-536.
Rodemann, H. P. and G. A. Muller (1991). "Characterization of human renal fibroblasts in health and disease: II. In vitro growth, differentiation, and collagen synthesis of fibroblasts from kidneys with interstitial fibrosis." Am J Kidney Dis **17**(6): 684-686.
Rojiani, M. V., J. Alidina, et al. (2010). "Expression of MMP-2 correlates with increased angiogenesis in CNS metastasis of lung carcinoma." Int J Clin Exp Pathol **3**(8): 775-781.
Ronco, P. and C. Chatziantoniou (2008). "Matrix metalloproteinases and matrix receptors in progression and reversal of kidney disease: therapeutic perspectives." Kidney Int **74**(7): 873-878.
Ronco, P., B. Lelongt, et al. (2007). "Matrix metalloproteinases in kidney disease progression and repair: a case of flipping the coin." Semin Nephrol **27**(3): 352-362.
Rossin, F., M. D'Eletto, et al. (2011). "TG2 transamidating activity acts as a reostat controlling the interplay between apoptosis and autophagy." Amino Acids.
Rubenstein, R., H. H. Roenigk, Jr., et al. (1986). "Atypical keloids after dermabrasion of patients taking isotretinoin." J Am Acad Dermatol **15**(2 Pt 1): 280-285.
Salbert, G., A. Fanjul, et al. (1993). "Retinoic acid receptors and retinoid X receptor-alpha down-regulate the transforming growth factor-beta 1 promoter by antagonizing AP-1 activity." Mol Endocrinol **7**(10): 1347-1356.
Sanchez, M., E. Gionti, et al. (1993). "Alpha 2(I) collagen gene expression is up-regulated in quail chondrocytes pretreated with retinoic acid." Biochem J **295 (Pt 1)**: 115-119.
Sanderson, N., V. Factor, et al. (1995). "Hepatic expression of mature transforming growth factor beta 1 in transgenic mice results in multiple tissue lesions." Proc Natl Acad Sci U S A **92**(7): 2572-2576.
Sato, M., Y. Muragaki, et al. (2003). "Targeted disruption of TGF-beta1/Smad3 signaling protects against renal tubulointerstitial fibrosis induced by unilateral ureteral obstruction." J Clin Invest **112**(10): 1486-1494.
Satre, M. A., K. E. Ugen, et al. (1992). "Developmental changes in endogenous retinoids during pregnancy and embryogenesis in the mouse." Biol Reprod **46**(5): 802-810.
Schaier, M., T. Jocks, et al. (2003). "Retinoid agonist isotretinoin ameliorates obstructive renal injury." J Urol **170**(4 Pt 1): 1398-1402.
Schaier, M., I. Lehrke, et al. (2001). "Isotretinoin alleviates renal damage in rat chronic glomerulonephritis." Kidney Int **60**(6): 2222-2234.

Schaier, M., S. Liebler, et al. (2004). "Retinoic acid receptor alpha and retinoid X receptor specific agonists reduce renal injury in established chronic glomerulonephritis of the rat." J Mol Med **82**(2): 116-125.
Schainuck, L. I., G. E. Striker, et al. (1970). "Structural-functional correlations in renal disease. II. The correlations." Hum Pathol **1**(4): 631-641.
Schmierer, B. and C. S. Hill (2007). "TGFbeta-SMAD signal transduction: molecular specificity and functional flexibility." Nat Rev Mol Cell Biol **8** (12): 970-982.
Schnaper, H. W., T. Hayashida, et al. (2003). "TGF-beta signal transduction and mesangial cell fibrogenesis." Am J Physiol Renal Physiol **284**(2): F243-252.
Schug, T. T., D. C. Berry, et al. (2007). "Opposing effects of retinoic acid on cell growth result from alternate activation of two different nuclear receptors." Cell **129**(4): 723-733.
Schug, T. T., D. C. Berry, et al. (2008). "Overcoming retinoic acid-resistance of mammary carcinomas by diverting retinoic acid from PPARbeta/delta to RAR." Proc Natl Acad Sci U S A **105**(21): 7546-7551.
Scott, W. J., Jr., R. Walter, et al. (1994). "Endogenous status of retinoids and their cytosolic binding proteins in limb buds of chick vs mouse embryos." Dev Biol **165**(2): 397-409.
Sharma, A. K., S. M. Mauer, et al. (1995). "Altered expression of matrix metalloproteinase-2, TIMP, and TIMP-2 in obstructive nephropathy." J Lab Clin Med **125**(6): 754-761.
Sharma, K., F. N. Ziyadeh, et al. (1997). "Increased renal production of transforming growth factor-beta1 in patients with type II diabetes." Diabetes **46**(5): 854-859.
Shaw, N., M. Elholm, et al. (2003). "Retinoic acid is a high affinity selective ligand for the peroxisome proliferator-activated receptor beta/delta." J Biol Chem **278**(43): 41589-41592.
Shearer, B. G., D. J. Steger, et al. (2008). "Identification and characterization of a selective peroxisome proliferator-activated receptor beta/delta (NR1C2) antagonist." Mol Endocrinol **22**(2): 523-529.
Shi, Y. and J. Massague (2003). "Mechanisms of TGF-beta signaling from cell membrane to the nucleus." Cell **113**(6): 685-700.
Shigematsu, T. and S. Tajima (1995). "Modulation of collagen synthesis and cell proliferation by retinoids in human skin fibroblasts." J Dermatol Sci **9**(2): 142-145.
Shweke, N., N. Boulos, et al. (2008). "Tissue transglutaminase contributes to interstitial renal fibrosis by favoring accumulation of fibrillar collagen through TGF-beta activation and cell infiltration." Am J Pathol **173**(3): 631-642.
Singh, R., R. H. Song, et al. (2001). "High glucose decreases matrix metalloproteinase-2 activity in rat mesangial cells via transforming growth factor-beta1." Exp Nephrol **9**(4): 249-257.
Skill, N. J., M. Griffin, et al. (2001). "Increases in renal epsilon-(gamma-glutamyl)-lysine crosslinks result from compartment-specific changes in tissue transglutaminase in early experimental diabetic nephropathy: pathologic implications." Lab Invest **81**(5): 705-716.

Skill, N. J., T. S. Johnson, et al. (2004). "Inhibition of transglutaminase activity reduces extracellular matrix accumulation induced by high glucose levels in proximal tubular epithelial cells." J Biol Chem **279**(46): 47754-47762.
Somerville, R. P., S. A. Oblander, et al. (2003). "Matrix metalloproteinases: old dogs with new tricks." Genome Biol **4**(6): 216.
Starkey, J. M., Y. Zhao, et al. (2010). "Altered retinoic acid metabolism in diabetic mouse kidney identified by O isotopic labeling and 2D mass spectrometry." PLoS One **5**(6): e11095.
Stehlin-Gaon, C., D. Willmann, et al. (2003). "All-trans retinoic acid is a ligand for the orphan nuclear receptor ROR beta." Nat Struct Biol **10**(10): 820-825.
Stevens, P. E., D. J. O'Donoghue, et al. (2007). "Chronic kidney disease management in the United Kingdom: NEOERICA project results." Kidney Int **72**(1): 92-99.
Sun, S. Z., Y. Wang, et al. (2006). "Effects of benazepril on renal function and kidney expression of matrix metalloproteinase-2 and tissue inhibitor of metalloproteinase-2 in diabetic rats." Chin Med J (Engl) **119**(10): 814-821.
Surendran, K., T. C. Simon, et al. (2004). "Matrilysin (MMP-7) expression in renal tubular damage: association with Wnt4." Kidney Int **65**(6): 2212-2222.
Sutton, A. B., A. E. Canfield, et al. (1991). "The response of endothelial cells to TGF beta-1 is dependent upon cell shape, proliferative state and the nature of the substratum." J Cell Sci **99 (Pt 4)**: 777-787.
Suzui, M., M. Shimizu, et al. (2004). "Acyclic retinoid activates retinoic acid receptor beta and induces transcriptional activation of p21(CIP1) in HepG2 human hepatoma cells." Mol Cancer Ther **3**(3): 309-316.
Suzuki, S., I. Ebihara, et al. (1993). "Transcriptional activation of matrix genes by transforming growth factor beta 1 in mesangial cells." Exp Nephrol **1** (4): 229-237.
Suzuki, Y., J. Shimada, et al. (1999). "Physical interaction between retinoic acid receptor and Sp1: mechanism for induction of urokinase by retinoic acid." Blood **93**(12): 4264-4276.
Sznaidman, M. L., C. D. Haffner, et al. (2003). "Novel selective small molecule agonists for peroxisome proliferator-activated receptor delta (PPARdelta)--synthesis and biological activity." Bioorg Med Chem Lett **13**(9): 1517-1521.
Tabata, C., Y. Kadokawa, et al. (2006). "All-trans-retinoic acid prevents radiation- or bleomycin-induced pulmonary fibrosis." Am J Respir Crit Care Med **174**(12): 1352-1360.
Tan, N. S., N. S. Shaw, et al. (2002). "Selective cooperation between fatty acid binding proteins and peroxisome proliferator-activated receptors in regulating transcription." Mol Cell Biol **22**(14): 5114-5127.
Taneja, R., C. Rochette-Egly, et al. (1997). "Phosphorylation of activation functions AF-1 and AF-2 of RAR alpha and RAR gamma is indispensable for differentiation of F9 cells upon retinoic acid and cAMP treatment." EMBO J **16**(21): 6452-6465.

Tang, X. H. and L. J. Gudas (2011). "Retinoids, Retinoic Acid Receptors, and Cancer." Annu Rev Pathol **28**(6): 345-364.
ten Dijke, P., P. Hansen, et al. (1988). "Identification of another member of the transforming growth factor type beta gene family." Proc Natl Acad Sci U S A **85**(13): 4715-4719.
Theodosiou, M., V. Laudet, et al. (2010). "From carrot to clinic: an overview of the retinoic acid signaling pathway." Cell Mol Life Sci **67**(9): 1423-1445.
Tomooka, S., W. A. Border, et al. (1992). "Glomerular matrix accumulation is linked to inhibition of the plasmin protease system." Kidney Int **42**(6): 1462-1469.
Tsou, H. C., X. Lee, et al. (1994). "Regulation of retinoic acid receptor expression in dermal fibroblasts." Exp Cell Res **211**(1): 74-81.
Tsou, H. C., X. X. Xie, et al. (1997). "Expression of retinoid X receptors in human dermal fibroblasts." Exp Cell Res **236**(2): 493-500.
Turgut, F. and W. K. Bolton (2010). "Potential new therapeutic agents for diabetic kidney disease." Am J Kidney Dis **55**(5): 928-940.
Uchida, G., K. Yoshimura, et al. (2003). "Tretinoin reverses upregulation of matrix metalloproteinase-13 in human keloid-derived fibroblasts." Exp Dermatol **12 Suppl 2**: 35-42.
Urbach, J. and R. R. Rando (1994). "Isomerization of all-trans-retinoic acid to 9-cis-retinoic acid." Biochem J **299 (Pt 2)**: 459-465.
Varani, J., R. S. Mitra, et al. (1990). "All-trans retinoic acid stimulates growth and extracellular matrix production in growth-inhibited cultured human skin fibroblasts." J Invest Dermatol **94**(5): 717-723.
Vasios, G. W., J. D. Gold, et al. (1989). "A retinoic acid-responsive element is present in the 5' flanking region of the laminin B1 gene." Proc Natl Acad Sci U S A **86**(23): 9099-9103.
Verderio, E., B. Nicholas, et al. (1998). "Regulated expression of tissue transglutaminase in Swiss 3T3 fibroblasts: effects on the processing of fibronectin, cell attachment, and cell death." Exp Cell Res **239**(1): 119-138.
Verrecchia, F., M. L. Chu, et al. (2001). "Identification of novel TGF-beta / Smad gene targets in dermal fibroblasts using a combined cDNA microarray/promoter transactivation approach." J Biol Chem **276**(20): 17058-17062.
Villa, R., L. Morey, et al. (2006). "The methyl-CpG binding protein MBD1 is required for PML-RARalpha function." Proc Natl Acad Sci U S A **103**(5): 1400-1405.
Visse, R. and H. Nagase (2003). "Matrix metalloproteinases and tissue inhibitors of metalloproteinases: structure, function, and biochemistry." Circ Res **92**(8): 827-839.
Vollmar, B., C. Heckmann, et al. (2002). "High, but not low, dietary retinoids aggravate manifestation of rat liver fibrosis." J Gastroenterol Hepatol **17**(7): 791-799.
Vuligonda, V., S. M. Thacher, et al. (2001). "Enantioselective syntheses of potent retinoid X receptor ligands: differential biological activities of individual antipodes." J Med Chem **44**(14): 2298-2303.

Wagner, J., C. Dechow, et al. (2000). "Retinoic acid reduces glomerular injury in a rat model of glomerular damage." J Am Soc Nephrol **11**(8): 1479-1487.
Wang, H., Z. Dan, et al. (2008). "Effect of all-trans retinoic acid on liver fibrosis induced by common bile duct ligation in rats." J Huazhong Univ Sci Technolog Med Sci **28**(5): 553-557.
Wang, L., J. J. Potter, et al. (2007). "Effects of retinoic acid on the development of liver fibrosis produced by carbon tetrachloride in mice." Biochim Biophys Acta **1772**(1): 66-71.
Wang, L., L. R. Tankersley, et al. (2002). "Regulation of the murine alpha(2)(I) collagen promoter by retinoic acid and retinoid X receptors." Arch Biochem Biophys **401**(2): 262-270.
Wang, L., L. R. Tankersley, et al. (2004). "Regulation of alpha 2(I) collagen expression in stellate cells by retinoic acid and retinoid X receptors through interactions with their cofactors." Arch Biochem Biophys **428** (1): 92-98.
Wang, Z., J. Xu, et al. (2011). "Effect of the regulation of retinoid X receptor-alpha gene expression on rat hepatic fibrosis." Hepatol Res **41**(5): 475-483.
Watanabe, A., H. Kanai, et al. (2002). "Retinoids induce the PAI-1 gene expression through tyrosine kinase-dependent pathways in vascular smooth muscle cells." J Cardiovasc Pharmacol **39**(4): 503-512.
Weiner, F. R., W. S. Blaner, et al. (1992). "Ito cell expression of a nuclear retinoic acid receptor." Hepatology **15**(2): 336-342.
Wells, D. J. (2010). "Electroporation and ultrasound enhanced non-viral gene delivery in vitro and in vivo." Cell Biol Toxicol **26**(1): 21-28.
Wen, X., Y. Li, et al. (2005). "Hepatocyte growth factor receptor signaling mediates the anti-fibrotic action of 9-cis-retinoic acid in glomerular mesangial cells." Am J Pathol **167**(4): 947-957.
Wotton, D., R. S. Lo, et al. (1999). "Multiple modes of repression by the Smad transcriptional corepressor TGIF." J Biol Chem **274**(52): 37105-37110.
Wozel, G., A. Chang, et al. (1991). "The effect of topical retinoids on the leukotriene-B4-induced migration of polymorphonuclear leukocytes into human skin." Arch Dermatol Res **283**(3): 158-161.
Wu, L. N., Y. Ishikawa, et al. (1997). "Retinoic acid stimulates matrix calcification and initiates type I collagen synthesis in primary cultures of avian weight-bearing growth plate chondrocytes." J Cell Biochem **65** (2): 209-230.
Xu, Q., B. M. Hendry, et al. (2010). "Kidneys of Alb/TGF-beta1 transgenic mice are deficient in retinoic acid and exogenous retinoic acid shows dose-dependent toxicity." Nephron Exp Nephrol **114**(4): e127-132.
Xu, Q., J. Lucio-Cazana, et al. (2004). "Retinoids in nephrology: promises and pitfalls." Kidney Int **66**(6): 2119-2131.
Xu, Q., J. T. Norman, et al. (2007). "In vitro models of TGF-beta-induced fibrosis suitable for high-throughput screening of antifibrotic agents." Am J Physiol Renal Physiol **293**(2): F631-640.
Yamaguchi, I., J. M. Lopez-Guisa, et al. (2007). "Endogenous urokinase lacks antifibrotic activity during progressive renal injury." Am J Physiol Renal Physiol **293**(1): F12-19.

Yamamoto, T., N. A. Noble, et al. (1996). "Expression of transforming growth factor-beta isoforms in human glomerular diseases." Kidney Int **49**(2): 461-469.
Yamamoto, T., N. A. Noble, et al. (1994). "Sustained expression of TGF-beta 1 underlies development of progressive kidney fibrosis." Kidney Int **45**(3): 916-927.
Yamane, A., N. Tsukamoto, et al. (2009). "Successful treatment by all-trans retinoic acid in a patient with acute promyelocytic leukemia complicated by liver cirrhosis and polycystic kidney." Intern Med **48**(18): 1691-1694.
Yan, Z. H., S. Noonan, et al. (1996). "Retinoic acid induction of the tissue transglutaminase promoter is mediated by a novel response element." Mol Cell Endocrinol **120**(2): 203-212.
Yang, J., R. W. Shultz, et al. (2002). "Disruption of tissue-type plasminogen activator gene in mice reduces renal interstitial fibrosis in obstructive nephropathy." J Clin Invest **110**(10): 1525-1538.
Yoshioka, K., T. Takemura, et al. (1993). "Transforming growth factor-beta protein and mRNA in glomeruli in normal and diseased human kidneys." Lab Invest **68**(2): 154-163.
Yu, V. C., C. Delsert, et al. (1991). "RXR beta: a coregulator that enhances binding of retinoic acid, thyroid hormone, and vitamin D receptors to their cognate response elements." Cell **67**(6): 1251-1266.
Zechel, C., X. Q. Shen, et al. (1994). "The dimerization interfaces formed between the DNA binding domains of RXR, RAR and TR determine the binding specificity and polarity of the full-length receptors to direct repeats." EMBO J **13**(6): 1425-1433.
Zeisberg, E. M., S. E. Potenta, et al. (2008). "Fibroblasts in kidney fibrosis emerge via endothelial-to-mesenchymal transition." J Am Soc Nephrol **19**(12): 2282-2287.
Zelent, A., C. Mendelsohn, et al. (1991). "Differentially expressed isoforms of the mouse retinoic acid receptor beta generated by usage of two promoters and alternative splicing." EMBO J **10**(1): 71-81.
Zhang, G. and A. A. Eddy (2008). "Urokinase and its receptors in chronic kidney disease." Front Biosci **13**: 5462-5478.
Zhang, G., K. A. Kernan, et al. (2007). "Plasmin(ogen) promotes renal interstitial fibrosis by promoting epithelial-to-mesenchymal transition: role of plasmin-activated signals." J Am Soc Nephrol **18**(3): 846-859.
Zhang, W., J. Ou, et al. (2000). "Synergistic cooperation between Sp1 and Smad3/Smad4 mediates transforming growth factor beta1 stimulation of alpha 2(I)-collagen (COL1A2) transcription." J Biol Chem **275**(50): 39237-39245.
Zhang, Y. E. (2009). "Non-Smad pathways in TGF-beta signaling." Cell Res **19**(1): 128-139.
Zhong, H., H. R. Wang, et al. (2010). "Targeting Smad4 links microRNA-146a to the TGF-beta pathway during retinoid acid induction in acute promyelocytic leukemia cell line." Int J Hematol **92**(1): 129-135.
Zhong, Y., Y. Wu, et al. (2011). "Novel retinoic acid receptor alpha agonists for treatment of kidney disease." PLoS One **6**(11): e27945.

Zhou, T. B., Y. H. Qin, et al. (2012). "All-trans retinoic Acid treatment is associated with prohibitin expression in renal interstitial fibrosis rats." Int J Mol Sci **13**(3): 2769-2782.
Zhou, T. B., Y. H. Qin, et al. (2011). "All-trans retinoic acid can regulate the expressions of gelatinases and apolipoprotein E in glomerulosclerosis rats." Vascul Pharmacol **55**(5-6): 167-177.

Chapter 10. Appendix

Appendix A. Supplementary figures

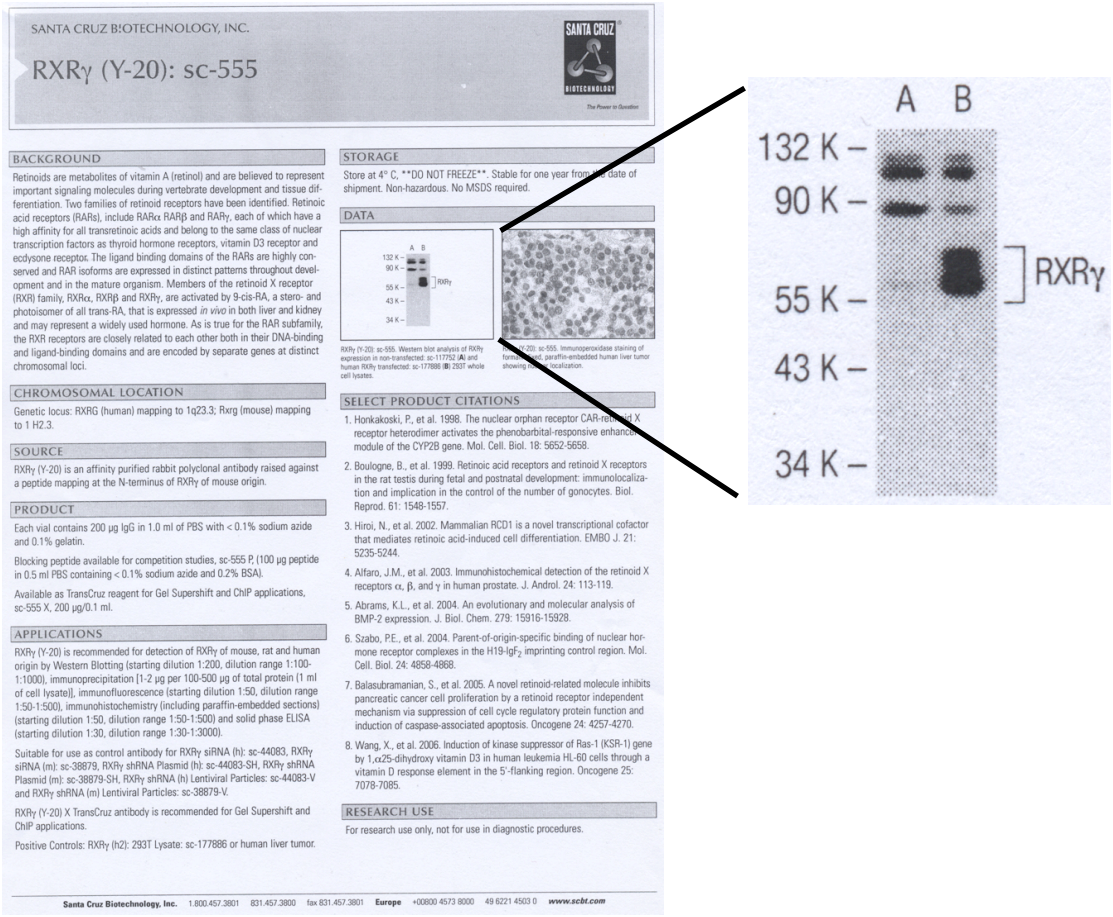

SANTA CRUZ BIOTECHNOLOGY, INC.

RXRγ (Y-20): sc-555

BACKGROUND

Retinoids are metabolites of vitamin A (retinol) and are believed to represent important signaling molecules during vertebrate development and tissue differentiation. Two families of retinoid receptors have been identified. Retinoic acid receptors (RARs), include RARα RARβ and RARγ, each of which have a high affinity for all transretinoic acids and belong to the same class of nuclear transcription factors as thyroid hormone receptors, vitamin D3 receptor and ecdysone receptor. The ligand binding domains of the RARs are highly conserved and RAR isoforms are expressed in distinct patterns throughout development and in the mature organism. Members of the retinoid X receptor (RXR) family, RXRα, RXRβ and RXRγ, are activated by 9-cis-RA, a stero- and photoisomer of all trans-RA, that is expressed *in vivo* in both liver and kidney and may represent a widely used hormone. As is true for the RAR subfamily, the RXR receptors are closely related to each other both in their DNA-binding and ligand-binding domains and are encoded by separate genes at distinct chromosomal loci.

CHROMOSOMAL LOCATION

Genetic locus: RXRG (human) mapping to 1q23.3; Rxrg (mouse) mapping to 1 H2.3.

SOURCE

RXRγ (Y-20) is an affinity purified rabbit polyclonal antibody raised against a peptide mapping at the N-terminus of RXRγ of mouse origin.

PRODUCT

Each vial contains 200 µg IgG in 1.0 ml of PBS with < 0.1% sodium azide and 0.1% gelatin.

Blocking peptide available for competition studies, sc-555 P, (100 µg peptide in 0.5 ml PBS containing < 0.1% sodium azide and 0.2% BSA).

Available as TransCruz reagent for Gel Supershift and ChIP applications, sc-555 X, 200 µg/0.1 ml.

APPLICATIONS

RXRγ (Y-20) is recommended for detection of RXRγ of mouse, rat and human origin by Western Blotting (starting dilution 1:200, dilution range 1:100-1:1000), immunoprecipitation [1-2 µg per 100-500 µg of total protein (1 ml of cell lysate)], immunofluorescence (starting dilution 1:50, dilution range 1:50-1:500), immunohistochemistry (including paraffin-embedded sections) (starting dilution 1:50, dilution range 1:50-1:500) and solid phase ELISA (starting dilution 1:30, dilution range 1:30-1:3000).

Suitable for use as control antibody for RXRγ siRNA (h): sc-44083, RXRγ siRNA (m): sc-38879, RXRγ shRNA Plasmid (h): sc-44083-SH, RXRγ shRNA Plasmid (m): sc-38879-SH, RXRγ shRNA (h) Lentiviral Particles: sc-44083-V and RXRγ shRNA (m) Lentiviral Particles: sc-38879-V.

RXRγ (Y-20) X TransCruz antibody is recommended for Gel Supershift and ChIP applications.

Positive Controls: RXRγ (h2): 293T Lysate: sc-177886 or human liver tumor.

STORAGE

Store at 4° C, **DO NOT FREEZE**. Stable for one year from the date of shipment. Non-hazardous. No MSDS required.

DATA

RXRγ (Y-20): sc-555. Western blot analysis of RXRγ expression in non-transfected: sc-117752 (A) and human RXRγ transfected: sc-177886 (B) 293T whole cell lysates.

SELECT PRODUCT CITATIONS

1. Honkakoski, P., et al. 1998. The nuclear orphan receptor CAR-retinoid X receptor heterodimer activates the phenobarbital-responsive enhancer module of the CYP2B gene. Mol. Cell. Biol. 18: 5652-5658.
2. Boulogne, B., et al. 1999. Retinoic acid receptors and retinoid X receptors in the rat testis during fetal and postnatal development: immunolocalization and implication in the control of the number of gonocytes. Biol. Reprod. 61: 1548-1557.
3. Hiroi, N., et al. 2002. Mammalian RCD1 is a novel transcriptional cofactor that mediates retinoic acid-induced cell differentiation. EMBO J. 21: 5235-5244.
4. Alfaro, J.M., et al. 2003. Immunohistochemical detection of the retinoid X receptors α, β, and γ in human prostate. J. Androl. 24: 113-119.
5. Abrams, K.L., et al. 2004. An evolutionary and molecular analysis of BMP-2 expression. J. Biol. Chem. 279: 15916-15928.
6. Szabo, P.E., et al. 2004. Parent-of-origin-specific binding of nuclear hormone receptor complexes in the H19-IgF_2 imprinting control region. Mol. Cell. Biol. 24: 4858-4868.
7. Balasubramanian, S., et al. 2005. A novel retinoid-related molecule inhibits pancreatic cancer cell proliferation by a retinoid receptor independent mechanism via suppression of cell cycle regulatory protein function and induction of caspase-associated apoptosis. Oncogene 24: 4257-4270.
8. Wang, X., et al. 2006. Induction of kinase suppressor of Ras-1 (KSR-1) gene by 1,α25-dihydroxy vitamin D3 in human leukemia HL-60 cells through a vitamin D response element in the 5'-flanking region. Oncogene 25: 7078-7085.

RESEARCH USE

For research use only, not for use in diagnostic procedures.

Santa Cruz Biotechnology, Inc. 1.800.457.3801 831.457.3800 fax 831.457.3801 Europe +00800 4573 8000 49 6221 4503 0 www.scbt.com

A B

132 K –
90 K –
55 K –
43 K –
34 K –

RXRγ

Supplementary figure 1. RXRγ (Y-20):sc-555 antibody datasheet from Santa Cruz Biotechnology, INC. with enlarged picture of RXRγ immunoblot. Western blot analysis of RXRγ protein expression in non-transfected :sc-117752 (A) and human RXRγ transfected: sc-177886 (B) 293T whole cell lysates. Website address: http://www.scbt.com/datasheet-555-rxrgamma-y-20-antibody.html.

Appendix B. Supplementary tables

Supplementary table 1. PCR array dataset showing fold change of tRA-treated group compared to vehicle.

		Group 1 tRA		
		Fold Change	95% CI	Comments
A01	Adamts1	0.9463	(0.60, 1.29)	OKAY
A02	Adamts5	0.8375	(0.42, 1.26)	OKAY
A03	Adamts8	0.5106	(0.18, 0.84)	B
A04	Catna1	1.1402	(0.89, 1.39)	OKAY
A05	Ctnna2	0.5936	(0.12, 1.07)	C
A06	Cd44	0.7571	(0.15, 1.36)	B
A07	Cdh1	0.4761	(0.00001, 0.98)	B
A08	Cdh2	1.0256	(0.44, 1.61)	OKAY
A09	Cdh3	1.044	(0.50, 1.59)	OKAY
A10	Cdh4	0.5936	(0.12, 1.07)	C
A11	Cntn1	0.1183	(0.06, 0.18)	OKAY
A12	Col1a1	0.9333	(0.16, 1.70)	OKAY
B01	Col2a1	0.5936	(0.12, 1.07)	C
B02	Col3a1	1.3306	(0.85, 1.81)	OKAY
B03	Col4a1	1.125	(0.76, 1.49)	OKAY
B04	Col4a2	1.4434	(0.63, 2.25)	OKAY
B05	Col4a3	0.5068	(0.32, 0.70)	OKAY
B06	Col5a1	0.8534	(0.36, 1.34)	OKAY
B07	Col6a1	0.6072	(0.38, 0.83)	OKAY
B08	Col8a1	0.5523	(0.27, 0.83)	OKAY
B09	Vcan	0.8921	(0.67, 1.11)	OKAY
B10	Ctgf	0.4991	(0.25, 0.75)	OKAY
B11	Ctnnb1	1.1814	(0.20, 2.16)	OKAY
B12	Ecm1	0.4708	(0.00001, 1.13)	OKAY
C01	Emilin1	1.9568	(0.08, 3.84)	OKAY
C02	Entpd1	0.5936	(0.12, 1.07)	C
C03	Fbln1	2.7423	(1.84, 3.64)	OKAY
C04	Fn1	0.6504	(0.19, 1.11)	OKAY
C05	Hapln1	0.1715	(0.00001, 0.39)	OKAY
C06	Icam1	0.8271	(0.10, 1.56)	OKAY
C07	Itga2	0.7606	(0.35, 1.18)	B
C08	Itga3	1.6376	(0.84, 2.44)	OKAY
C09	Itga4	0.6933	(0.26, 1.12)	B
C10	Itga5	0.9508	(0.56, 1.34)	OKAY
C11	Itgad	0.5936	(0.12, 1.07)	C
C12	Itgae	0.6312	(0.18, 1.09)	B
D01	Itgal	0.5936	(0.12, 1.07)	C
D02	Itgam	0.5936	(0.12, 1.07)	C
D03	Itgav	1.2746	(0.62, 1.93)	OKAY
D04	Itgb1	1.7988	(0.18, 3.42)	OKAY
D05	Itgb2	0.5936	(0.12, 1.07)	C
D06	Itgb3	1.6009	(0.00001, 3.21)	OKAY
D07	Itgb4	0.4349	(0.25, 0.62)	A
D08	Lama1	1.0885	(0.52, 1.66)	B
D09	Lama2	0.6356	(0.04, 1.23)	B
D10	Lama3	0.4812	(0.31, 0.65)	OKAY
D11	Lamb2	0.695	(0.43, 0.96)	OKAY
D12	Lamb3	0.4931	(0.04, 0.94)	B
E01	Lamc1	1.6337	(0.54, 2.73)	OKAY
E02	Mmp10	0.1952	(0.00001, 0.41)	B
E03	Mmp11	1.1807	(0.82, 1.54)	OKAY
E04	Mmp12	0.4312	(0.19, 0.67)	OKAY
E05	Mmp13	0.0411	(0.02, 0.06)	OKAY
E06	Mmp14	1.1015	(0.00001, 2.38)	OKAY
E07	Mmp15	0.5936	(0.12, 1.07)	C
E08	Mmp16	0.7768	(0.39, 1.16)	OKAY
E09	Mmp1a	0.5132	(0.07, 0.96)	B
E10	Mmp2	1.4998	(0.95, 2.05)	OKAY
E11	Mmp3	0.2116	(0.14, 0.29)	OKAY

E12	Mmp7	13.6639	(8.01, 19.32)	OKAY
F01	Mmp8	0.5936	(0.12, 1.07)	C
F02	Mmp9	0.3025	(0.07, 0.54)	OKAY
F03	Ncam1	2.175	(1.30, 3.05)	OKAY
F04	Ncam2	0.5936	(0.12, 1.07)	C
F05	Pecam1	0.3475	(0.00001, 0.72)	B
F06	Postn	2.1045	(0.00001, 4.35)	OKAY
F07	Adamts2	0.9556	(0.35, 1.56)	OKAY
F08	Sele	0.5936	(0.12, 1.07)	C
F09	Sell	0.5936	(0.12, 1.07)	C
F10	Selp	0.5936	(0.12, 1.07)	C
F11	Sgce	0.5758	(0.15, 1.00)	OKAY
F12	Sparc	42.6872	(0.00001, 383.00)	OKAY
G01	Spock1	0.8628	(0.37, 1.36)	A
G02	Spp1	0.6896	(0.51, 0.87)	OKAY
G03	Syt1	0.3357	(0.01, 0.66)	A
G04	Tgfbi	0.4401	(0.23, 0.65)	OKAY
G05	Thbs1	0.3962	(0.24, 0.55)	OKAY
G06	Thbs2	2.2811	(0.12, 4.44)	OKAY
G07	Timp1	0.5726	(0.23, 0.92)	OKAY
G08	Timp2	0.5553	(0.29, 0.82)	OKAY
G09	Timp3	0.7366	(0.66, 0.81)	OKAY
G10	Tnc	0.7611	(0.26, 1.26)	OKAY
G11	Vcam1	10.2021	(0.00001, 20.71)	OKAY
G12	Vtn	0.5936	(0.12, 1.07)	C
H01	Rplp1	0.7018	(0.29, 1.11)	OKAY
H02	Hprt1	1.2145	(1.00, 1.43)	OKAY
H03	Rpl13a	1.5083	(0.96, 2.06)	OKAY
H04	Ldha	0.9453	(0.77, 1.12)	OKAY
H05	Actb	0.8229	(0.10, 1.54)	OKAY
H06	RGDC	0.6492	(0.21, 1.09)	B
H07	RTC	0.7834	(0.46, 1.11)	OKAY
H08	RTC	0.8111	(0.45, 1.18)	OKAY
H09	RTC	0.6593	(0.41, 0.90)	OKAY
H10	PPC	19.868	(0.00001, 155.85)	OKAY
H11	PPC	0.5718	(0.10, 1.04)	OKAY
H12	PPC	0.6292	(0.13, 1.13)	OKAY

Comments:

A: This gene's average threshold cycle is relatively high (> 30) in either the control or the test sample, and is reasonably low in the other sample (< 30).

These data mean that the gene's expression is relatively low in one sample and reasonably detected in the other sample suggesting that the actual fold-change value is at least as large as the calculated and reported fold-change result.

This fold-change result may also have greater variations if p value > 0.05; therefore, it is important to have a sufficient number of biological replicates to validate the result for this gene.

B: This gene's average threshold cycle is relatively high (> 30), meaning that its relative expression level is low, in both control and test samples, and the p-value for the fold-change is either unavailable or relatively high (p > 0.05).

This fold-change result may also have greater variations; therefore, it is important to have a sufficient number of biological replicates to validate the result for this gene.

C: This gene's average threshold cycle is either not determined or greater than the defined cut-off value (default 35), in both samples meaning that its expression was undetected, making this fold-change result erroneous and un-interpretable.

Fold Change & Fold Regulation:

Fold-Change (2^(- Delta Delta Ct)) is the normalized gene expression (2^(- Delta Ct)) in the Test Sample divided the normalized gene expression (2^(- Delta Ct)) in the Control Sample.

Fold-Regulation represents fold-change results in a biologically meaningful way. Fold-change values greater than one indicate a positive- or an up-regulation, and the fold-regulation is equal to the fold-change.

Fold-change values less than one indicate a negative or down-regulation, and the fold-regulation is the negative inverse of the fold-change.

Fold-change and fold-regulation values greater than 2 are indicated in red; fold-change values less than 0.5 and fold-regulation values less than -2 are indicated in blue.

Supplementary Table 2. PCR array dataset showing fold change of TGF-β1-treated group compared to vehicle.

		Group 2 TGF		
		Fold Change	95% CI	Comments
A01	Adamts1	1.8948	(0.98, 2.80)	OKAY
A02	Adamts5	0.4675	(0.29, 0.65)	OKAY
A03	Adamts8	0.5255	(0.20, 0.85)	B
A04	Catna1	0.6053	(0.42, 0.79)	OKAY
A05	Ctnna2	0.6386	(0.29, 0.99)	C
A06	Cd44	2.6187	(0.93, 4.31)	B
A07	Cdh1	0.5756	(0.06, 1.09)	B
A08	Cdh2	0.7254	(0.36, 1.09)	OKAY
A09	Cdh3	0.2541	(0.11, 0.40)	OKAY
A10	Cdh4	0.6386	(0.29, 0.99)	C
A11	Cntn1	0.3036	(0.10, 0.51)	OKAY
A12	Col1a1	0.9764	(0.36, 1.59)	OKAY
B01	Col2a1	0.6386	(0.29, 0.99)	C
B02	Col3a1	3.7563	(2.79, 4.72)	OKAY
B03	Col4a1	2.1044	(1.43, 2.78)	OKAY
B04	Col4a2	1.5535	(0.58, 2.52)	OKAY
B05	Col4a3	0.5742	(0.19, 0.96)	B
B06	Col5a1	1.848	(1.44, 2.26)	OKAY
B07	Col6a1	0.5475	(0.21, 0.89)	OKAY
B08	Col8a1	1.0965	(0.44, 1.75)	OKAY
B09	Vcan	0.5109	(0.39, 0.63)	OKAY
B10	Ctgf	1.0759	(0.50, 1.65)	OKAY
B11	Ctnnb1	0.4026	(0.09, 0.72)	OKAY
B12	Ecm1	0.1905	(0.00001, 0.41)	OKAY
C01	Emilin1	1.606	(0.00001, 3.51)	OKAY
C02	Entpd1	0.6386	(0.29, 0.99)	C
C03	Fbln1	3.5942	(2.21, 4.98)	OKAY
C04	Fn1	2.0625	(1.31, 2.81)	OKAY
C05	Hapln1	0.3609	(0.24, 0.48)	OKAY
C06	Icam1	0.1737	(0.05, 0.30)	OKAY
C07	Itga2	8.6921	(2.02, 15.37)	A
C08	Itga3	0.5092	(0.25, 0.77)	OKAY
C09	Itga4	0.6554	(0.30, 1.01)	B
C10	Itga5	1.8212	(1.08, 2.56)	OKAY
C11	Itgad	0.6386	(0.29, 0.99)	C
C12	Itgae	0.6386	(0.29, 0.99)	C
D01	Itgal	0.6386	(0.29, 0.99)	C
D02	Itgam	0.6386	(0.29, 0.99)	C
D03	Itgav	1.6384	(0.92, 2.36)	OKAY
D04	Itgb1	2.5893	(1.40, 3.78)	OKAY
D05	Itgb2	0.6386	(0.29, 0.99)	C
D06	Itgb3	2.1995	(0.04, 4.36)	OKAY
D07	Itgb4	0.327	(0.20, 0.45)	A
D08	Lama1	4.3578	(1.97, 6.75)	A
D09	Lama2	0.2574	(0.00001, 0.54)	B
D10	Lama3	5.6291	(3.39, 7.87)	OKAY
D11	Lamb2	0.2332	(0.11, 0.35)	OKAY
D12	Lamb3	335.4897	(0.00001, 769.29)	A
E01	Lamc1	1.9206	(0.58, 3.26)	OKAY
E02	Mmp10	1.8539	(0.67, 3.04)	B
E03	Mmp11	0.3727	(0.29, 0.45)	OKAY
E04	Mmp12	0.3375	(0.19, 0.49)	OKAY
E05	Mmp13	0.8518	(0.63, 1.08)	OKAY
E06	Mmp14	1.0058	(0.00001, 2.27)	OKAY
E07	Mmp15	0.6386	(0.29, 0.99)	C
E08	Mmp16	0.971	(0.50, 1.44)	OKAY
E09	Mmp1a	0.6537	(0.09, 1.22)	B
E10	Mmp2	0.6656	(0.42, 0.91)	OKAY
E11	Mmp3	0.1408	(0.08, 0.20)	OKAY

E12	Mmp7	0.6386	(0.29, 0.99)	C
F01	Mmp8	0.6386	(0.29, 0.99)	C
F02	Mmp9	2.6053	(0.92, 4.29)	B
F03	Ncam1	1.2809	(1.06, 1.50)	OKAY
F04	Ncam2	0.6386	(0.29, 0.99)	C
F05	Pecam1	1.27	(0.00001, 2.68)	B
F06	Postn	86.2131	(3.13, 169.29)	OKAY
F07	Adamts2	0.7716	(0.25, 1.29)	OKAY
F08	Sele	0.6386	(0.29, 0.99)	C
F09	Sell	0.6386	(0.29, 0.99)	C
F10	Selp	0.9263	(0.09, 1.76)	B
F11	Sgce	0.2735	(0.06, 0.48)	OKAY
F12	Sparc	67.9995	(0.00001, 610.82)	OKAY
G01	Spock1	0.6405	(0.33, 0.95)	B
G02	Spp1	2.4626	(1.64, 3.28)	OKAY
G03	Syt1	0.7953	(0.12, 1.47)	OKAY
G04	Tgfbi	2.8865	(2.17, 3.61)	OKAY
G05	Thbs1	0.7108	(0.44, 0.98)	OKAY
G06	Thbs2	5.8709	(0.00001, 11.82)	OKAY
G07	Timp1	1.4481	(0.23, 2.67)	OKAY
G08	Timp2	0.3106	(0.16, 0.46)	OKAY
G09	Timp3	3.8951	(1.69, 6.10)	OKAY
G10	Tnc	53.0506	(16.22, 89.88)	OKAY
G11	Vcam1	0.1012	(0.00001, 0.20)	A
G12	Vtn	0.6386	(0.29, 0.99)	C
H01	Rplp1	0.6607	(0.46, 0.87)	OKAY
H02	Hprt1	1.3396	(1.19, 1.49)	OKAY
H03	Rpl13a	1.568	(0.65, 2.49)	OKAY
H04	Ldha	0.7706	(0.45, 1.09)	OKAY
H05	Actb	0.935	(0.75, 1.12)	OKAY
H06	RGDC	0.6256	(0.27, 0.98)	B
H07	RTC	1.1031	(0.51, 1.70)	OKAY
H08	RTC	1.1467	(0.51, 1.78)	OKAY
H09	RTC	0.8815	(0.49, 1.27)	OKAY
H10	PPC	21.9409	(0.00001, 171.58)	OKAY
H11	PPC	0.666	(0.37, 0.96)	OKAY
H12	PPC	0.5398	(0.18, 0.90)	OKAY

Comments:

A: This gene's average threshold cycle is relatively high (> 30) in either the control or the test sample, and is reasonably low in the other sample (< 30).

These data mean that the gene's expression is relatively low in one sample and reasonably detected in the other sample suggesting that the actual fold-change value is at least as large as the calculated and reported fold-change result.

This fold-change result may also have greater variations if p value > 0.05; therefore, it is important to have a sufficient number of biological replicates to validate the result for this gene.

B: This gene's average threshold cycle is relatively high (> 30), meaning that its relative expression level is low, in both control and test samples, and the p-value for the fold-change is either unavailable or relatively high (p > 0.05).

This fold-change result may also have greater variations; therefore, it is important to have a sufficient number of biological replicates to validate the result for this gene.

C: This gene's average threshold cycle is either not determined or greater than the defined cut-off value (default 35), in both samples meaning that its expression was undetected, making this fold-change result erroneous and un-interpretable.

Fold Change & Fold Regulation:

Fold-Change (2^(- Delta Delta Ct)) is the normalized gene expression (2^(- Delta Ct)) in the Test Sample divided the normalized gene expression (2^(- Delta Ct)) in the Control Sample.

Fold-Regulation represents fold-change results in a biologically meaningful way. Fold-change values greater than one indicate a positive- or an up-regulation, and the fold-regulation is equal to the fold-change.

Fold-change values less than one indicate a negative or down-regulation, and the fold-regulation is the negative inverse of the fold-change.

Fold-change and fold-regulation values greater than 2 are indicated in red; fold-change values less than 0.5 and fold-regulation values less than -2 are indicated in blue.

Supplementary Table 3. PCR array dataset showing fold change of the dual-treated group compared to the TGF-β1-treated group.

		Group 3 dual		
		Fold Change	**95% CI**	**Comments**
A01	Adamts1	0.1876	(0.07, 0.31)	OKAY
A02	Adamts5	1.3789	(0.83, 1.93)	OKAY
A03	Adamts8	0.6887	(0.34, 1.03)	B
A04	Catna1	1.0327	(0.72, 1.34)	OKAY
A05	Ctnna2	0.9647	(0.26, 1.66)	B
A06	Cd44	0.4985	(0.26, 0.74)	B
A07	Cdh1	0.6857	(0.34, 1.03)	B
A08	Cdh2	1.2062	(1.02, 1.39)	OKAY
A09	Cdh3	0.9636	(0.51, 1.42)	OKAY
A10	Cdh4	0.7708	(0.42, 1.13)	C
A11	Cntn1	0.1338	(0.06, 0.21)	OKAY
A12	Col1a1	0.9903	(0.58, 1.40)	OKAY
B01	Col2a1	0.7708	(0.42, 1.13)	C
B02	Col3a1	0.9061	(0.75, 1.06)	OKAY
B03	Col4a1	0.8118	(0.58, 1.04)	OKAY
B04	Col4a2	0.6426	(0.23, 1.06)	OKAY
B05	Col4a3	2.5618	(0.00001, 5.42)	B
B06	Col5a1	0.755	(0.57, 0.94)	OKAY
B07	Col6a1	0.4663	(0.16, 0.77)	OKAY
B08	Col8a1	0.2295	(0.10, 0.36)	OKAY
B09	Vcan	1.4914	(1.13, 1.85)	OKAY
B10	Ctgf	0.2054	(0.13, 0.28)	OKAY
B11	Ctnnb1	1.5039	(0.72, 2.29)	OKAY
B12	Ecm1	0.5055	(0.36, 0.65)	OKAY
C01	Emilin1	0.4488	(0.00001, 0.93)	OKAY
C02	Entpd1	0.7708	(0.42, 1.13)	C
C03	Fbln1	1.8752	(1.15, 2.60)	OKAY
C04	Fn1	0.8744	(0.55, 1.19)	OKAY
C05	Hapln1	0.3641	(0.27, 0.46)	OKAY
C06	Icam1	1.2736	(0.77, 1.78)	OKAY
C07	Itga2	1.3085	(0.52, 2.09)	OKAY
C08	Itga3	1.4985	(0.84, 2.16)	OKAY
C09	Itga4	0.8661	(0.34, 1.39)	B
C10	Itga5	1.0695	(0.80, 1.34)	OKAY
C11	Itgad	0.7708	(0.42, 1.13)	C
C12	Itgae	0.7708	(0.42, 1.13)	C
D01	Itgal	0.7781	(0.43, 1.13)	B
D02	Itgam	0.7708	(0.42, 1.13)	C
D03	Itgav	0.5509	(0.31, 0.80)	OKAY
D04	Itgb1	0.7025	(0.53, 0.87)	OKAY
D05	Itgb2	1.0141	(0.20, 1.83)	B
D06	Itgb3	0.5937	(0.11, 1.08)	OKAY
D07	Itgb4	0.8391	(0.46, 1.22)	B
D08	Lama1	0.6083	(0.39, 0.82)	OKAY
D09	Lama2	0.8038	(0.19, 1.42)	B
D10	Lama3	0.3984	(0.22, 0.57)	OKAY
D11	Lamb2	1.2126	(0.59, 1.84)	OKAY
D12	Lamb3	0.856	(0.00001, 1.92)	OKAY
E01	Lamc1	0.7047	(0.25, 1.16)	OKAY
E02	Mmp10	0.6454	(0.51, 0.78)	OKAY
E03	Mmp11	1.6439	(1.36, 1.93)	OKAY
E04	Mmp12	1.2478	(0.65, 1.85)	B
E05	Mmp13	0.2724	(0.20, 0.34)	OKAY
E06	Mmp14	0.4132	(0.09, 0.73)	OKAY
E07	Mmp15	0.7708	(0.42, 1.13)	C
E08	Mmp16	0.6528	(0.54, 0.76)	OKAY
E09	Mmp1a	1.1303	(0.11, 2.16)	B
E10	Mmp2	0.6106	(0.34, 0.88)	OKAY
E11	Mmp3	0.5144	(0.29, 0.74)	OKAY

E12	Mmp7	3.506	(1.41, 5.61)	OKAY
F01	Mmp8	0.7708	(0.42, 1.13)	C
F02	Mmp9	1.295	(0.50, 2.09)	B
F03	Ncam1	1.6203	(1.26, 1.98)	OKAY
F04	Ncam2	0.7708	(0.42, 1.13)	C
F05	Pecam1	0.5979	(0.00001, 1.24)	B
F06	Postn	0.0218	(0.01, 0.04)	OKAY
F07	Adamts2	0.4678	(0.21, 0.73)	OKAY
F08	Sele	0.7708	(0.42, 1.13)	C
F09	Sell	0.7708	(0.42, 1.13)	C
F10	Selp	2.0933	(0.35, 3.84)	B
F11	Sgce	1.2613	(0.74, 1.78)	OKAY
F12	Sparc	0.4527	(0.08, 0.82)	OKAY
G01	Spock1	1.2025	(0.67, 1.74)	A
G02	Spp1	0.7527	(0.54, 0.97)	OKAY
G03	Syt1	0.5644	(0.16, 0.97)	OKAY
G04	Tgfbi	0.2818	(0.22, 0.34)	OKAY
G05	Thbs1	0.3343	(0.20, 0.47)	OKAY
G06	Thbs2	0.31	(0.03, 0.59)	OKAY
G07	Timp1	0.3997	(0.13, 0.67)	OKAY
G08	Timp2	0.4675	(0.36, 0.57)	OKAY
G09	Timp3	0.1167	(0.04, 0.19)	OKAY
G10	Tnc	0.0607	(0.03, 0.09)	OKAY
G11	Vcam1	51.1681	(14.42, 87.91)	A
G12	Vtn	0.7708	(0.42, 1.13)	C
H01	Rplp1	0.9726	(0.80, 1.14)	OKAY
H02	Hprt1	1.1873	(1.07, 1.31)	OKAY
H03	Rpl13a	0.809	(0.29, 1.33)	OKAY
H04	Ldha	1.3536	(0.64, 2.07)	OKAY
H05	Actb	0.7907	(0.55, 1.03)	OKAY
H06	RGDC	0.7708	(0.42, 1.13)	C
H07	RTC	0.7663	(0.39, 1.14)	OKAY
H08	RTC	0.7158	(0.35, 1.08)	OKAY
H09	RTC	0.7705	(0.48, 1.06)	OKAY
H10	PPC	0.7001	(0.34, 1.06)	OKAY
H11	PPC	0.8023	(0.48, 1.12)	OKAY
H12	PPC	0.9054	(0.31, 1.50)	OKAY

Comments:

A: This gene's average threshold cycle is relatively high (> 30) in either the control or the test sample, and is reasonably low in the other sample (< 30).

These data mean that the gene's expression is relatively low in one sample and reasonably detected in the other sample suggesting that the actual fold-change value is at least as large as the calculated and reported fold-change result.

This fold-change result may also have greater variations if p value > 0.05; therefore, it is important to have a sufficient number of biological replicates to validate the result for this gene.

B: This gene's average threshold cycle is relatively high (> 30), meaning that its relative expression level is low, in both control and test samples, and the p-value for the fold-change is either unavailable or relatively high (p > 0.05).

This fold-change result may also have greater variations; therefore, it is important to have a sufficient number of biological replicates to validate the result for this gene.

C: This gene's average threshold cycle is either not determined or greater than the defined cut-off value (default 35), in both samples meaning that its expression was undetected, making this fold-change result erroneous and un-interpretable.

Fold Change & Fold Regulation:

Fold-Change (2^(- Delta Delta Ct)) is the normalized gene expression (2^(- Delta Ct)) in the Test Sample divided the normalized gene expression (2^(- Delta Ct)) in the Control Sample.

Fold-Regulation represents fold-change results in a biologically meaningful way. Fold-change values greater than one indicate a positive- or an up-regulation, and the fold-regulation is equal to the fold-change.

Fold-change values less than one indicate a negative or down-regulation, and the fold-regulation is the negative inverse of the fold-change.

Fold-change and fold-regulation values greater than 2 are indicated in red; fold-change values less than 0.5 and fold-regulation values less than -2 are indicated in blue.

Supplementary Table 4. LC/MS/MS analysis of 1D polyacrylamide gel bands of interest in NRK-49F total cell lysate. AR2_1 and AR2_2 represent bands of interest corresponding to the TG2 immunoblot (see Figure 3.12); AR3_1, AR3_2 and AR3_3 represent bands of interest corresponding to the CRABP-II immunoblot (see Figure 4.9).

Band No.	Protein I.D.	Species	Accession No.	MW (Da)	pI	No. Peptides Matched	No. Unique Peptides	Peptide Identity Score	Peptide Identity Threshold	Percentage Coverage	Sequence
AR2_1	78 kDa glucose-regulated protein	Rat	P06761	72302	5.07	53	30	62.1	49.9	48%	AKFEELNMDLFR
								80.4	49.7		AVEEKIEWLESHQDADIEDFK
								60.0	50.0		DAGTIAGLNVMR
								117.0	49.8		DNHLLGTFDLTGIPPAPR
								42.8	49.7		ELEEIVQPIISK
								68.1	50.0		FEELNMDLFR
								75.4	49.7		IEIESFFEGEDFSETLTR
								84.4	49.7		IEWLESHQDADIEDFK
								71.8	49.8		IEWLESHQDADIEDFKAK
								68.8	49.9		IINEPTAAAIAYGLDK
								93.1	49.8		IINEPTAAAIAYGLDKR
								54.6	49.6		ITPSYVAFTPEGER
								50.0	49.4		KKELEEIVQPIISK
								102.1	50.0		KSDIDEIVLVGGSTR
								74.1	49.9		KTKPYIQVDIGGGQTK
								64.8	49.8		KVTHAVVTVPAYFNDAQR
								34.1	50.1		LTPEEIER
								86.0	49.9		MKETAEAYLGK
								52.3	49.6		MVNDAEKFAEEDKK
								50.6	50.1		NELESYAYSLK
								39.8	49.9		NGRVEIIANDQGNR
								95.2	49.8		NQLTSNPENTVFDAK
								56.1	49.9		NQLTSNPENTVFDAKR
								76.0	49.8		SQIFSTASDNQPTVTIK
								66.6	49.7		TFAPEEISAMVLTK
								59.9	49.9		TKPYIQVDIGGGQTK
								63.7	50.0		TWNDPSVQQDIK
								57.8	50.3		VLEDSDLK
								51.9	50.2		VLEDSDLKK
								58.8	49.8		VTHAVVTVPAYFNDAQR
								49.0	49.9		VYEGERPLTK
	Stress-70 protein, mitochondrial	Rat	P48721	73812	5.97	44	23	57.2	49.8	41%	AQFEGIVTDLIK
								59.3	49.9		AQFEGIVTDLIKR
								84.1	49.8		ASNGDAWVEAHGK
								63.8	49.8		DAGQISGLNVLR
								63.9	50.0		EQQIVIQSSGGLSK
								43.8	49.8		EQQIVIQSSGGLSKDDIENMVK
								82.8	49.8		ERVEAVNMAEGIIHDTETK
								91.5	49.9		ETAENYLGHTAK
								47.8	49.9		ETGVDLTKDNMALQR
								47.5	50.3		LFEMAYK
								55.7	49.5		LLGQFTLIGIPPAPR
								45.0	49.4		MEEFKDQLPADECNK
								69.2	49.6		MKETAENYLGHTAK
								55.3	49.8		NAVITVPAYFNDSQR
								93.8	50.1		QAASSLQQASLK
								101.2	49.8		QAVTNPNNTFYATK
								61.7	49.7		RYDDPEVQKDTK
								63.3	50.0		SDIGEVILVGGMTR
								92.4	49.6		STNGDTFLGGEDFDQALLR
								74.6	49.9		TTPSVVAFTPDGER
								95.1	49.8		VEAVNMAEGIIHDTETK
								63.7	49.8		VINEPTAAALAYGLDKSEDK
								62.6	50.0		VQQTVQDLFGR
	Heat shock cognate 71 kDa protein	Rat	P63018	70827	5.37	32	15	72.1	49.7	32%	ARFEELNADLFR
								75.9	49.4		FEELNADLFR
								53.2	49.8		HWPFMVVNDAGRPK
								73.7	49.9		IINEPTAAAIAYGLDKK
								47.1	49.0		LLQDFFNGK
								55.4	50.3		LSKEDIER
								80.0	49.4		MKEIAEAYLGK
								52.5	49.4		MVNHFIAEFK
								38.7	49.8		MVQEAEKYKAEDEK
								100.3	49.7		NQVAMNPTNTVFDAK
								57.5	50.0		NSLESYAFNMK
								118.2	49.5		QTQTFTTYSDNQPGVLIQVYEGER
								69.4	49.6		RFDDAVVQSDMK

								79.9	49.6		STAGDTHLGGEDFDNR
								50.7	50.0		TTPSYVAFTDTER
								55.9	49.7		TVTNAVVTVPAYFNDSQR
	Non-muscle caldesmon	Rat	Q62736	60548	6.34	15	8	59.5	49.9	22%	ASGDKEAEGAPQVEAGKR
								67.1	49.6		GSVFSSPSASGTPNK
								86.5	49.5		LEQYTNAIEGTK
								96.6	49.8		QKEFDPTITDGSLSVPSR
								40.1	50.0		QQEAALELEELK
								49.4	49.5		QTENAFSPSR
								69.1	49.6		RGETESEEFEKLK
								44.1	49.6		SGRYEMEETEVVITSYQK
	Src substrate cortactin	Mouse	Q60598	61222	5.24	13	8	39.7	49.9	15%	CALGWDHQEK
								56.2	50.0		ENVFQEHQTLK
								40.7	50.0		LQLHESQKDYK
								56.6	49.8		LRENVFQEHQTLK
								62.4	49.8		NASTFEEVVQVPSAYQK
								97.6	50.1		QDSSAVGFDYK
								62.7	49.8		SAVGFEYQGK
								38.4	49.3		YGIDKDKVDK
	Protein disulfide-isomerase A4	Rat	P38659	72721	5.16	11	7	54.9	49.4	12%	FDVSGYPTIK
								45.0	50.1		FIDEHATKR
								47.0	49.7		IASTLKDNDPPIAVAK
								59.5	49.4		RFDVSGYPTLK
								27.9	49.7		TFDAIVMDPK
								60.7	49.2		VDATEQTDLAK
	Peptidyl-prolyl cis-trans isomerase FKBP10	Mouse	Q61576	64628	5.38	13	7	58.6	49.0	16%	EVQMGDFVR
								56.2	50.0		GGTYDTYIGSGWLIK
								68.8	49.1		GLMGMCVNER
								39.8	49.7		GLQGMCVGER
								38.9	49.9		IIIPPFLAYGEK
								100.0	49.8		LFSSHDYEAPQEITLGANK
								45.1	49.8		QLIVPPHLAHGENGAR
	Prelamin-A/C	Rat	P48679	74279	6.54	7	4	46.5	50.0	8%	AQHEDQVEQYKK
								62.8	49.9		ITESEEVVSR
								69.3	49.8		MQQQLDEYQELLDIK
								48.6	50.0		SGAQASSTPLSPTR
	LETM1 and EF-hand domain-containing protein 1, mitochondrial	Rat	Q5XIN6	83008	6.22	5	3	80.1	49.5	6%	AKLEATLQEEAAIQQEHLEELKR
								40.9	49.6		FLQDTIEEMALK
								46.0	49.8		STLQTLPEIVAK
	Septin-9	Rat	Q9QZR6	63752	8.65	4	2	50.2	50.1	5%	QVESTASTPGPSR
								56.8	48.7		RTEITIVKPQESGLR
	Sorting nexin-1	Rat	Q99N27	59008	5.15	4	2	65.4	49.9	5%	AVGTQALSGAGLLK
								57.9	50.0		ELALNTALFAK
	Zyxin	Mouse	Q62523	60751	6.47	3	2	50.3	49.8	4%	GPLSQAPTPAPK
								67.0	49.1		SPGGPGPLTLK
	Protein phosphatase 1G	Mouse	Q61074	58691	4.27	2	2	65.4	50.0	4%	ALQDAFLAIDAK
								83.1	50.0		QLIVANAGDSR
	Dihydropyrimidinase-related protein 3	Rat	Q62952	61928	6.04	3	2	37.6	49.4	4%	QIGDNLIVPGGVK
								45.2	50.1		SAADLISQAR
	Glucosidase 2 subunit beta	Mouse	O08795	58756	4.41	2	1	50.1	50.1	4%	ESLQQLAEVTR
								50.3	50.0		KLWEEQQAAAK
	Eukaryotic translation initiation factor 4B	Mouse	Q8BGD9	68799	5.47	3	1	46.5	50.1	2%	RGDDSFGDKYR
	Far upstream element-binding protein 1	Rat	Q32PX7	67155	7.18	1	1	81.7	49.7	2%	IGGNEGIDVPIPR
	Splicing factor 1	Mouse	Q64213	70363	8.98	2	1	52.5	49.9	2%	AYIVQLQIEDLTR
	Calnexin	Rat	P35565	67213	4.49	1	1	62.5	49.8	3%	APVPTGEVYFADSFDR
	Peptidyl-prolyl cis-trans isomerase FKBP9	Rat	Q66H94	63086	4.93	1	1	48.5	49.8	2%	LAPGFNAEMIVK
	Neuroplastin	Rat	P97546	43904	8.6	1	1	47.7	50.1	3%	IVTSEEVIIR
AR2_2	Cytoskeleton-associated protein 4	Mouse	Q8BMK4	63654	5.46	30	17	68.6	52.1	27%	DFTSLENTVEER
								44.6	51.7		DLSDGIHVVK
								66.0	52.1		ERDFTSLENTVEER
								53.7	53.0		ERDIEALK
								38.2	53.3		ISEVLQK
								57.3	52.9		LALQALTEK
								43.6	53.0		LQNEILK
								60.1	52.4		LQNEILKDLSDGIHVVK
								64.2	52.3		MKVASLEESKGDR
								42.9	53.0		QIEGLGAR
								63.1	52.5		QRDELGQGLQGVEQK
								54.4	52.6		RLEEELQQLK
								75.5	52.5		SINDNIAIFTDVQK
								108.6	52.2		SSLQTMESDVYTEVR

								52.8	52.3		SSVSQVESDLK
								101.3	51.9		TAVDSLVAYSVK
								78.6	52.6		VASLEESKGDR
	Stress-induced-phosphoprotein 1	Rat	O35814	62530	6.4	32	15	54.5	52.3	26%	AAALEFLNRFEEAK
								52.9	51.7		ALDLDSSCK
								65.4	52.7		EGLQNMEAR
								61.4	52.5		ELIEQLQNKPSDLGTK
								94.6	52.6		IGNSYFKEER
								47.1	52.5		KAAALEAMKDYTK
								75.6	52.7		KAAALEFLNR
								55.6	52.4		KAAALEFLNRFEEAK
								84.7	52.7		LAYINPDLALEEK
								66.3	52.8		LMDVGLIAIR
								51.9	52.7		MEQVNELKEK
								58.6	52.5		RTYEEGLKHEANNLQLK
								45.7	51.8		TLLSDPTYR
								46.1	52.5		TYEEGLKHEANNLQLK
								40.4	52.5		YKDAIHFYNK
	Heterogeneous nuclear ribonucleoprotein K	Rat	P61980	50944	5.39	19	13	53.8	52.2	35%	GGDLMAYDR
								41.5	52.1		GGDLMAYDRR
								37.6	51.6		GSDFDCELR
								69.3	52.5		GSYGDLGGPIITTQVTIPK
								74.8	52.6		IDEPLEGSEDR
								97.6	52.4		IITITGTQDQIQNAQYLLQNSVK
								51.1	51.7		LFQECCPHSTDR
								52.7	52.5		LLIHQSLAGGIIGVK
								44.2	51.9		NLPLPPPPPPR
								54.9	51.7		NTDEMVELR
								72.4	52.2		RPAEDMEEEQAFKR
								71.8	51.9		TDYNASVSVPDSSGPER
								52.8	51.6		VVLIGGKPDR
	Nucleobindin-1	Rat	Q63083	53474	5.04	11	7	54.1	52.7	18%	DLELLIQTATR
								41.6	52.6		ELQQAVLQMEQR
								50.0	52.4		KVPEQPPVLPQLDSQHL
								51.2	52.8		LQAANAEDIK
								67.3	52.7		LSQETEALGR
								53.6	52.0		VNVPGSQAQLK
								50.3	51.9		YLESLGEEQR
	Prolyl 4-hydroxylase subunit alpha-1	Rat	P54001	60860	5.63	8	6	52.5	52.5	14%	FILAPAKQEDEWDKPR
								51.9	52.7		GIAVDYLPER
								52.1	51.9		HAACPVLVGNK
								68.0	52.3		LLELDPEHQR
								56.2	52.3		LQDTYNLDTNTISK
								44.0	52.0		QYFPNDEDQVGAAK
	Prelamin-A/C	Rat	P48679	P48679	6.54	10	5	42.5	52.6	9%	AQHEDQVEQYKK
								56.8	52.7		LADALQELR
								46.6	52.7		LKDLEALLNSK
								38.7	52.6		LQEKEDLQELNDR
								45.0	52.7		SGAQASSTPLSPTR
	Dihydropyrimidinase-related protein 2	Rat	P47942	62239	5.95	9	4	48.3	52.4	11%	IVLEDGTLHVTEGSGR
								45.0	52.3		NLHQSGFSLSGAQIDDNIPR
								49.6	52.1		QIGENLIVPGGVK
								82.8	52.5		SITIANQTNCPLYVTK
	Protein kinase C and casein kinase substrate in neurons 2 protein	Rat	Q9QY17	55943	5.04	8	4	62.5	51.6	10%	AGDELTKIEDEDEQGWCK
								66.1	52.2		AYAQQLTEWAR
								67.4	52.7		HLDLSNVASYK
								49.7	51.6		VSELHLEVK
	Vimentin	Rat	P31000	53700	5.06	5	2	59.2	52.5	5%	KVESLQEEIAFLKK
								58.3	51.9		LGDLYEEEMR
	RNA-binding protein FUS	Mouse	P56959	52642	9.4	6	2	45.4	52.3	6%	AAIDWFDGKEFSGNPIK
								50.2	52.5		LKGEATVSFDDPPSAK
	Sulfated glycoprotein 1	Rat	P10960	61084	5.13	4	2	56.8	52.8	4%	LVTDIQTAVR
								39.6	52.6		QLESNKIPEVDLAR
	Gamma-glutamyltranspeptidase 1	Rat	P07314	61571	7.21	3	2	49.8	52.7	4%	LFQPSIQLAR
								44.0	52.5		VLQEGETVTMPK
	Brain acid soluble protein 1	Mouse	Q91XV3	22074	4.5	2	2	54.5	52.7	16%	ETPAASEAPSSAAK
								49.8	52.1		SDAAPAASDSKPSSAEPAPSSK
	Abl interactor 1	Rat	Q9QZM5	51673	6.57	1	1	62.7	52.5	3%	KPIDYTVLDDVGHGVK
AR3_1	Vinculin	Rat	P85972	116542	5.83	51	30	67.9	52.3	37%	AGEVINQPMMMAAR
								67.5	52.7		ALASQLQDSLK
								94.2	52.6		AQQVSQGLDVLTAK

								59.8	52.3		AVAGNISDPGLQK
								65.3	52.3		CDRVDQLAAQLADLAAR
								69.1	51.5		EAFQPQEPDFPPPPPDLEQLR
								59.3	52.5		ELLPVLISAMK
								64.5	52.5		ETVQTTEDQILK
								101.4	51.8		GILEYLTVAEVVETMEDLVTYTK
								93.0	51.9		GWLRDPNASPGDAGEQAIR
								42.0	52.8		IPTISTQLK
								59.2	52.5		KIAELCDDPKER
								105.7	51.6		KIDAAQNWLADPNGGPEGEEQIR
								109.8	52.2		LVQAAQMLQSDPYSVPAR
								64.8	52.0		MALLMAEMSR
								92.6	51.8		MLGQMTDQVADLR
								89.3	52.5		MSAEINEIIR
								85.3	51.9		MTGLVDEAIDTK
								45.6	53.0		NQGIEEALK
								48.0	51.5		QILDEAGK
								79.1	52.7		QVATALQNLQTK
								47.1	53.0		SFLDSGYR
								57.9	52.7		SLGEIAALTSK
								92.2	52.7		SLLDASEEAIKK
								48.2	52.1		TISPMVMDAK
								106.8	50.9		TQMQEAMTQEVSDVFSDTTTPIK
								71.0	52.5		VDQLAAQLADLAAR
								64.1	52.7		VGELCAGKER
								93.4	52.0		VLQLTSWDEDAWASK
								67.0	52.4		WIDNPTVDDR
	Endoplasmin	Rat	Q66HD0	92713	4.72	47	27	50.0	52.4	36%	DISTNYYASQK
								85.0	52.1		EATEKEFEPLLNWMK
								35.8	52.2		EFEPLLNWMK
								46.9	50.9		EGSRTDDEVVQREEEAIQLDGLNASQIR
								67.3	51.5		EGVKFDESEK
								67.1	52.0		EGVKFDESEKSK
								84.4	52.6		ELISNASDALDK
								88.8	52.7		ELISNASDALDKIR
								43.6	51.5		FAFQAEVNR
								116.8	51.4		FQSSHHSTDITSLDQYVER
								33.8	52.8		GLFDEYGSK
								80.9	52.4		GVVDSDDLPLNVSR
								50.6	50.8		GYEVIYLTEPVDEYCIQALPEFDGKR
								43.2	52.6		IYFMAGSSR
								84.8	52.1		KEAESSPFVER
								79.9	50.9		KGYEVIYLTEPVDEYCIQALPEFDGK
								59.8	50.9		KGYEVIYLTEPVDEYCIQALPEFDGKR
								41.4	52.8		KTFEINPR
								42.8	52.6		KTLDMIK
								75.2	51.6		LGVIEDHSNR
								127.8	52.3		LISLTDENALAGNEELTVK
								97.1	51.1		LTESPCALVASQYGWSGNMER
								40.9	52.3		NLLHVTDTGVGMTREELVK
								58.0	51.2		SGTSEFLNK
								55.6	51.9		SGYLLPDTK
								51.7	52.8		SILFVPTSAPR
								90.1	51.5		TDDEVVQREEEAIQLDGLNASQIR
	Alpha-actinin-4	Rat	Q9QXQ0	104849	5.27	37	17	68.8	51.9	26%	ACLISLGYDVENDR
								64.1	51.9		AGTQIENIDEDFRDGLK
								67.2	51.5		ASFNHFDKDHGGALGPEEFK
								57.8	52.3		DGLAFNALIHR
								122.6	51.7		ETTDTDTADQVIASFK
								65.1	51.7		GISQEQMQEFR
								67.3	52.3		HRDYETATLSDIK
								77.2	51.9		ICDQWDNLGSLTHSR
								45.8	52.1		KAGTQIENIDEDFRDGLK
								124.6	52.2		KDDPVTNLNNAFEVAEK
								137.4	52.4		LSGSNPYTSVTPQIINSK
								111.5	51.9		MAPYQGPDAAPGALDYK
								85.1	52.5		QLETIDQLHLEYAK
								74.7	52.2		RDHALLEEQSK
								102.2	52.6		VLAGDKNFITAEELR
								68.1	51.5		VLAVNQENEHLMEDYER
								32.4	50.4		VQQLVPK
	Alpha-actinin-1	Rat	Q9Z1P2	102896	5.23	39	17	92.0	51.1	31%	ACLISLGYDIGNDPQGEAEFAR
								49.0	52.0		AGTQIENIEEDFRDGLK
								64.5	51.7		GISQEQMNEFR

								50.7	52.5		HRPELIDYGK
								96.2	52.2		ICDQWDNLGALTQK
								64.9	52.0		IDQLEGDHQLIQEALIFDNK
								68.4	52.4		ILAGDKNYITGDELR
								44.6	52.8		IMSIVDPNR
								80.4	52.1		ISIEMHGTLEDQLSHLR
								118.0	52.1		KDDPLTNLNTAFDVAER
								71.6	52.1		LAILGIHNEVSK
								38.5	49.8		MDHYDSQQTNDYMQPEEDWDRDLLLDPAWEK
								47.4	52.1		MLDAEDIVGTARPDEK
								70.4	51.3		MVSDINNAWGCLEQAEK
								113.0	52.5		QFGAQANVIGPWIQTK
								68.8	52.2		QKDYETATLSEIK
								55.2	51.5		VLAVNQENEQLMEDYEK
	Transitional endoplasmic reticulum ATPase	Rat	P46462	89293	5.14	18	12	130.3	52.4	23%	ASGADSKGDDLSTAILK
								63.2	52.0		ETVVEVPQVTWEDIGGLEDVKR
								54.0	52.6		EVDIGIPDATGR
								46.4	52.6		IVSQLLTLMDGLK
								48.2	52.8		KGDIFLVR
								63.9	50.4		LADDVDLEQVANETHGHVGADLAALCSEAALQAIR
								69.7	52.7		LAGESESNLR
								101.1	52.2		LIVDEAINEDNSVVSLSQPK
								50.9	51.4		MDELQLFR
								106.1	52.5		NAPAIIFIDELDAIAPK
								55.5	52.1		VINQILTEMDGMSTK
								63.9	52.6		WALSQSNPSALR
	Nucleolin	Rat	P13383	77101	4.67	13	11	40.3	51.0	18%	ALVPTPGKK
								51.1	52.2		ATFIKVPQNPHGK
								45.4	52.3		EVFEDAVEIR
								82.9	51.6		FGYVDFESAEDLEK
								64.7	51.9		GYAFIEFASFEDAK
								113.6	52.0		KFGYVDFESAEDLEK
								59.5	52.1		NLSFNITEDELK
								100.9	52.1		QKIEGSEPTTPFNLFIGNLNPNK
								43.4	52.3		SKGIAYIEFK
								51.0	52.7		SVSLYYTGEK
								52.2	52.5		VAISELFAK
	Calnexin	Rat	P35565	67213	4.49	21	10	82.9	51.5	19%	APVPTGEVYFADSFDR
								50.1	52.7		GSLSGWILSK
								53.1	51.1		KDDTDDEIAKYDGKWEVDEMK
								96.6	52.2		KIPNPDFFEDLEPFR
								54.2	52.4		KPEDWDERPK
								73.8	51.8		VTYKAPVPTGEVYFADSFDR
								88.3	52.2		VVDDWANDGWGLK
								47.8	52.1		WKPPMIDNPNYQGIWKPR
								43.2	52.0		YDGKWEVDEMK
								67.6	51.6		YDGKWEVDEMKETK
	Glucosidase 2 subunit beta	Mouse	O08795	58756	4.41	13	10	67.4	52.6	18%	EKESLQQLAEVTR
								78.0	52.7		ESLQQLAEVTR
								63.0	52.2		ETVVTSTTEPSR
								42.4	52.9		KILIEEWK
								82.0	52.7		KLWEEQQAAAK
								40.9	52.8		LLELQAGK
								43.3	52.7		LWEEQQAAAK
								101.9	51.4		MPPYDEETQAIIDAAQEAR
								51.5	52.1		SLKEMEESIR
								67.8	51.3		YEQGTGCWQGPNR
	Heat shock protein HSP 90-beta	Rat	P34058	83229	4.97	13	9	71.1	52.6	16%	ADLINNLGTIAK
								49.7	52.2		EQVANSAFVER
								75.9	52.6		GVVDSEDLPLNISR
								76.3	52.4		HLEINPDHPIVETLR
								97.9	51.3		NPDDITQEEYGEFYK
								76.3	52.3		TLTLVDTGIGMTK
								56.0	52.4		VILHLKEDQTEYLEER
								40.9	51.9		YESLTDPSKLDSGK
								51.8	51.8		YIDQEELNK
	Transcription intermediary factor 1-beta	Rat	O08629	88900	5.52	10	8	46.3	51.9	17%	FQWDLNAWTK
								55.2	52.2		IVAERPGTNSTGPGPMAPPR
								75.8	50.3		LASPSGSTSSGLEVVAPEVTSAPVSGPGILDDSATICR
								96.2	52.5		LDLDLTSDSQPPVFK
								96.4	52.0		LSPPYSSPQEFAQDVGR
								110.7	52.6		LTEDKADVQSIIGLQR

								75.2	52.0		SGEGEVSGLMR
								79.2	52.2		VFPGSTTEDYNLIVIER
	Kinesin-1 heavy chain	Rat	Q2PQA9	109463	6.06	10	8	49.9	51.7	11%	HVAVTNMNEHSSR
								42.9	52.6		ILQDSLGGNCR
								66.9	52.5		ISFLENNLEQLTK
								73.9	52.0		QAVEQQIQSHR
								72.1	51.8		QLDDKDEEINQQSQLVEK
								102.1	52.2		QLEESVDSLGEELVQLR
								68.0	52.7		SATLASIDAELQK
								63.3	52.7		TGAEGAVLDEAK
	Splicing factor, proline- and glutamine-rich	Mouse	Q8VIJ6	75394	9.45	13	8	69.3	51.4	18%	DKLESEMEDAYHEHQANLLR
								86.1	52.3		FGQGGAGPVGGQGPR
								50.4	52.7		GIVEFASKPAAR
								70.7	52.2		LFVGNLPADITEDEFKR
								44.9	51.6		MPGGPKPGGGPGMGAPGGHPKPPHR
								56.3	51.8		RMEELHSQEMQK
								49.0	52.0		SPPPGMGLNQNR
								59.1	51.8		YGEPGEVFINK
	Catenin alpha-1	Mouse	P26231	100044	5.91	11	7	61.8	52.1	11%	AHVLAASVEQATENFLEKGDK
								83.2	52.3		IAEQVASFQEEK
								91.3	52.1		LIEVANLACSISNNEEGVK
								90.9	52.5		LLEPLVTQVTTLVNTNSK
								55.7	52.2		LLILADMADVYK
								57.8	52.6		QDLLAYLQR
								65.3	52.5		QIIVDPLSFSEER
	Calpastatin	Rat	P27321	77266	5.09	12	5	54.0	51.7	9%	DKELDDALDELSDSLGQR
								46.2	52.5		GVVPDDAVETLAR
								83.6	52.4		QPDPQSHLR
								54.9	52.6		SLTPTLPMESTLNK
								53.2	52.0		SQSSEPPVIHEK
	Importin-5	Mouse	Q8BKC5	123511	4.82	9	5	53.7	51.7	7%	HIVENAVQK
								61.6	52.1		LLSSAFDEVYPALPSDVQTAIK
								81.2	52.1		STACQMLVCYAK
								64.8	52.5		VAAAESMPLLLECAR
								85.8	52.4		VIAALLQTMEDQGNQR
	Caprin-1	Rat	Q5M9G3	78073	5.14	7	5	55.0	52.4	13%	QILGVIDKK
								66.3	52.1		SFMALSQDIQK
								122.6	51.1		SSFSNTPNSGYTQSQFNAPR
								44.2	50.2		SSGPPPPSGSSGSEAAAGAAAPASQHPATGTGAVQTEAMK
								51.9	52.3		YQEVTNNLEFAK
	Drebrin	Rat	Q07266	77424	4.46	6	5	54.2	52.1	11%	KSESEVEEAAAIIAQRPDNPR
								61.0	51.9		LAASGEGGLQELSGHFENQK
								65.1	52.0		LREDENAEPVGTTYQK
								53.8	51.6		LSSPVLHR
								78.1	52.4		YVLINWVGEDVPDAR
	78 kDa glucose-regulated protein	Rat	P06761	72302	5.07	6	4	92.0	52.6	9%	IINEPTAAAIAYGLDKR
								81.7	52.6		KSDIDEIVLVGGSTR
								49.0	52.3		TFAPEEISAMVLTK
								69.1	52.4		TWNDPSVQQDIK
	Heterogeneous nuclear ribonucleoprotein U	Mouse	Q8VEK3	87863	5.92	5	4	40.5	51.3	7%	DIDIHEVR
								41.5	52.3		DLPEHAVLK
								53.6	51.2		EKPYFPIPEDCTFIQNVPLEDR
								108.8	52.5		SSGPTSLFAVTVAPPGAR
	Integrin beta-1	Rat	P49134	88436	5.77	5	4	48.6	51.6	6%	IGFGSFVEK
								52.5	52.5		LRPEDITQIQPQQLLLK
								74.6	51.6		SLGTDLMNEMR
								61.4	51.8		WDTGENPIYK
	Ubiquitin-like modifier-activating enzyme 1	Rat	Q5U300	117713	5.36	2	2	69.1	52.4	3%	LAGTQPLEVLEAVQR
								159.2	52.0		NEEDATELVTLAQAVNAR
	Heat shock protein 105 kDa	Rat	Q66HA8	96357	5.4	3	2	52.6	52.0	3%	DLLNMYIETEGK
								81.2	52.3		GCALQCAILSPAFK
	Catenin delta-1	Mouse	P30999	104860	6.41	3	2	41.8	52.6	2%	QDVYGPQPQVR
	Lon protease homolog, mitochondrial	Rat	Q924S5	105726	6.17	2	1	92.1	52.4	2%	VLFICTANVTDTIPEPLR
	Heterogeneous nuclear ribonucleoprotein U-like protein 2	Mouse	Q00PI9	84948	4.83	2	1	67.8	52.3	2%	YNVLGAETVLTQMR
	Transmembrane glycoprotein NMB	Rat	Q6P7C7	63691	6.67	1	1	92.6	50.9	3%	GWSSDENEWDEQLYPVWR
	Ankycorbin	Rat	Q5U312	109066	5.81	2	1	58.1	52.7	1%	EKENIQTLLK
	Src substrate cortactin	Mouse	Q60598	61222	5.24	2	1	50.1	52.5	2%	YGLFPANYVELR
	Gelsolin	Rat	Q68FP1	86014	5.76	1	1	65.3	52.6	2%	AGALNSNDAFVLK
	Lysosome membrane protein 2	Rat	P27615	54056	4.91	1	1	66.0	52.3	3%	KLDDFVETGNIR
	Importin subunit beta-1	Rat	P52296	97062	4.66	1	1	54.3	52.1	1%	VLANPGNSQVAR
	LIM domain and actin-binding protein 1	Mouse	Q9ERG0	84038	6.18	1	1	49.5	52.5	1%	LSETSIKDR

AR3_2	Actin, cytoplasmic 1	Rat	P60711	41710	5.29	40	15	72.2	52.5	59%	AGFAGDDAPR
								60.5	52.5		AVFPSIVGRPR
								65.7	50.9		DDDIAALVVDNGSGMCK
								36.2	51.6		DLTDYLMK
								120.4	51.0		DLYANTVLSGGTTMYPGIADR
								44.9	51.4		DSYVGDEAQSK
								56.1	52.7		EITALAPSTMK
								52.2	52.1		GYSFTTTAER
								79.0	52.3		HQGVMVGMGQK
								61.5	52.1		IWHHTFYNELR
								101.8	51.6		KDLYANTVLSGGTTMYPGIADR
								124.0	50.8		LCYVALDFEQEMATAASSSSLEK
								98.3	51.5		QEYDESGPSIVHR
								89.8	52.0		SYELPDGQVITIGNER
								81.7	50.8		TTGIVMDSGDGVTHTVPIYEGYALPHAILR
	Fructose-bisphosphate aldolase A	Rat	P05065	39327	8.31	19	14	85.1	51.9	52%	AAQEEYIKR
								44.8	52.5		ADDGRPFPQVIK
								63.7	52.6		ALANSLACQGK
								52.4	51.1		ELADIAHR
								122.9	51.8		FSNEEIAMATVTALR
								73.9	52.5		GILAADESTGSIAK
								82.8	51.4		GVVPLAGTNGETTTQGLDGLSER
								103.4	51.8		IGEHTPSSLAIMENANVLAR
								80.5	51.8		LQSIGTENTEENR
								53.4	51.9		LQSIGTENTEENRR
								42.9	52.3		PHPYPALTPEQK
								51.9	51.9		RLQSIGTENTEENRR
								61.4	50.8		YASICQQNGIVPIVEPEILPDGDHDLK
								65.6	50.9		YTPSGQSGAAASESLFISNHAY
	Phosphoglycerate kinase 1	Rat	P16617	44510	8.02	19	13	59.2	52.1	40%	AHSSMVGVNLPQK
								81.4	52.5		ALESPERPFLAILGGAK
								46.0	50.8		FCLDNGAK
								47.1	52.8		FHVEEEGK
								97.2	51.2		GCITIIGGGDTATCCAK
								88.3	51.7		ITLPVDFVTADKFDENAK
								45.6	52.1		KYAEAVAR
								84.1	51.5		LGDVYVNDAFGTAHR
								52.7	52.9		LTLDKLDVK
								117.0	51.0		VLNNMEIGTSLYDEEGAK
								97.6	52.2		VSHVSTGGGASLELLEGK
								87.7	51.3		WNTEDKVSHVSTGGGASLELLEGK
								55.9	52.5		YSLEPVAAELK
	Annexin A2	Rat	Q07936	38654	7.55	15	13	123.7	51.1	41%	AEDGSVIDYELIDQDAR
								55.5	52.8		DALNIETAIK
								43.2	51.6		DIISDTSGEFR
								101.4	51.8		GLGTDEDSLIEIICSR
								93.5	52.5		GVDEVTIVNILTNR
								57.4	51.5		KLLVALAK
								67.3	51.2		RAEDGSVIDYELIDQDAR
								68.2	52.5		SALSGHLETVMLGLLK
								57.6	52.5		STVHEILCK
								45.7	51.8		SYSPYDMLESIR
								77.4	51.6		TDLEKDIISDTSGEFR
								70.8	52.5		TNQELQEINR
								79.7	51.6		TPAQYDASELK
	Glyceraldehyde-3-phosphate dehydrogenase	Rat	P04797	35805	8.14	17	8	60.5	52.1	41%	GAAQNIIPASTGAAK
								107.3	51.8		IVSNASCTTNCLAPLAK
								77.9	50.7		LISWYDNEYGYSNR
								104.5	51.6		VIHDNFGIVEGLMTTVHAITATQK
								44.2	51.7		VIISAPSADAPMFVMGVNHEK
								91.9	51.7		VPTPNVSVVDLTCR
								70.5	52.0		VVDLMAYMASKE
								99.5	50.9		WGDAGAEYVVESTGVFTTMEK
	Annexin A1	Rat	P07150	38805	6.97	10	8	61.7	52.3	25%	AAYLQETGKPLDETLKK
								46.9	51.9		CATSTPAFFAEK
								110.7	52.5		GLGTDEDTLIEILTTR
								81.8	52.2		GTDVNVFNTILTTR
								89.6	52.3		KGTDVNVFNTILTTR
								39.1	51.3		KVFQNYR
								72.6	52.0		QEQEYVQAVK
								101.6	52.2		TPAQFDADELR
	Nucleophosmin	Rat	P13084	32540	4.62	9	7	63.6	50.9	35%	ADKDYHFKVDNDENEHQLSLR
								47.8	52.4		DLKPSTPR

								43.2	53.0		GPSSVEDIK
								73.1	52.3		MSVQPTVSLGGFEITPPVVLR
								125.4	51.2		MTDQEAIQDLWQWR
								112.7	51.0		TVSLGAGAKDELHIVEAEAMNYEGSPIK
								103.0	51.4		VDNDENEHQLSLR
	Macrophage-capping protein	Rat	Q6AYC4	38775	6.11	11	7	47.7	51.9	37%	AQVEIITDGEEPAEMIQVLGPKPALK
								58.4	52.6		EGGVESAFHK
								109.5	50.8		EGNPEEDITADQTNAQAAALYK
								99.4	51.0		EVQGNESDLFMSYFPQGLK
								46.3	51.0		MYTPIPQSGSPFPASVQDPGLHIWR
								82.0	51.9		VSDATGQMNLTK
								87.5	52.4		YSPNTQVEILPQGR
	Malate dehydrogenase, mitochondrial	Rat	P04636	35661	8.93	8	6	40.9	51.7	25%	EGVIECSFVQSK
								74.5	51.9		ETECTYFSTPLLLGK
								46.5	52.3		GYLGPEQLPDCLK
								55.2	52.6		IFGVTTLDIVR
								55.0	52.8		IQEAGTEVVK
								116.2	51.9		LTLYDIAHTPGVAADLSHIETR
	Poly(rC)-binding protein 1	Mouse	P60335	37474	6.66	6	6	69.7	52.5	24%	AITIAGVPQSVTECVK
								95.0	51.1		ESTGAQVQVAGDMLPNSTER
								65.1	52.7		IITLTGPTNAIFK
								71.1	52.1		INISEGNCPER
								64.5	52.7		QGANINEIR
								109.3	51.9		QICLVMLETLSQSPQGR
	Elongation factor 1-delta	Rat	Q68FR9	31311	4.94	8	6	46.4	51.6	25%	ATAPQTQHVSPMR
								46.6	52.3		ATNFLMHEK
								83.8	51.5		FYEQMNGPVTAGSR
								70.0	52.6		GVVQDLQQAISK
								41.1	52.8		QENGASVILR
								61.6	52.7		SIQLDGLVWGASK
	Heterogeneous nuclear ribonucleoprotein A3	Rat	Q6URK4	39628	9.1	8	5	64.5	52.1	19%	EDSVKPGAHLTVK
								55.0	52.2		IETIEVMEDR
								43.7	52.0		IFVGGIKEDTEEYNLR
								145.2	50.8		SSGSPYGGGYGSGGGSGGYGSR
								45.9	51.5		YHTINGHNCEVK
	Alcohol dehydrogenase [NADP+]	Rat	P51635	36483	6.84	7	5	50.5	51.6	16%	ALGLSNFSSR
								64.0	52.1		AWRHPDEPVLLEEPVVLALAEK
								62.4	52.3		HPDEPVLLEEPVVLALAEK
								52.3	52.8		MPLIGLGTWK
								54.8	51.9		YIVPMITVDGK
	Thioredoxin domain-containing protein 5	Mouse	Q91W90	46386	5.51	7	4	61.6	52.1	15%	ALAPTWEQLALGLEHSETVK
								62.3	52.6		DLDSLHSFVLR
								82.0	52.2		SFEDTIAQGITFVK
								93.5	50.9		VDCTADSDVCSAQGVR
	LIM and SH3 domain protein 1	Rat	Q99MZ8	29951	6.61	5	4	63.0	52.4	18%	GFSVVADTPELQR
								78.4	52.6		LKQQSELQSQVR
								63.0	51.8		QSFTMVADTPENLR
								51.0	52.8		TQDQISNIK
	Isocitrate dehydrogenase [NAD] subunit alpha, mitochondrial	Rat	Q99NA5	39588	6.47	6	4	48.4	52.6	14%	APIQWEER
								72.6	51.2		ENTEGEYSGIEHVIVDGVVQSIK
								60.6	52.6		IAEFAFEYAR
								65.4	52.4		TPYTDVNIVTIR
	Alpha-2-macroglobulin receptor-associated protein	Rat	Q99068	42006	6.85	4	4	89.8	52.1	14%	HVESIGDPEHISR
								46.5	52.6		IHEYNVLLDTLSR
								78.5	51.4		KVSHQGYGPATEFEEPR
								53.2	51.4		LAELHSDLK
	PDZ and LIM domain protein 1	Rat	P52944	35562	6.79	5	4	50.1	52.6	18%	DFEQPLAISR
								55.1	51.8		MNLASEPQEVLHIGSAHNR
								59.5	52.1		SAMPFTASPAPGTR
								49.8	52.1		TTQQIVLQGPGPWGFR
	Poly(rC)-binding protein 2	Mouse	Q61990	38197	6.33	5	3	54.8	52.5	12%	AITIAGIPQSIIECVK
								51.7	52.7		IITLAGPTNAIFK
								65.0	52.6		LVVPASQCGSLIGK
	Nascent polypeptide-associated complex subunit alpha	Mouse	Q60817	23370	4.52	3	3	74.5	52.2	19%	DIELVMSQANVSR
								124.8	52.3		IEDLSQQAQLAAAEK
								73.9	52.4		NILFVITKPDVYK
	Reticulocalbin-1	Mouse	Q05186	38090	4.7	5	3	76.0	51.5	14%	HWILPQDYDHAQAEAR
								84.2	51.8		IVDRIDSDGDGLVTTEELK
								67.2	51.5		TFDQLSPDESK
	60S acidic ribosomal protein P0	Rat	P19945	34194	5.91	5	3	54.0	52.0	11%	GHLENNPALEK
								48.6	52.6		GTIEILSDVQLIK

								60.2	52.6		TSFFQALGITTK
	Leucine-rich repeat-containing protein 59	Rat	Q5RJR8	34848	9.57	3	3	117.7	51.6	14%	DKLDGNELDLSLSDLNEVPVK
								57.8	52.7		LQQLPADFGR
								43.2	52.8		LVTLPVSFAQLK
	Tropomyosin beta chain	Rat	P58775	32817	4.66	3	3	78.9	52.2	15%	ATDAEADVASLNR
								57.8	51.8		LDKENAIDRAEQAEADKK
								66.1	52.4		QLEEEQQALQK
	26S protease regulatory subunit 10B	Mouse	P62334	44145	7.1	3	3	75.0	52.5	10%	ALQSVGQIVGEVLK
								69.2	52.4		EVIELPLTNPELFQR
								42.8	51.8		IHAGPITK
	Cathepsin L1	Rat	P07154	37636	6.37	4	2	75.2	51.4	7%	FDQTFNAQWHQWK
								55.4	52.6		LFQEPLMLQIPK
	Succinyl-CoA ligase [GDP-forming] subunit beta, mitochondrial	Mouse	Q9Z2I8	46811	6.58	3	2	86.0	51.8	7%	MAENLGFLGSLK
								88.9	52.3		SSGLPITSAVDLEDAAK
	Heterogeneous nuclear ribonucleoprotein A/B	Mouse	Q99020	30812	7.68	4	2	45.6	52.8	8%	DLKDYFTK
								72.1	52.5		IFVGGLNPEATEEK
	SPARC	Rat	P16975	34274	4.81	3	2	75.2	52.5	10%	RLEAGDHPVELLAR
								123.3	51.7		YIAPCLDSELTEFPLR
	Vimentin	Rat	P31000	53700	5.06	3	2	57.9	51.7	4%	FADLSEAANR
								79.6	52.7		QDVDNASLAR
	Septin-2	Rat	Q91Y81	41566	6.15	2	2	75.2	52.5	8%	ASIPFSVVGSNQLIEAK
								48.8	52.2		TIISYIDEQFER
	Alpha-enolase	Rat	P04764	47098	6.16	2	2	57.3	52.2	6%	GNPTVEVDLYTAK
								59.7	52.1		YITPDQLADLYK
	Adenosine deaminase	Rat	Q920P6	39874	5.32	2	2	40.7	52.7	7%	AQTPAFNKPK
								63.8	52.4		GIDLPADTVEGLR
	Heterogeneous nuclear ribonucleoprotein D0	Rat	Q9JJ54	38168	7.62	2	2	52.0	51.4	7%	FGDVVDCTLK
								54.2	52.5		IFVGGLSPDTPEEK
	Ribonuclease inhibitor	Rat	P29315	49942	4.67	2	1	122.2	51.6	5%	TNELGDAGVGLVLQGLQNPTCK
	TAR DNA-binding protein 43	Mouse	Q921F2	44519	6.26	1	1	120.2	51.2	4%	FGGNPGGFGNQGGFGNSR
	Cathepsin B	Rat	P00787	37446	5.36	1	1	104.5	51.5	5%	VGFSEDINLPESFDAR
	Heterogeneous nuclear ribonucleoproteins A2/B1	Rat	A7VJC2	37455	8.97	2	1	57.4	51.8	4%	GGGGNFGPGPGSNFR
	DnaJ homolog subfamily B member 1	Mouse	Q9QYJ3	38143	8.75	2	1	62.8	51.9	5%	EGDQTSNNIPADIVFVLK
	Isocitrate dehydrogenase [NADP] cytoplasmic	Rat	P41562	46705	6.53	1	1	83.3	52.1	3%	TVEAEAAHGTVTR
	L-lactate dehydrogenase A chain	Rat	P04642	36427	8.45	2	1	60.7	52.0	3%	QVVDSAYEVIK
	UBX domain-containing protein 1	Rat	Q499N6	33561	5.22	2	1	78.3	52.3	5%	AELTALESLIEMGFPR
	Aldose reductase	Rat	P07943	35774	6.26	3	1	51.9	52.5	4%	AIGVSNFNPLQIER
	Protein kinase C delta-binding protein	Rat	Q9Z1H9	27894	5.79	1	1	68.4	52.4	6%	KGSEAAQPTPVKPPR
	Transcriptional activator protein Pur-alpha (Fragments)	Rat	P86252	15313	4.69	1	1	67.8	52.1	17%	GPGLGSTQGQTIALPAQGLIEFR
	Peroxisomal 3,2-trans-enoyl-CoA isomerase	Rat	Q5XIC0	42994	9.11	1	1	65.0	52.5	3%	WDAWNALGSLPK
	Calponin-3	Rat	P37397	36412	5.47	1	1	62.4	51.9	3%	GPSYGLSAEVK
	3-ketoacyl-CoA thiolase B, peroxisomal	Rat	P07871	43793	8.53	1	1	62.2	52.4	4%	IAQFLSGIPETVPLSAVNR
	Brain acid soluble protein 1	Mouse	Q91XV3	22074	4.5	1	1	61.4	52.3	6%	ETPAASEAPSSAAK
	Protein disulfide-isomerase	Rat	P04785	56916	4.82	1	1	59.3	51.5	2%	YKPESDELTAEK
	Malate dehydrogenase, cytoplasmic	Rat	O88989	36460	6.16	1	1	59.0	52.1	4%	FVEGLPINDFSR
	Isocitrate dehydrogenase [NADP], mitochondrial	Rat	P56574	50935	8.88	1	1	83.3	52.1	3%	GKLDGNQDLIR
	Stomatin-like protein 2	Rat	Q4FZT0	38390	8.74	1	1	54.7	51.9	4%	APVPGAQNSSEAR
	Small glutamine-rich tetratricopeptide repeat-containing protein alph	Rat	O70593	34136	5.05	1	1	46.1	51.6	3%	HAEAVAYYK
AR3_3	Peptidyl-prolyl cis-trans isomerase A	Mouse	P17742	17960	7.74	26	12	52.4	48.3	71%	EGMNIVEAMER
								48.6	48.7		FEDENFILK
								111.7	48.0		HTGPGILSMANAGPNTNGSQFFICTAK
								68.8	48.4		IIPGFMCQGGDFTR
								54.2	49.8		KITISDCGQL
								70.7	48.2		MVNPTVFFDITADDEPLGR
								87.1	48.5		SIYGEKFEDENFILK
								36.8	50.1		TEWLDGK
								77.0	49.2		VKEGMNIVEAMER
								69.6	48.4		VNPTVFFDITADDEPLGR
								52.1	48.9		VSFELFADK
								47.9	49.4		VSFELFADKVPK
	Cellular retinoic acid-binding protein 1	Mouse	P62965	15582	5.3	10	8	47.5	50.3	55%	ALGVNAMLR
								79.7	48.8		IHCTQTLLEGDGPK
								101.2	49.9		KVAVAAASKPHVEIR
								51.7	49.9		PNFAGTWK

								48.6	48.7		QDGDQFYIK
								46.7	49.2		SLPTWENENK
								76.5	48.6		SSENFDELLK
								70.3	49.9		VAVAAASKPHVEIR
	Galectin-1	Mouse	P16045	14856	5.32	16	7	97.0	48.8	60%	ACGLVASNLNLKPGECLK
								90.2	48.6		DSNNLCLHFNPR
								112.4	48.5		FNAHGDANTIVCNTK
								110.4	48.2		LNMEAINYMAADGDFK
								36.3	49.0		LPDGHEFK
								54.8	49.0		LPDGHEFKFPNR
								46.9	50.1		SFVLNLGK
	Eukaryotic translation initiation factor 5A-1	Mouse	P63242	16821	5.08	11	7	108.0	48.1	67%	ADDLDFETGDAGASATFPMQCSALR
								49.5	49.3		EDLRLPEGDLGK
								80.2	48.9		EDLRLPEGDLGKEIEQK
								48.4	49.0		IVEMSTSK
								57.0	48.3		KYEDICPSTHNMDVPNIK
								96.6	48.2		NDFQLIGIQDGYLSLLQDSGEVR
								76.5	49.7		VHLVGIDIFTGK
	Histidine triad nucleotide-binding protein 1	Mouse	P70349	13768	6.36	8	6	59.6	49.6	73%	AQVAQPGGDTIFGK
								53.8	50.3		CAADLGLK
								71.9	48.8		CLAFHDISPQAPTHFLVIPK
								63.0	50.3		KCAADLGLK
								87.1	48.3		KHISQISVADDDDESLLGHLMIVGK
								34.0	48.2		MVVNEGADGGQSVYHIHLHVLGGR
	Actin, cytoplasmic 1	Mouse	P607110	41710	5.29	8	5	65.5	48.2	19%	DDDIAALVVDNGSGMCK
								75.1	48.3		DLYANTVLSGGTTMYPGIADR
								41.7	49.9		EITALAPSTMK
								79.3	48.3		KDLYANTVLSGGTTMYPGIADR
								113.4	48.0		LCYVALDFEQEMATAASSSSLEK
	Profilin-1	Mouse	P62962	14948	8.46	15	5	46.8	48.1	50%	CYEMASHLR
								64.0	49.3		DSPSVWAAVPGK
								67.9	49.3		SSFFVNGLTLGGQK
								55.0	48.7		STGGAPTFNVTVTMTAK
								109.4	49.6		TFVSITPAEVGVLVGKDR
	Nucleoside diphosphate kinase B	Mouse	Q01768	17352	6.97	10	5	81.0	49.0	44%	EIHLWFKPEELIDYK
								49.7	48.7		GDFCIQVGR
								86.7	48.8		NIIHGSDSVESAEK
								75.0	50.1		TFIAIKPDGVQR
								66.6	49.0		VMLGETNPADSKPGTIR
	Myosin light polypeptide 6	Mouse	Q60605	16919	4.56	7	5	72.3	49.4	42%	ALGQNPTNAEVLK
								61.8	48.9		HVLVTLGEK
								48.2	48.7		ILYSQCGDVMR
								98.5	48.4		NKDQGTYEDYVEGLR
								44.2	48.6		VFDKEGNGTVMGAEIR
	40S ribosomal protein S19	Mouse	Q9CZX8	16076	10.4	8	5	42.1	49.6	30%	DVNQQEFVR
								62.7	48.4		ELAPYDENWFYTR
								50.2	49.9		LKVPEWVDTVK
								50.5	49.4		RVLQALEGLK
								47.5	50.0		VPEWVDTVK
	Fatty acid-binding protein, epidermal	Mouse	Q05816	15127	6.14	10	4	63.2	50.3	33%	ASLKDLEGK
								51.1	49.3		ELGVGLALR
								40.0	48.2		LMESHGFEEYMK
								69.8	48.1		MIVECVMNNATCTR
	40S ribosomal protein S14	Mouse	P62264	16263	10.1	5	4	61.5	49.2	19%	IEDVTPIPSDSTR
								59.3	49.2		IGRIEDVTPIPSDSTR
								76.7	49.4		TKTPGPGAQSALR
								73.0	48.8		TPGPGAQSALR
	40S ribosomal protein S25	Mouse	P62852	13734	10.1	5	4	54.3	50.2	24%	AALQELLSK
								67.1	49.9		DKLNNLVLFDK
								58.0	49.5		LITPAVVSER
								50.2	50.1		LNNLVLFDK
	Superoxide dismutase [Cu-Zn]	Mouse	P08228	15933	6.02	6	3	64.3	49.5	23%	DGVANVSIEDR
								85.6	48.8		HVGDLGNVTAGK
								87.0	49.4		VISLSGEHSIIGR
	40S ribosomal protein S13	Mouse	P62301	17212	10.5	4	3	78.3	49.6	28%	KGLTPSQIGVILR
								97.3	49.1		LTSDDVKEQIYK
								58.5	49.4		SKGLAPDLPEDLYHLIK
	40S ribosomal protein S17	Mouse	P63276	15514	9.85	5	3	66.8	48.1	41%	DNYVPEVSALDQEIIEVDPDTK
								97.2	48.4		LLDFGSLSNLQVTQPTVGMNFK
								66.7	49.9		VCEEIAIIPSK
	Ubiquitin-conjugating enzyme E2 N	Mouse	P61089	17127	6.13	6	3	58.4	49.4	27%	LLAEPVPGIK
								79.9	49.6		TNEAQAIETAR

								44.2	48.5		YFHVVIAGPQDSPFEGGTFK
	40S ribosomal protein S18	Mouse	P62270	17708	11	8	2	43.2	49.7	16%	SLVIPEKFQHILR
								77.4	49.3		YSQVLANGLDNK
	Low molecular weight phosphotyrosine protein phosphatase	Mouse	Q9D358	18180	6.3	3	2	116.9	48.1	18%	IDSAATSTYEVGNPPDYR
								58.3	49.7		IELLGSYDPQK
	Cytochrome c oxidase subunit 4 isoform 1, mitochondrial	Mouse	P19783	19518	9.25	4	2	61.5	48.3	12%	SEDYAEPTYADR
								44.7	48.3		WDYDKNEWK
	Glyceraldehyde-3-phosphate dehydrogenase	Rat	P04797	35805	8.14	3	2	41.1	49.4	11%	GAAQNIIPASTGAAK
								110.8	48.2		WGDAGAEYVVESTGVFTTMEK
	ATP synthase subunit delta, mitochondrial	Mouse	Q9D3D9	17589	5.03	2	2	79.9	49.2	14%	AQSELSGAADEAAR
								69.3	50.1		IEANEALVK
	60S ribosomal protein L36	Rat	P39032	12260	11.6	4	2	61.7	49.8	12%	EELSNVLAAMR
								42.1	49.6		KREELSNVLAAMR
	Putative RNA-binding protein 3	Mouse	O89086	16595	6.84	4	2	45.0	48.5	19%	DYSGSQGGYDR
								47.3	48.2		GFGFITFTNPEHASDAMR
	Peptidyl-prolyl cis-trans isomerase NIMA-interacting 1	Mouse	Q9QUR7	18359	8.93	2	2	56.5	48.5	21%	GQMQKPFEDASFALR
								70.4	48.8		TGEMSGPVFTDSGIHIILR
	Peroxiredoxin-5, mitochondrial	Mouse	P99029	21884	9.1	3	2	51.0	50.1	10%	KVNLAELFK
								59.6	50.0		LLADPTGAFGK
	Prothymosin alpha	Mouse	P26350	12247	3.7	2	1	75.1	48.6	13%	SDAAVDTSSEITTK
	Thioredoxin	Mouse	P10639	11668	4.8	3	1	63.0	49.1	12%	EAFQEALAAAGDK
	Ubiquitin-conjugating enzyme E2 variant 1	Mouse	Q9CZY3	16344	7.74	3	1	48.6	49.8	7%	WTGMIIGPPR
	Prefoldin subunit 2	Mouse	O70591	16524	6.19	2	1	77.2	49.9	8%	IIETLSQQLQAK
	60S acidic ribosomal protein P1	Mouse	P47955	11468	4.28	1	1	94.9	47.2	38%	ALANVNIGSLICNVGAGGPAPAAGAAPAGGAAPSTAAAPAEEK
	60S ribosomal protein L23	Muse	P62830	14856	10.5	2	1	53.3	49.4	6%	ECADLWPR